The Detroit Edison Company
One Energy Plaza, Detroit, MI 48226-1279

DTE Energy
Detroit Edison

10 CFR 52.79

June 15, 2012
NRC3-12-0019

U. S. Nuclear Regulatory Commission
Attention: Document Control Desk
Washington, DC 20555-0001

References:
1) Fermi 3
Docket No. 52-033
2) Letter from Jerry Hale (USNRC) to Jack M. Davis (Detroit Edison), "Request for Additional Information Letter No. 70 Related to Chapters 2.0 and 3.0 for the Fermi 3 Combined License Application," dated January 18, 2012
3) Letter from Peter W. Smith (Detroit Edison) to USNRC, "Detroit Edison Company Response to NRC Request for Additional Information Letter No. 70," NRC3-12-0003, dated February 16, 2012
4) Letter from Peter W. Smith (Detroit Edison) to USNRC, "Detroit Edison Company Response to NRC Request for Additional Information Letter No. 70," NRC3-12-0007, dated March 1, 2012
5) Letter from Peter W. Smith (Detroit Edison) to USNRC, "Detroit Edison Company Response to NRC Request for Additional Information Letter No. 70," NRC3-12-0008, dated March 23, 2012
6) Letter from Peter W. Smith (Detroit Edison) to USNRC, "Detroit Edison Company Response to NRC Request for Additional Information Letter No. 70," NRC3-12-0013, dated April 30, 2012
7) Letter from Peter W. Smith (Detroit Edison) to USNRC, "Detroit Edison Company Response to NRC Request for Additional Information Letter No. 70," NRC3-12-0016, dated May 22, 2012

Subject: Detroit Edison Company Response to NRC Request for Additional Information Letter No. 70

In Reference 2, the NRC requested additional information to support the review of certain portions of the Fermi 3 Combined License Application (COLA). Detroit Edison provided responses to several Requests for Additional Information (RAIs) associated with Reference 2 in References 3, 4, and 5. Attachment 1 provides a table of the eighteen RAIs of Reference 2, broken down into 40 parts, with submittal dates identified for each RAI part.

DO95
NRO

During the week of April 23, 2012, the NRC conducted an audit of responses to RAIs provided in References 3, 4, and 5, draft responses to the remaining RAIs in Reference 2, and the Fermi 3 site-specific soil-structure interaction (SSI) analyses. In Reference 6, Detroit Edison indicated that, as requested by the staff during the audit, an additional direct method SSI analysis would be performed in order to validate the subtraction method analyses performed to respond to the remaining RAIs in Reference 2. The staff indicated that a fully embedded direct method analysis of the Control Building (CB) that utilizes the most recent seismic inputs would be appropriate for comparison with the subtraction method. In Reference 6, Detroit Edison committed to provide responses to the remaining RAIs in Reference 2, including validation, no later than June 15, 2012. Additionally, the staff requested supplemental responses to several RAIs in Reference 2, which Detroit Edison committed to provide no later than June 15, 2012, in Reference 6. Reference 7 provided supplemental responses to several of the RAIs in Reference 2.

Attachment 2 provides a table containing the list of issues that were unresolved as of the audit during the week of April 23, 2012. This table also identifies which letter(s) and attachment(s) addresses each of the issues.

Attachments 3 through 6 provide responses to the remaining RAIs in Reference 2, as well as one supplemental response requested by the staff during the audit. The remaining unresolved issues that were identified at the audit during the week of April 23, 2012, are addressed in Attachments 7 through 9, as described in Attachment 2.

If you have any questions, or need additional information, please contact me at (313) 235-3341.

I state under penalty of perjury that the foregoing is true and correct. Executed on the 15th day of June 2012.

Sincerely,

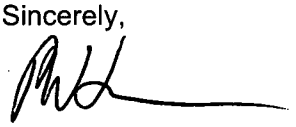

Peter W. Smith, Director
Nuclear Development – Licensing and Engineering
Detroit Edison Company

Attachments:
1) Table of RAI Letter No. 70 Response Dates
2) Table of Supplemental Issues Identified During the April 23 through 27, 2012, Audit
3) Supplemental Response to RAI Letter No. 70 (Question No. 03.07.01-3)
4) Response to RAI Letter No. 70 (Question No. 03.07.02-6)
5) Response to RAI Letter No. 70 (Question No. 03.07.02-8)
6) Response to RAI Letter No. 70 (Question No. 03.08.05-4)
7) SER-DTF-006, Rev. 1
8) SER-DTF-009, Rev. 0
9) COLA Markups

cc: Adrian Muniz, NRC Fermi 3 Project Manager
Jerry Hale, NRC Fermi 3 Project Manager
Michael Eudy, NRC Fermi 3 Project Manager (w/o attachments)
Bruce Olson, NRC Fermi 3 Environmental Project Manager (w/o attachments)
Fermi 2 Resident Inspector (w/o attachments)
NRC Region III Regional Administrator (w/o attachments)
NRC Region II Regional Administrator (w/o attachments)
Supervisor, Electric Operators, Michigan Public Service Commission (w/o attachments)
Michigan Department of Natural Resources and Environment
Radiological Protection Section (w/o attachments)

Attachment 1
NRC3-12-0019
(7 pages)

Table of RAI Letter No. 70 Response Dates

RAI Number	Part	Question Summary	Submittal Date
02.05.02-17	1	Explain why such a model is appropriate for use at the Fermi site.	March 1, 2012 (Detroit Edison Letter NRC3-12-0007, ML12065A194)
02.05.02-17	2	What is the impact of this assumed correlation model on site amplification?	March 1, 2012 (Detroit Edison Letter NRC3-12-0007, ML12065A194)
02.05.02-17	3	If a fully correlated model were to be assumed, for example, what would be the expected increase in amplification, particularly at higher frequencies above 15 Hz?	March 1, 2012 (Detroit Edison Letter NRC3-12-0007, ML12065A194)
02.05.02-18	1	Please provide more detail regarding the scaling process.	February 16, 2012 (Detroit Edison Letter NRC3-12-0003, ML120520154)
02.05.02-18	2	In addition, please quantitatively compare the mean response spectrum of each suite of scaled time histories to the respective target spectrum.	February 16, 2012 (Detroit Edison Letter NRC3-12-0003, ML120520154)
02.05.04-39	1	The technical basis for eliminating the ESBWR DCD site parameter requirement $K_0\gamma \geq 47$ lb/ft^3 from EF3 FSAR Table 2.0-201 and Section 2.5.4.5.4.2.	February 16, 2012 (Detroit Edison Letter NRC3-12-0003, ML120520154)
02.05.04-39	2	An explanation of why site Design Commitment Item 2 of engineering properties in EF3 COL Application Part 10: ITAAC, Section 2.4 and Table 2.4.2-1 are not applicable, as well as the basis for eliminating Item 2 of site-specify ITAAC corresponding to "backfill adjacent to Seismic Category I structures" from EF3 COL Application Part 10: ITAAC, Section 2.4 and Table 2.4.2-1.	February 16, 2012 (Detroit Edison Letter NRC3-12-0003, ML120520154)
03.07.01-3	1	Explain why it is appropriate to define the FIRS for this facility on the basis of a 1D column of concrete material if the lateral extension of this material is limited to its footprint.	March 23, 2012 (Detroit Edison Letter NRC3-12-0008, ML12086A091)

RAI Number	Part	Question Summary	Submittal Date
03.07.01-4	1	Therefore, explain the impact of the increased shear wave velocity on the computed FIRS for the FWSC, particularly at high frequency.	March 23, 2012 (Detroit Edison Letter NRC3-12-0008, ML12086A091)
03.07.01-4	2	Also explain how the data from EF3 FSAR Reference 2.5.2-288 (Hasek, 2002), which is based on lean concrete with shear wave velocities between 900 fps and 1400 fps, is applicable to the aforementioned Fermi 3 site conditions.	March 23, 2012 (Detroit Edison Letter NRC3-12-0008, ML12086A091)
03.07.01-5	1	Since the backfill material is limited in lateral extent, following a relatively complicated geometry in plan, explain why it is appropriate to define the PBSRS and FIRS for the RB/FB and CB (EF3 FSAR Section 3.7.1) on the basis of a 1D column of backfill material.	March 23, 2012 (Detroit Edison Letter NRC3-12-0008, ML12086A091)
03.07.01-6	1	Based on the above discussion, the staff needs additional technical basis for using two components of ground motion with correlation coefficient of approximately 0.30.	February 16, 2012 (Detroit Edison Letter NRC3-12-0003, ML120520154)
03.07.01-6	2	If Regulatory Position C.2.2(2) of RG 1.92 is used for determining the total site-specific seismic demand for the SSCs, the applicant is requested to provide a comparison with the seismic demand as determined from the use of Regulatory Position C.2.2(1), and demonstrate that the current site-specific seismic demand as specified in EF3 FSAR is not under predicted.	February 16, 2012 (Detroit Edison Letter NRC3-12-0003, ML120520154)
03.07.01-7	1	As such, the applicant is requested to provide further justification of the acceptability of the PGV/PGA values for the artificial time histories being higher than the selected controlling earthquake.	February 16, 2012 (Detroit Edison Letter NRC3-12-0003, ML120520154)
03.07.01-7	2	The applicant is also requested to provide comparison of the response spectra of the artificial time histories and the estimated target spectra (SSI FIRS) at 2% and 10% damping values for RB/FB and CB.	February 16, 2012 (Detroit Edison Letter NRC3-12-0003, ML120520154)

RAI Number	Part	Question Summary	Submittal Date
03.07.01-8	1	Therefore, the applicant is requested to provide in the FSAR comparison plots of the RB/FB and CB horizontal FIRS with the RG 1.60 horizontal spectrum anchored at 0.1 g, which demonstrate that the RB/FB and CB horizontal FIRS envelope the RG 1.60 spectrum at all frequencies of interest.	February 16, 2012 (Detroit Edison Letter NRC3-12-0003, ML120520154)
03.07.02-5	1	Since the backfill requirements are not being met for the Fermi 3 site, the applicant is requested to describe in the FSAR how the above ESBWR DCD commitments and ITAAC are implemented for the site-specific conditions of the Fermi 3 site, including a description of the site-specific analysis to be performed	February 16, 2012 (Detroit Edison Letter NRC3-12-0003, ML120520154)
03.07.02-5	2	The applicant is also requested to describe how the seismic input for the Seismic Category II structures (for the site specific analysis) will consider the site-specific scale factors, including the effect of structure-soil-structure interaction, to ensure that the seismic input specified in the DCD for these structures will still be bounding.	February 16, 2012 (Detroit Edison Letter NRC3-12-0003, ML120520154)
03.07.02-5	3	In addition, explain why EF3 FSAR Figures 2.5.4-201 through 2.5.4-204, as modified by the markups included with the response to RAI Letter 55 Question 02.05.04-38, only show the TB and RW, and not the SB and ADB, and why Table 2.5.4-224 lists the TB as "nonseismic" and not as Seismic Category II.	February 16, 2012 (Detroit Edison Letter NRC3-12-0003, ML120520154)
03.07.02-6	1	As such, the applicant is requested to provide further justification for ignoring embedment effects on SSI response. The justification should include the potential impact of this modeling approach on in-structure response spectra (over the entire frequency range of interest), lateral wall pressures, and other seismic loads.	June 15, 2012
03.07.02-7	1	The applicant is requested to provide the geometry and properties of the excavated volume modeled in both SASSI analyses.	March 1, 2012 (Detroit Edison Letter NRC3-12-0007, ML12065A194)
03.07.02-7	2	Therefore, the applicant is requested to provide an additional comparative study for the RB/FB along the lines of the study performed for the CB.	February 16, 2012 (Detroit Edison Letter NRC3-12-0003, ML120520154)

RAI Number	Part	Question Summary	Submittal Date
03.07.02-7	3	Details of the comparative studies discussed above should be included in the relevant sections of the EF3 FSAR.	February 16, 2012 (Detroit Edison Letter NRC3-12-0003, ML120520154)
03.07.02-8	1	Since these site conditions deviate significantly from cases CL-6 and FL-5, analyzed in the ESBWR DCD, the applicant is requested to explain how SSSI effects are evaluated between these structures.	June 15, 2012
03.07.02-8	2	What is the basis for neglecting the granular fill in the site-specific analyses in the context of SSSI, given that these structures are deeply embedded and in close proximity to each other?	June 15, 2012
03.07.02-8	3	What is the basis for including concrete fill between the RB/FB and CB gap?	June 15, 2012
03.07.02-8	4	Does the addition of the stiff concrete fill between the CB and the RB/FB introduce potential interaction between the two structures?	June 15, 2012
03.08.05-1	1	The applicant is requested to provide justification for using 2006 code edition of ACI 349.	February 16, 2012 (Detroit Edison Letter NRC3-12-0003, ML120520154)
03.08.05-2	1	(a) Provide the numerical values for each of the terms in the equation used to evaluate the factors of safety against sliding (see ESBWR DCD Section 3.8.5.5).	March 1, 2012 (Detroit Edison Letter NRC3-12-0007, ML12065A194)
03.08.05-2	2	Also provide a detailed explanation of how each value was obtained, including the assumed coefficient of friction at the various foundation-rock interfaces.	March 1, 2012 (Detroit Edison Letter NRC3-12-0007, ML12065A194)
03.08.05-2	3	(b) Explain if shear keys are provided as described in ESBWR DCD. The staff notes that EF3 FSAR Figures 2.5.4-201 through 2.5.4-204 do not show shear keys.	February 16, 2012 (Detroit Edison Letter NRC3-12-0003, ML120520154)

RAI Number	Part	Question Summary	Submittal Date
03.08.05-3	1	The applicant is requested to explain how the seismic load (in the E-W direction) imposed by the CB bearing against the concrete fill is transferred to the underlying rock.	March 1, 2012 (Detroit Edison Letter NRC3-12-0007, ML12065A194)
03.08.05-3	2	Is base friction sufficient to resist the entire load or will a certain fraction of this load be transferred to the adjacent RB/FB?	March 1, 2012 (Detroit Edison Letter NRC3-12-0007, ML12065A194)
03.08.05-3	3	Has this been considered in the design?	March 1, 2012 (Detroit Edison Letter NRC3-12-0007, ML12065A194)
03.08.05-3	4	The above questions are also appropriate to the potential transfer of seismic loads from the RB/FB to the CB through the concrete fill.	March 1, 2012 (Detroit Edison Letter NRC3-12-0007, ML12065A194)
03.08.05-4	1	(a) Comparison of seismic lateral earth pressures shown in EF3 FSAR Figures 2.5.4-230 and 4-231 with those obtained using the method described in ASCE 4-98 Section 3.5.3.2 and also with those given in ESBWR DCD Tables 3A.8.8-1 and 3A.8.8-2, and ESBWR DCD Sections 3G.1.5.2.1 and 3G.2.5.2 (Figures 3G.1-19, 3G.1-27, 3G.2-12, and 3G.2-15), which were used for the design of the walls.	February 16, 2012 (Detroit Edison Letter NRC3-12-0003, ML120520154)
03.08.05-4	2	(b) For the portions of below-grade walls that are embedded in rock, provide estimates of the seismic lateral pressures imposed by the surrounding rock, which are compatible with the results of the site-specific SSI analyses performed and with the assumptions of the sliding stability calculations discussed in EF3 FSAR Sections 3.7.2 and 3.8.5, as modified by the markups included with the response to RAI Letter 55 Question 02.05.04-38.	June 15, 2012
03.08.05-4	3	(c) Provide estimates of additional static and dynamic lateral pressures imposed from adjacent Seismic Category I and II structures. This should also include possible effects of structure-to-structure interaction through the surrounding backfill, concrete fill, or rock.	June 15, 2012

RAI Number	Part	Question Summary	Submittal Date
03.08.05-4	4	(d) Modify EF3 FSAR Figures 2.5.4-230 and 4-231 to incorporate the pressures discussed in items (b) and (c) above and compare with the lateral pressures given in ESBWR DCD Tables 3A.8.8-1 and 3A.8.8-2, and ESBWR DCD Sections 3G.1.5.2.1 and 3G..2.5.2, which were used for the design of the walls. If site-specific SSI analyses that consider the backfill become available, include the lateral pressures from the SSI analyses in the comparison.	June 15, 2012
03.08.05-5	1	Therefore, explain whether the fill concrete below the FSWC is reinforced or not. If it is not, explain how the shear resistance is developed. If it is reinforced, describe how the reinforcement is selected.	February 16, 2012 (Detroit Edison Letter NRC3-12-0003, ML120520154)

Attachment 2
NRC3-12-0019
(8 pages)

Table of Supplemental Issues Identified
During the April 23 through 27, 2012, Audit

Issue	Details	Disposition
SSI analysis (licensing basis analysis, i.e., no backfill)	Provide the structural model including damping used, which should be consistent with the relative stress level of the structural elements. If SSE damping is used, provide the technical basis for this.	Attachment 8 of this letter, SER-DTF-009, Section 5.1
SSI analysis (licensing basis analysis, i.e., no backfill)	Provide the modeling of floor diaphragms in the structural model, which is not shown in the calculations. This information was shown to the staff but needs to be documented.	Attachment 4 of this letter, Figures 03.07.02-6(3) and 03.07.02-6(6) Attachment 7 of this letter, SER-DTF-006, Figures 4.3-4 and 4.3-7 Attachment 8 of this letter, SER-DTF-009, Figure 4.3-3
SSI analysis (licensing basis analysis, i.e., no backfill)	Provide plots of Fourier amplitude/power and cumulative Fourier power spectra for the input in- column motions, in order to identify the relative power of the input between 25 and 50 Hz.	Attachment 4 of NRC3-12-0016, dated May 22, 2012 (ML12144A322)
SSI analysis (licensing basis analysis, i.e., no backfill)	Confirm all SSI analyses consider the seismic input in both plus and minus directions.	Attachment 7 of this letter, SER-DTF-006, Section 4.1 Attachment 8 of this letter, SER-DTF-009, Section 4.1

Issue	Details	Disposition
SSI analysis (licensing basis analysis, i.e., no backfill)	Provide plots of transfer functions identified as having spikes, with clear representation of computed values and interpolated values, in order to judge numerical accuracy.	Attachment 4 of this letter, Figures 03.07.02-6(15)a through 03.07.02-6(20)b Attachment 5 of this letter, Figures 03.07.02-8(24)a through 03.07.02-8(29)d Attachment 7 of this letter, SER-DTF-006, Figures 5.2-1a through 5.3-6b Attachment 8 of this letter, SER-DTF-009, Figures A-4a through A-4b and B-1a through B-3b
SSI analysis (licensing basis analysis, i.e., no backfill)	Clarify why toe bearing pressures reported in GEH Calculation 002 and 006 are the same if the inputs are different (Tables 7-3, 7-4, B-7, and B-8).	Attachment 7 of this letter, SER-DTF-006, Tables 7-3, 7-4, B-7, and B-8 Attachment 9 of this letter
SSI analysis (licensing basis analysis, i.e., no backfill)	Provide plots of wall pressures for RB and CB.	Attachment 7 of this letter, SER-DTF-006, Figures 5.4-1 and 5.4-2
SSI analysis (licensing basis analysis, i.e., no backfill)	Explain the applicability of DCD mesh sensitivity study (for the excavated soil) to the Fermi site-specific conditions, especially if certain analyses only consider frequencies up to 25 Hz. Staff noted brick elements having aspect ratio 1(vertical):4(horizontal); what is the frequency transmission characteristics for such elements?	Attachment 8 of this letter, SER-DTF-009, Section 4.3

Issue	Details	Disposition
Validation of QUAD4 analysis	Supplemental response to provide response spectra computed at the center node at top of the concrete fill, for various widths of the analysis model, which demonstrate that the chosen width of 600 ft adequately represents the lateral boundary conditions. Also provide a discussion on the envelope function used and its impact on the design margin.	Attachment 3 of NRC3-12-0016, dated May 22, 2012 (ML12144A322) Supplemental Response contained in Attachment 3 of this letter
Disturbance of the material outside the diaphragm wall	NRC to assess if there is a need to evaluate the disturbance of the material outside the diaphragm wall, and evaluate whether it could cause an increase in the PBSRS as well as its potential impact on the SSI analysis.	NRC determined no additional information is required
Variability/uncertainty in geotechnical data for Bass Island Group and Salina Group F	Supplemental response to explain variability of Bass Island Group data and the uncertainty in the data for Salina F shown in the calculations.	Attachment 4 of NRC3-12-0016, dated May 22, 2012 (ML12144A322)
Minimum horizontal input for SSI	Supplemental response to provide FSAR markup that indicates minimum horizontal input requirements are met by NUREG/CR-0098 spectral shape for rock sites. Markup reviewed during audit is OK.	Attachment 5 of NRC3-12-0016, dated May 22, 2012 (ML12144A322)
ITAAC Commitments for Seismic Category II Structures	Supplemental response that clearly explains the design intent (i.e., generic DCD Cat. II design to be performed for DCD profiles and DCD seismic input, to address DCD ITAAC commitments), and FSAR markup with indication that all Seismic Category II structures will be founded on bedrock or concrete fill, not on engineered granular backfill, similarly to Seismic Category I structures.	Attachment 6 of NRC3-12-0016, dated May 22, 2012 (ML12144A322)
Embedment effects on SSI response	DTE to respond to outstanding RAI. Any analysis based on the subtraction method requires independent validation using the direct method.	Attachment 4 of this letter

Issue	Details	Disposition
Direct vs. Subtraction method of SASSI2000	DTE indicated a direct method-vs.-subtraction method validation study will be provided using the CB 3D model with backfill included. The model may have frequency transmission characteristics adequate up to 25 Hz only.	Attachment 8 of this letter, SER-DTF-009
Direct vs. Subtraction method of SASSI2000	Staff indicated that this validation study needs to provide a comparison of (a) wall pressures on both backfill and bedrock/concrete fill portions, (b) ISRS, and (c) amplified FIRS in adjacent nodes in the soil (used to assess SSSI effects.	Attachment 8 of this letter, SER-DTF-009
Direct vs. Subtraction method of SASSI2000	Validation study should use updated soil profiles and time histories. Use of BE soil profile is adequate.	Attachment 8 of this letter, SER-DTF-009
Direct vs. Subtraction method of SASSI2000	In all cases, the effect of the backfill and the SSSI effects need to be differentiated in order to address RAIs 03.07.02-6, 03.07.02-8, and 03.08.05-4.	Attachment 8 of this letter, SER-DTF-009
Direct vs. Subtraction method of SASSI2000	Since only the CB is being used for validation, staff needs to review the computed transfer functions obtained using the direct and subtraction methods with the backfill, to assess potential impact on the RB analysis, which is not part of the validation study.	Attachment 8 of this letter, SER-DTF-009
Direct vs. Subtraction method of SASSI2000	Staff indicated an acceptable alternative to using the subtraction method would be to perform a 2D slice-type analysis in either the time or frequency domain.	2D analysis approach was not utilized
Direct vs. Subtraction method of SASSI2000	Staff will issue new RAI to specifically request the validation study for the SSI analysis using the subtraction method with backfill.	NRC determined that no new RAI would be issued

Issue	Details	Disposition
SSSI effects between RB/FB and CB, and between CB and FWSC	DTE to respond to outstanding RAI. Any analysis based on the subtraction method requires independent validation using the direct method. For the RB acting on the CB, staff indicated the kinematic approach proposed by GEH may not capture inertial effects on wall pressures.	Attachments 5 and 6 of this letter
ACI 349-01 vs. -06	Supplemental response to provide FSAR markup that indicates that ACI 349-01 will be used, consistent with ESBWR DCD.	Attachment 7 of NRC3-12-0016, dated May 22, 2012 (ML12144A322)
Sliding factor of safety for FWSC	Supplemental response to provide FSAR markup that clarifies that the stated factor of safety of 15 is actually an upper bound; to ensure the minimum factor of safety is at least 1.1, a minimum 10% design margin needs to be specified for the design of shear friction reinforcement.	Attachment 8 of NRC3-12-0016, dated May 22, 2012 (ML12144A322)
SSSI effects and pressures transferred to concrete fill between RB/FB and CB	RAI response reviewed by NRC and not accepted; RAI to be submitted under 03.08.05-4.	Attachment 6 of this letter
Information regarding lateral pressures (backfill and bedrock)	Part (a) was reviewed and there are no further issues; Part (b) was reviewed and not accepted; Parts (c) and (d) are dependent on the SSI and SSSI analyses which are outstanding.	Attachment 6 of this letter
Information regarding lateral pressures (backfill and bedrock)	DTE to provide response to RAI to address staff's concerns regarding lateral wall pressures on both backfill and bedrock/concrete fill portions; in particular, whether the design of embedded sidewalls is adequate to resist the large lateral pressures expected at the top of rock elevation for the licensing basis SSI analysis (i.e., no backfill).	Attachment 6 of this letter

Issue	Details	Disposition
Information regarding lateral pressures (backfill and bedrock)	The RAI response should include plots of wall pressures for RB and CB for the licensing basis SSI analysis (i.e., no backfill) and for the SSI analyses that include backfill and SSSI.	No backfill – Attachment 7 of this letter, SER-DTF-006, Figures 5.4-1 and 5.4-2 Backfill – Attachment 6 of this letter
Information regarding lateral pressures (backfill and bedrock)	Any analysis based on the subtraction method requires independent validation using the direct method.	Attachment 8 of this letter, SER-DTF-009
Concrete fill under FWSC and surrounding other Cat I and II structures	Describe specific measures that will be implemented to control thermal cracking. Markup reviewed during audit is OK.	Attachment 9 of NRC3-12-0016, dated May 22, 2012 (ML12144A322)
Concrete fill under FWSC and surrounding other Cat I and II structures	Provide past precedent where unreinforced concrete fill has been used under similar conditions of f'c (i.e., high cement content, low water/cement ratio).	Attachment 9 of NRC3-12-0016, dated May 22, 2012 (ML12144A322)
Concrete fill under FWSC and surrounding other Cat I and II structures	Provide specific criteria to be used during detailed design to determine whether thermal reinforcement needs to be provided.	Attachment 9 of NRC3-12-0016, dated May 22, 2012 (ML12144A322)
Concrete fill under FWSC and surrounding other Cat I and II structures	Provide clarification of which edition of ACI 207R is being referenced.	Attachment 9 of NRC3-12-0016, dated May 22, 2012 (ML12144A322)
Concrete fill under FWSC and surrounding other Cat I and II structures	Reference other applicable standards for mass concrete construction (e.g., ACI 207.1R, 207.4, 211.1).	Attachment 9 of NRC3-12-0016, dated May 22, 2012 (ML12144A322)

Issue	Details	Disposition
Concrete fill under FWSC and surrounding other Cat I and II structures	Provide explanation that voids under concrete fill are not a concern because of the chemical composition/geological characteristics of the dolomite bedrock and groundwater, and also because of actual conditions observed on the bedrock surface.	Attachment 9 of NRC3-12-0016, dated May 22, 2012 (ML12144A322)

Attachment 3
NRC3-12-0019
(4 pages)

Response to RAI Letter No. 70
(eRAI Tracking No. 6244)

RAI Question No. 03.07.01-3

NRC RAI 03.07.01-3

EF3 FSAR Section 2.5.4.5 and Figure 2.5.4-202, as modified by the markups included with the response to RAI Letter 55 Question 02.05.04-38, indicate that the lateral extension of concrete fill under the FWSC is limited to its footprint. Explain why it is appropriate to define the FIRS for this facility on the basis of a 1D column of concrete material if the lateral extension of this material is limited to its footprint.

Supplemental Response

The initial response to this RAI was provided in Detroit Edison letter NRC3-12-0008, dated March 23, 2012 (ML12086A091). A previous supplemental response was provided in Detroit Edison letter NRC3-12-0016, dated May 22, 2012 (ML12144A322), and supplied supplemental information regarding the following supplemental requests made by the staff at an audit conducted during the week of April 23, 2012.

> *Provide response spectra computed at the center node at the top of the fill concrete for various widths of the analysis model which demonstrate that the chosen width of 600 feet adequately represents the lateral boundary conditions. Also provide additional discussion on the envelope function used and the impact on the design margin.*

This additional supplemental response provides supplemental information concerning variations in the response spectra in the 7 to 9 Hz frequency range requested by the staff during an open-items call on May 31, 2012.

The spectra in Figure 11 of the May 22, 2012, supplemental response to this RAI (replicated in this response); displays non-systematic differences in the frequency range of 5 to 9 Hz. As described in the March 23, 2012, initial response to this RAI, the first peak in the 2D/1D response spectral ratios occurs in the 6 to 9 Hz frequency range and there are small variations in the frequency location of the peaks depending on the foundation width (66 or 171 feet) and time history used. That same initial response to this RAI describes that the final envelope of the 2D/1D response spectral ratio shown on Figure 9 (replicated in this response) was increased in the frequency range of 5.8 to 20 Hz to account for possible larger ratios for the 171 foot fill concrete width that were not reduced and broadened by the use of additional time histories and randomized soil properties. The final envelope of the 2D/1D response spectral ratio also ignored a dip in the frequency range from 4 to 6 Hz. The 5 to 20 Hz frequency range with increased 2D/1D response spectral ratios includes the non-systematic differences from 5 to 9 Hz and is anticipated to capture the observed range of spectral ratios. Additionally, as stated in FSAR Subsection 2.5.2.6.1, the surface response spectra for the ground motion response spectrum (GMRS) and Foundation Input Response Spectra (FIRS) have a dip in the spectra in the frequency range of 6 to 12 Hz. This dip was conservatively removed from both the GMRS and the FIRS and indicates that the final FIRS for the FWSC are conservative in most of the frequency range of 5 to 9 Hz where the non-systematic differences were observed in the final envelope 2D/1D response spectral ratios. The increase in the final envelope of 2D/1D response spectral ratios and the conservative removal of a dip in the FIRS for the FWSC indicate the 2D/1D response spectral ratios presented in the March 23, 2012, initial response are acceptable using the 600 foot wide mesh in QUAD4MU.

Proposed COLA Revision

None.

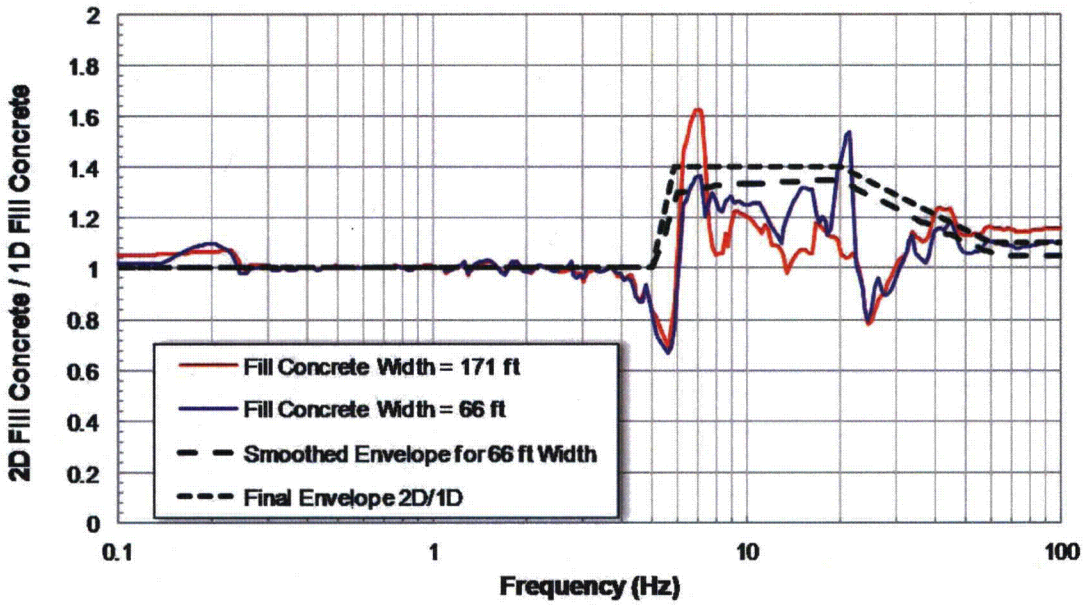

Figure 9 (From March 23, 2012, response): Final envelope 2D/1D response spectral ratios based on comparison of the smoothed envelope 2D/1D response spectral ratios for the 66 foot width FWSC with the results for the 66 and 171 foot FWSC widths computed using the H4DEL time history.

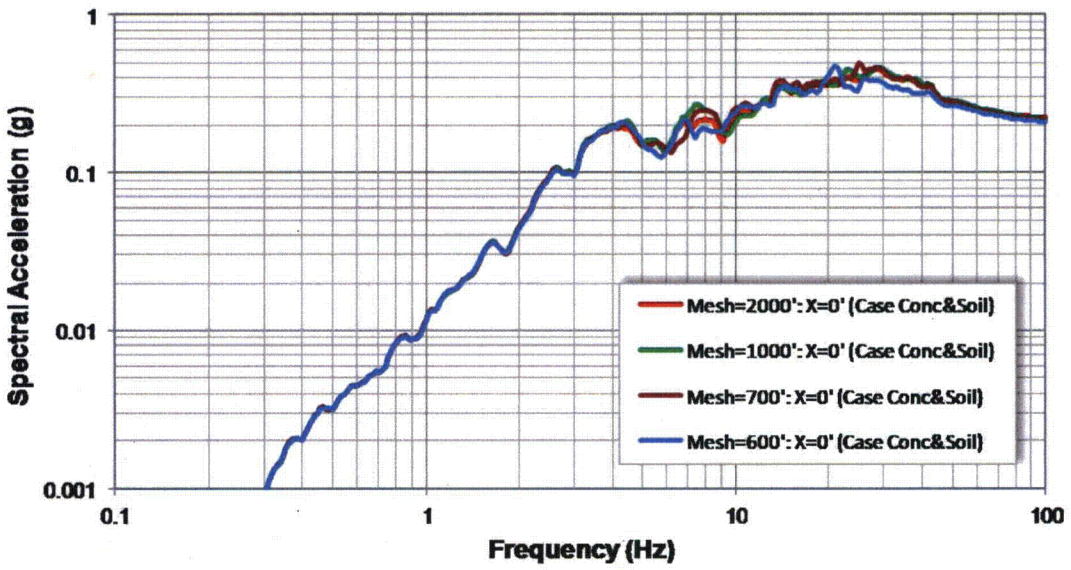

Figure 11 (From May 22, 2012, response): Response spectral acceleration (5 percent damping) for motions computed at the top center node of the fill concrete (66 foot width) for mesh widths of 600, 700, 1,000, and 2,000 feet.

Attachment 4
NRC3-12-0019
(84 pages)

Response to RAI Letter No. 70
(eRAI Tracking No. 6243)

RAI Question No. 03.07.02-6

NRC RAI 03.07.02-6

EF3 FSAR Sections 3.7.1, 3.7.2, and 3.8.5, as modified by the markups included with the response to RAI Letter 55 Question 02.05.04-38, indicate that engineered granular backfill above the Bass Islands Group rock is not included in the site-specific SSI analyses performed for the RB/FB and CB. The rationale given for exclusion of the backfill is that it is not credited for resistance of sliding and overturning forces, and thus serves no safety-related function. It is also implied that, because the site-specific SSI analyses "do not take credit for the benefits provided by the backfill surrounding the RB/FB and CB" (EF3 FSAR Section 3.7.2.4.1), the computed SSI responses (seismic loads, vertical accelerations, and in-structure response spectra) are appropriate for comparison to the reference ESBWR DCD design values.

However, EF3 FSAR Figures 2.5.4-201 through 2.5.4-204 show that the RB/FB and CB are deeply embedded structures with two-thirds or more of their depth in the granular fill (above rock and concrete). As such, the applicant is requested to provide further justification for ignoring embedment effects on SSI response. The justification should include the potential impact of this modeling approach on in-structure response spectra (over the entire frequency range of interest), lateral wall pressures, and other seismic loads.

Response

To justify ignoring engineered granular backfill embedment effects on the Fermi 3 Reactor Building/Fuel Building (RB/FB) and Control Building (CB) soil-structure interaction (SSI) response, additional SASSI2000 analyses for the RB/FB and CB with the backfill included in the model was performed using the Design Control Document (DCD) SASSI2000 model mesh size. The subtraction method of the SASSI2000 computer program was used for these analyses. The validity of using the subtraction method is confirmed in SER-DTE-009 by using the direct method of the SASSI2000 computer program with the same model.

The subsurface properties for the models for the RB/FB and CB SASSI2000 analyses are shown in Tables 03.07.02-6(1), 03.07.02-6(2) and 03.07.02-6(3) for the best estimate (BE), lower bound (LB) and upper bound (UB) subsurface profiles, respectively. Input motions are based on the markup of FSAR Section 3.7.1 submitted with the response to RAI 03.07.01-6.

The site-specific SSI analysis cases for the RB/FB and CB are summarized in Table 03.07.02-6(4).

The geometries of the excavated volumes for the RB/FB and CB SASSI2000 analyses are illustrated in Figures 03.07.02-6(1) through 03.07.02-6(6). The excavated volume is modeled from the top of the finished ground level grade (EL 4,500 mm) to the bottom of the basemat foundation. For the RB/FB, the bottom of the basemat foundation is EL -15,500 mm and for the CB, the bottom of the basemat foundation is EL -10,400 mm. The RB/FB stick model is connected to the basemat and side walls at floor EL -11,500 mm, -6,400 mm, -1,000 mm, and 4,500 mm by a set of rigid links shown in red on Figure 03.07.02-6(3). The CB stick model is connected to the basemat and side walls at floor EL -7,400 mm, -2,000 mm, and 4,500 mm by a set of rigid links shown in red on Figure 03.07.02-6(6). At the top of the basemat for the RB/FB and CB models at EL -11,500 mm and EL -7,400 mm, respectively, a rigid link is used to connect the stick models to the center of the each basemat.

The Fermi 3 floor response spectra for the Fermi 3 SSI accounting for embedment in the engineered granular backfill are shown in Figures 03.07.02-6(7) through 03.07.02-6(12). Also shown on these figures is the corresponding DCD floor response spectra. Comparison with the DCD response spectra demonstrates that the Fermi 3 floor response spectra for the RB/FB and CB are enveloped by the DCD floor response spectra for the BE, LB, and UB subsurface profiles.

The maximum shear and moment distributions along the RB/FB walls, RCCV, vent wall/pedestal, RSW, and RPV for the Fermi 3 SSI accounting for embedment in the engineered granular backfill are shown in Table 03.07.02-6(5) and along the CB walls are shown in Table 03.07.02-6(6) for all cases. The results are compared with the design envelopes specified in DCD Section 3A.9. The Fermi 3 maximum shear and moment distributions are enveloped by the DCD maximum shear and moment distributions for all the site conditions.

The maximum accelerations of the RB/FB and CB for the Fermi 3 SSI are shown in Tables 03.07.02-6(7) and 03.07.02-6(8) for all cases. They are all enveloped by the DCD maximum vertical acceleration except for the CB oscillators 9003 and 9103. However, the slab design accelerations are calculated by averaging the vertical accelerations of oscillators which are attached to the node representing the floor, as shown in Table 03.07.02-6(9). According to this procedure, it is found that the design accelerations of the slabs including the oscillators 9003 and 9103 are also enveloped by the DCD slab design accelerations.

Figures 03.07.02-6(13) and 03.07.02-6(14) show lateral soil pressures for the RB/FB and CB, respectively. Also shown on Figures 03.07.02-6(13) and 03.07.02-6(14) are the lateral soil pressures computed using the equivalent static pressure analysis in ASCE 4-98. The lateral soil pressure loads for the exterior walls are calculated by averaging lateral soil pressure along each wall height which is a floor height excluding the thickness of slabs. The calculated lateral soil pressures from the Fermi 3 SSI are summarized in Tables 03.07.02-6(10) and 03.07.02-6(11), respectively for the RB/FB and CB, comparing between the SASSI2000 soil pressures and the DCD design soil pressures.

For the RB/FB, the results in Table 03.07.02-6(10) show that the Fermi 3 SSI lateral soil pressures accounting for embedment in the engineered granular backfill are less than the DCD design soil pressure, except for the Floor Levels between EL -7,400 mm and EL- 11,500 mm. However, the Fermi 3 SSI lateral soil pressures between Floor Levels EL -7,400 mm and EL-11,500 mm are less than the DCD wall capacity passive pressures along the embedded exterior walls, which are considered for the stability evaluation. The DCD wall capacity passive pressure is a part of the passive soil pressure accounted as lateral resistance pressure to maintain the sliding factor of safety to be 1.1 minimum. As described in Section 3G.1.5.5 of the ESBWR DCD, the stress check has been performed to confirm that the stresses of the exterior walls against the DCD wall capacity passive pressure are within the allowable stress.

For the CB, the results in Table 03.07.02-6(11) show that the Fermi 3 SSI lateral soil pressures accounting for embedment in the engineered granular backfill are less than the all the DCD design lateral soil pressures.

For reference, Figures 03.07.02-6(15) through 03.07.02-6(20) show the transfer function values computed at each frequency for the Fermi 3 SSI analyses and the continuous transfer functions obtained by interpolation of the computed values from the Fermi 3 SSI analyses.

Figures 03.07.02-6(15) through 03.07.02-6(20) show that there are some spikes in the transfer functions; however, it can be found from the Figures that the spikes are generated from the interpolate process of SASSI2000 computer program. They are very narrow and not real transfer functions. Their effect does not appear in the FRS in Figures 03.07.02-6(7) through 03.07.02-6(12), which are calculated at intervals wider than the width of the spikes.

Proposed COLA Revision

None.

Table 03.07.02-6(1) Site-Specific Strain Compatible Dynamic Subsurface Properties – Best Estimate (BE) Soil Profile

Layer	Thickness (ft)	Unit Weight (pcf)	Shear Wave Velocity (ft/sec)	Damping Ratio (%)	Compression Wave Velocity (ft/sec)	Elevation at Top of Layer (ft)
1	2.9	132.5	557	2.73	1028	589.0
2	2.9	132.5	588	4.19	1148	586.1
3	4.2	132.5	622	5.09	1291	583.2
4	3.2	132.5	663	5.49	1422	579.0
5	2.6	132.5	680	5.87	5000	575.8
6	4.3	132.5	702	6.08	5000	573.2
7	5	132.5	750	4.39	5000	568.9
8	4.9	132.5	772	4.54	5000	563.9
9	7	132.5	795	4.56	5000	559.0
10	9.9	150	6689	0.95	13202	552.0
11	2	150	6592	0.95	13202	542.1
12	8	150	6592	0.95	13202	540.1
13	8	150	6745	0.95	13202	532.1
14	2	150	6745	0.95	13202	524.1
15	10.2	150	6825	0.95	13202	522.1
16	11.1	150	6790	0.95	13202	511.9
17	11.9	150	6853	0.95	13202	500.8
18	11.7	150	6609	0.95	13202	488.9
19	15	150	4752	1.37	9835	477.2
20	20	150	3309	1.91	7889	462.2
21	19.9	150	3252	1.91	7889	442.2
22	19.9	150	3235	1.91	7889	422.3
23	21.2	150	3218	1.91	7889	402.4
24	21.1	150	4072	1.91	9537	381.2
25	21.1	150	4132	1.91	9537	360.1
26	9.8	150	5650	0.73	10477	339.0
27	19.7	150	9523	0.73	17679	329.2
28	21	150	9439	0.73	17679	309.5
29	20.5	150	9525	0.73	17679	288.5
30	22.1	150	9491	0.73	17679	268.0
31	45	160	8943	0.73	16282	245.9
32	44.6	160	9049	0.73	16282	200.9
33	Half Space	169	9494	0.1	17100	

Notes: 1. The top of in-situ bedrock is at EL-6.77m (552.0 ft, top of layer #10)
2. The bottom of CB basemat is at EL -10.4m (540.1 ft, top of layer #12)
3. The bottom of RB/FB basemat is at EL -15.5m (523.4 ft, sublayer was generated within layer #14)
4. The properties of layers #1 through #33 are based on the markup of FSAR Section 3.7.1 submitted with the response to RAI 03.07.01-6.

Table 03.07.02-6(2) Site-Specific Strain Compatible Dynamic Subsurface Properties – Lower Bound (LB) Soil Profile

Layer	Thickness (ft)	Unit Weight (pcf)	Shear Wave Velocity (ft/sec)	Damping Ratio (%)	Compression Wave Velocity (ft/sec)	Elevation at Top of Layer (ft)
1	2.9	119	408	4.07	781	589.0
2	2.9	119	426	6.55	937	586.1
3	4.2	119	432	7.84	1054	583.2
4	3.2	119	485	8.23	1161	579.0
5	2.6	119	501	8.5	5000	575.8
6	4.3	119	513	8.65	5000	573.2
7	5	119	574	6.45	5000	568.9
8	4.9	119	610	6.59	5000	563.9
9	7	119	608	6.9	5000	559.0
10	9.9	150	5666	1.51	10779	552.0
11	2	150	5780	1.51	10779	542.1
12	8	150	5780	1.51	10779	540.1
13	8	150	5761	1.51	10779	532.1
14	2	150	5761	1.51	10779	524.1
15	10.2	150	5766	1.51	10779	522.1
16	11.1	150	5659	1.51	10779	511.9
17	11.9	150	5877	1.51	10779	500.8
18	11.7	150	5609	1.51	10779	488.9
19	15	150	4003	2.18	8030	477.2
20	20	150	2616	2.88	6441	462.2
21	19.9	150	2529	2.88	6441	442.2
22	19.9	150	2611	2.88	6441	422.3
23	21.2	150	2478	2.88	6441	402.4
24	21.1	150	3111	2.88	7787	381.2
25	21.1	150	3189	2.88	7787	360.1
26	9.8	150	4998	1.12	8554	339.0
27	19.7	150	8501	1.12	14435	329.2
28	21	150	8628	1.12	14435	309.5
29	20.5	150	8542	1.12	14435	288.5
30	22.1	150	8516	1.12	14435	268.0
31	45	160	8156	1.12	13294	245.9
32	44.6	160	8202	1.12	13294	200.9
33	Half Space	169	8490	0.1	13962	

Notes: 1. The top of in-situ bedrock is at EL-6.77m (552.0 ft, top of layer #10)
2. The bottom of CB basemat is at EL -10.4m (540.1 ft, top of layer #12)
3. The bottom of RB/FB basemat is at EL -15.5m (523.4 ft, sublayer was generated within layer #14)
4. The properties of layers #1 through #33 are based on the markup of FSAR Section 3.7.1 submitted with the response to RAI 03.07.01-6.

Table 03.07.02-6(3) Site-Specific Strain Compatible Dynamic Subsurface Properties – Upper Bound (UB) Soil Profile

Layer	Thickness (ft)	Unit Weight (pcf)	Shear Wave Velocity (ft/sec)	Damping Ratio (%)	Compression Wave Velocity (ft/sec)	Elevation at Top of Layer (ft)
1	2.9	146	734	1.79	1259	589.0
2	2.9	146	751	2.84	1406	586.1
3	4.2	146	816	3.39	1581	583.2
4	3.2	146	891	3.48	1742	579.0
5	2.6	146	939	3.61	5000	575.8
6	4.3	146	930	3.85	5000	573.2
7	5	146	1021	2.81	5000	568.9
8	4.9	146	1032	2.86	5000	563.9
9	7	146	1041	2.97	5000	559.0
10	9.9	150	8063	0.48	16169	552.0
11	2	150	7967	0.48	16169	542.1
12	8	150	7967	0.48	16169	540.1
13	8	150	8042	0.48	16169	532.1
14	2	150	8042	0.48	16169	524.1
15	10.2	150	8130	0.48	16169	522.1
16	11.1	150	7924	0.48	16169	511.9
17	11.9	150	7928	0.48	16169	500.8
18	11.7	150	7754	0.48	16169	488.9
19	15	150	5439	0.68	12046	477.2
20	20	150	4221	0.95	9662	462.2
21	19.9	150	4042	0.95	9662	442.2
22	19.9	150	4041	0.95	9662	422.3
23	21.2	150	4033	0.95	9662	402.4
24	21.1	150	4898	0.95	11681	381.2
25	21.1	150	4989	0.95	11681	360.1
26	9.8	150	6264	0.36	12831	339.0
27	19.7	150	10472	0.36	21653	329.2
28	21	150	10596	0.36	21653	309.5
29	20.5	150	10526	0.36	21653	288.5
30	22.1	150	10456	0.36	21653	268.0
31	45	160	10247	0.36	19941	245.9
32	44.6	160	10276	0.36	19941	200.9
33	Half Space	169	10476	0.1	20943	

Notes: 1. The top of in-situ bedrock is at EL-6.77m (552.0 ft, top of layer #10)
2. The bottom of CB basemat is at EL -10.4m (540.1 ft, top of layer #12)
3. The bottom of RB/FB basemat is at EL -15.5m (523.4 ft, sublayer was generated within layer #14)
4. The properties of layers #1 through #33 are based on the markup of FSAR Section 3.7.1 submitted with the response to RAI 03.07.01-6.

Table 03.07.02-6(4) RB/FB & CB SSI Analysis Cases

Building	Case	ID No.	Model * (DCD)	Input Motion	Site Condition		
					BE	LB	UB
RB/FB	RFB	RFB-1	Base	RB/FB FIRS	✓	--	--
		RFB-2			--	✓	--
		RFB-3			--	--	✓
CB	CFB1	CFB1-1	Base	CB FIRS	✓	--	--
		CFB1-2			--	✓	--
		CFB1-3			--	--	✓

Note *: As shown in DCD Table 3A.6-1, there are some models with minor modifications to evaluate the modeling effects. For this Fermi 3 SSI analysis, the most basic model, "Base" is applied.

Table 03.07.02-6(5)a Ratio with DCD Enveloping Seismic Loads: RB/FB Stick - Case RBF

(a) Enveloping Seismic Loads

Elev. (m)	Elem No.	Node No.	Shear		Moment		Torsion
			X-Dir. (MN)	Y-Dir. (MN)	X-Dir. (MN-m)	Y-Dir. (MN-m)	(MN-m)
52.40*	1110	110			835.8	961.3	
		109	61.3	71.2	1809.8	2057.2	512.5
34.00	1109	109			2466.8	2803.9	
		108	73.0	64.6	2667.1	3191.1	892.2
27.00	1108	108			2855.7	3691.2	
		107	176.7	166.1	3437.3	4161.1	1472.4
22.50	1107	107			3824.2	4481.8	
		106	191.1	188.8	4622.0	5045.0	2589.8
17.50	1106	106			5092.7	5267.8	
		105	202.1	184.8	5711.4	5815.4	2272.3
13.57	1105	105			5951.0	6042.6	
		104	215.4	194.7	6650.7	6616.6	2387.5
9.06	1104	104			6785.2	6831.1	
		103	228.3	204.3	7510.6	7411.6	2606.9
4.65	1103	103			5001.3	4174.4	
		102	270.3	202.7	6260.1	4584.4	2864.6
-1.00	1102	102			6239.3	4767.2	
		101	302.4	301.8	7615.3	5610.9	3090.9
-6.40	1101	101			4625.1	3885.8	
-11.50		2	149.9	169.4	5148.1	4017.5	2029.6

(b) Ratio with DCD ((a)/DCD Loads)

Elev. (m)	Elem No.	Node No.	Shear		Moment		Torsion
			X-Dir.	Y-Dir.	X-Dir.	Y-Dir.	
52.40*	1110	110			51%	53%	
		109	40%	45%	42%	46%	37%
34.00	1109	109			44%	51%	
		108	38%	42%	41%	51%	37%
27.00	1108	108			37%	52%	
		107	42%	41%	38%	48%	44%
22.50	1107	107			39%	49%	
		106	40%	41%	40%	45%	43%
17.50	1106	106			41%	44%	
		105	38%	33%	41%	42%	45%
13.57	1105	105			42%	42%	
		104	38%	32%	40%	40%	46%
9.06	1104	104			40%	40%	
		103	37%	31%	39%	38%	44%
4.65	1103	103			26%	21%	
		102	32%	23%	27%	19%	25%
-1.00	1102	102			26%	19%	
		101	35%	32%	28%	19%	27%
-6.40	1101	101			16%	13%	
-11.50		2	16%	16%	16%	11%	17%

Note: Total torsional moments are obtained by the absolute sum of the accidental torsional moments and the values of the geometric torsional moments shown. The accidental torsional moment is the product of the horizontal force component and an eccentricity of 5% of the larger horizontal dimension at various elevations.

* : The difference between the modeled elevation 52.4 m and the actual elevation 52.7 m at the RB roof is negligibly small.

Table 03.07.02-6(5)b Ratio with DCD Enveloping Seismic Loads: RCCV Stick - Case RBF

(a) Enveloping Seismic Loads

Elev. (m)	Elem No.	Node No.	Shear		Moment		Torsion (MN-m)
			X-Dir. (MN)	Y-Dir. (MN)	X-Dir. (MN-m)	Y-Dir. (MN-m)	
34.00	1209	209			71.0	202.1	
		208	59.4	76.0	432.5	710.5	13.4
27.00	1208	208			723.3	1234.5	
		206	71.4	86.3	1170.7	1805.2	810.1
17.50	1206	206			1291.5	2042.6	
		205	93.5	93.1	1545.5	2274.2	899.6
13.57	1205	205			1600.0	2454.7	
		204	103.5	98.0	1937.5	2682.6	1000.0
9.06	1204	204			2028.1	2902.3	
		203	114.8	106.3	2410.7	3159.1	1145.7
4.65	1203	203			2498.9	3334.8	
		202	80.8	63.6	2695.1	3598.3	771.9
-1.00	1202	202			2749.4	3597.0	
		201	111.5	95.3	3280.1	3848.5	783.8
-6.40	1201	201			3421.7	3865.2	
-11.50		2	39.9	44.2	3461.7	3931.6	342.8

(b) Ratio with DCD ((a)/DCD Loads)

Elev. (m)	Elem No.	Node No.	Shear		Moment		Torsion
			X-Dir.	Y-Dir.	X-Dir.	Y-Dir.	
34.00	1209	209			36%	35%	
		208	43%	42%	41%	48%	37%
27.00	1208	208			42%	49%	
		206	43%	35%	40%	41%	45%
17.50	1206	206			39%	43%	
		205	41%	32%	37%	39%	45%
13.57	1205	205			37%	41%	
		204	39%	30%	36%	37%	46%
9.06	1204	204			36%	39%	
		203	38%	29%	36%	35%	44%
4.65	1203	203			36%	36%	
		202	36%	22%	34%	34%	27%
-1.00	1202	202			34%	33%	
		201	41%	29%	35%	31%	27%
-6.40	1201	201			36%	31%	
-11.50		2	15%	15%	32%	28%	17%

Note: Total torsional moments are obtained by the absolute sum of the accidental torsional moments and the values of the geometric torsional moments shown. The accidental torsional moment is the product of the horizontal force component and an eccentricity of 5% of the larger horizontal dimension at various elevations.

Table 03.07.02-6(5)c Ratio with DCD Enveloping Seismic Loads: Vent Wall/Pedestal Stick - Case RBF

(a) Enveloping Seismic Loads

Elev. (m)	Elem No.	Node No.	Shear		Moment		Torsion (MN-m)
			X-Dir. (MN)	Y-Dir. (MN)	X-Dir. (MN-m)	Y-Dir. (MN-m)	
17.50	701	701			21.2	17.5	
		702	7.2	7.9	26.9	30.9	13.6
14.50	702	702			27.7	33.4	
		703	7.3	7.5	38.5	54.0	14.4
11.50	703	703			39.6	56.0	
		704	7.7	9.1	55.3	73.7	15.4
8.50	704	704			55.1	74.4	
		705	8.2	9.8	62.7	80.3	16.0
7.4625	705	705			75.0	77.1	
		706,303	5.6	5.0	85.6	85.9	8.2
4.65	1303	303			212.2	177.7	
		377	12.0	13.4	210.8	188.3	38.1
2.4165	1377	377			258.9	231.6	
		302	17.3	19.6	253.8	255.1	46.3
-1.00	1302	302			238.3	238.9	
		376	27.5	27.5	258.9	249.8	39.2
-2.75	1376	376			259.0	249.8	
		301	28.0	27.6	335.3	322.8	39.2
-6.40	1301	301			308.3	314.3	
-11.50		2	16.5	16.7	369.7	380.5	20.7

(b) Ratio with DCD ((a)/DCD Loads)

Elev. (m)	Elem No.	Node No.	Shear		Moment		Torsion
			X-Dir.	Y-Dir.	X-Dir.	Y-Dir.	
17.50	701	701			27%	21%	
		702	21%	21%	24%	23%	12%
14.50	702	702			23%	23%	
		703	20%	19%	17%	21%	12%
11.50	703	703			17%	21%	
		704	21%	22%	16%	19%	13%
8.50	704	704			16%	19%	
		705	22%	22%	17%	18%	13%
7.4625	705	705			21%	18%	
		706,303	14%	12%	19%	16%	8%
4.65	1303	303			37%	29%	
		377	36%	30%	35%	28%	27%
2.4165	1377	377			35%	28%	
		302	36%	30%	33%	28%	27%
-1.00	1302	302			28%	25%	
		376	42%	34%	28%	24%	27%
-2.75	1376	376			28%	24%	
		301	42%	34%	30%	24%	27%
-6.40	1301	301			27%	23%	
-11.50		2	16%	14%	22%	19%	18%

Note: Total torsional moments are obtained by the absolute sum of the accidental torsional moments and the values of the geometric torsional moments shown. The accidental torsional moment is the product of the horizontal force component and an eccentricity of 5% of the larger horizontal dimension at various elevations.

Table 03.07.02-6(5)d Ratio with DCD Enveloping Seismic Loads: RSW Stick - Case RBF

(a) Enveloping Seismic Loads

Elev. (m)	Elem No.	Node No.	Shear		Moment		Torsion (MN-m)
			X-Dir. (MN)	Y-Dir. (MN)	X-Dir. (MN-m)	Y-Dir. (MN-m)	
24.18	707	707			1.00	0.72	
			1.04	0.75	5.10	3.67	0.12
20.20	708	708			8.30	6.11	
			5.03	4.49	26.44	24.91	0.42
15.775	709	709			28.69	26.13	
			5.84	5.09	52.12	48.28	0.56
11.35	710	710			52.43	48.90	
			6.62	5.79	77.90	69.79	0.63
7.4625	711	711			73.48	75.65	
			14.46	13.00	98.39	98.27	8.64
4.65	712	712			47.03	37.51	
			5.18	5.85	46.57	43.22	8.13
2.4165	713	713			1.31	1.14	
			0.44	0.49	1.11	0.96	0.06
1.96	714	714			0.98	0.86	
-0.80		715	0.29	0.30	0.20	0.16	0.04

(b) Ratio with DCD ((a)/DCD Loads)

Elev. (m)	Elem No.	Node No.	Shear		Moment		Torsion
			X-Dir.	Y-Dir.	X-Dir.	Y-Dir.	
24.18	707	707			48%	43%	
			34%	27%	39%	30%	31%
20.20	708	708			45%	36%	
			35%	37%	33%	36%	30%
15.775	709	709			35%	37%	
			34%	35%	33%	36%	30%
11.35	710	710			33%	36%	
			33%	35%	33%	35%	27%
7.4625	711	711			37%	41%	
			35%	36%	34%	39%	37%
4.65	712	712			38%	28%	
			36%	30%	35%	29%	27%
2.4165	713	713			36%	35%	
			29%	39%	38%	36%	26%
1.96	714	714			36%	36%	
-0.80		715	33%	40%	37%	31%	27%

Note: Total torsional moments are obtained by the absolute sum of the accidental torsional moments and the values of the geometric torsional moments shown. The accidental torsional moment is the product of the horizontal force component and an eccentricity of 5% of the larger horizontal dimension at various elevations.

Table 03.07.02-6(5)e Ratio with DCD Enveloping Seismic Loads: RPV Stick - Case RBF

(a) Enveloping Seismic Loads

Elev. (m)	Elem No.	Node No.	Shear		Moment	
			X-dir. (MN)	Y-dir. (MN)	X-dir. (MN·m)	Y-dir. (MN·m)
27.64	801	801			0.0	0.0
26.792		802	0.2	0.2	0.2	0.2
26.792	802	802			0.2	0.2
25.944		803	0.7	0.5	0.8	0.6
25.944	803	803			0.8	0.6
25.03		804	1.3	1.0	2.0	1.6
25.03	804	804			2.0	1.6
24.3188		805	1.8	1.6	3.2	2.7
24.3188	805	805			3.2	2.7
22.276		806	2.5	2.1	8.2	7.0
22.276	806	806			8.2	7.0
21.8247		807	3.3	2.8	9.7	8.2
21.8247	807	807			9.7	8.2
20.2		808	3.6	3.0	15.6	13.1
20.2	808	808			15.6	13.1
19.5278		809	1.1	1.2	16.3	13.7
19.5278	809	809			16.3	13.7
17.2677		810	1.8	1.7	20.5	17.4
17.2677	810	810			20.5	17.4
16.365		811	2.3	2.1	22.3	19.0

(b) Ratio with DCD ((a)/DCD Loads)

Elev. (m)	Elem No.	Node No.	Shear		Moment	
			X-dir.	Y-dir.	X-dir.	Y-dir.
27.64	801	801				
26.792		802	40%	34%	40%	34%
26.792	802	802			40%	34%
25.944		803	40%	34%	40%	34%
25.944	803	803			40%	34%
25.03		804	41%	34%	41%	34%
25.03	804	804			41%	34%
24.3188		805	40%	38%	40%	35%
24.3188	805	805			40%	35%
22.276		806	40%	36%	40%	36%
22.276	806	806			40%	36%
21.8247		807	41%	35%	40%	35%
21.8247	807	807			40%	35%
20.2		808	41%	35%	40%	35%
20.2	808	808			40%	35%
19.5278		809	31%	41%	40%	36%
19.5278	809	809			40%	36%
17.2677		810	35%	42%	40%	37%
17.2677	810	810			40%	37%
16.365		811	38%	40%	39%	38%

Table 03.07.02-6(5)e Ratio with DCD Enveloping Seismic Loads: RPV Stick - Case RBF (Continued)

(a) Enveloping Seismic Loads

Elev. (m)	Elem No.	Node No.	Shear		Moment	
			X-dir. (MN)	Y-dir. (MN)	X-dir. (MN·m)	Y-dir. (MN·m)
16.365	811	811			22.3	19.0
14.51		812	4.3	3.4	28.0	24.3
14.51	812	812			28.0	24.3
12.491		813	3.7	3.2	35.1	30.4
12.491	813	813			35.1	30.4
10.472		814	3.6	2.7	41.0	35.4
10.472	814	814			41.0	35.4
8.453		815	4.0	3.0	47.6	39.4
8.453	815	815			36.3	24.0
7.8071		816	6.4	3.8	32.2	21.2
7.8071	816	816			32.2	21.2
7.111		817	6.3	3.8	27.1	19.0
7.111	817	817			27.1	19.0
6.401		818	5.9	3.8	23.0	16.7
6.401	818	818			23.0	16.7
5.691		819	5.8	3.4	20.6	14.5
5.691	819	819			20.6	14.5
4.981		820	5.6	3.3	16.6	12.5
4.981	820	820			16.6	12.5
4.2713		821	5.2	3.2	14.1	10.6

(b) Ratio with DCD ((a)/DCD Loads)

Elev. (m)	Elem No.	Node No.	Shear		Moment	
			X-dir.	Y-dir.	X-dir.	Y-dir.
16.365	811	811			39%	38%
14.51		812	48%	43%	41%	39%
14.51	812	812			41%	39%
12.491		813	39%	40%	42%	39%
12.491	813	813			42%	39%
10.472		814	36%	34%	39%	39%
10.472	814	814			39%	39%
8.453		815	40%	34%	38%	37%
8.453	815	815			50%	39%
7.8071		816	50%	33%	50%	39%
7.8071	816	816			50%	39%
7.111		817	50%	34%	49%	40%
7.111	817	817			49%	40%
6.401		818	48%	35%	49%	41%
6.401	818	818			49%	41%
5.691		819	49%	31%	50%	43%
5.691	819	819			50%	43%
4.981		820	49%	31%	45%	45%
4.981	820	820			45%	45%
4.2713		821	49%	32%	43%	48%

Table 03.07.02-6(5)e Ratio with DCD Enveloping Seismic Loads: RPV Stick - Case RBF (Continued)

(a) Enveloping Seismic Loads

Elev. (m)	Elem No.	Node No.	Shear		Moment	
			X-dir. (MN)	Y-dir. (MN)	X-dir. (MN·m)	Y-dir. (MN·m)
4.2713	821	821			14.1	10.6
3.7593		822	5.2	3.1	12.9	9.3
3.7593	822	822			12.9	9.3
3.215		823	5.1	3.0	12.2	9.5
3.215	823	823			12.2	9.5
2.365		824	4.9	2.9	12.0	10.3
2.365	824	824			4.5	2.8
1.785		825	2.6	1.9	2.6	1.7
1.785	825	825			2.6	1.7
1.2		826	2.6	1.7	1.0	0.7
1.2	826	826			1.0	0.7
0.7657		827	2.3	1.5	0.2	0.2
0.7657	827	827			0.2	0.2
-0.1315		828	1.6	1.1	1.4	1.1

(b) Ratio with DCD ((a)/DCD Loads)

Elev. (m)	Elem No.	Node No.	Shear		Moment	
			X-dir.	Y-dir.	X-dir.	Y-dir.
4.2713	821	821			43%	48%
3.7593		822	51%	32%	43%	44%
3.7593	822	822			43%	44%
3.215		823	53%	32%	44%	47%
3.215	823	823			44%	47%
2.365		824	54%	32%	49%	49%
2.365	824	824			53%	44%
1.785		825	46%	44%	51%	44%
1.785	825	825			51%	44%
1.2		826	51%	45%	48%	39%
1.2	826	826			48%	39%
0.7657		827	51%	47%	36%	31%
0.7657	827	827			34%	31%
-0.1315		828	51%	49%	48%	50%

Table 03.07.02-6(5)e Ratio with DCD Enveloping Seismic Loads: RPV Stick - Case RBF (Continued)

(a) Enveloping Seismic Loads

Elev. (m)	Elem No.	Node No.	Shear		Moment	
			X-dir. (MN)	Y-dir. (MN)	X-dir. (MN·m)	Y-dir. (MN·m)
21.8247	828	829			0.0	0.0
20.2		830	0.1	0.1	0.2	0.2
20.2	829	830			0.2	0.2
19.5278		831	0.3	0.3	0.4	0.7
19.5278	830	831			0.4	0.7
17.2677		832	0.4	0.4	1.2	1.3
17.2677	831	832			1.2	1.3
16.365		833	0.4	0.5	1.6	1.8
16.365	832	833			1.6	1.8
14.51		834	2.4	1.6	4.8	4.6
14.51	833	834			4.8	4.6
12.491		835	1.5	0.7	7.8	5.6
12.491	834	835			7.8	5.6
10.472		836	0.6	0.5	8.2	4.5
10.472	835	836			8.2	4.5
8.453		837	1.2	0.9	6.2	3.4
8.453	836	837			6.2	3.4
7.8071		838	1.7	1.1	5.2	2.7
7.8071	837	838			5.2	2.7
7.111		839	2.0	1.6	4.0	2.6

(b) Ratio with DCD ((a)/DCD Loads)

Elev. (m)	Elem No.	Node No.	Shear		Moment	
			X-dir.	Y-dir.	X-dir.	Y-dir.
21.8247	828	829				
20.2		830	23%	22%	23%	22%
20.2	829	830			23%	22%
19.5278		831	30%	29%	34%	45%
19.5278	830	831			34%	45%
17.2677		832	35%	29%	30%	30%
17.2677	831	832			30%	30%
16.365		833	33%	34%	30%	31%
16.365	832	833			30%	31%
14.51		834	47%	32%	51%	47%
14.51	833	834			51%	47%
12.491		835	50%	23%	52%	38%
12.491	834	835			52%	38%
10.472		836	38%	26%	50%	27%
10.472	835	836			50%	27%
8.453		837	45%	40%	42%	23%
8.453	836	837			42%	23%
7.8071		838	47%	35%	38%	19%
7.8071	837	838			38%	19%
7.111		839	50%	38%	35%	20%

Table 03.07.02-6(5)e Ratio with DCD Enveloping Seismic Loads: RPV Stick - Case RBF (Continued)

(a) Enveloping Seismic Loads

Elev. (m)	Elem No.	Node No.	Shear		Moment	
			X-dir. (MN)	Y-dir. (MN)	X-dir. (MN·m)	Y-dir. (MN·m)
7.111	838	839			4.0	2.6
6.401		840	2.4	1.8	3.6	2.7
6.401	839	840			3.6	2.7
5.691		841	2.8	2.0	2.8	2.5
5.691	840	841			2.8	2.5
4.981		842	3.2	2.2	3.7	2.8
4.981	841	842			3.7	2.8
4.2713		843	3.6	2.3	5.2	3.9
4.2713	842	843			5.2	3.9
3.7593		844	4.1	2.4	6.8	5.0
3.7593	843	844			6.8	5.0
3.215		845	3.2	1.9	8.1	6.1
3.215	844	845			8.1	6.1
2.365		846	3.3	2.0	9.8	8.2

(b) Ratio with DCD ((a)/DCD Loads)

Elev. (m)	Elem No.	Node No.	Shear		Moment	
			X-dir.	Y-dir.	X-dir.	Y-dir.
7.111	838	839			35%	20%
6.401		840	51%	40%	33%	24%
6.401	839	840			33%	24%
5.691		841	56%	39%	28%	24%
5.691	840	841			28%	24%
4.981		842	56%	40%	40%	26%
4.981	841	842			40%	26%
4.2713		843	56%	39%	47%	36%
4.2713	842	843			47%	36%
3.7593		844	63%	39%	49%	40%
3.7593	843	844			49%	40%
3.215		845	45%	29%	50%	43%
3.215	844	845			50%	43%
2.365		846	46%	29%	46%	47%

Table 03.07.02-6(5)e Ratio with DCD Enveloping Seismic Loads: RPV Stick - Case RBF (Continued)

(a) Enveloping Seismic Loads

Elev. (m)	Elem No.	Node No.	Shear		Moment	
			X-dir. (MN)	Y-dir. (MN)	X-dir. (MN·m)	Y-dir. (MN·m)
0.7657	859	827			0.1	0.0
-0.788		861	0.1	0.1	0.1	0.1
-0.788	861	861			0.1	0.1
-1.443		863	0.0	0.0	0.1	0.1
-1.443	863	863			0.1	0.1
-2.098		865	0.0	0.0	0.1	0.1
-2.098	865	865			0.1	0.1
-2.753		867	0.1	0.1	0.1	0.1
-2.753	867	867			0.1	0.1
-3.4715		869	0.1	0.1	0.0	0.0
-3.4715	869	869			0.0	0.0
-4.2237		871	0.0	0.0	0.0	0.0
8.453	871	815			56.3	51.5
7.4625		711	10.1	6.8	55.0	51.7

(b) Ratio with DCD ((a)/DCD Loads)

Elev. (m)	Elem No.	Node No.	Shear		Moment	
			X-dir.	Y-dir.	X-dir.	Y-dir.
0.7657	859	827			30%	23%
-0.788		861	51%	52%	48%	38%
-0.788	861	861			48%	38%
-1.443		863	35%	28%	51%	41%
-1.443	863	863			51%	41%
-2.098		865	37%	28%	51%	36%
-2.098	865	865			51%	36%
-2.753		867	32%	32%	43%	34%
-2.753	867	867			43%	34%
-3.4715		869	44%	34%	44%	34%
-3.4715	869	869			44%	34%
-4.2237		871	44%	34%	1%	0%
8.453	871	815			39%	38%
7.4625		711	54%	38%	39%	38%

Table 03.07.02-6(5)e Ratio with DCD Enveloping Seismic Loads: RPV Stick - Case RBF (Continued)

(a) Enveloping Seismic Loads

Elev. (m)	Elem No.	Node No.	Shear		Moment	
			X-dir. (MN)	Y-dir. (MN)	X-dir. (MN·m)	Y-dir. (MN·m)
7.896	845	847			0.0	0.0
7.8071		848	0.6	0.7	0.1	0.1
7.8071	846	848			0.1	0.1
7.111		849	0.5	0.8	0.4	0.5
7.111	847	849			0.4	0.5
6.401		850	0.3	0.4	0.7	0.9
6.401	848	850			0.7	0.9
5.691		851	0.1	0.1	0.7	0.9
5.691	849	851			0.7	0.9
4.981		852	0.3	0.4	0.5	0.6
4.981	850	852			0.5	0.6
4.2713		853	0.6	0.7	0.1	0.1
4.2713	851	853			0.1	0.1
4.1784		854	0.6	0.7	0.0	0.0

(b) Ratio with DCD ((a)/DCD Loads)

Elev. (m)	Elem No.	Node No.	Shear		Moment	
			X-dir.	Y-dir.	X-dir.	Y-dir.
7.896	845	847				
7.8071		848	48%	60%	48%	60%
7.8071	846	848			48%	60%
7.111		849	50%	76%	50%	65%
7.111	847	849			50%	65%
6.401		850	60%	65%	53%	73%
6.401	848	850			53%	73%
5.691		851	46%	36%	58%	71%
5.691	849	851			58%	71%
4.981		852	53%	61%	60%	70%
4.981	850	852			60%	70%
4.2713		853	61%	73%	56%	66%
4.2713	851	853			56%	66%
4.1784		854	56%	66%	3%	4%

Table 03.07.02-6(5)e Ratio with DCD Enveloping Seismic Loads: RPV Stick - Case RBF (Continued)

(a) Enveloping Seismic Loads

Elev. (m)	Elem No.	Node No.	Shear		Moment	
			X-dir. (MN)	Y-dir. (MN)	X-dir. (MN·m)	Y-dir. (MN·m)
4.1784	852	854			0.0	0.0
4.065		855	0.5	0.4	0.1	0.0
4.065	853	855			0.1	0.0
3.215		856	0.5	0.3	0.5	0.3
3.215	854	856			0.5	0.3
2.365		857	0.1	0.1	0.6	0.4
2.365	855	857			0.6	0.4
1.785		858	0.3	0.2	0.4	0.3
1.785	856	858			0.4	0.3
1.2		859	0.7	0.5	0.0	0.0
1.2	857	859			0.0	0.0
0.7657		860	0.9	0.7	0.4	0.3
0.7657	858	860			0.4	0.3
-0.1315		828	1.1	0.8	1.4	1.0

(b) Ratio with DCD ((a)/DCD Loads)

Elev. (m)	Elem No.	Node No.	Shear		Moment	
			X-dir.	Y-dir.	X-dir.	Y-dir.
4.1784	852	854				
4.065		855	48%	50%	48%	50%
4.065	853	855			48%	50%
3.215		856	49%	51%	48%	51%
3.215	854	856			48%	51%
2.365		857	50%	45%	49%	51%
2.365	855	857			49%	51%
1.785		858	49%	51%	49%	50%
1.785	856	858			49%	50%
1.2		859	49%	50%	24%	19%
1.2	857	859			1%	2%
0.7657		860	49%	50%	49%	50%
0.7657	858	860			49%	50%
-0.1315		828	48%	51%	48%	51%

Table 03.07.02-6(5)e Ratio with DCD Enveloping Seismic Loads: RPV Stick - Case RBF (Continued)

(a) Enveloping Seismic Loads

Elev. (m)	Elem No.	Node No.	Shear		Moment	
			X-dir. (MN)	Y-dir. (MN)	X-dir. (MN·m)	Y-dir. (MN·m)
-0.1315	860	828			0.1	0.1
-0.788		862	0.1	0.1	0.1	0.1
-0.788	862	862			0.1	0.1
-1.443		864	0.0	0.1	0.1	0.1
-1.443	864	864			0.1	0.1
-2.098		866	0.0	0.1	0.1	0.1
-2.098	866	866			0.1	0.1
-2.753		868	0.1	0.1	0.1	0.1
-2.753	868	868			0.1	0.1
-3.4715		870	0.1	0.1	0.0	0.0
-3.4715	870	870			0.0	0.0
-4.2237		872	0.0	0.1	0.0	0.0

(b) Ratio with DCD ((a)/DCD Loads)

Elev. (m)	Elem No.	Node No.	Shear		Moment	
			X-dir.	Y-dir.	X-dir.	Y-dir.
-0.1315	860	828			43%	43%
-0.788		862	43%	36%	47%	43%
-0.788	862	862			47%	43%
-1.443		864	39%	37%	48%	43%
-1.443	864	864			48%	43%
-2.098		866	34%	31%	46%	44%
-2.098	866	866			46%	44%
-2.753		868	35%	29%	45%	36%
-2.753	868	868			45%	36%
-3.4715		870	46%	37%	42%	36%
-3.4715	870	870			42%	36%
-4.2237		872	42%	36%	0%	0%

Table 03.07.02-6(6) Ratio with DCD Enveloping Seismic Loads: CB Stick - Case CBF1

(a) Enveloping Seismic Loads

Elev. (m)	Node No.	Elem No.	Shear		Moment		Torsion (MN-m)
			X-Dir. (MN)	Y-Dir. (MN)	X-Dir. (MN-m)	Y-Dir. (MN-m)	
13.80	6				34.5	42.1	
		6	11.2	13.9	76.8	70.7	10.0
9.06	5				98.3	86.3	
		5	20.5	24.0	185.5	187.2	18.0
4.65	4				141.3	85.2	
		4	37.8	40.7	330.5	303.1	13.3
-2.00	3				324.7	252.7	
-7.40	2	3	72.9	69.9	555.1	545.3	16.2

(b) Ratio with DCD ((a)/DCD Loads)

Elev. (m)	Node No.	Elem No.	Shear		Moment		Torsion
			X-Dir.	Y-Dir.	X-Dir.	Y-Dir.	
13.80	6				22%	34%	
		6	34%	48%	31%	36%	14%
9.06	5				27%	31%	
		5	38%	44%	32%	42%	14%
4.65	4				20%	16%	
		4	50%	51%	29%	31%	7%
-2.00	3				26%	24%	
-7.40	2	3	59%	70%	35%	36%	7%

Note: Total torsional moments are obtained by the absolute sum of the accidental torsional moments and the values of the geometric torsional moments shown. The accidental torsional moment is the product of the horizontal force component and an eccentricity of 5% of the larger horizontal dimension at various elevations.

Table 03.07.02-6(7)a Ratio with DCD Maximum Vertical Acceleration: RB/FB - Case RBF

(a) Enveloping Maximum Vertical Acceleration

Elev. (m)	Node No.	Stick Model	Max. Vertical Acceleration
52.40*	110	RB/FB	0.36
34.00	109	RB/FB	0.31
27.00	108	RB/FB	0.28
22.50	107	RB/FB	0.27
17.50	106	RB/FB	0.25
13.57	105	RB/FB	0.22
9.06	104	RB/FB	0.20
4.65	103	RB/FB	0.20
-1.00	102	RB/FB	0.21
-6.40	101	RB/FB	0.20
-11.50	2	RB/FB	0.18
-15.50	1	RB/FB	0.18

(b) Ratio with DCD ((a)/DCD Acceleration)

Elev. (m)	Node No.	Stick Model	Max. Vertical Acceleration
52.40*	110	RB/FB	29%
34.00	109	RB/FB	38%
27.00	108	RB/FB	39%
22.50	107	RB/FB	37%
17.50	106	RB/FB	34%
13.57	105	RB/FB	30%
9.06	104	RB/FB	28%
4.65	103	RB/FB	26%
-1.00	102	RB/FB	28%
-6.40	101	RB/FB	29%
-11.50	2	RB/FB	29%
-15.50	1	RB/FB	36%

Note: For structural design use only. Unit: g

* : The difference between the modeled elevation 52.4 m and the actual elevation 52.7 m at the RB roof is negligibly small.

Table 03.07.02-6(7)b Ratio with DCD Enveloping Maximum Vertical Acceleration: RCCV - Case RBF

(a) Enveloping Maximum Vertical Acceleration

Elev. (m)	Node No.	Stick Model	Max. Vertical Acceleration
34.00	209	RCCV	0.31
27.00	208	RCCV	0.31
17.50	206	RCCV	0.26
13.57	205	RCCV	0.23
9.06	204	RCCV	0.21
4.65	203	RCCV	0.19
-1.00	202	RCCV	0.17
-6.40	201	RCCV	0.18

Note: For structural design use only. Unit: g

(b) Ratio with DCD ((a)/DCD Acceleration)

Elev. (m)	Node No.	Stick Model	Max. Vertical Acceleration
34.00	209	RCCV	35%
27.00	208	RCCV	36%
17.50	206	RCCV	35%
13.57	205	RCCV	30%
9.06	204	RCCV	33%
4.65	203	RCCV	27%
-1.00	202	RCCV	28%
-6.40	201	RCCV	31%

Table 03.07.02-6(7)c Ratio with DCD Enveloping Maximum Vertical Acceleration: VW/Pedestal - Case RBF

(a) Enveloping Maximum Vertical Acceleration

Elev. (m)	Node No.	Stick Model	Max. Vertical Acceleration
17.50	701	VW	0.26
14.50	702	VW	0.25
11.50	703	VW	0.24
8.50	704	VW	0.22
7.4625	705	VW	0.22
4.65	706,303	Pedestal	0.20
-1.00	302	Pedestal	0.17
-6.40	301	Pedestal	0.18

(b) Ratio with DCD ((a)/DCD Acceleration)

Elev. (m)	Node No.	Stick Model	Max. Vertical Acceleration
17.50	701	VW	23%
14.50	702	VW	24%
11.50	703	VW	26%
8.50	704	VW	29%
7.4625	705	VW	32%
4.65	706,303	Pedestal	30%
-1.00	302	Pedestal	30%
-6.40	301	Pedestal	36%

Note: For structural design use only. Unit: g

Table 03.07.02-6(7)d Ratio with DCD Enveloping Maximum Vertical Acceleration: RSW - Case RBF

(a) Enveloping Maximum Vertical Acceleration

Elev. (m)	Node No.	Stick Model	Max. Vertical Acceleration
24.18	707	RSW	0.31
20.20	708	RSW	0.30
15.775	709	RSW	0.28
11.35	710	RSW	0.24
7.4625	711	RSW	0.22
4.65	712	RSW	0.20
2.4615	713	RSW	0.19
1.96	714	RSW	0.19
-0.80	715	RSW	0.19

Note: For structural design use only. Unit: g

(b) Ratio with DCD ((a)/DCD Acceleration)

Elev. (m)	Node No.	Stick Model	Max. Vertical Acceleration
24.18	707	RSW	32%
20.20	708	RSW	32%
15.775	709	RSW	34%
11.35	710	RSW	32%
7.4625	711	RSW	32%
4.65	712	RSW	30%
2.4615	713	RSW	30%
1.96	714	RSW	30%
-0.80	715	RSW	30%

Table 03.07.02-6(7)e Ratio with DCD Enveloping Maximum Vertical Acceleration: RB/FB Flexible Slab Oscillators - Case RBF

(a) Enveloping Maximum Vertical Acceleration

Elev. (m)	Node No.	Stick Model	Max. Vertical Acceleration
52.40*	9101	Oscillator	0.20
	9102	Oscillator	0.46
	9103	Oscillator	0.93
	9104	Oscillator	0.79
	9105	Oscillator	0.71
	9106	Oscillator	0.75
	9107	Oscillator	0.75
	9108	Oscillator	0.82
34.00	9091	Oscillator	0.42
	9092	Oscillator	0.44
27.00	9081	Oscillator	0.49
	9082	Oscillator	0.37
	9083	Oscillator	0.33
	9084	Oscillator	0.56
	9085	Oscillator	0.34
22.50	9071	Oscillator	0.38
	9072	Oscillator	0.49
	9073	Oscillator	0.75
	9074	Oscillator	0.46
	9075	Oscillator	0.45
17.50	9061	Oscillator	0.56
	9062	Oscillator	0.49
	9063	Oscillator	0.31
	9064	Oscillator	0.64
	9065	Oscillator	0.49

(b) Ratio with DCD ((a)/DCD Acceleration)

Elev. (m)	Node No.	Stick Model	Max. Vertical Acceleration
52.40*	9101	Oscillator	17%
	9102	Oscillator	26%
	9103	Oscillator	30%
	9104	Oscillator	32%
	9105	Oscillator	31%
	9106	Oscillator	25%
	9107	Oscillator	27%
	9108	Oscillator	31%
34.00	9091	Oscillator	33%
	9092	Oscillator	41%
27.00	9081	Oscillator	42%
	9082	Oscillator	37%
	9083	Oscillator	30%
	9084	Oscillator	42%
	9085	Oscillator	35%
22.50	9071	Oscillator	24%
	9072	Oscillator	37%
	9073	Oscillator	37%
	9074	Oscillator	35%
	9075	Oscillator	39%
17.50	9061	Oscillator	31%
	9062	Oscillator	33%
	9063	Oscillator	38%
	9064	Oscillator	35%
	9065	Oscillator	35%

Note: For structural design use only. Unit: g

* : The difference between the modeled elevation 52.4 m and the actual elevation 52.7 m at the RB roof is negligibly small.

Table 03.07.02-6(7)e Ratio with DCD Enveloping Maximum Vertical Acceleration: RB/FB Flexible Slab Oscillators - Case RBF (Continued)

(a) Enveloping Maximum Vertical Acceleration

Elev. (m)	Node No.	Stick Model	Max. Vertical Acceleration
13.57	9051	Oscillator	0.33
	9052	Oscillator	0.47
9.06	9041	Oscillator	0.34
	9042	Oscillator	0.51
4.65	9031	Oscillator	0.68
	9032	Oscillator	0.39
	9033	Oscillator	0.46
	9034	Oscillator	0.70
	9035	Oscillator	0.51
-1.00	9021	Oscillator	0.51
	9022	Oscillator	0.48
	9023	Oscillator	0.43
	9024	Oscillator	0.35
	9025	Oscillator	0.48
	9026	Oscillator	0.58
	9027	Oscillator	0.28
-6.40	9011	Oscillator	0.42
	9012	Oscillator	0.37
	9013	Oscillator	0.37

(b) Ratio with DCD ((a)/DCD Acceleration)

Elev. (m)	Node No.	Stick Model	Max. Vertical Acceleration
13.57	9051	Oscillator	41%
	9052	Oscillator	33%
9.06	9041	Oscillator	39%
	9042	Oscillator	36%
4.65	9031	Oscillator	58%
	9032	Oscillator	41%
	9033	Oscillator	45%
	9034	Oscillator	46%
	9035	Oscillator	37%
-1.00	9021	Oscillator	46%
	9022	Oscillator	33%
	9023	Oscillator	43%
	9024	Oscillator	40%
	9025	Oscillator	36%
	9026	Oscillator	37%
	9027	Oscillator	32%
-6.40	9011	Oscillator	46%
	9012	Oscillator	41%
	9013	Oscillator	28%

Note: For structural design use only. Unit: g

Table 03.07.02-6(8) Ratio with DCD Enveloping Maximum Vertical Acceleration: CB - Case CBF1

(a) Enveloping Maximum Vertical Acceleration

Elev. (m)	Node No.	Stick Model	X-dir. (g)	Y-dir. (g)	Max. Vertical
13.80	6	CB	0.42	0.56	0.51
9.06	5	CB	0.32	0.38	0.47
4.65	4	CB	0.42	0.36	0.40
-2.00	3	CB	0.24	0.42	0.31
-7.40	2	CB	0.23	0.22	0.20
-10.40	1	CB	0.23	0.21	0.20
13.80	9001	Oscillator	---	---	1.05
	9002	Oscillator	---	---	0.99
	9003	Oscillator	---	---	1.71
9.06	9101	Oscillator	---	---	0.85
	9102	Oscillator	---	---	0.98
	9103	Oscillator	---	---	1.83
4.65	9201	Oscillator	---	---	0.77
	9202	Oscillator	---	---	1.40
-2.00	9301	Oscillator	---	---	1.05

(b) Ratio with DCD ((a)/DCD Acceleration)

Elevation (m)	Node No.	Stick Model	X-dir. (g)	Y-dir. (g)	Max. Vertical Acceleration
13.80	6	CB	33%	50%	51%
9.06	5	CB	36%	42%	55%
4.65	4	CB	49%	44%	54%
-2.00	3	CB	31%	59%	55%
-7.40	2	CB	43%	41%	39%
-10.40	1	CB	43%	40%	39%
13.80	9001	Oscillator	---	---	48%
	9002	Oscillator	---	---	74%
	9003	Oscillator	---	---	120%
9.06	9101	Oscillator	---	---	43%
	9102	Oscillator	---	---	78%
	9103	Oscillator	---	---	128%
4.65	9201	Oscillator	---	---	59%
	9202	Oscillator	---	---	98%
-2.00	9301	Oscillator	---	---	76%

Note: For structural design use only. Unit: g

Table 03.07.02-6(9) Design Slab Vertical Acceleration: CB - Case CBF1

Elevation H (m)	Node No.	Slab Weight $_sW_i$ (kN)	Total Weight $\Sigma\ _sW_i$ (kN)	Slab Vertical Acceleration $_sA_i$ (g)	$_sW_i * {}_sA_i$	$_sA_{eq}$ (g)	$_wW$ (kN)	Wall Vertical Acceleration $_wA$ (g)	Design Vertical Acceleration $_sA_{ave}$ (g)	DCD Design Vertical Acceleration $_sA_{ave}$ (g)
13.80	9001	5478		1.05	5753.71					
	9002	6390		0.99	6326.79					
	9003	781	12650	1.71	1335.22	1.06	10745	0.51	0.81	1.39
9.06	9101	3494		0.85	2969.85					
	9102	4907		0.98	4809.18					
	9103	850	9250	1.83	1554.62	1.01	19785	0.47	0.64	1.08
4.65	9201	8022		0.77	6177.48					
	9202	227	8249	1.40	318.36	0.79	27986	0.40	0.49	0.87
-2.00	9301	4325	4325	1.05	4541.28	1.05	32570	0.31	0.40	0.66

Notes : 1. Equivalent vertical slab acceleration are calculated with the following equation for each floor.

$$_sA_{eq} = \Sigma\ (\ _sW_i * {}_sA_i\ ) / \Sigma_s W_i$$

where, $_sA_i$: Maximum acceleration of i-th mass in the dynamic analysis results.

$_sW_i$: Weight of i-th mass in the dynamic analysis model.

2. Average slab accelerations are calculated with the following equation for the slab design loads.

$$_sA_{ave} = (\ _sA_{eq} * \Sigma_s W_i + {}_wA * {}_wW\ ) / (\Sigma_s W_i + {}_wW\ )$$

where, $_sA_{ave}$: Average slab acceleration .

$_wA$: Maximum acceleration of the wall masses.

$_wW$: Slab weights included in the wall masses.

Table 03.07.02-6(10) Comparison of Lateral Soil Pressure - RB/FB - Case RBF

Floor Level (m)	R1 and F3 Averaged Soil Pressure (MPa)			RA and RG Averaged Soil Pressure (MPa)			Envelope (MPa)		DCD Design Soil Pressure (MPa)		DCD Wall Capacity Passive Pressure (MPa)	
	RFB-1 (BE)	RFB-2 (LB)	RFB-3 (UB)	RFB-1 (BE)	RFB-2 (LB)	RFB-3 (UB)	R1 and F3 Wall	RA and RG Wall	R1 and F3 Wall	RA and RG Wall	R1 and F3 Wall	RA and RG Wall
4.65												
Slab												
3.65	0.09	0.06	0.14	0.11	0.07	0.14	0.14	0.14	0.30	0.33	0.19	0.12
-1.00												
Slab												
-2.00	0.17	0.12	0.21	0.19	0.11	0.22	0.21	0.22	0.29	0.29	0.51	0.33
-6.40												
Slab												
-7.40	0.41	0.38	0.40	0.42	0.37	0.38	0.41	0.42	0.25	0.23	0.82	0.53
-11.50												

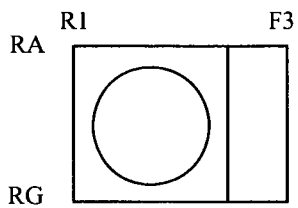

Table 03.07.02-6(11) Comparison of Lateral Soil Pressure - CB - Case CFB1

Floor Level (m)	C1 and C5 Averaged Soil Pressure (MPa)			CA and CD Averaged Soil Pressure (MPa)			Envelope (MPa)		DCD Design Soil Pressure (MPa)	
	CFB1-1 (BE)	CFB1-2 (LB)	CFB1-3 (UB)	CFB1-1 (BE)	CFB1-2 (LB)	CFB1-3 (UB)	C1 and C5 Wall	CA and CD Wall	C1 and C5 Wall	CA and CD Wall
4.65										
Slab										
3.95 -2.00	0.12	0.10	0.11	0.12	0.09	0.10	0.12	0.12	0.22	0.22
Slab										
-2.50 -7.40	0.14	0.14	0.13	0.16	0.13	0.12	0.14	0.16	0.18	0.18

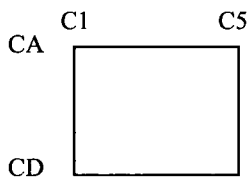

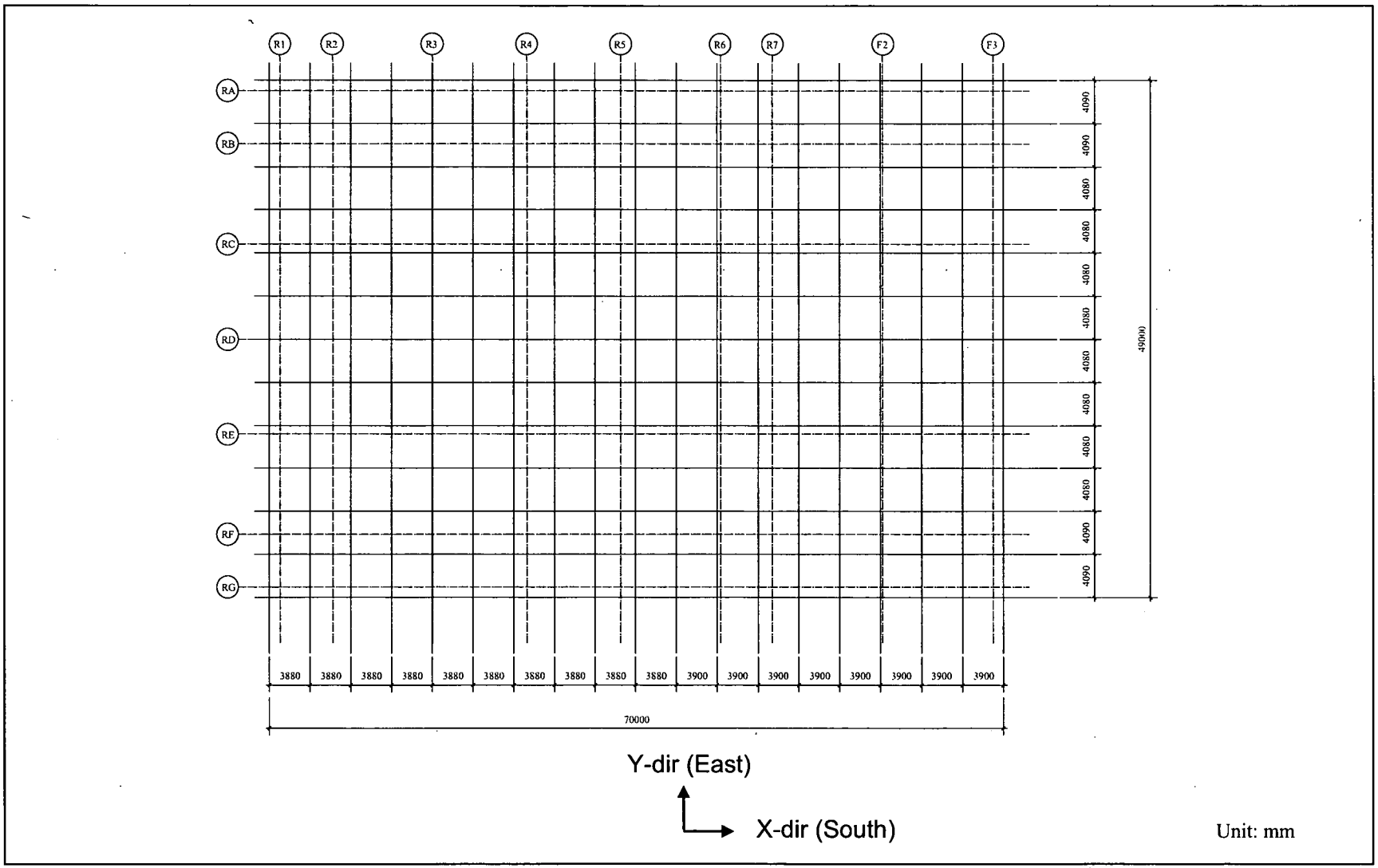

Figure 03.07.02-6(1) SASSI2000 Plate Elements for RB/FB Basemat

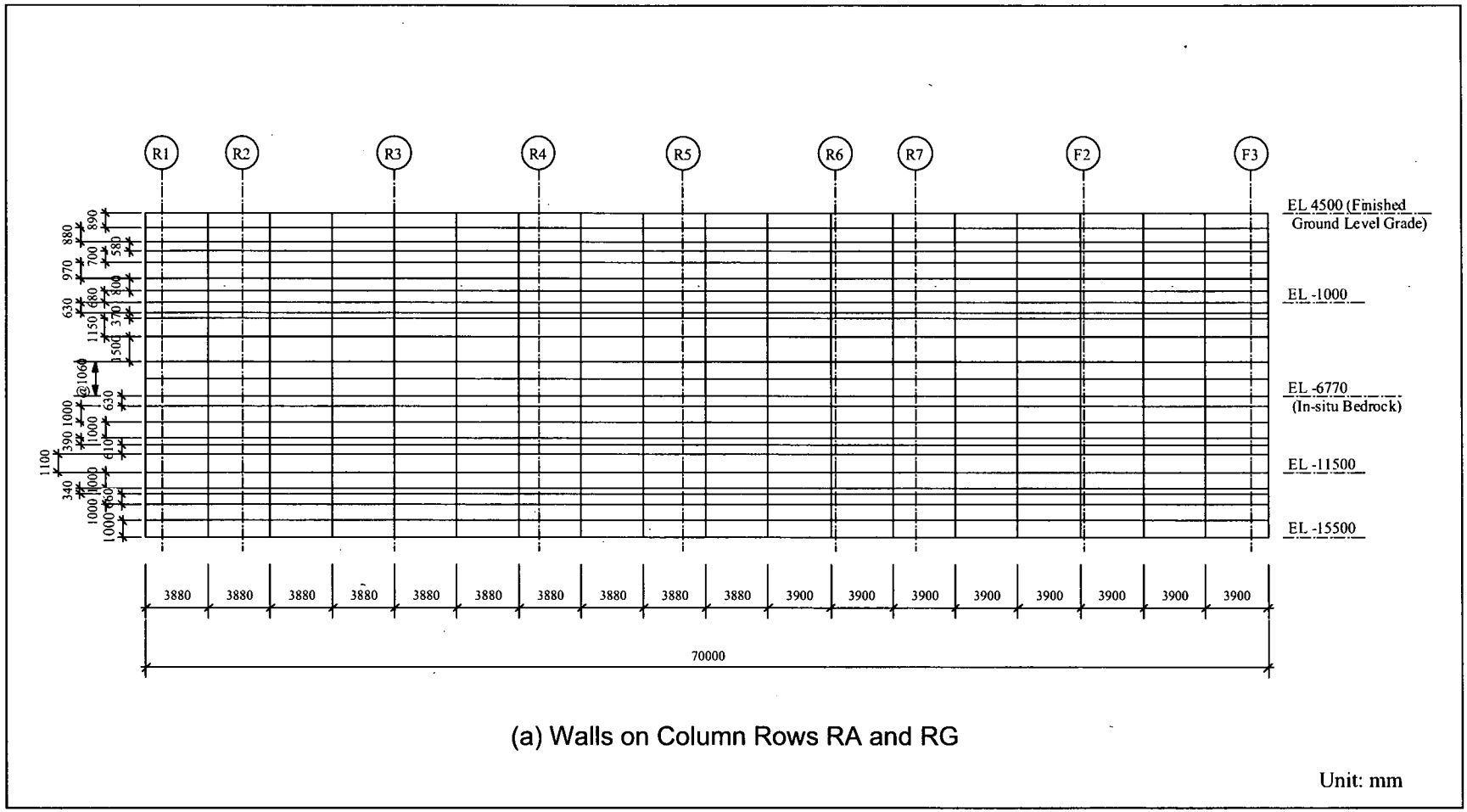

Figure 03.07.02-6(2) SASSI2000 Plate Elements for RB/FB Exterior Walls

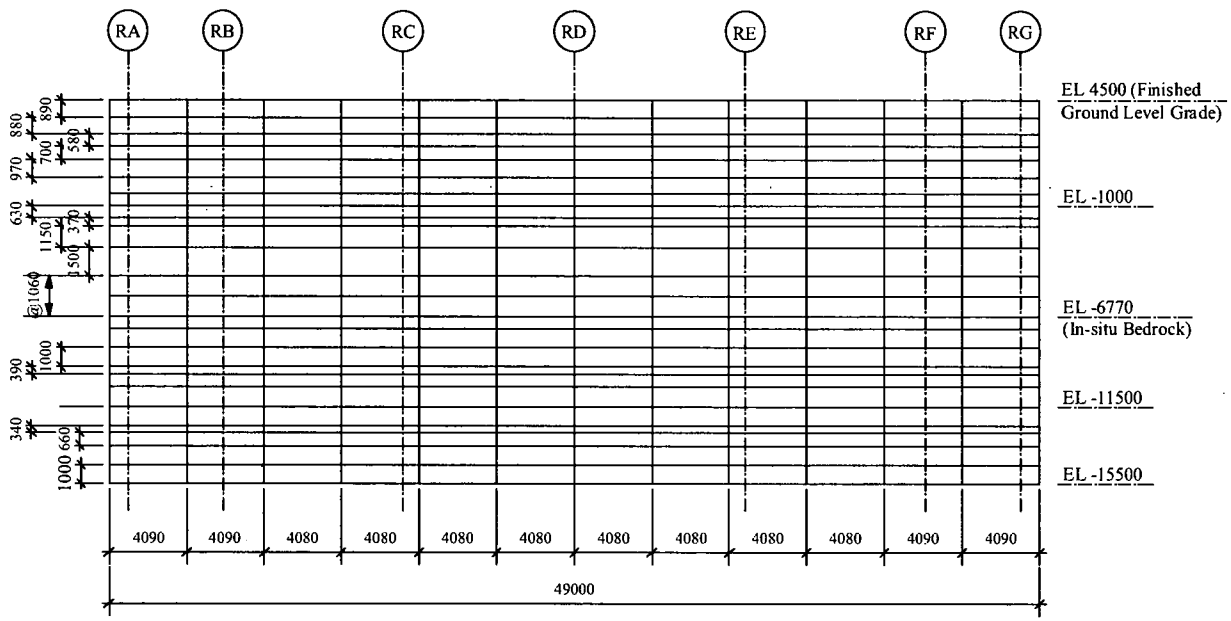

(b) Walls on Column Rows R1 and F3

Unit: mm

Figure 03.07.02-6(2) SASSI2000 Plate Elements for RB/FB Exterior Walls (Continued)

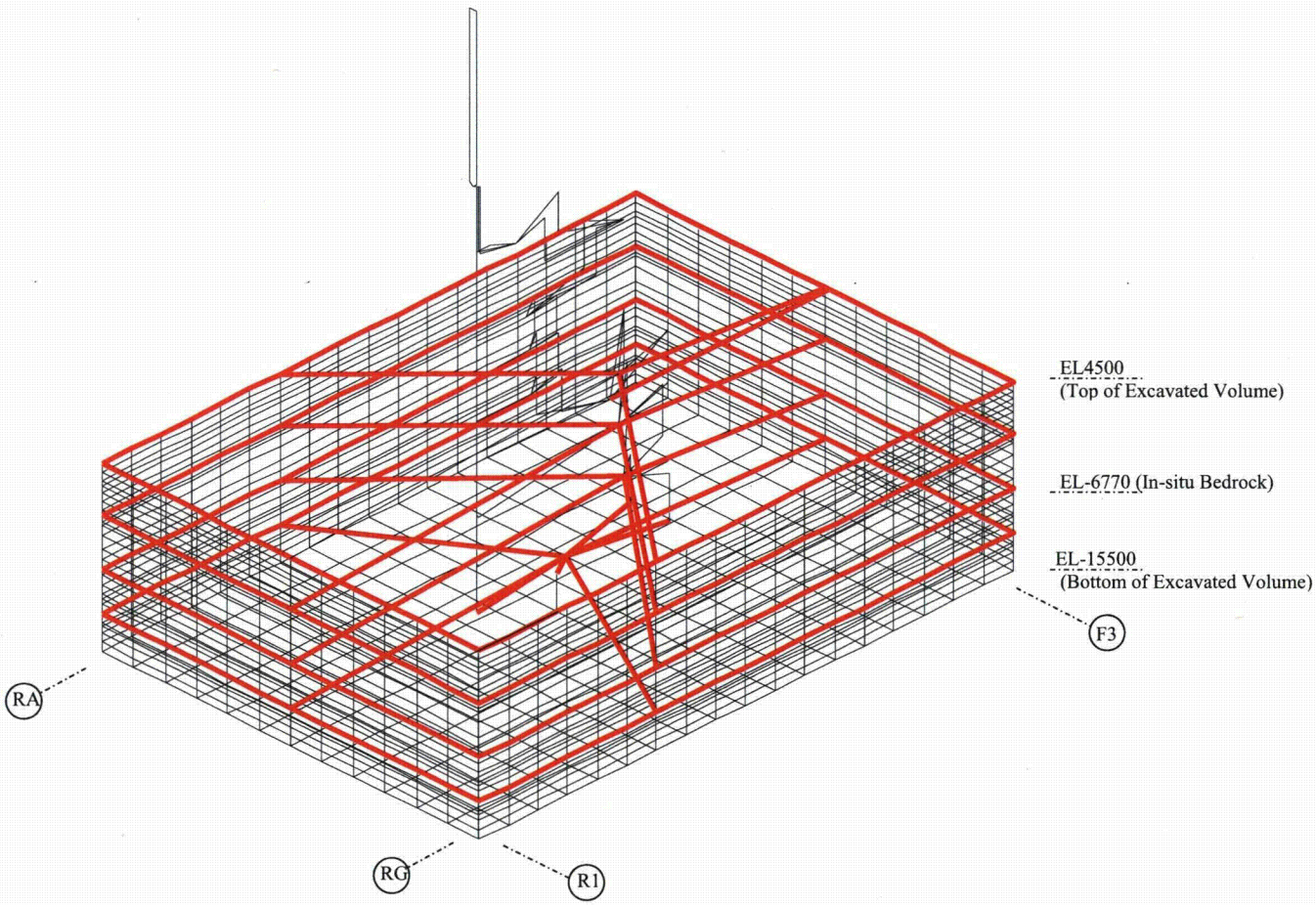

Note: 1) Wall and basemat are modeled with shell element without mass.
2) Rigid beams indicated in red are installed at the floor levels.

Unit: mm

Figure 03.07.02-6(3) Overview of SASSI2000 SSI RB/FB Model

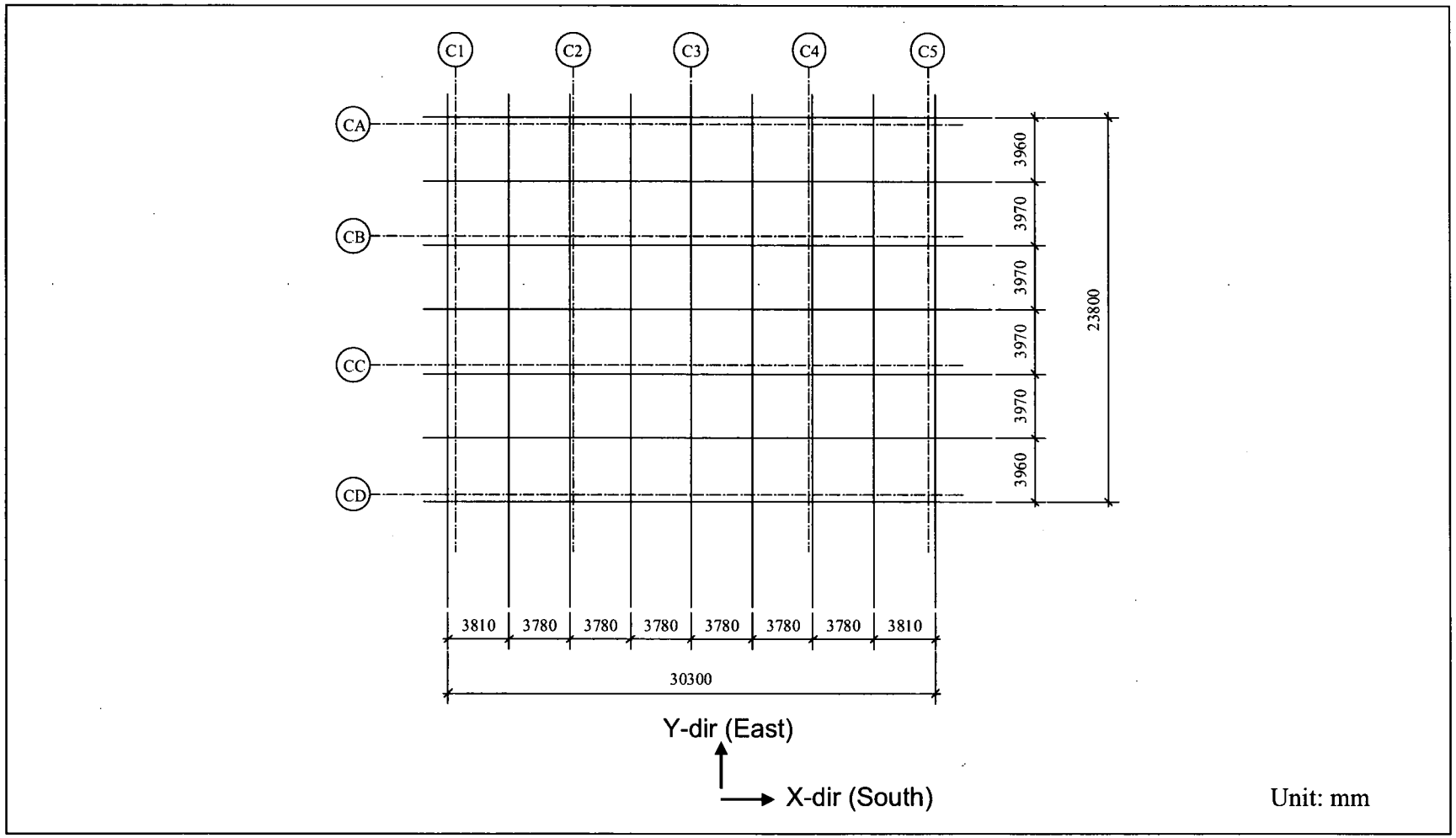

Figure 03.07.02-6(4) SASSI2000 Plate Elements for CB Basemat

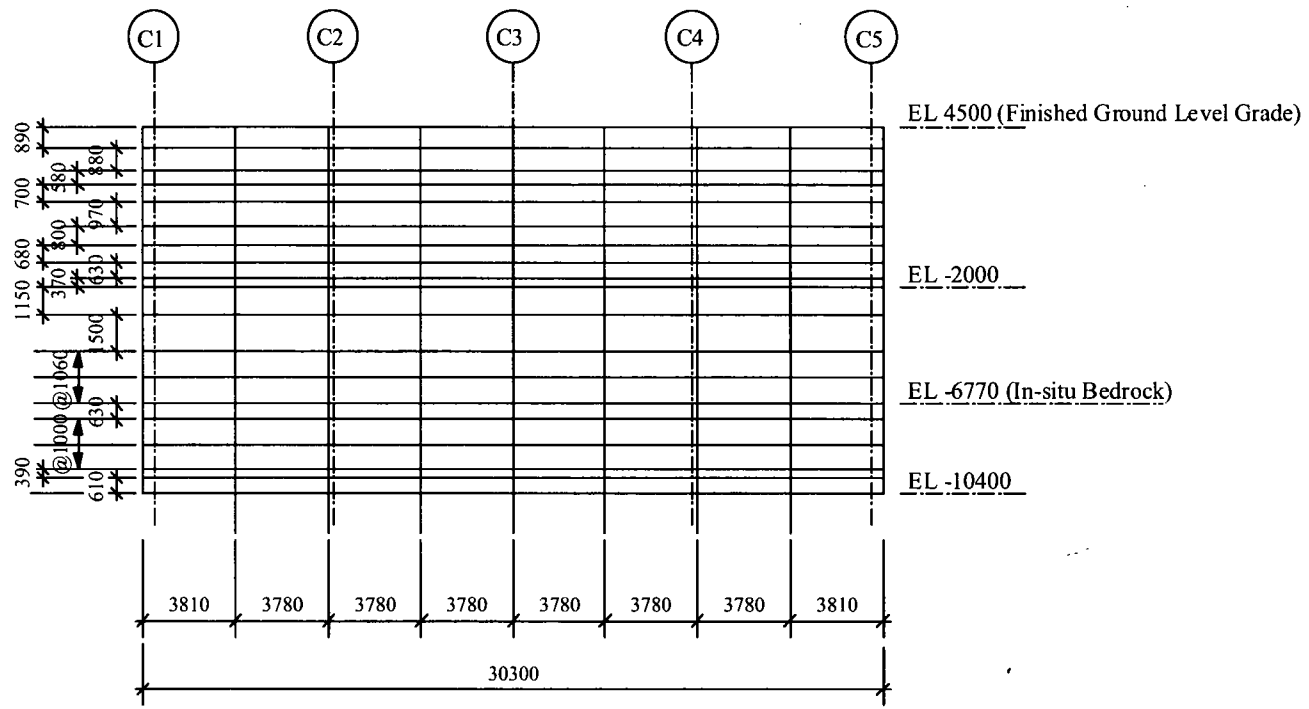

(a) Walls on Column Rows CA and CD

Unit: mm

Figure 03.07.02-6(5) SASSI2000 Plate Elements for CB Exterior Walls

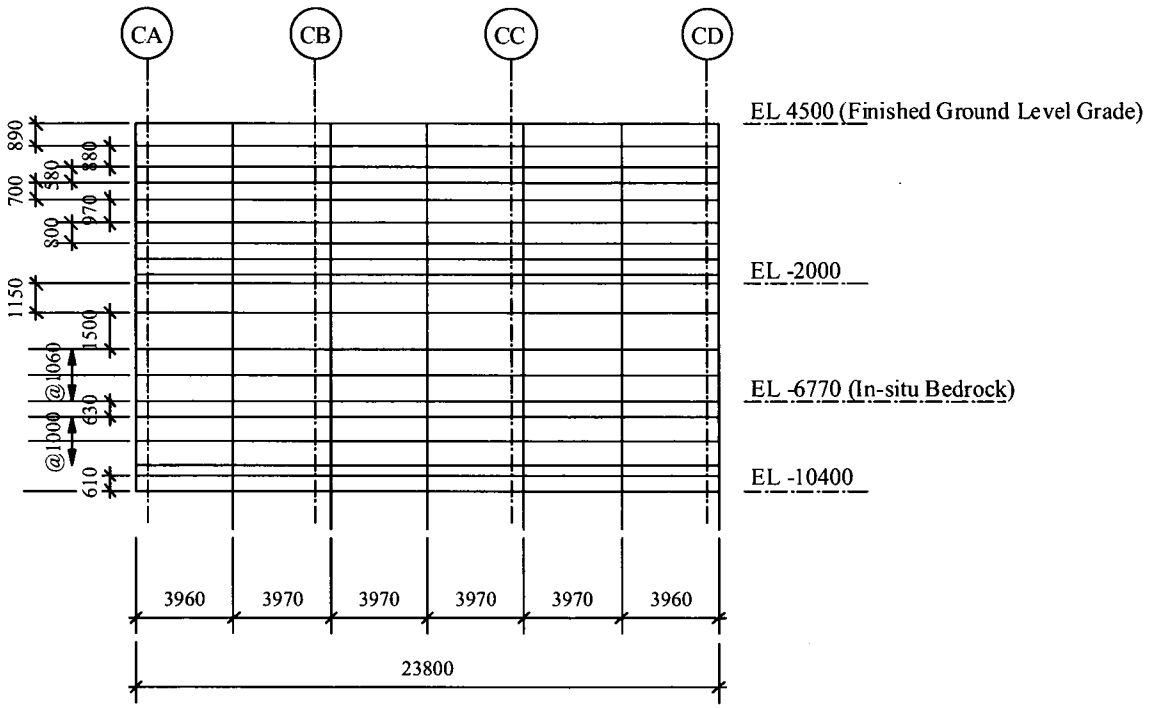

(b) Walls on Column Rows C1 and C5

Unit: mm

Figure 03.07.02-6(5) SASSI2000 Plate Elements for CB Exterior Walls (Continued)

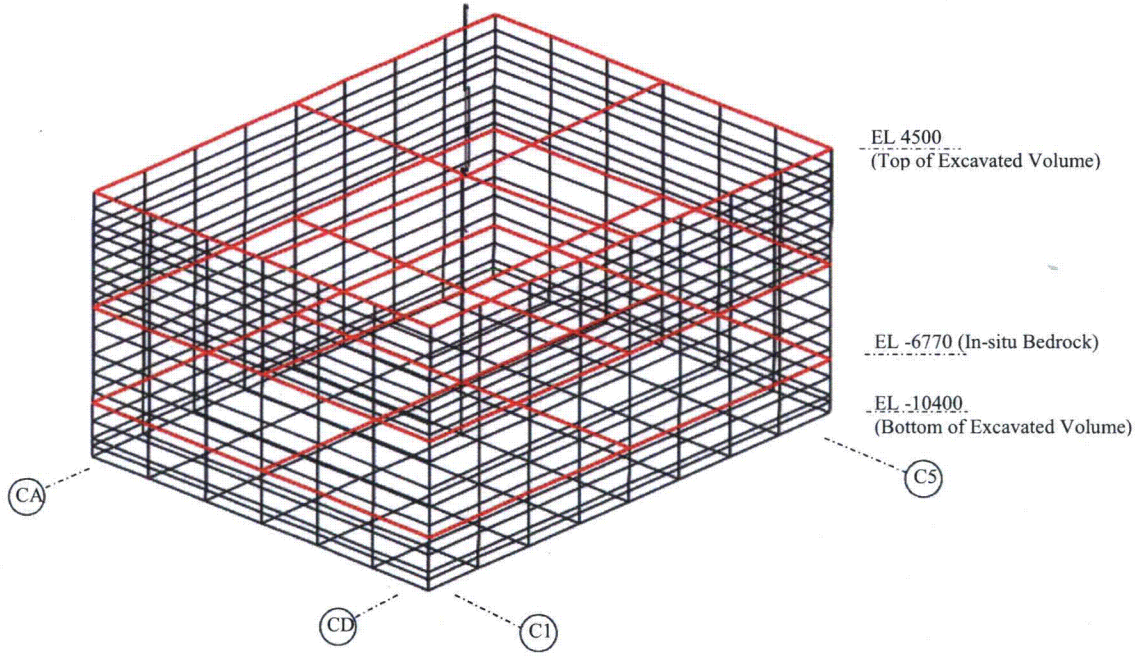

Unit: mm

Note: 1) Wall and basemat are modeled with shell element without mass.
2) Rigid beams indicated in red are installed at the floor levels.

Figure 03.07.02-6(6) Overview of CB SASSI2000 SSI Model

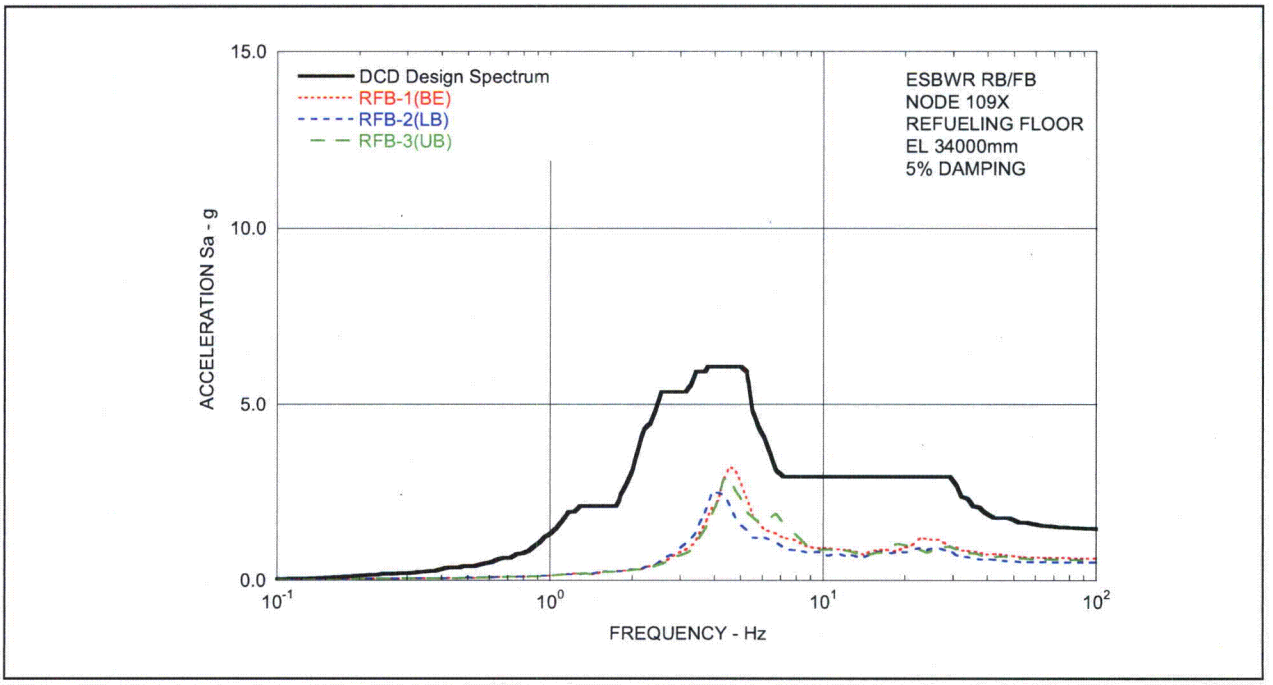

Figure 03.07.02-6(7)a Comparison of Floor Response Spectra - RB/FB Refueling Floor in X-Direction - Case RFB

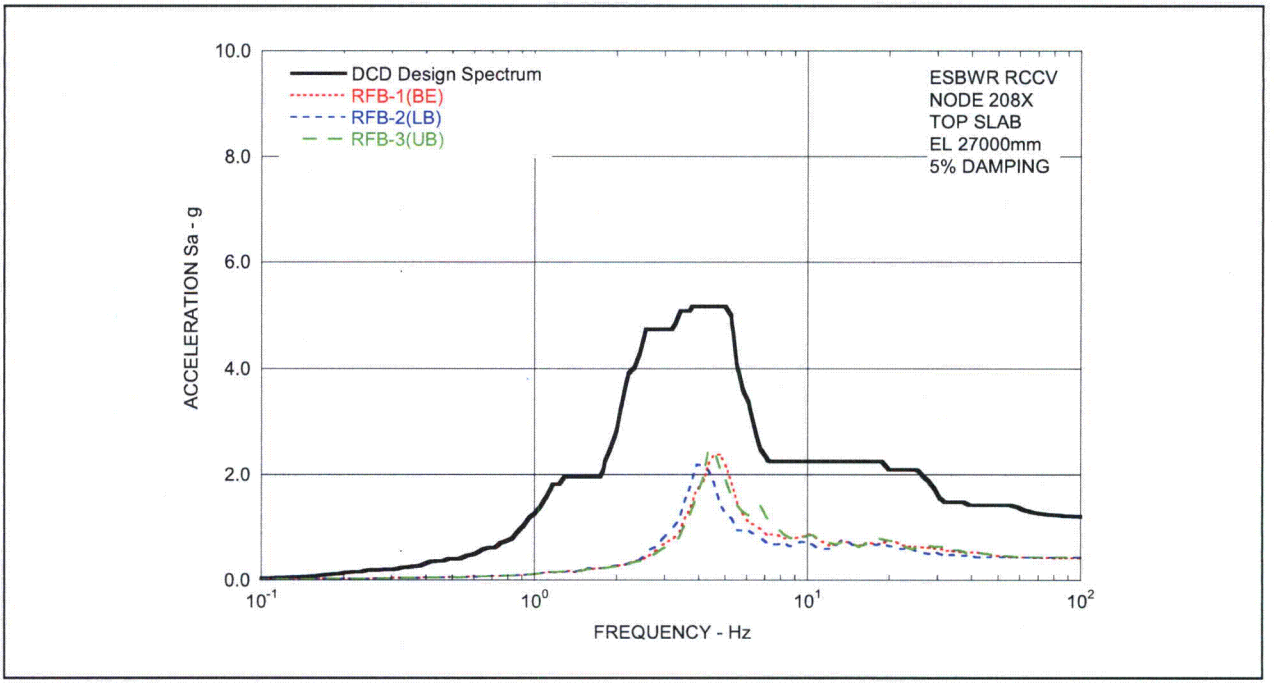

Figure 03.07.02-6(7)b Comparison of Floor Response Spectra - RCCV Top Slab in X-Direction - Case RFB

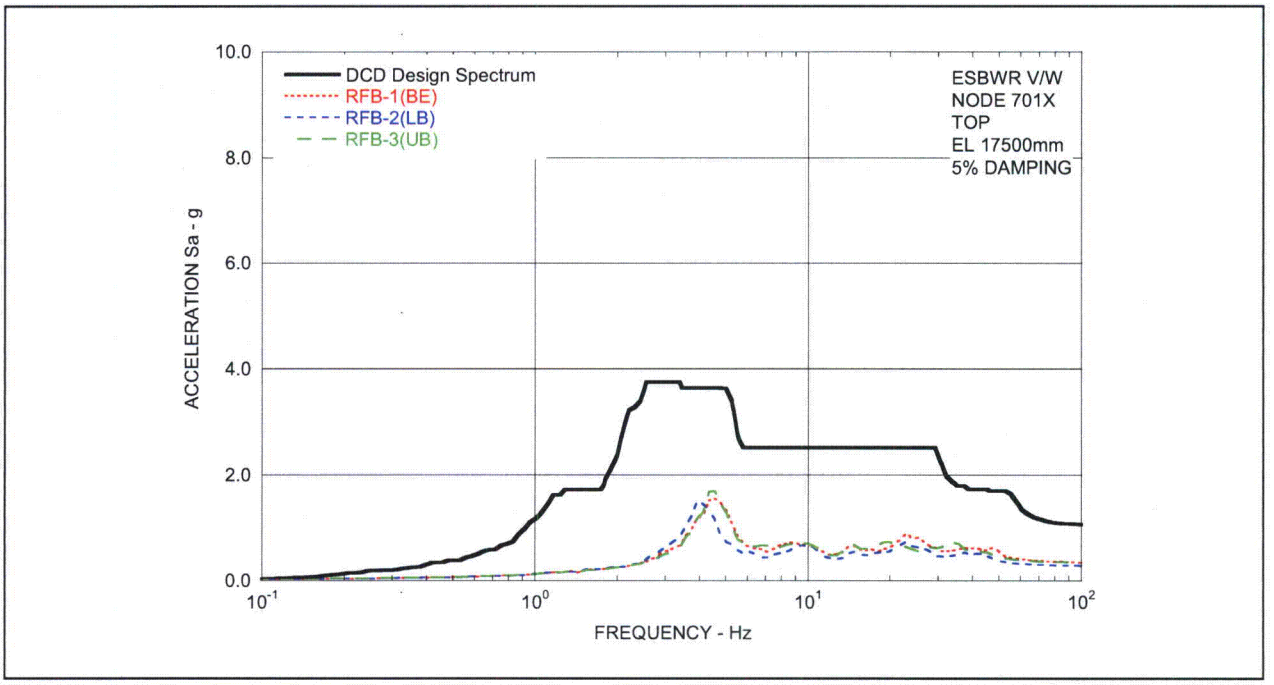

Figure 03.07.02-6(7)c Comparison of Floor Response Spectra - Vent Wall Top in X-Direction - Case RFB

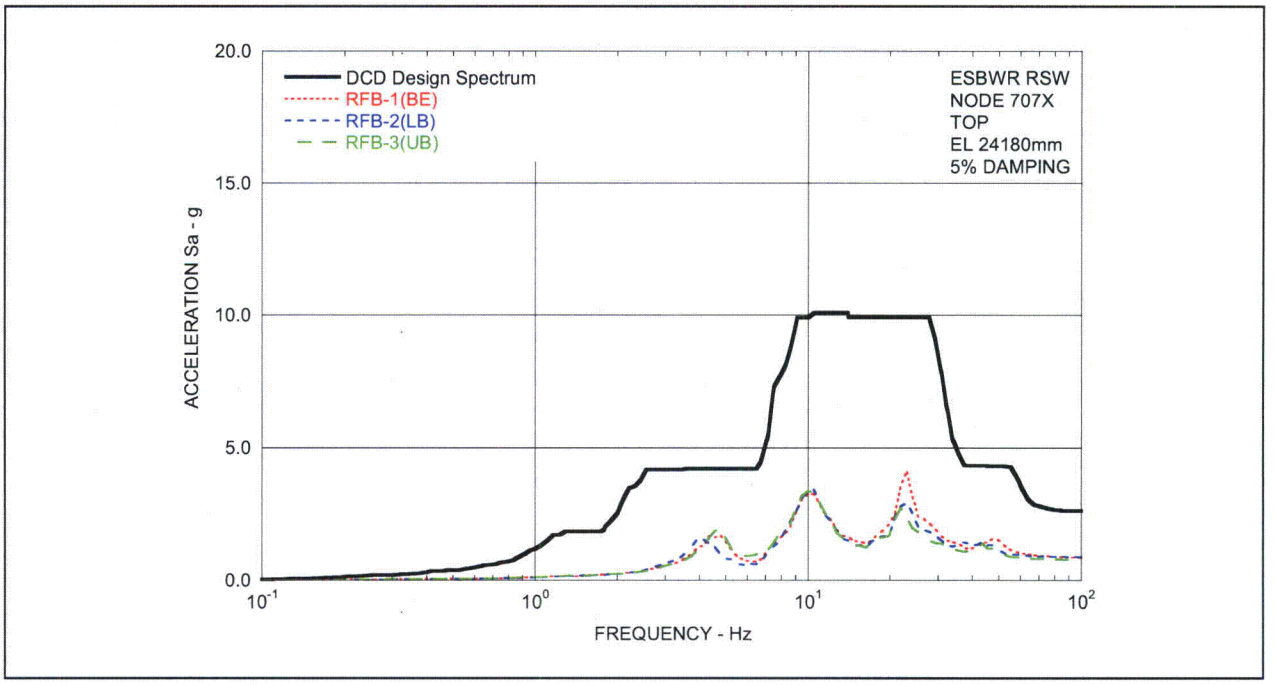

Figure 03.07.02-6(7)d Comparison of Floor Response Spectra - RSW Top in X-Direction - Case RFB

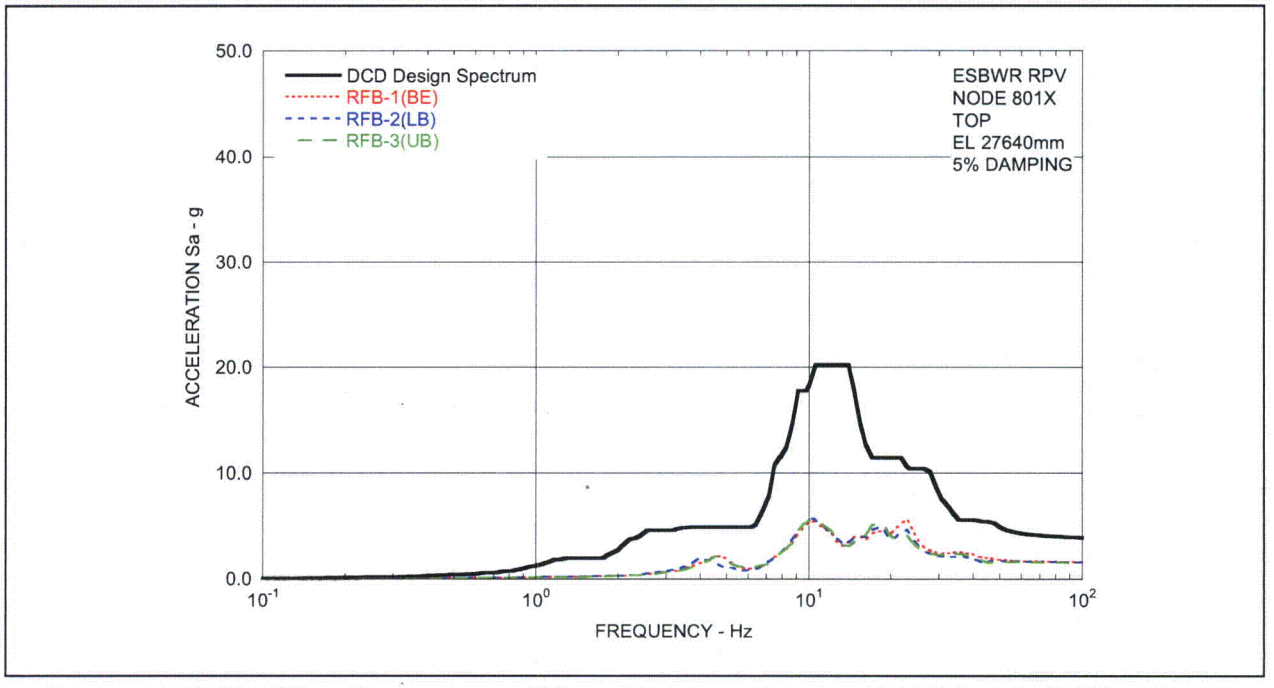

Figure 03.07.02-6(7)e Comparison of Floor Response Spectra - RPV Top in X-Direction - Case RFB

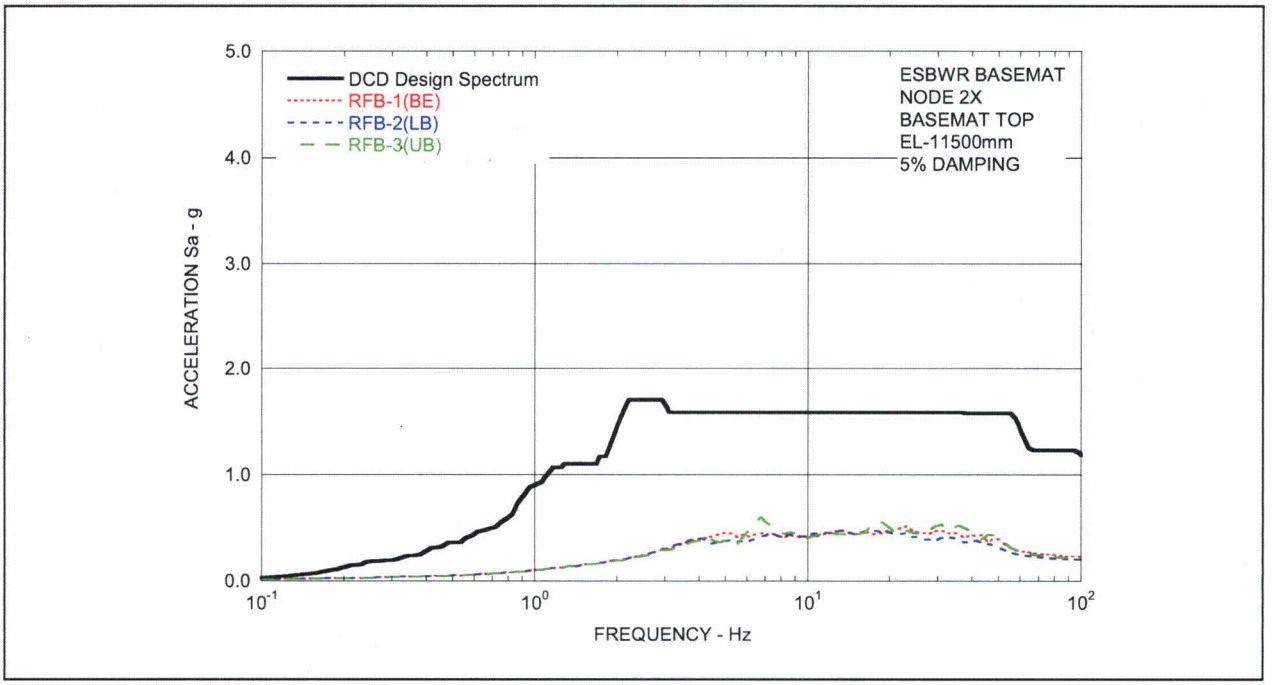

Figure 03.07.02-6(7)f Comparison of Floor Response Spectra - RB/FB Basemat in X-Direction - Case RFB

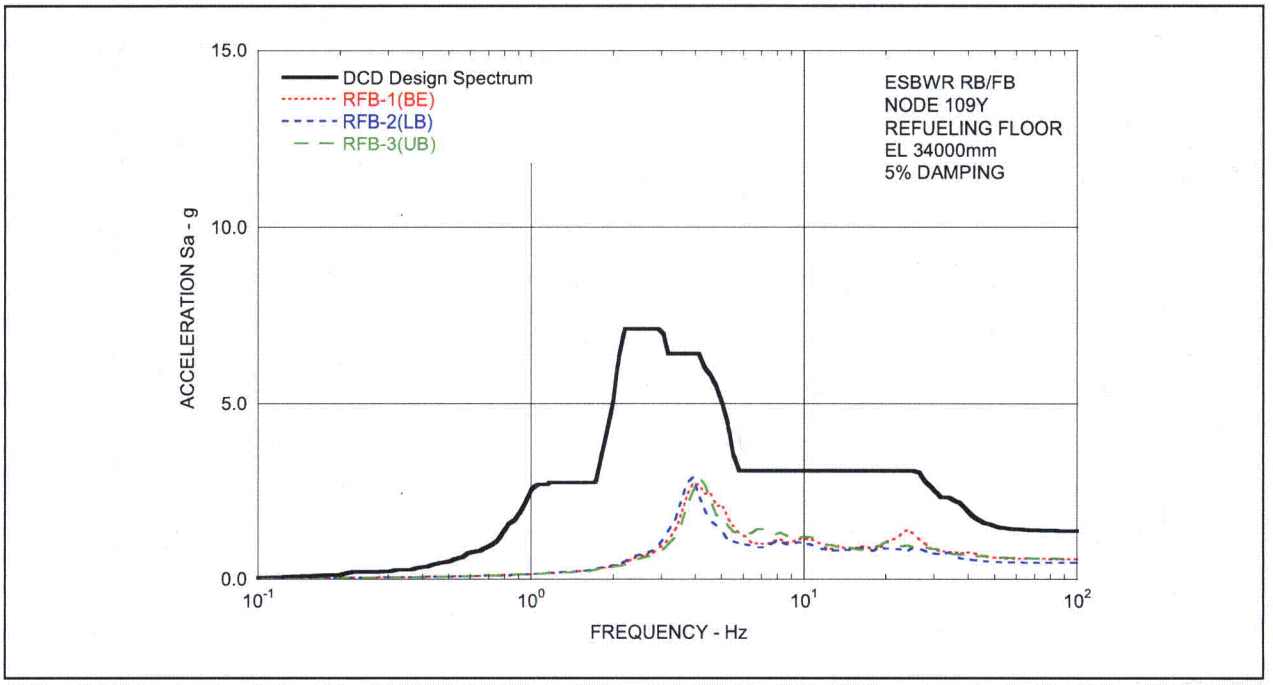

Figure 03.07.02-6(8)a Comparison of Floor Response Spectra - RB/FB Refueling Floor in Y-Direction - Case RFB

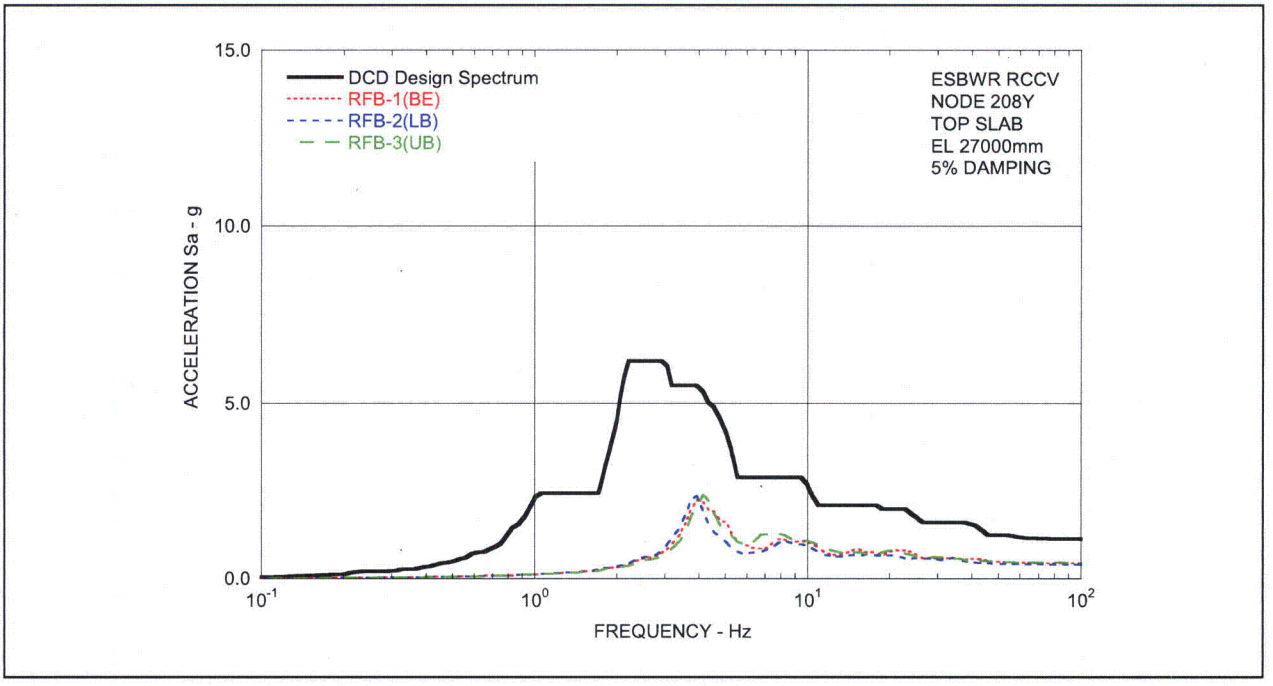

Figure 03.07.02-6(8)b Comparison of Floor Response Spectra - RCCV Top Slab in Y-Direction - Case RFB

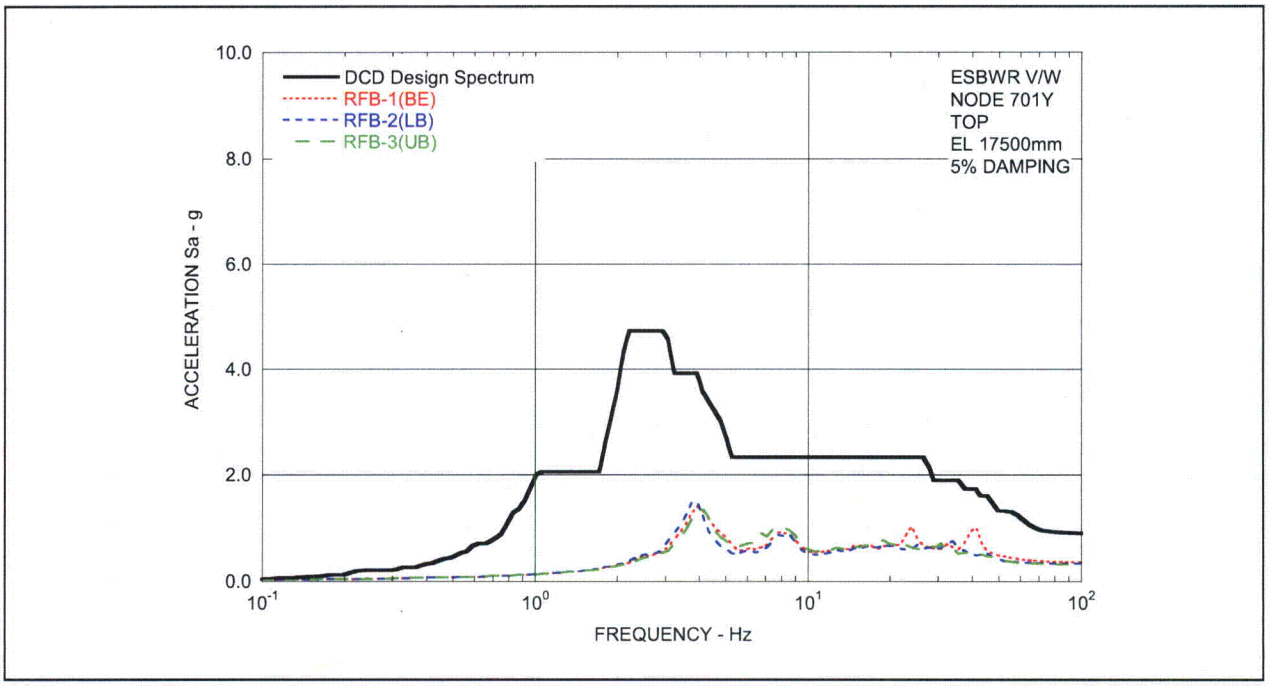

Figure 03.07.02-6(8)c Comparison of Floor Response Spectra - Vent Wall Top in Y-Direction - Case RFB

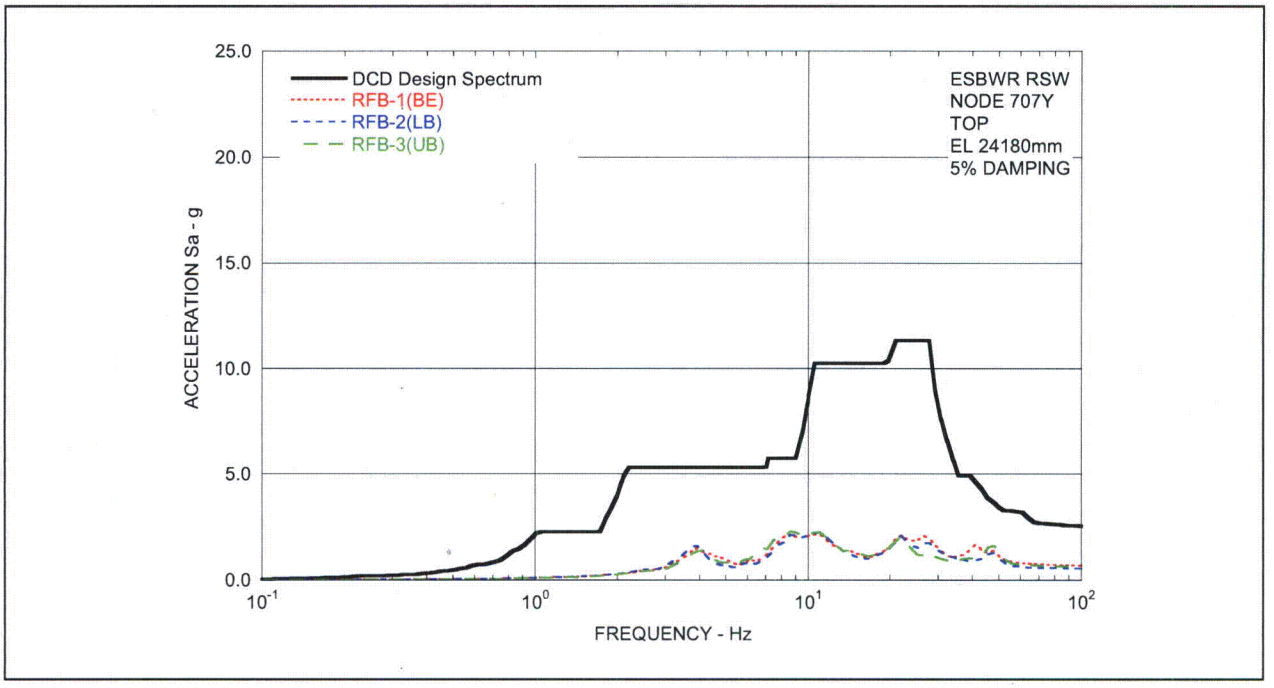

Figure 03.07.02-6(8)d Comparison of Floor Response Spectra - RSW Top in Y-Direction - Case RFB

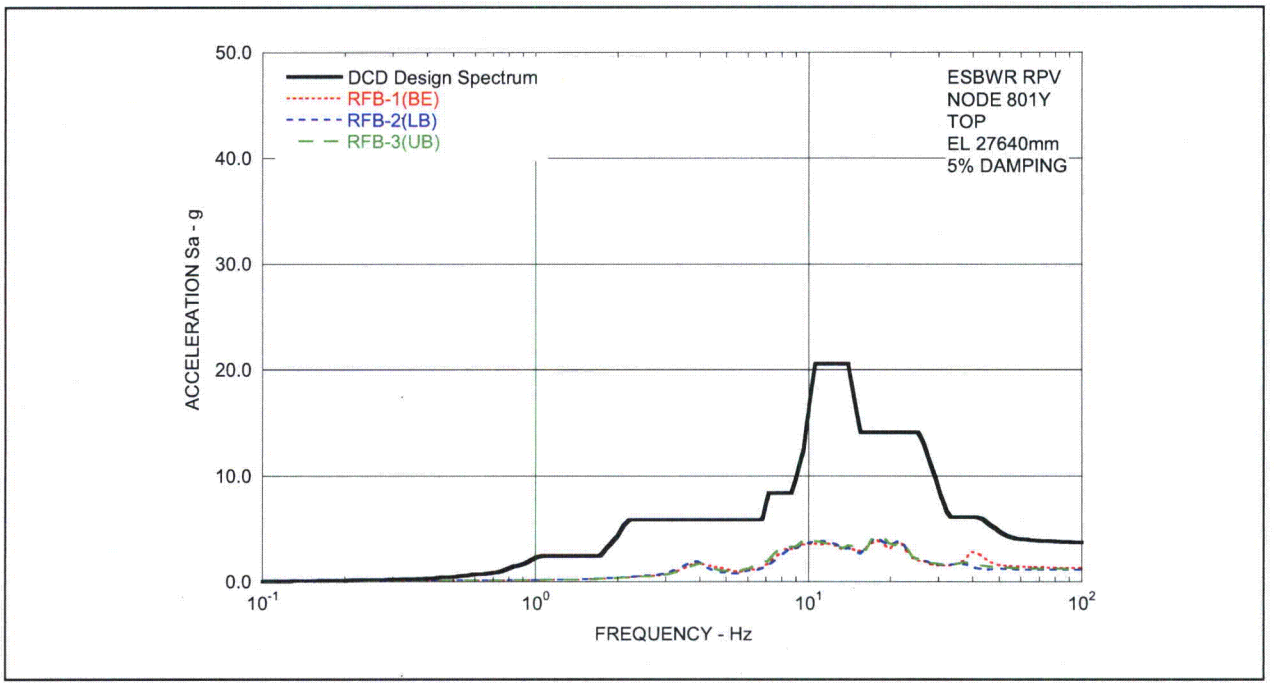

Figure 03.07.02-6(8)e Comparison of Floor Response Spectra - RPV Top in Y-Direction - Case RFB

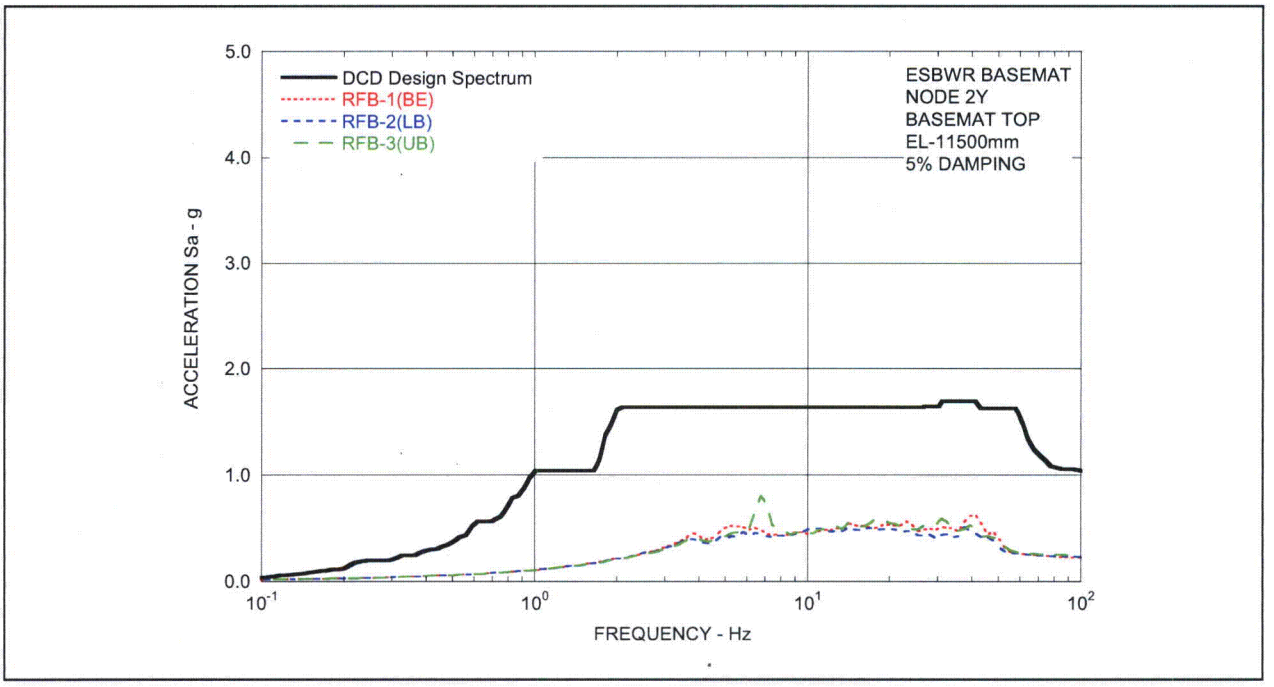

Figure 03.07.02-6(8)f Comparison of Floor Response Spectra - RB/FB Basemat in Y-Direction - Case RFB

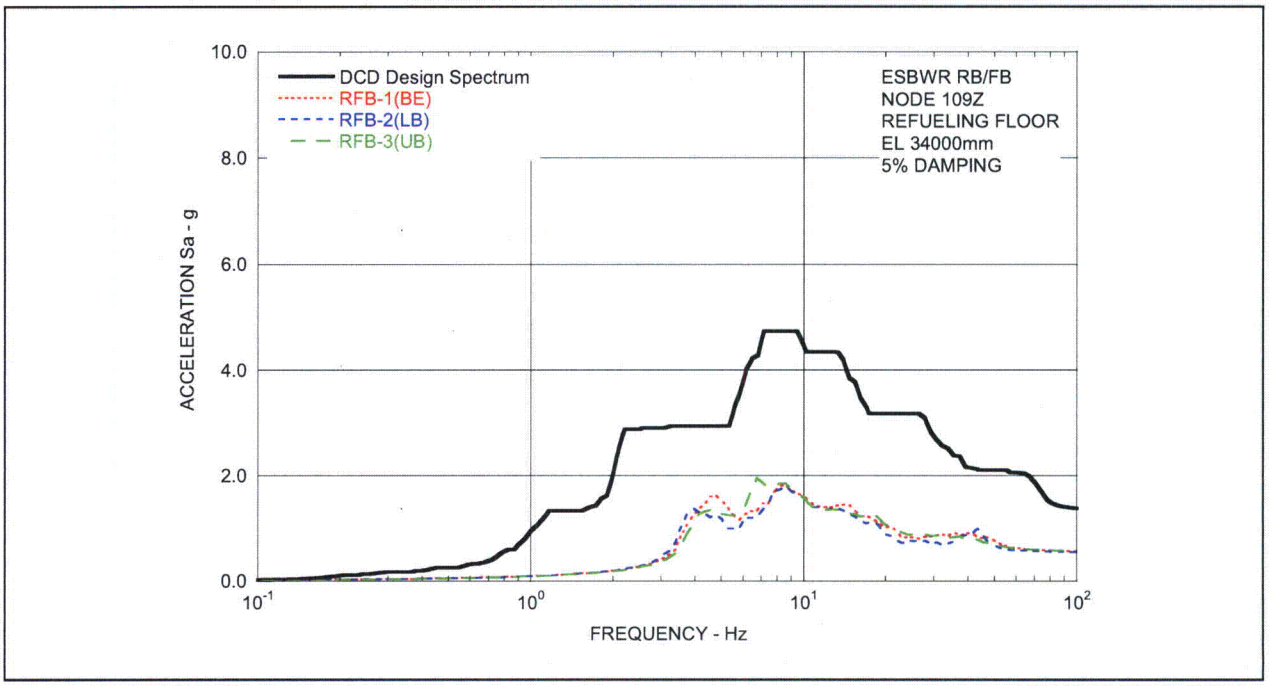

Figure 03.07.02-6(9)a Comparison of Floor Response Spectra - RB/FB Refueling Floor in Z-Direction - Case RFB

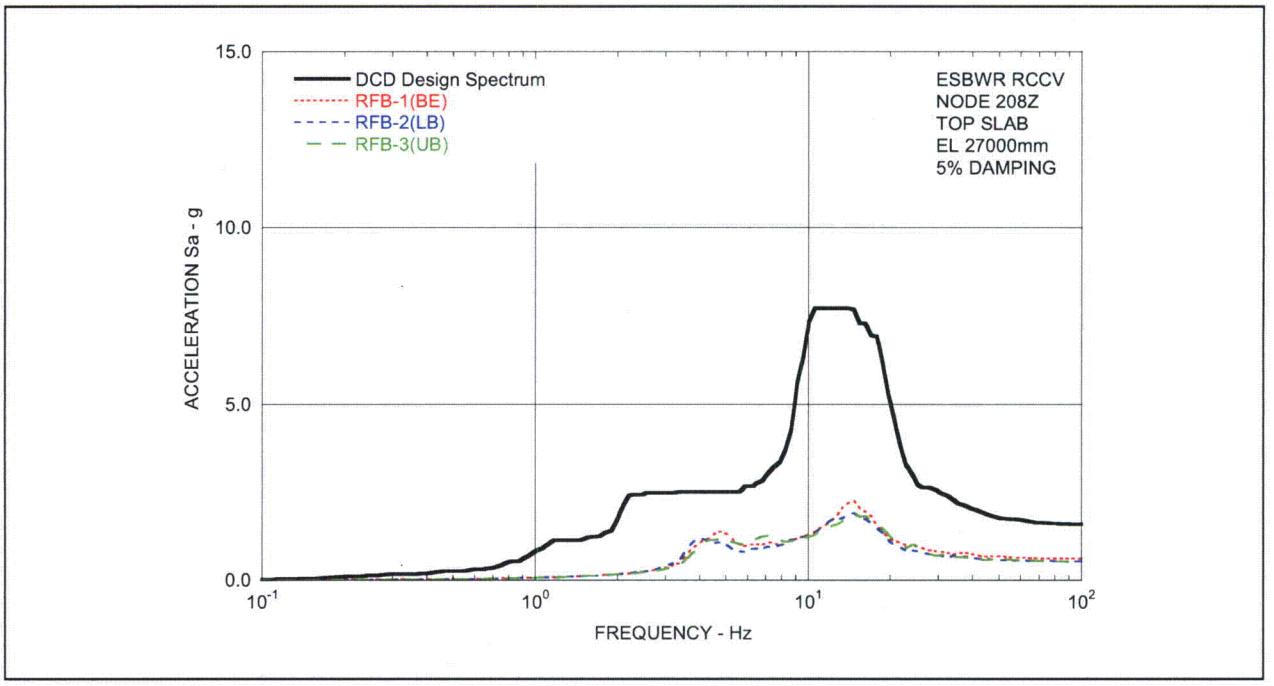

Figure 03.07.02-6(9)b Comparison of Floor Response Spectra - RCCV Top Slab in Z-Direction - Case RFB

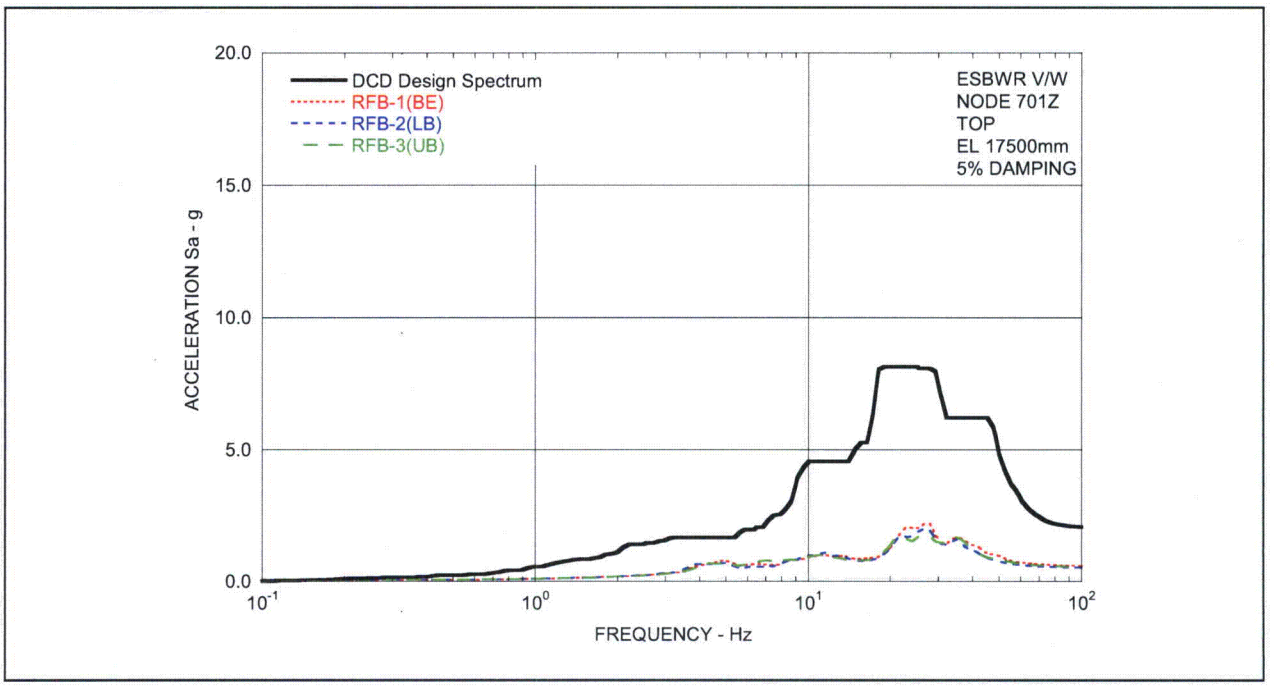

Figure 03.07.02-6(9)c Comparison of Floor Response Spectra - Vent Wall Top in Z-Direction - Case RFB

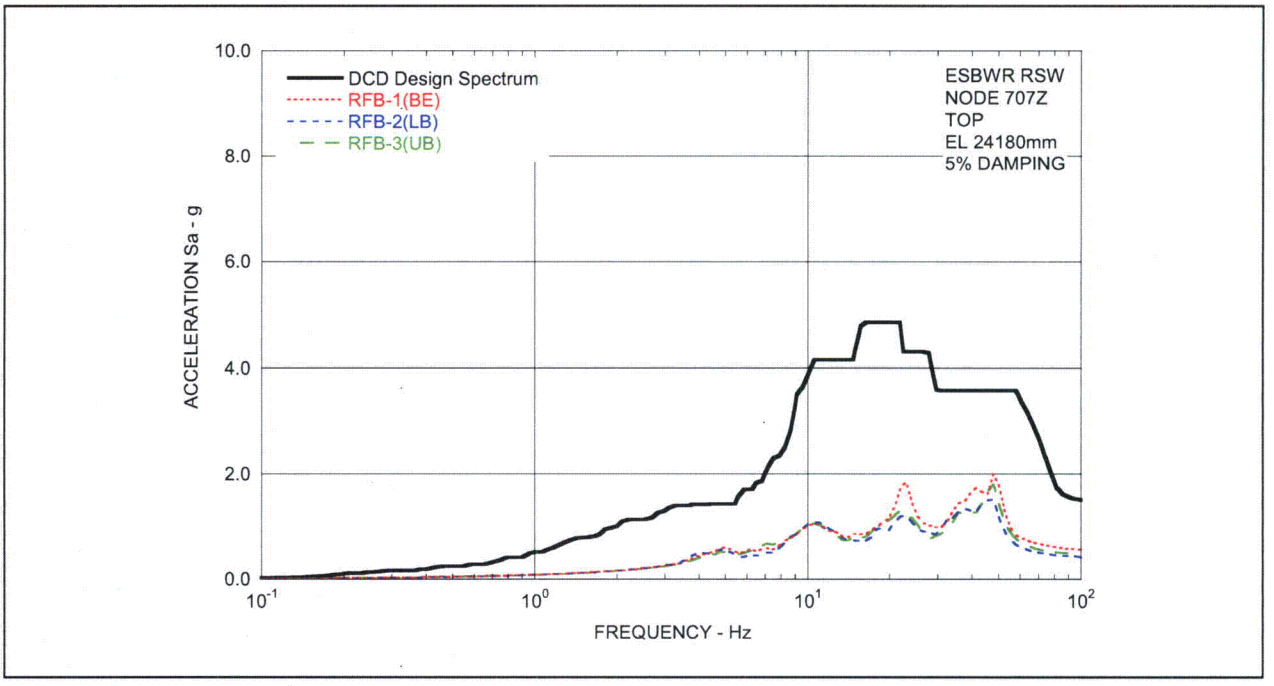

Figure 03.07.02-6(9)d Comparison of Floor Response Spectra - RSW Top in Z-Direction - Case RFB

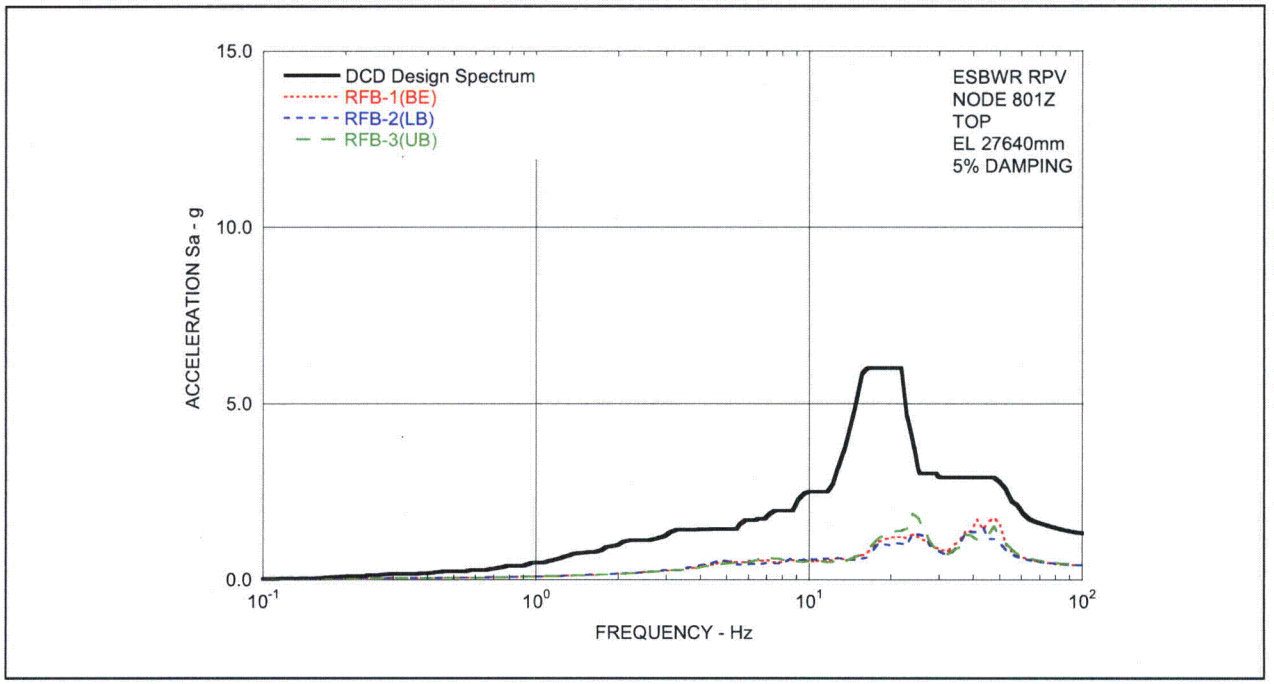

Figure 03.07.02-6(9)e Comparison of Floor Response Spectra - RPV Top in Z-Direction - Case RFB

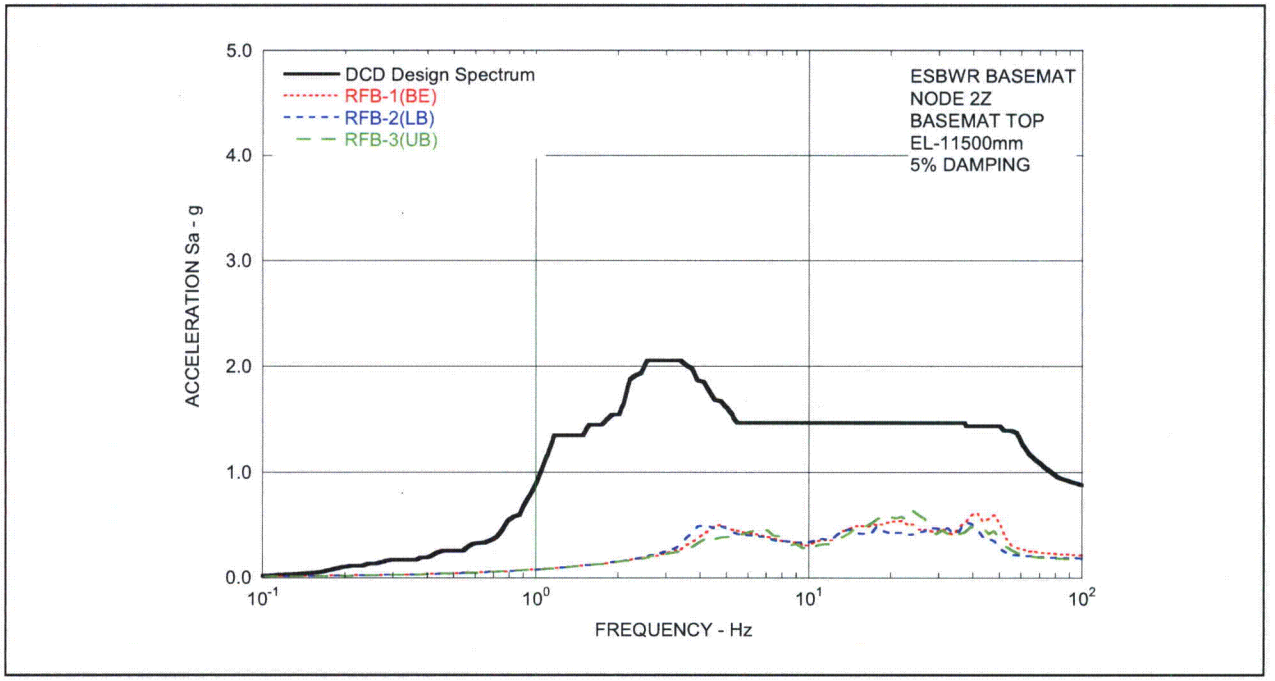

Figure 03.07.02-6(9)f Comparison of Floor Response Spectra - RB/FB Basemat in Z-Direction - Case RFB

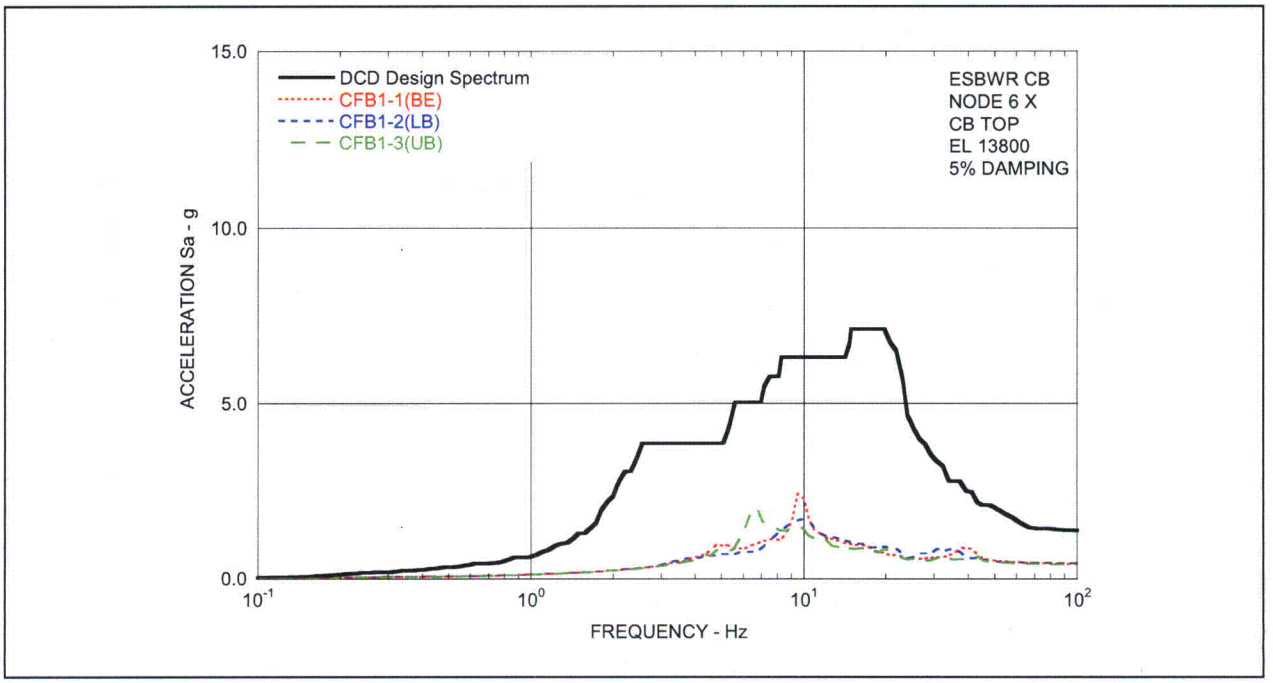

Figure 03.07.02-6(10)a Comparison of Floor Response Spectra - CB Top in X-Direction - Case CFB1

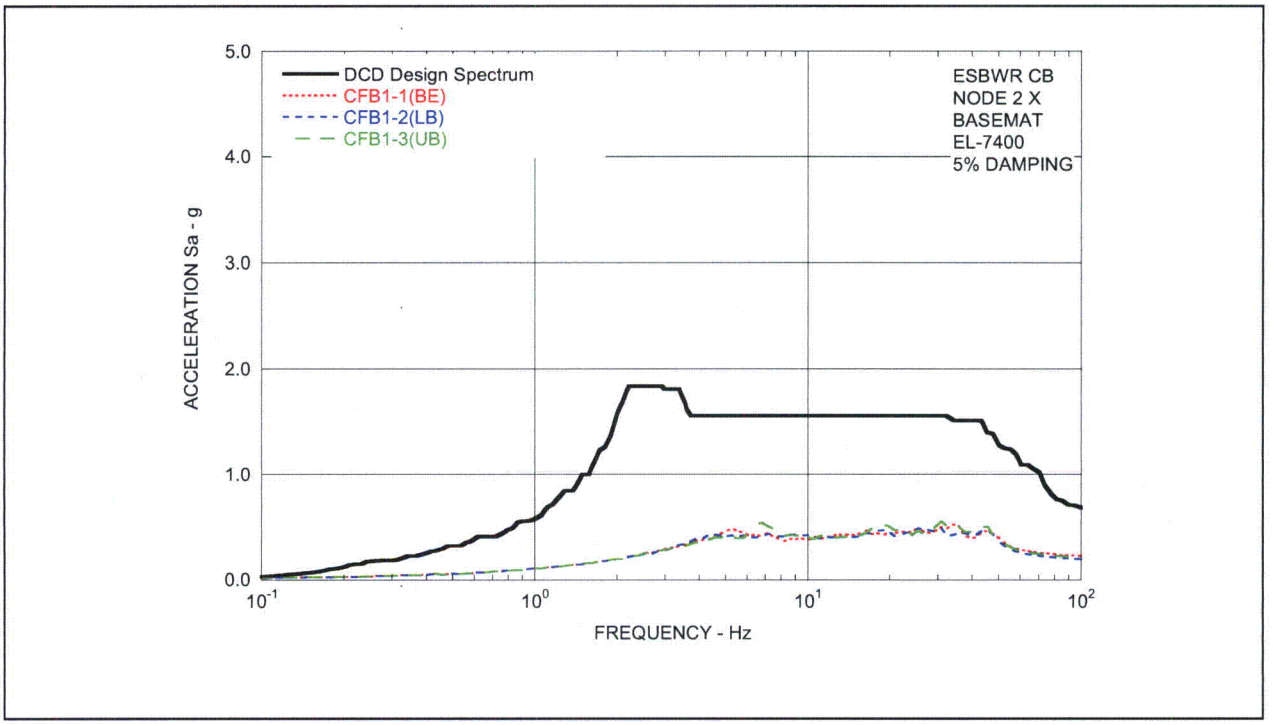

Figure 03.07.02-6(10)b Comparison of Floor Response Spectra - CB Basemat in X-Direction - Case CFB1

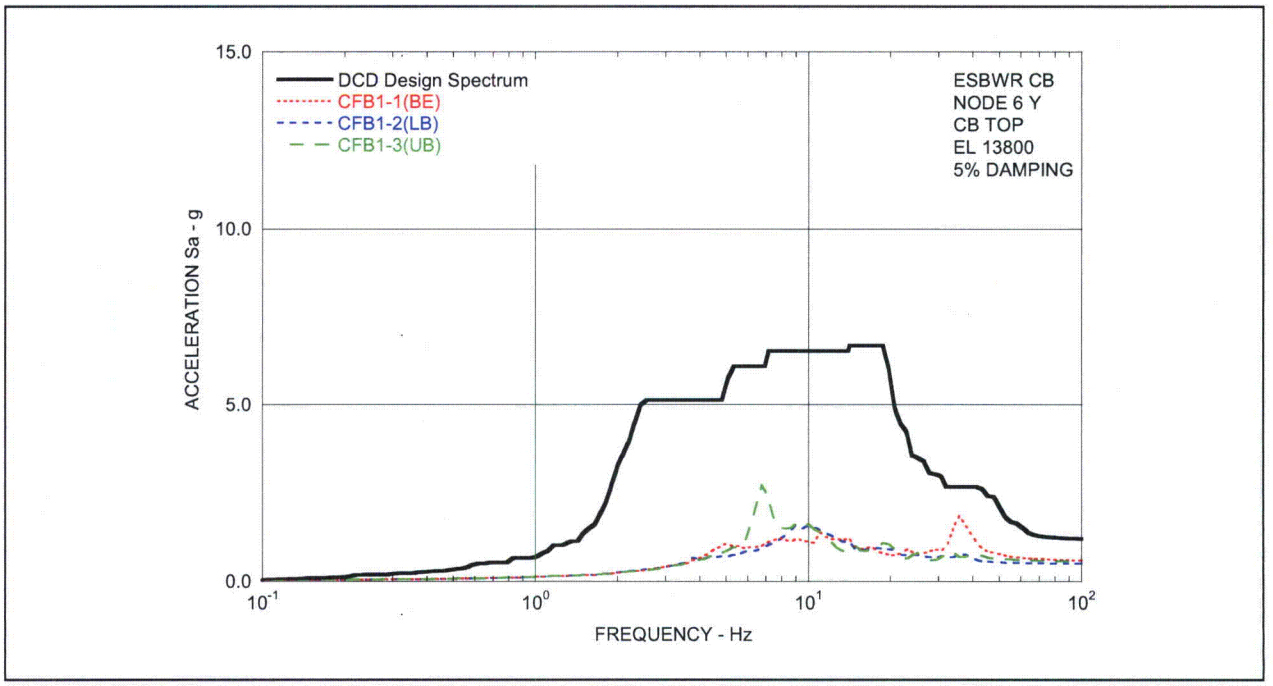

Figure 03.07.02-6(11)a Comparison of Floor Response Spectra - CB Top in Y-Direction - Case CFB1

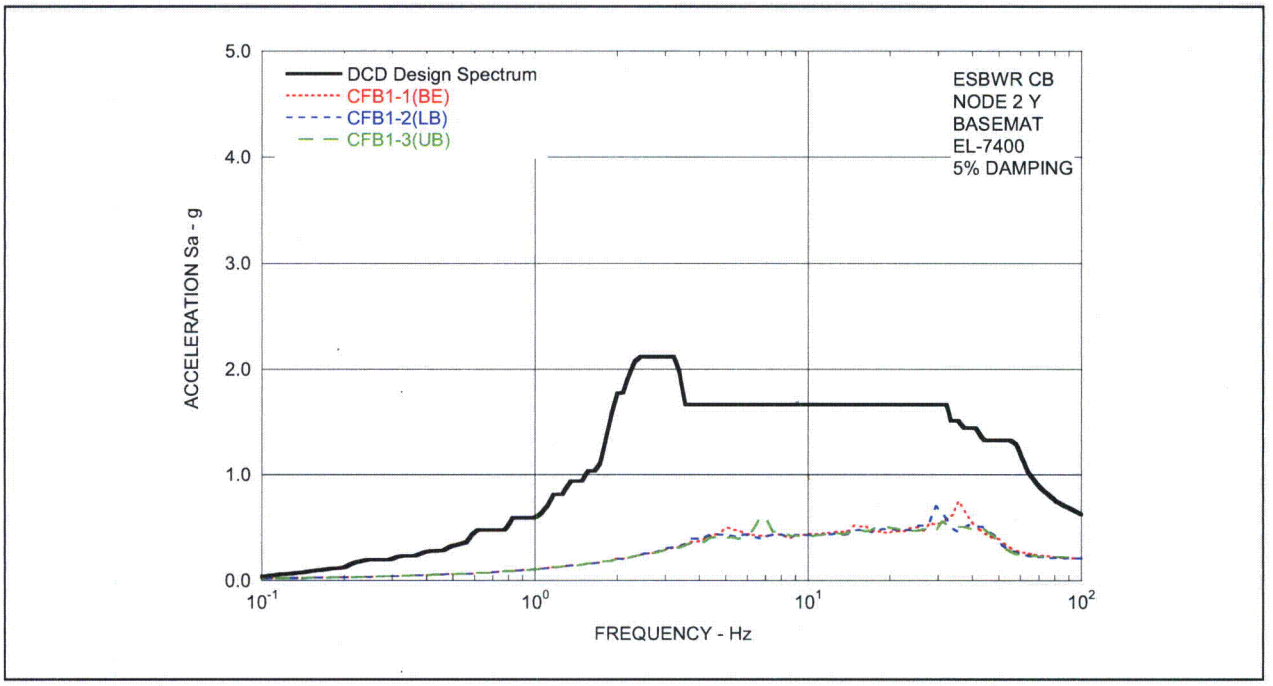

Figure 03.07.02-6(11)b Comparison of Floor Response Spectra - CB Basemat in Y-Direction - Case CFB1

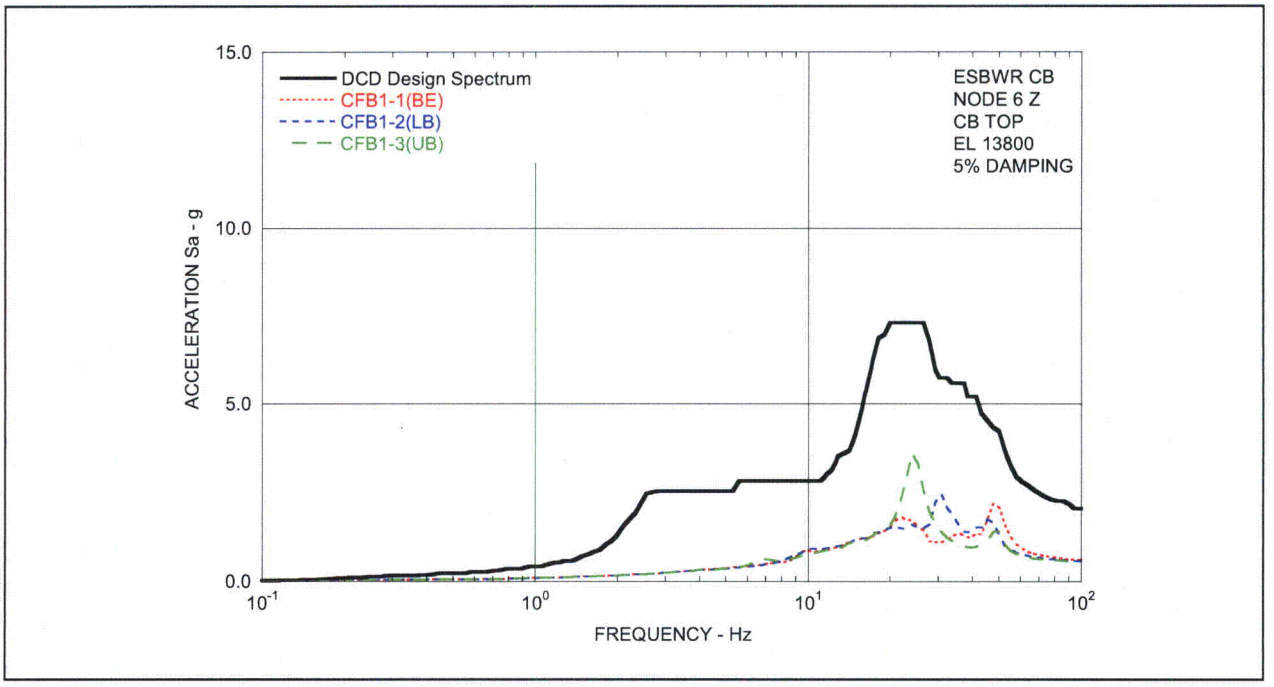

Figure 03.07.02-6(12)a Comparison of Floor Response Spectra - CB Top in Z-Direction - Case CFB1

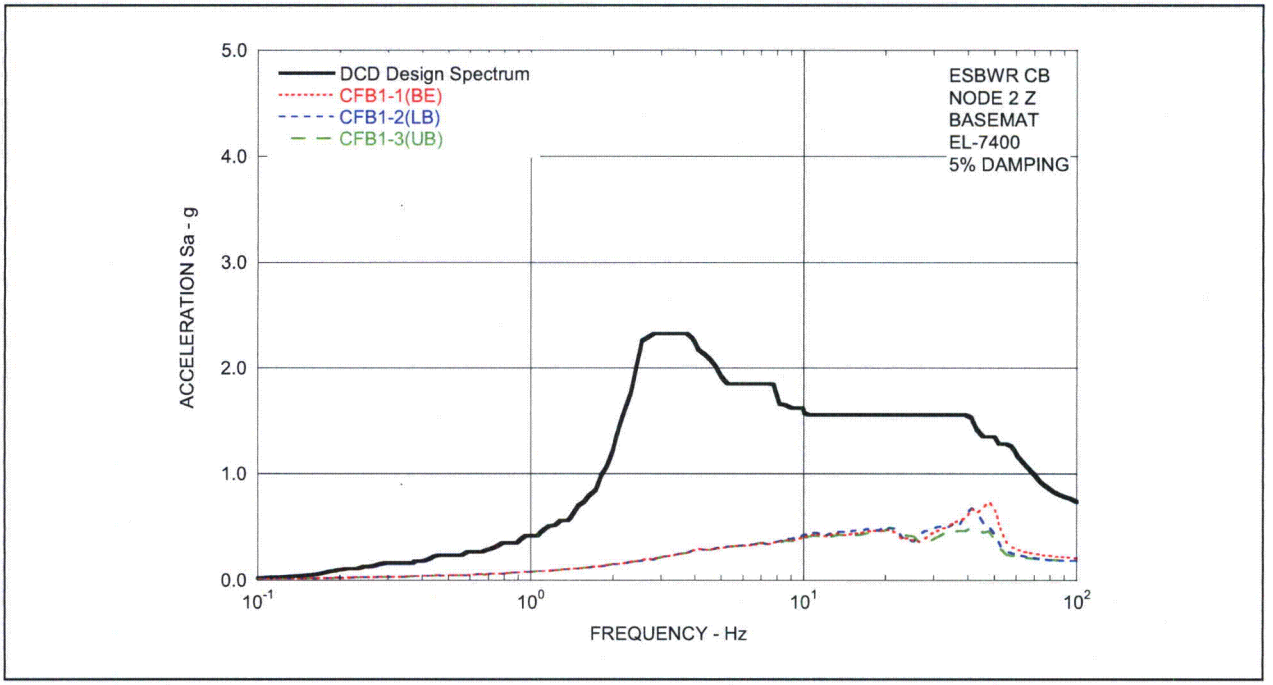

Figure 03.07.02-6(12)b Comparison of Floor Response Spectra - CB Basemat in -Z-Direction - Case CFB1

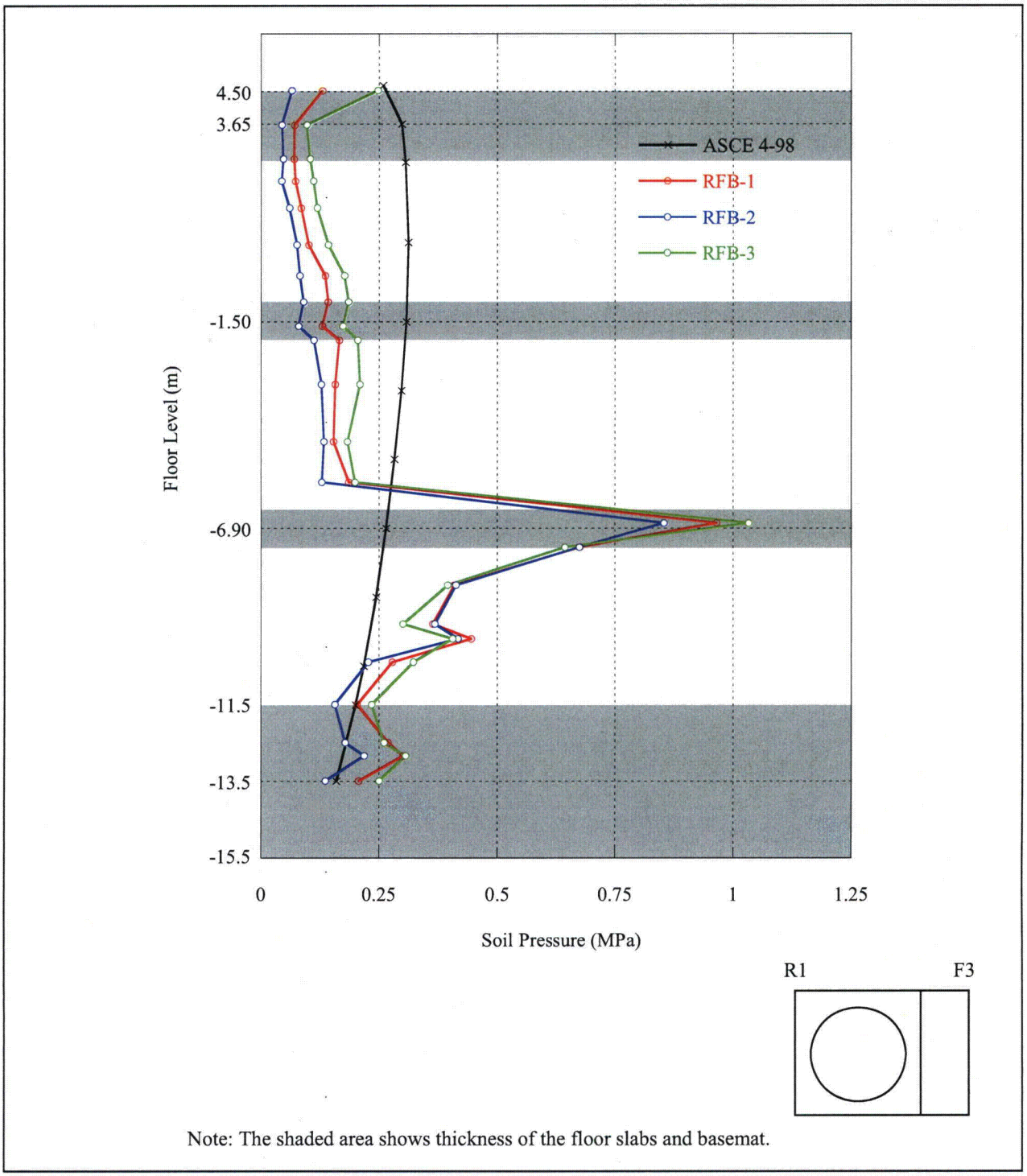

Note: The shaded area shows thickness of the floor slabs and basemat.

Figure 03.07.02-6(13)a Lateral Soil Pressure - RB/FB R1 Wall – Case RFB

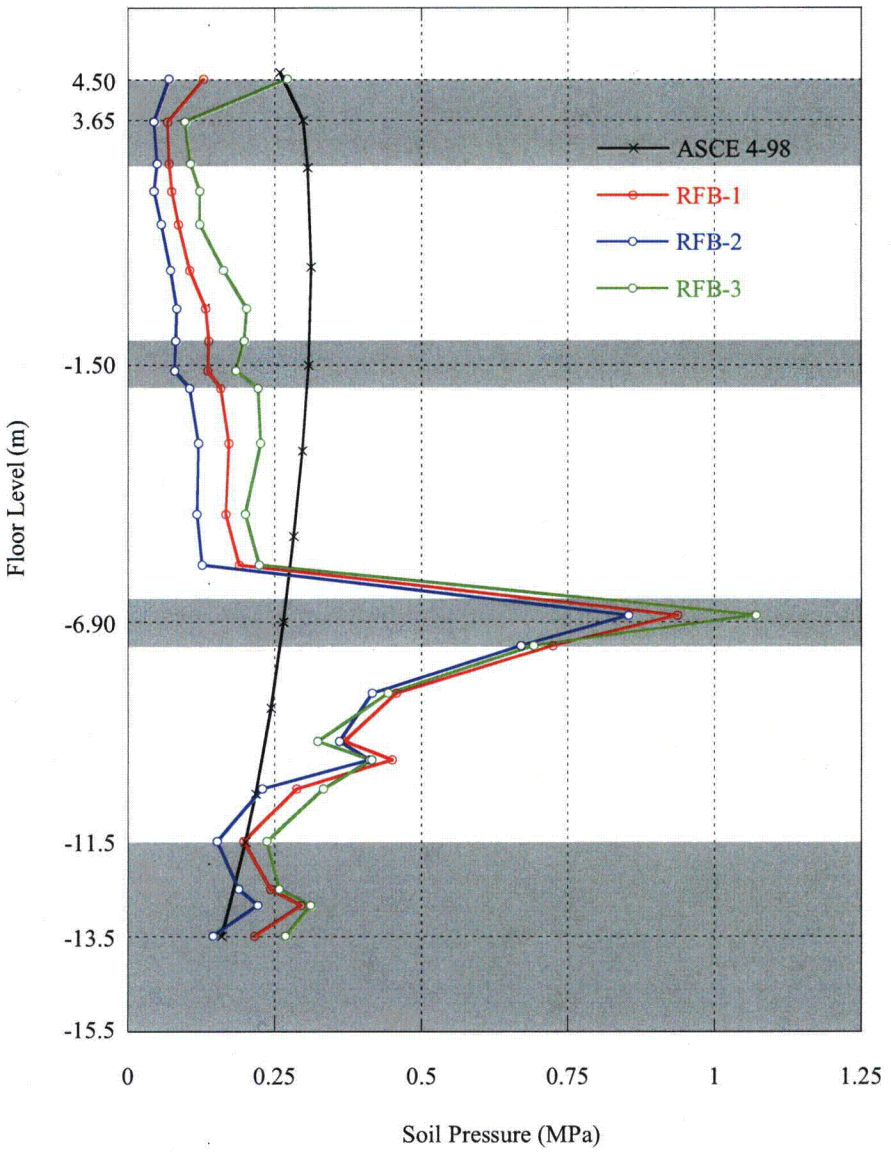

Note: The shaded area shows thickness of the floor slabs and basemat.

Figure 03.07.02-6(13)b Lateral Soil Pressure - RB/FB F3 Wall – Case RFB

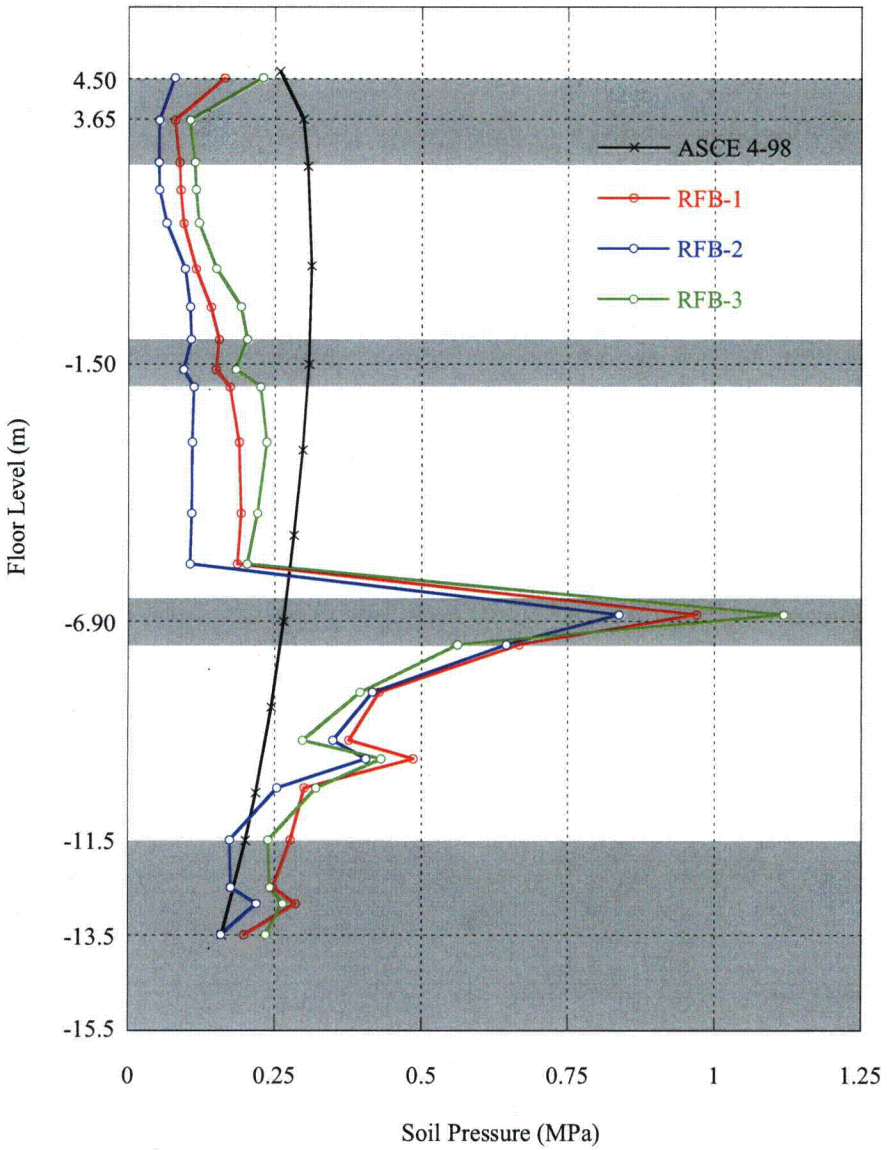

Note: The shaded area shows thickness of the floor slabs and basemat.

Figure 03.07.02-6(13)c Lateral Soil Pressure - RB/FB RA Wall – Case RFB

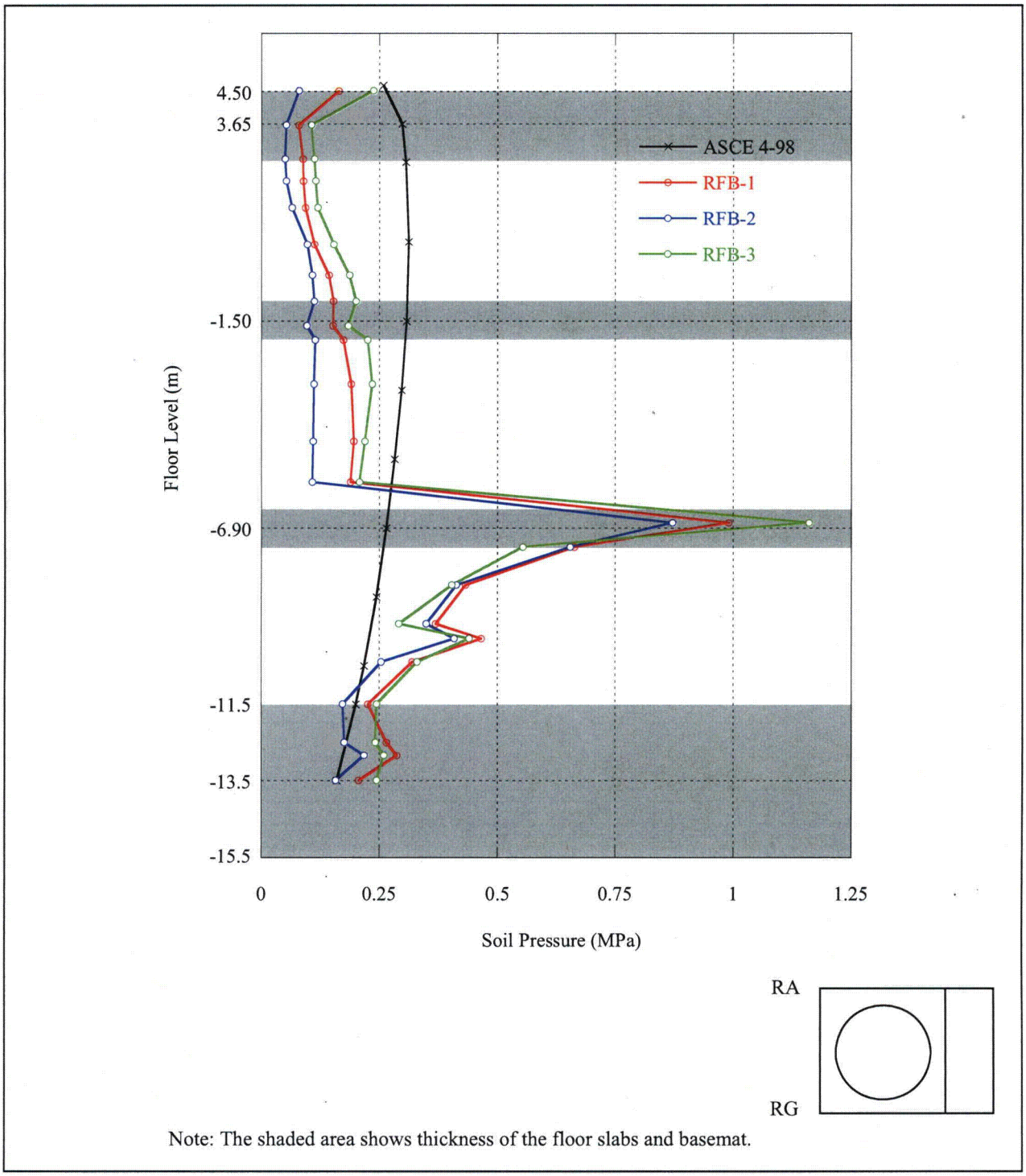

Note: The shaded area shows thickness of the floor slabs and basemat.

Figure 03.07.02-6(13)d Lateral Soil Pressure - RB/FB RG Wall – Case RFB

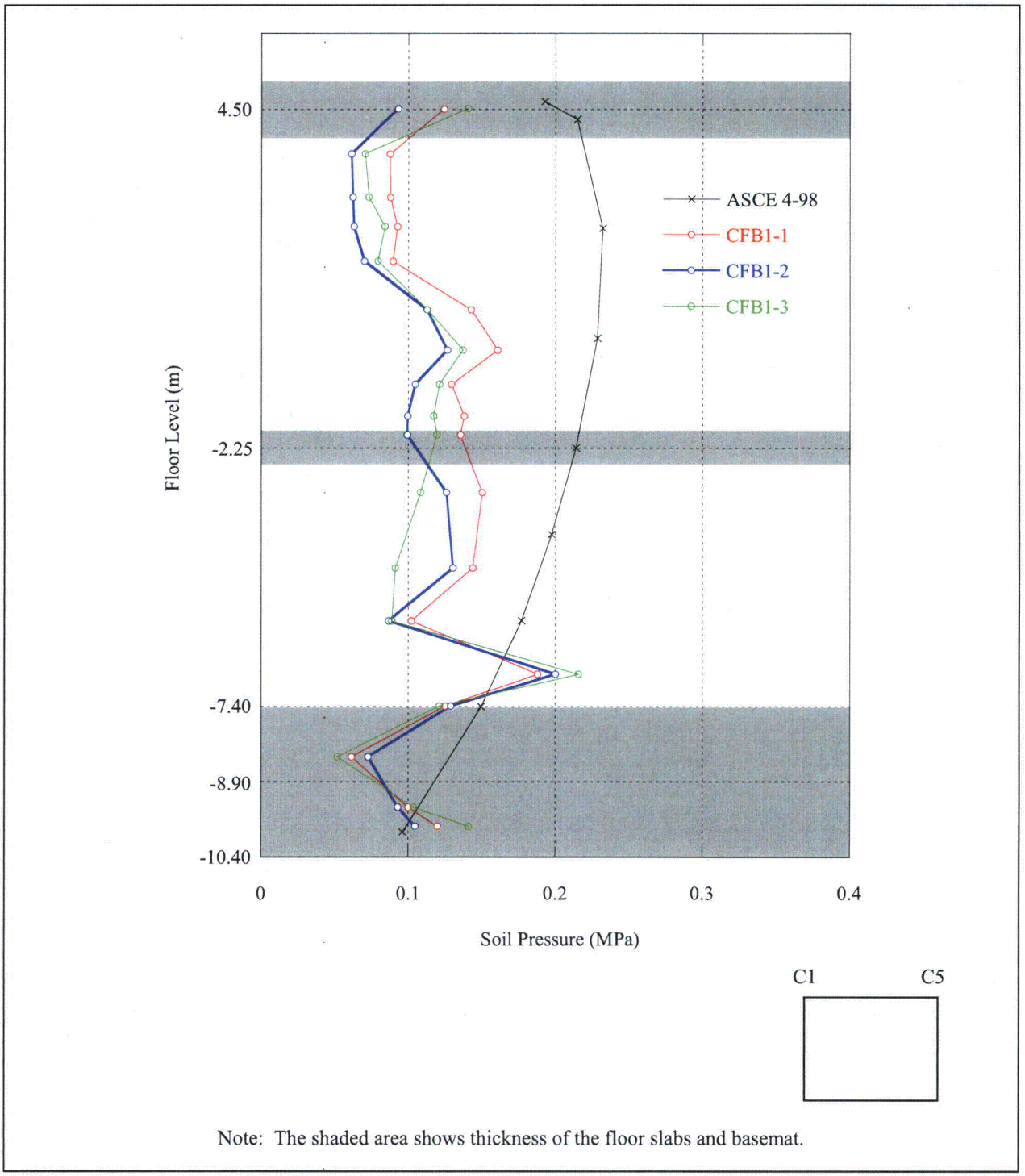

Note: The shaded area shows thickness of the floor slabs and basemat.

Figure 03.07.02-6(14)a Lateral Soil Pressure - CB C1 Wall – Case CFB1

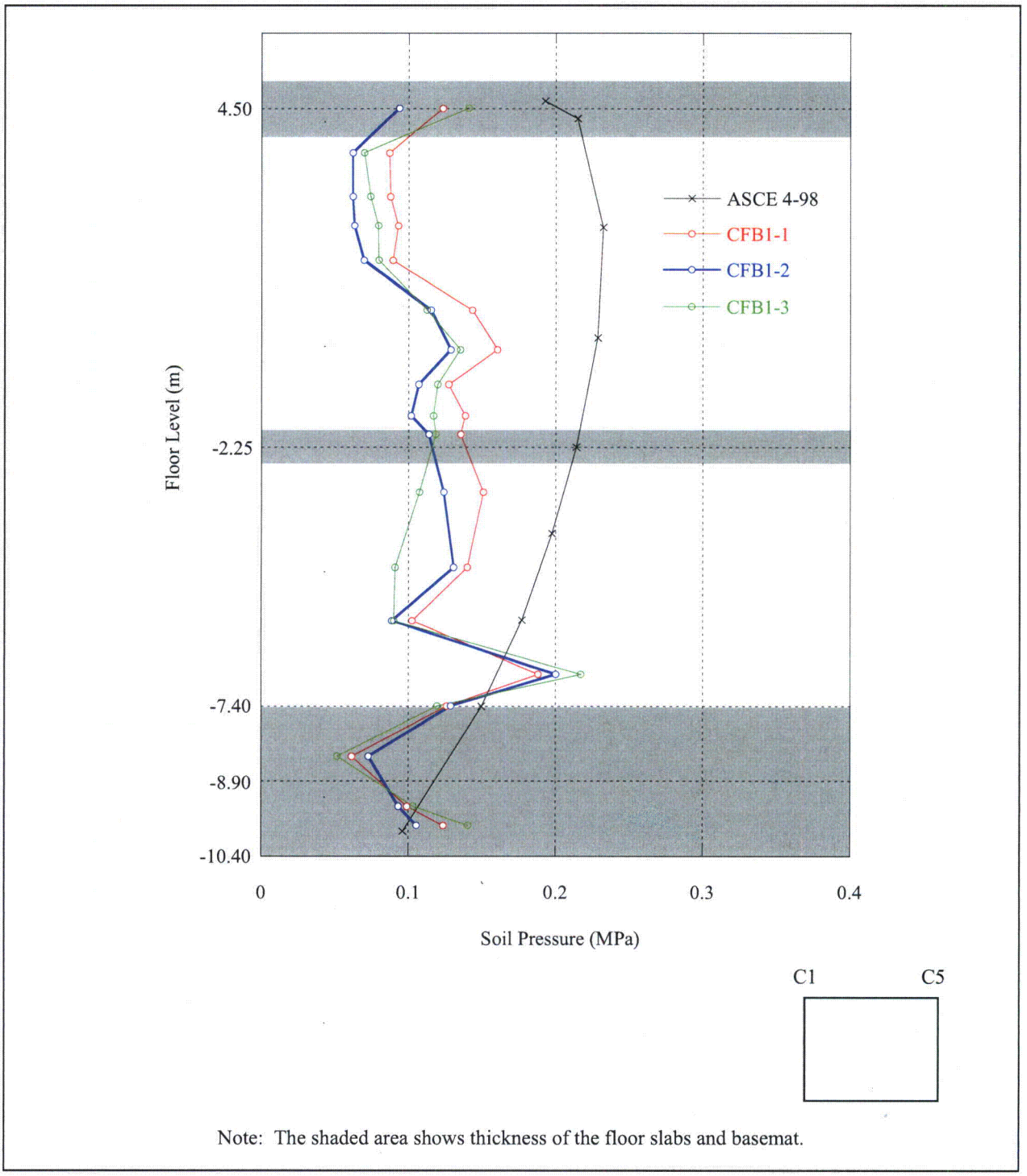

Figure 03.07.02-6(14)b Lateral Soil Pressure - CB C5 Wall – Case CFB1

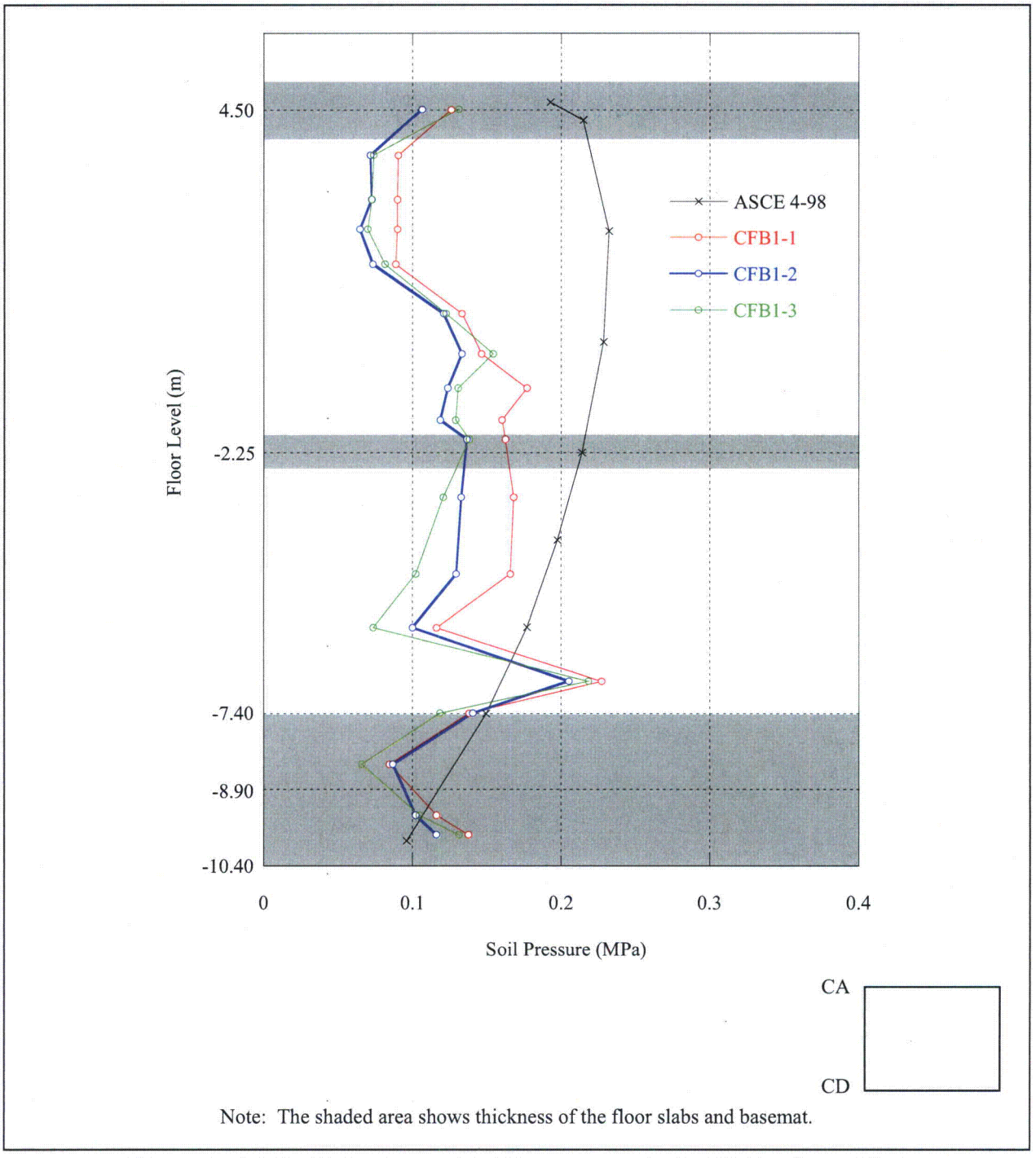

Figure 03.07.02-6(14)c Lateral Soil Pressure - CB CA Wall – Case CFB1

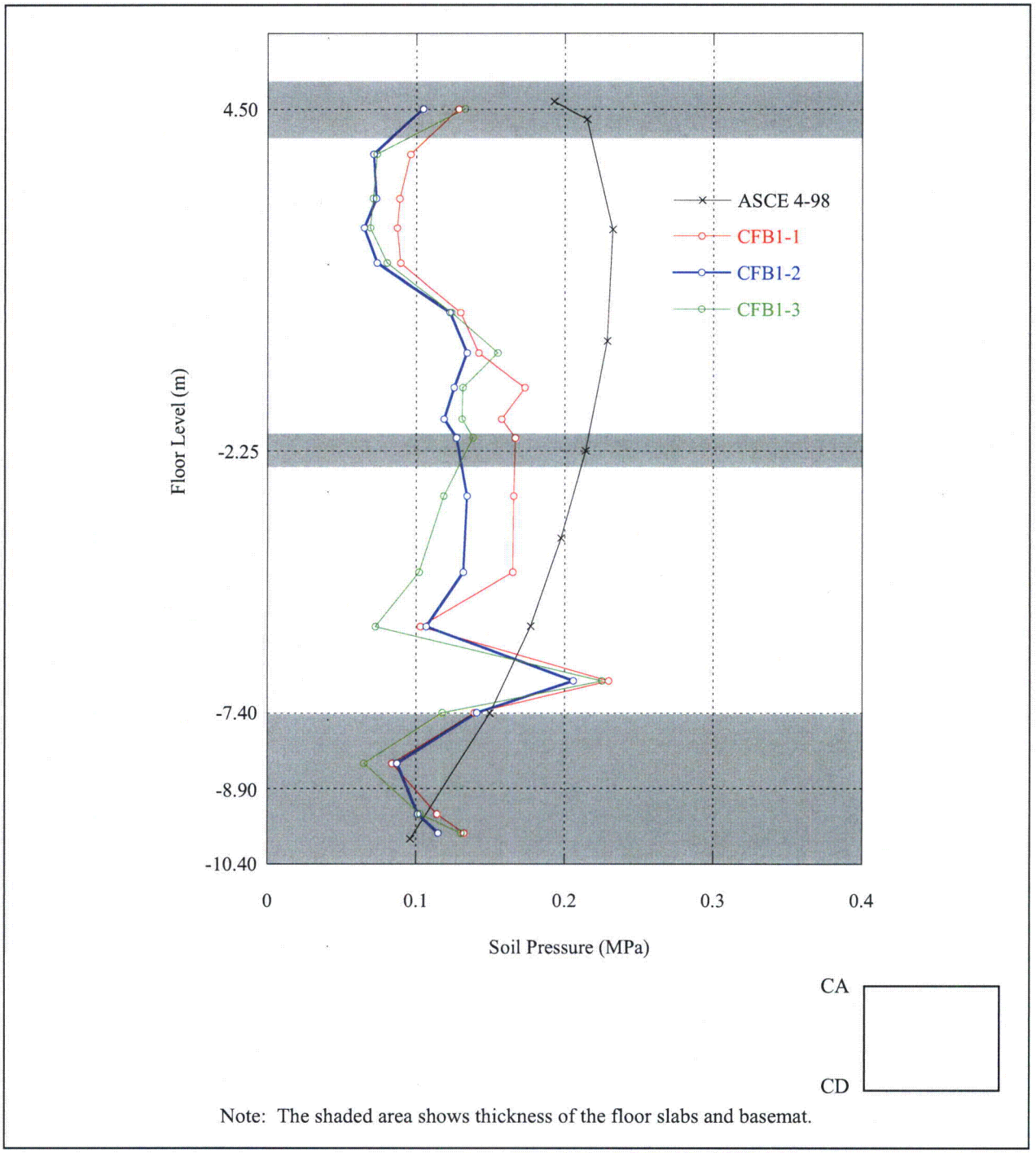

Figure 03.07.02-6(14)d Lateral Soil Pressure - CB CD Wall – Case CFB1

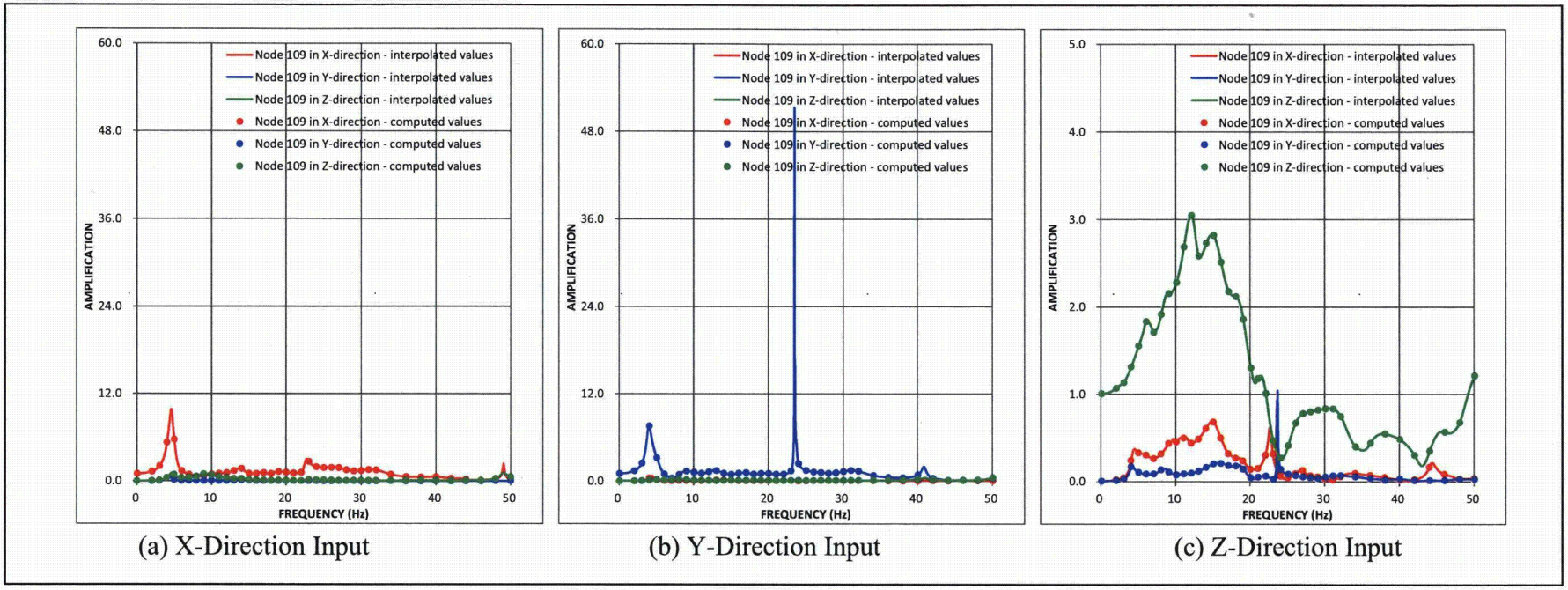

Figure 03.07.02-6(15)a Transfer functions – RB/FB Refueling Floor at Best Estimate Subsurface Profile - Case RFB

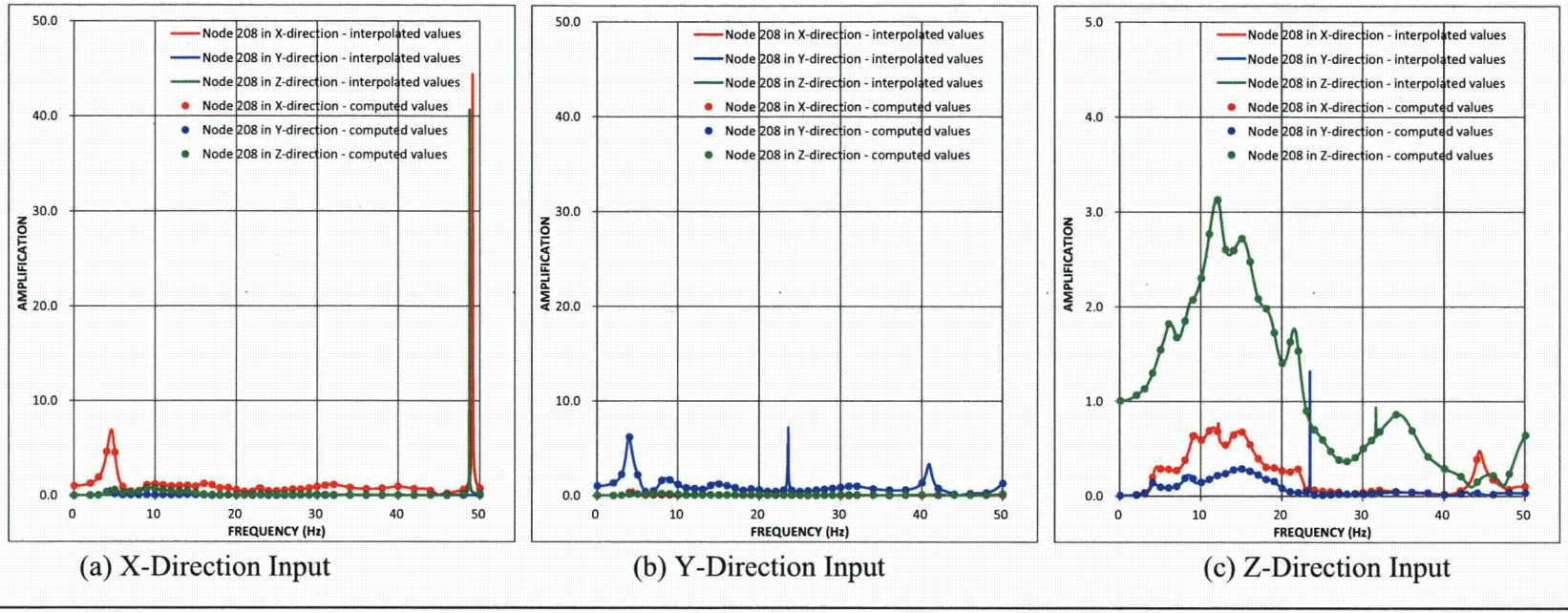

Figure 03.07.02-6(15)b Transfer functions – RCCV Top Slab at Best Estimate Subsurface Profile - Case RFB

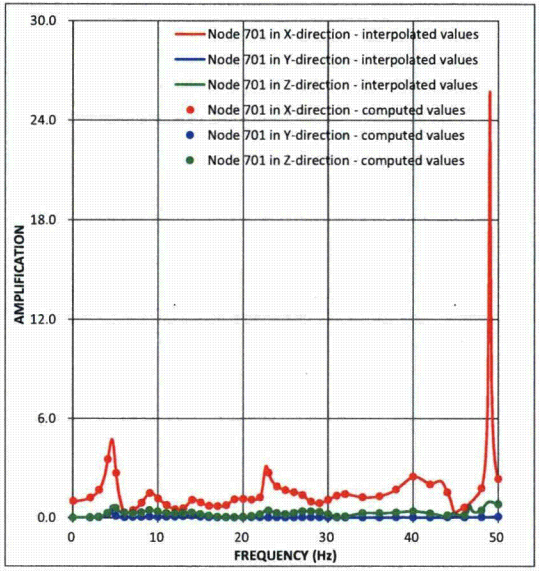

(a) X-Direction Input

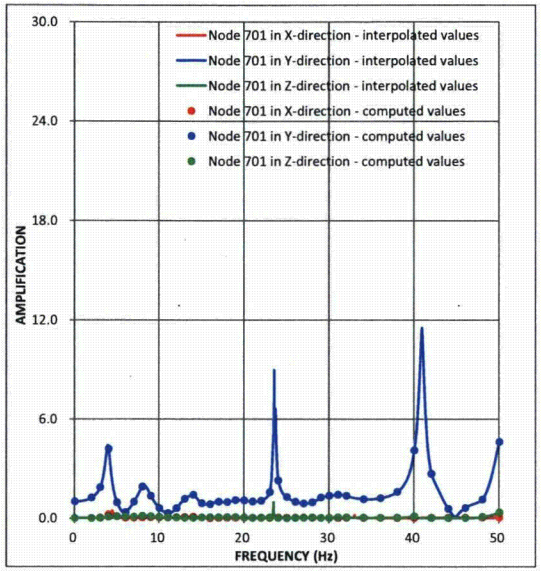

(b) Y-Direction Input

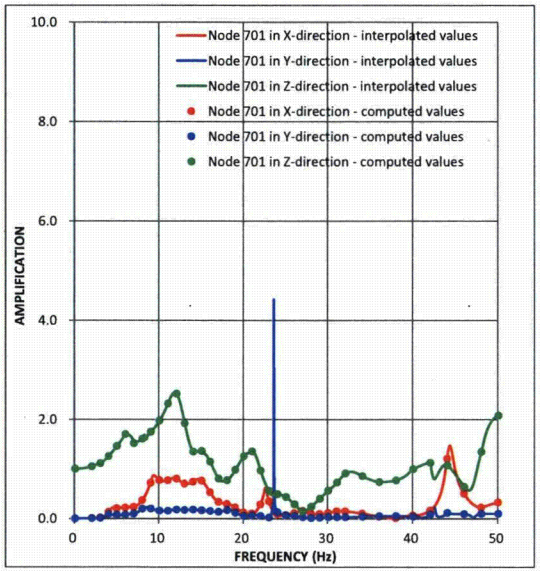

(c) Z-Direction Input

Figure 03.07.02-6(15)c Transfer functions – Vent Wall Top at Best Estimate Subsurface Profile - Case RFB

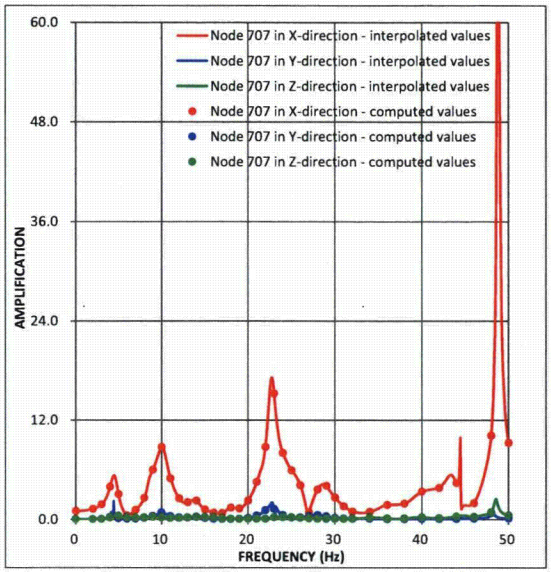

(a) X-Direction Input

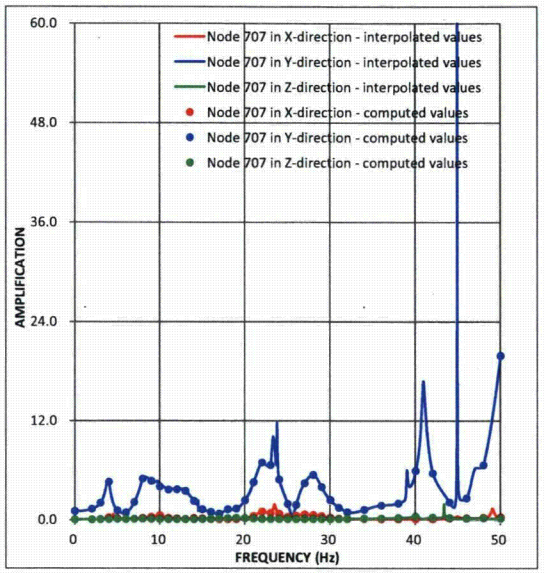

(b) Y-Direction Input

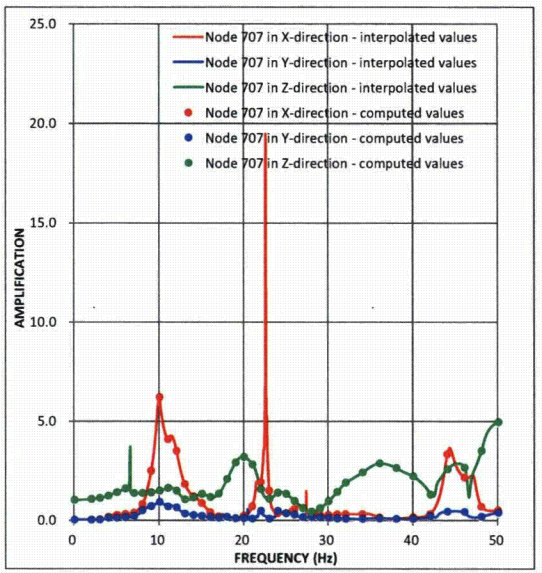

(c) Z-Direction Input

Figure 03.07.02-6(15)d Transfer functions – RSW Top at Best Estimate Subsurface Profile - Case RFB

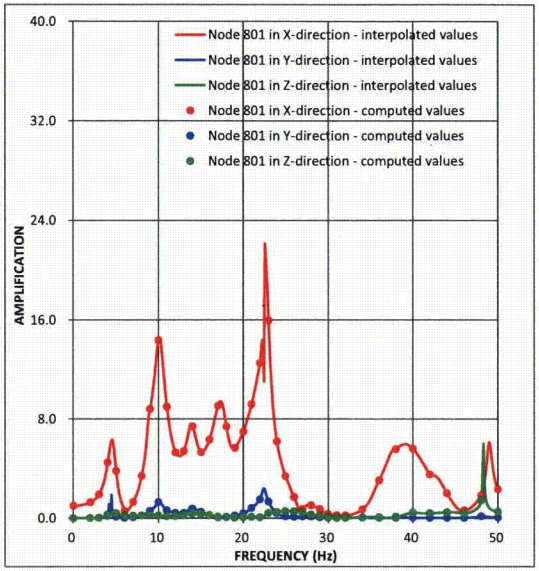

(a) X-Direction Input

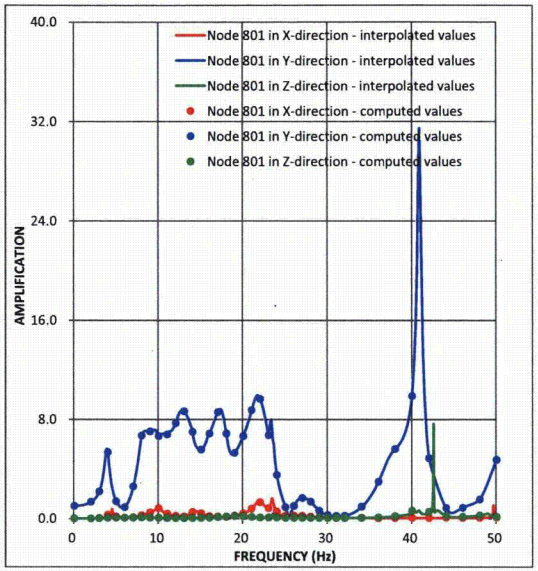

(b) Y-Direction Input

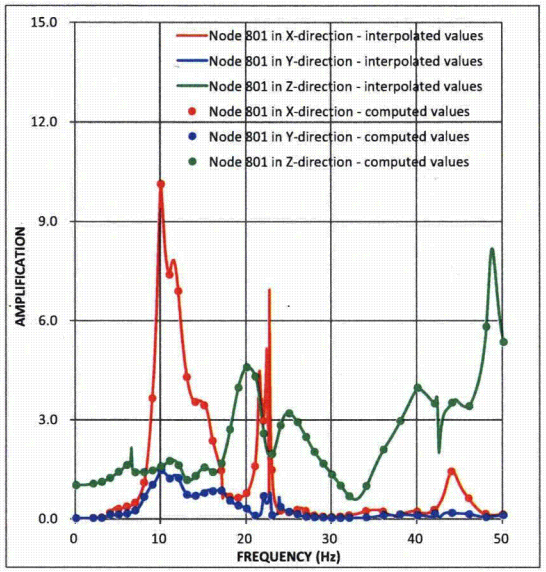

(c) Z-Direction Input

Figure 03.07.02-6(15)e Transfer functions – RPV Top at Best Estimate Subsurface Profile - Case RFB

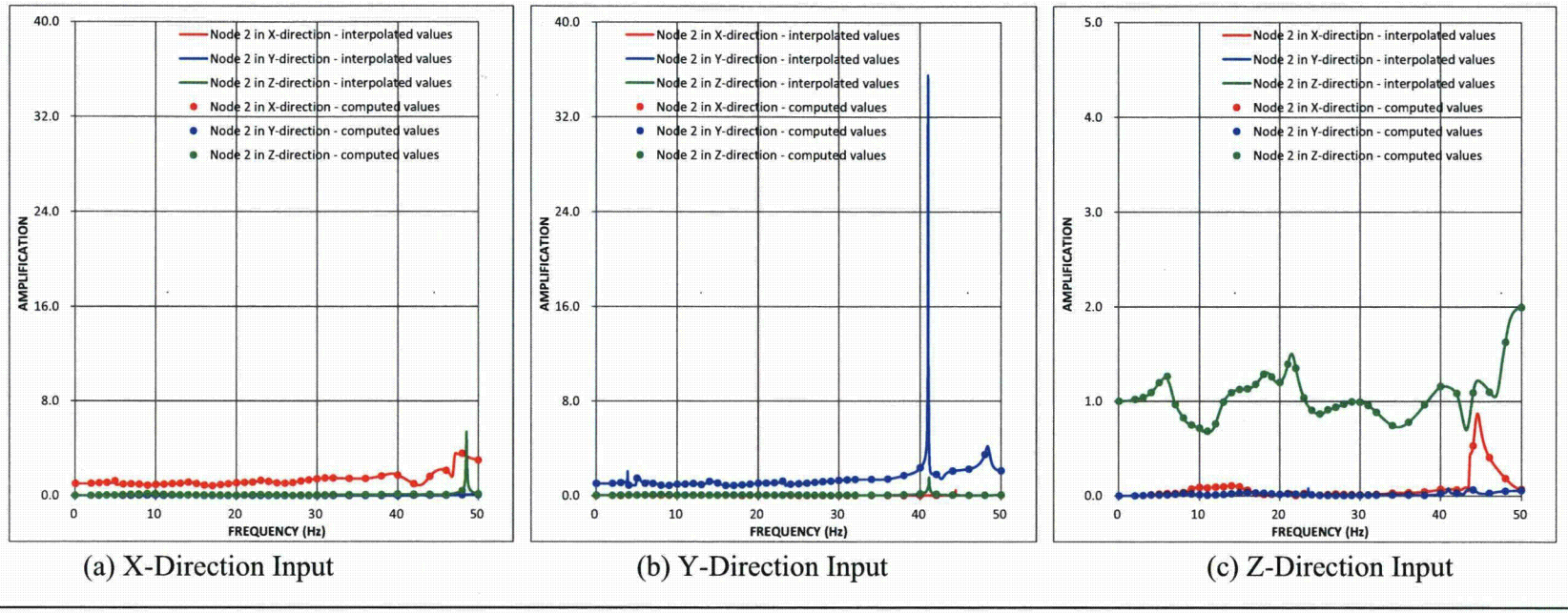

(a) X-Direction Input (b) Y-Direction Input (c) Z-Direction Input

Figure 03.07.02-6(15)f Transfer functions – RB/FB Basemat at Best Estimate Subsurface Profile - Case RFB

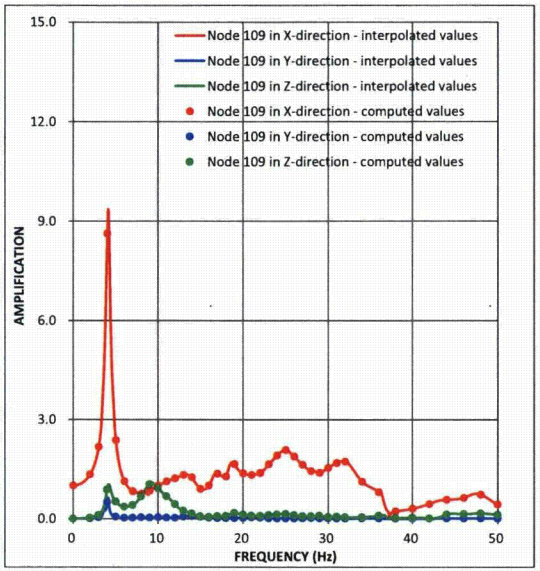

(a) X-Direction Input

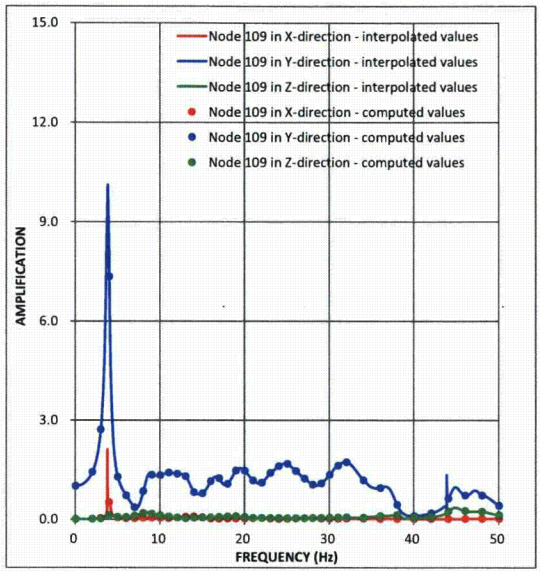

(b) Y-Direction Input

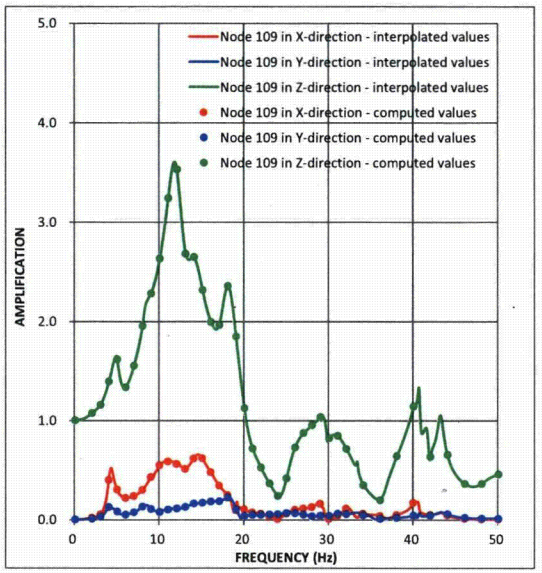

(c) Z-Direction Input

Figure 03.07.02-6(16)a Transfer functions – RB/FB Refueling Floor at Lower Bound Subsurface Profile - Case RFB

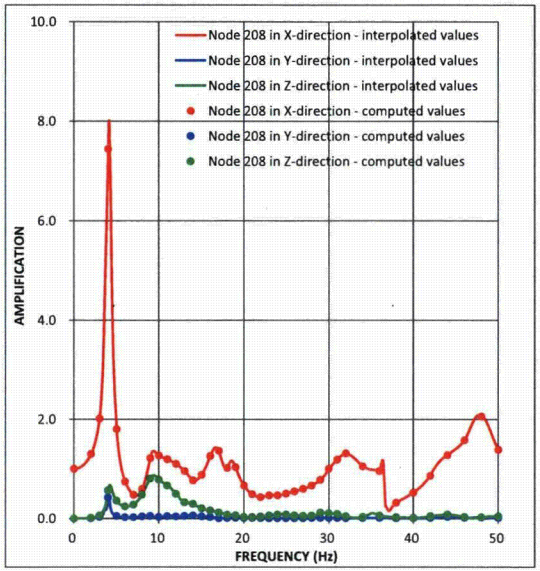

(a) X-Direction Input

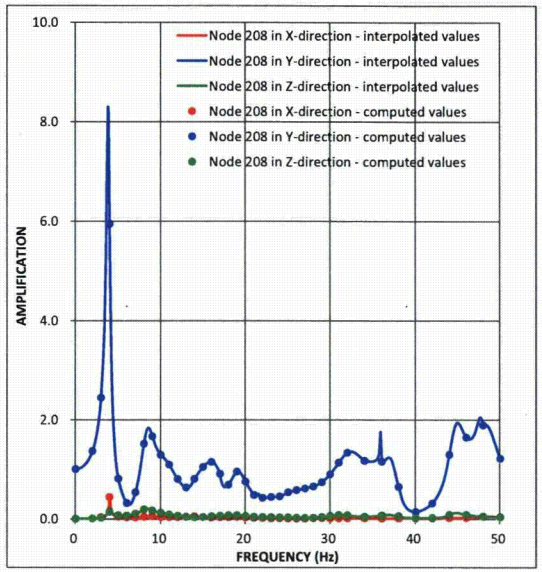

(b) Y-Direction Input

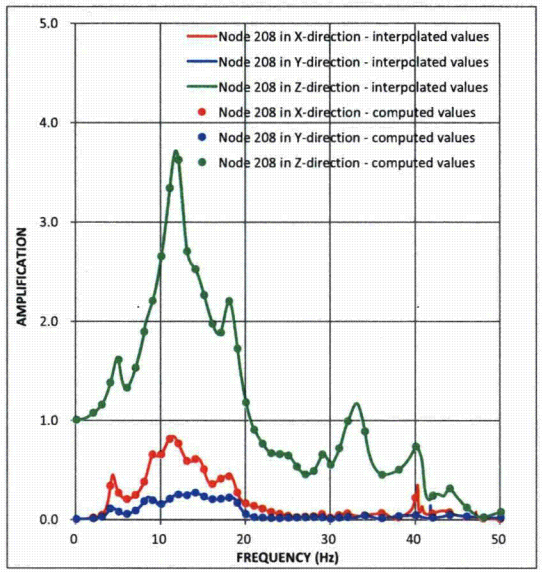

(c) Z-Direction Input

Figure 03.07.02-6(16)b Transfer functions – RCCV Top Slab at Lower Bound Subsurface Profile - Case RFB

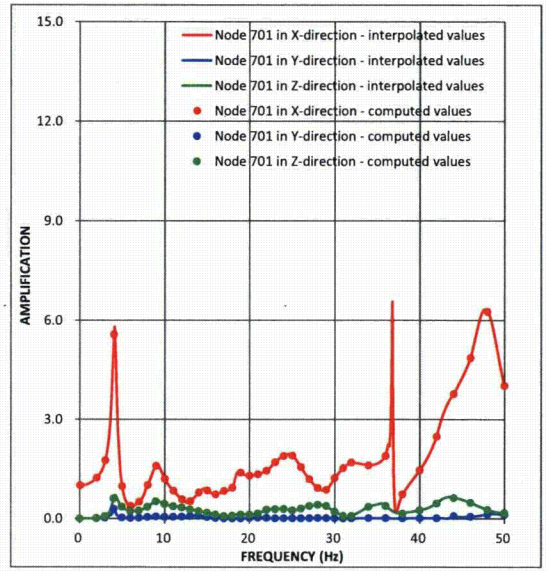

(a) X-Direction Input

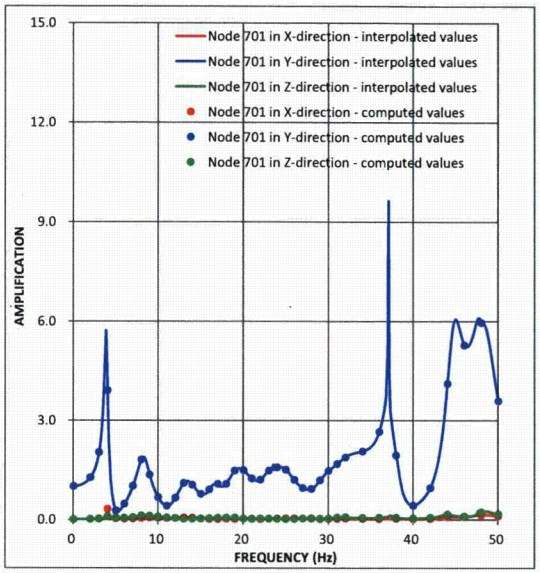

(b) Y-Direction Input

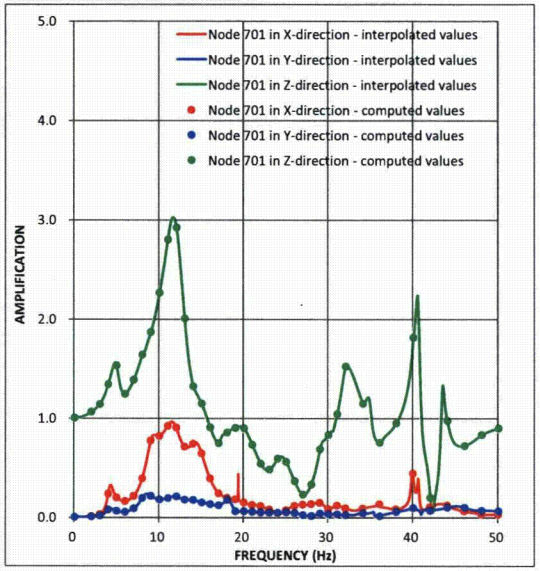

(c) Z-Direction Input

Figure 03.07.02-6(16)c Transfer functions – Vent Wall Top at Lower Bound Subsurface Profile - Case RFB

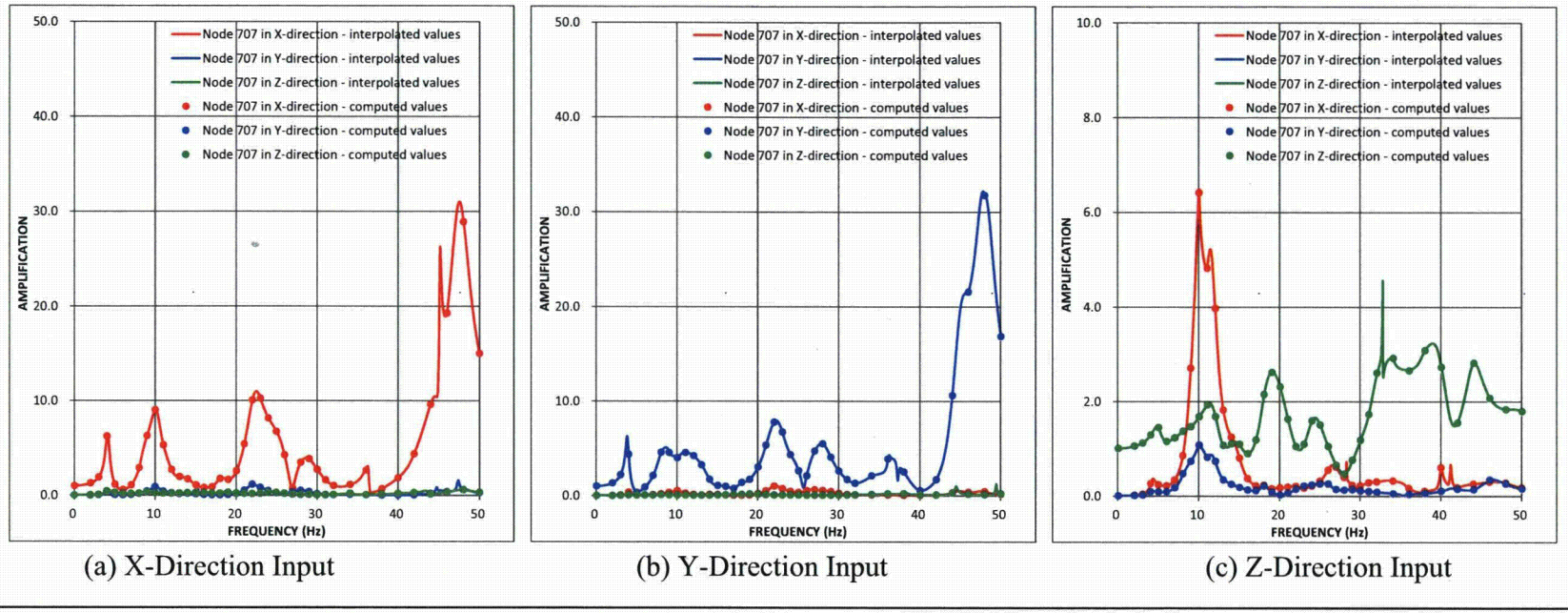

Figure 03.07.02-6(16)d Transfer functions – RSW Top at Lower Bound Subsurface Profile - Case RFB

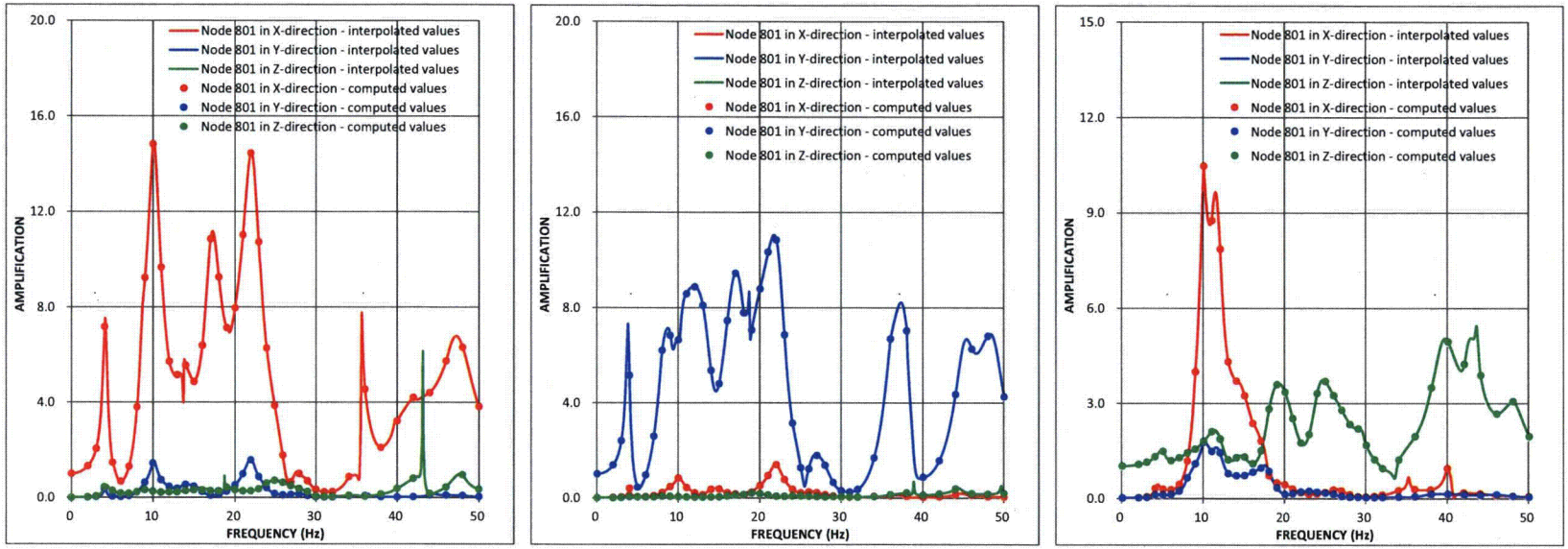

Figure 03.07.02-6(16)e Transfer functions – RPV Top at Lower Bound Subsurface Profile - Case RFB

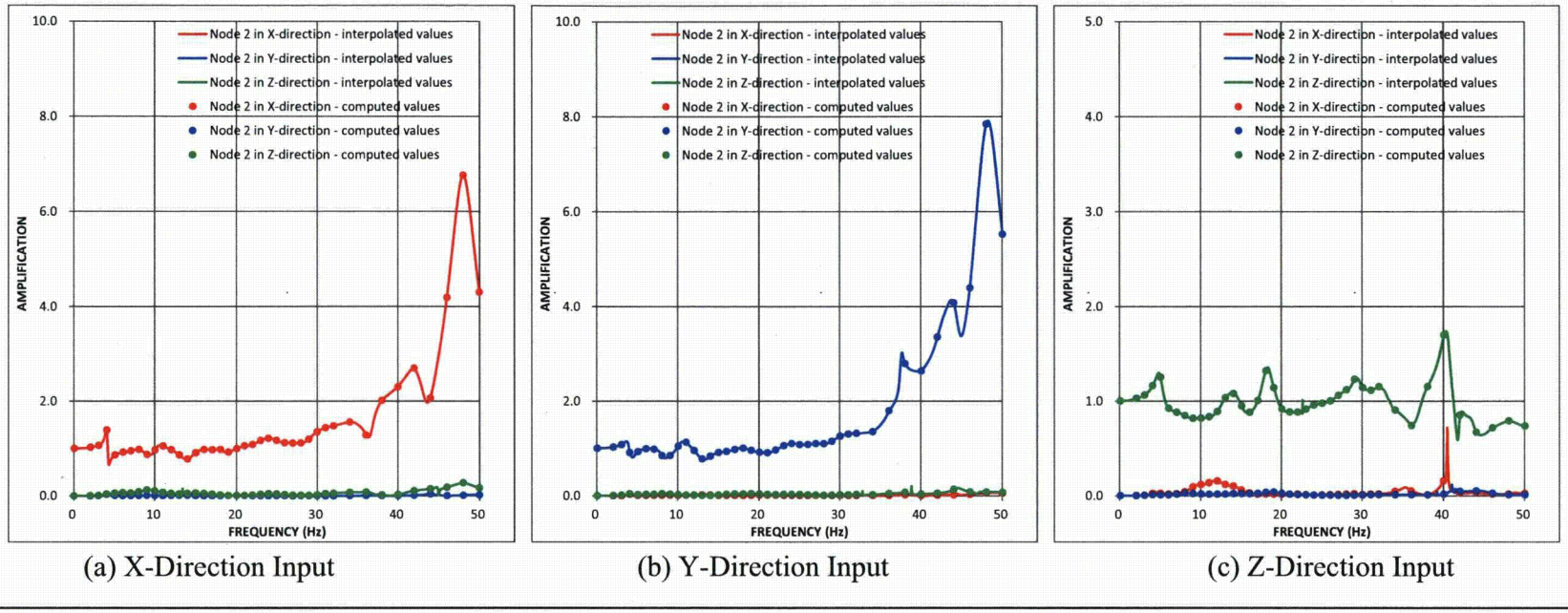

Figure 03.07.02-6(16)f Transfer functions – RB/FB Basemat at Lower Bound Subsurface Profile - Case RFB

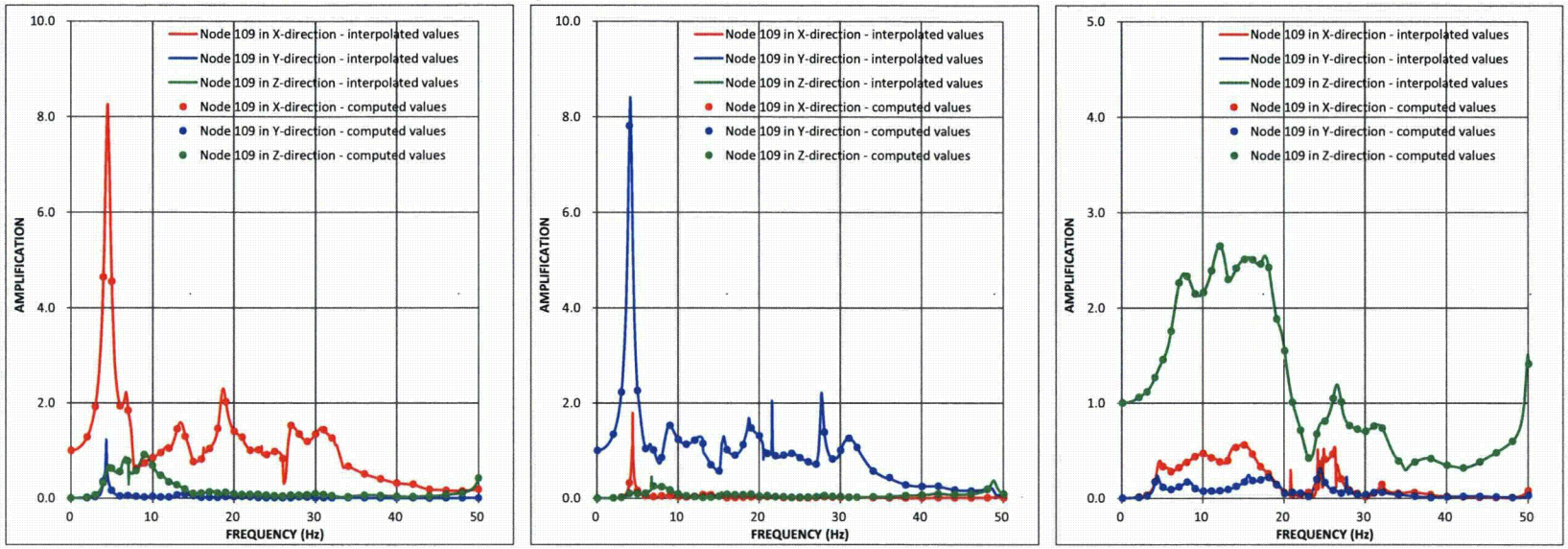

Figure 03.07.02-6(17)a Transfer functions – RB/FB Refueling Floor at Upper Bound Subsurface Profile - Case RFB

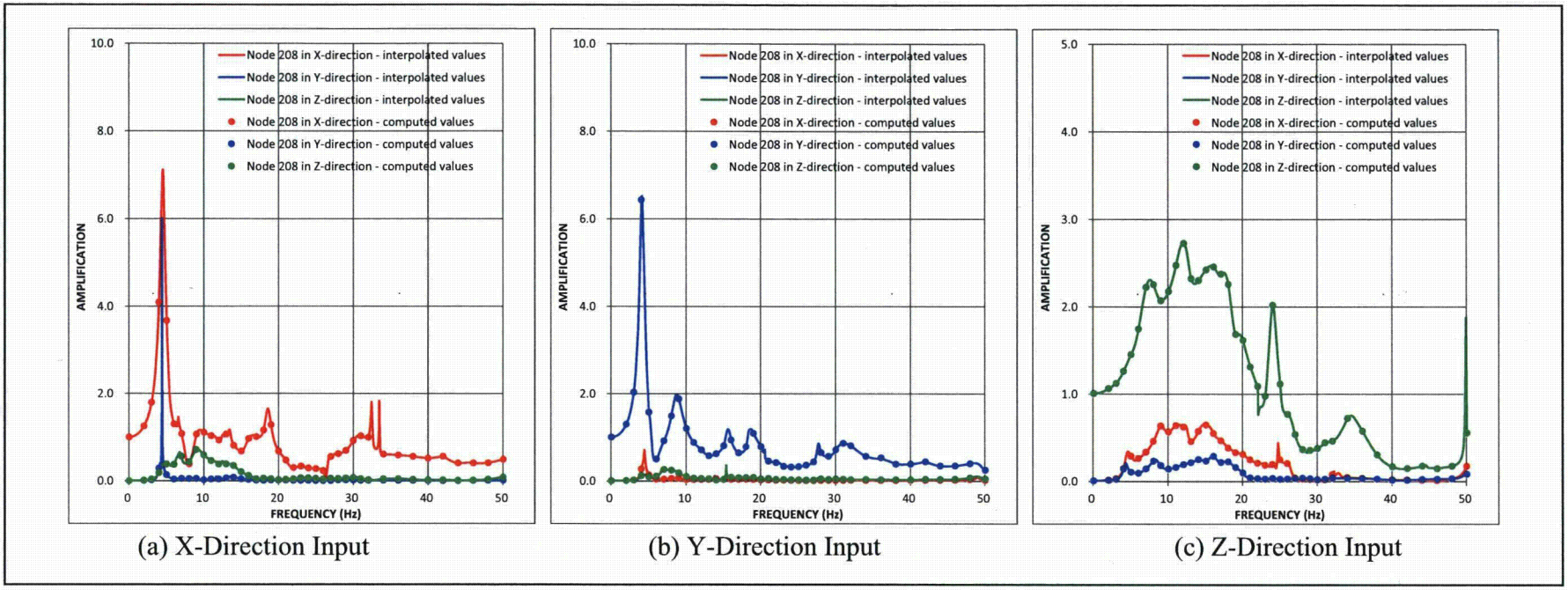

Figure 03.07.02-6(17)b Transfer functions – RCCV Top Slab at Upper Bound Subsurface Profile - Case RFB

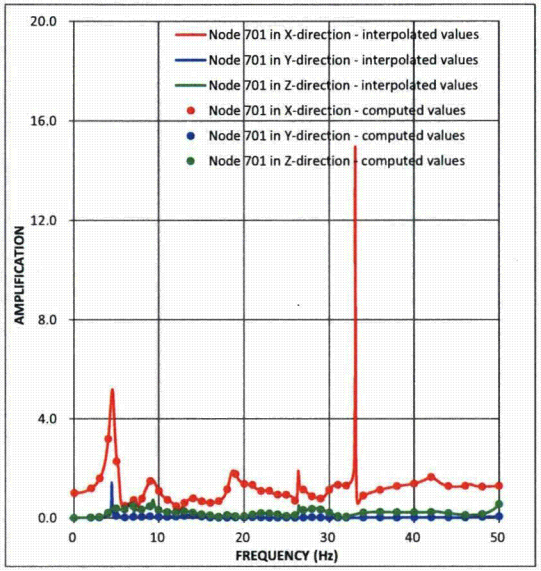

(a) X-Direction Input

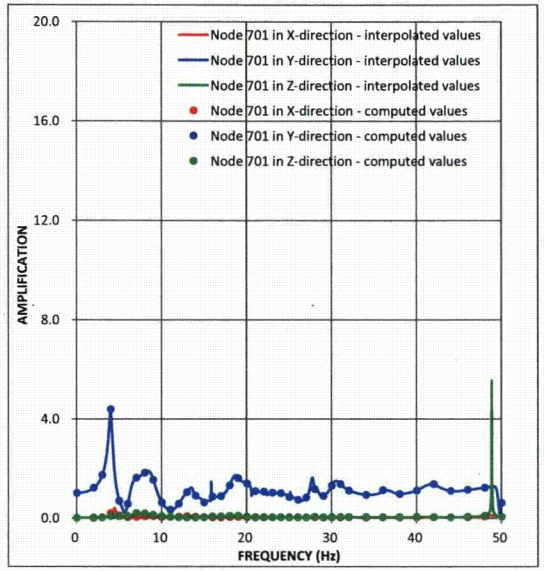

(b) Y-Direction Input

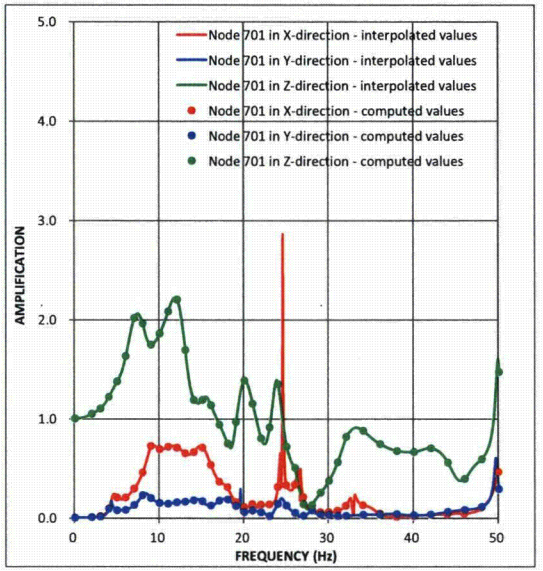

(c) Z-Direction Input

Figure 03.07.02-6(17)c Transfer functions – Vent Wall Top at Upper Bound Subsurface Profile - Case RFB

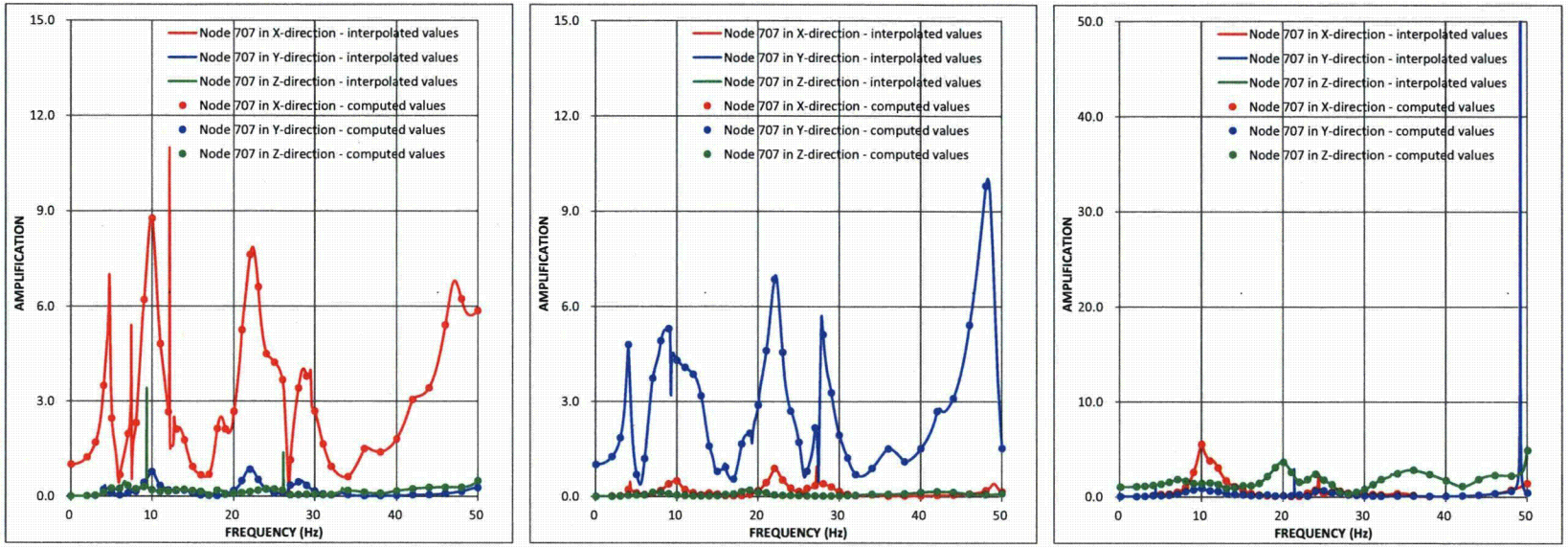

Figure 03.07.02-6(17)d Transfer functions – RSW Top at Upper Bound Subsurface Profile - Case RFB

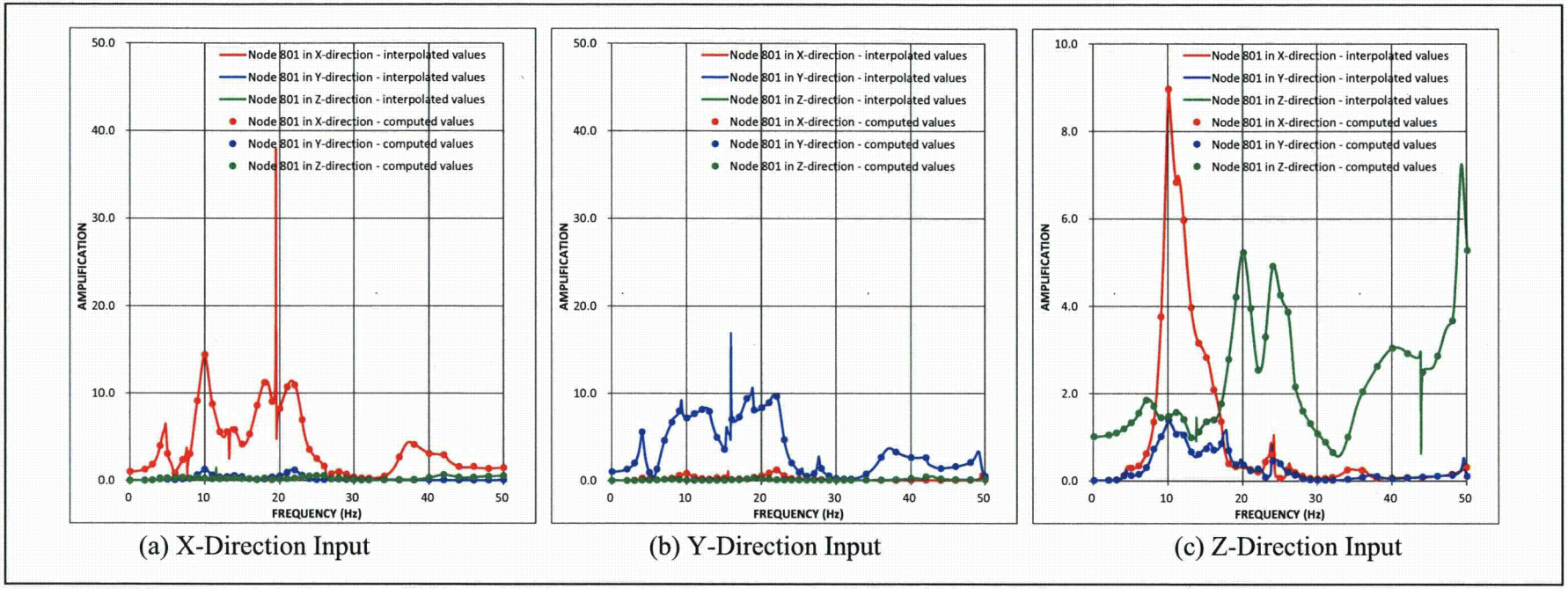

Figure 03.07.02-6(17)e Transfer functions – RPV Top at Upper Bound Subsurface Profile - Case RFB

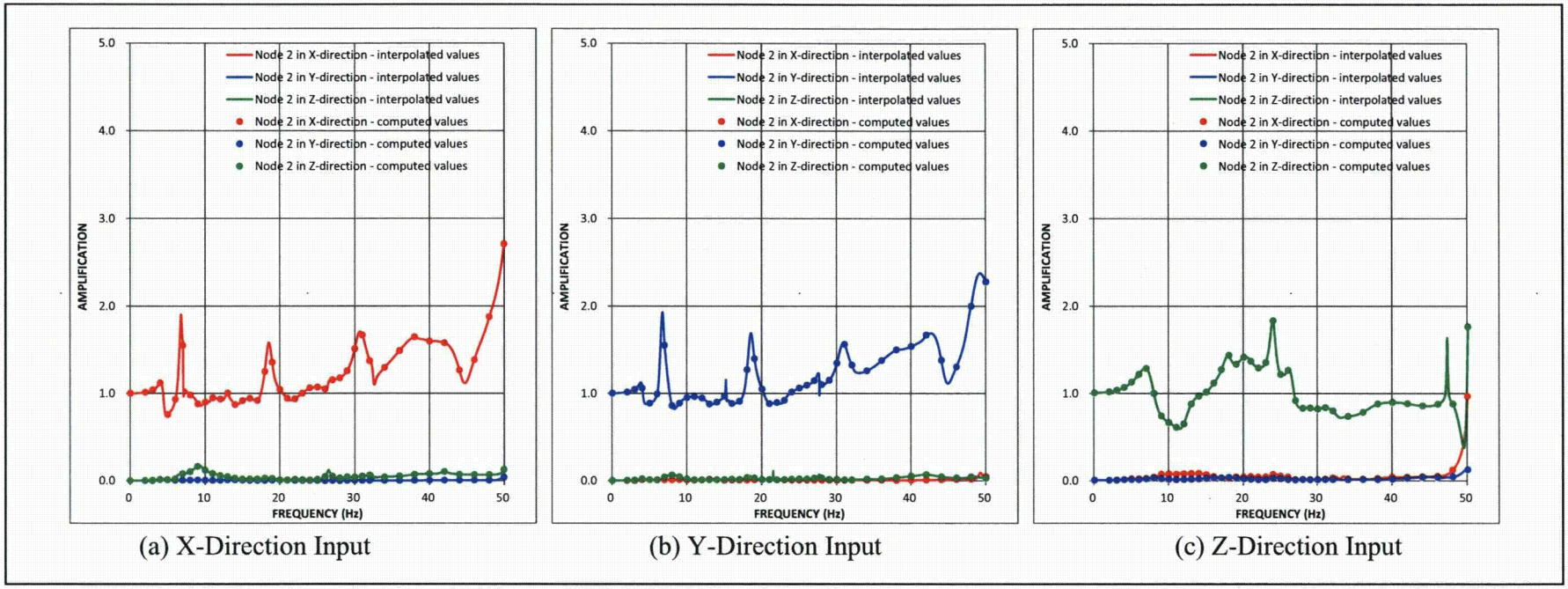

(a) X-Direction Input (b) Y-Direction Input (c) Z-Direction Input

Figure 03.07.02-6(17)f Transfer functions – RB/FB Basemat at Upper Bound Subsurface Profile - Case RFB

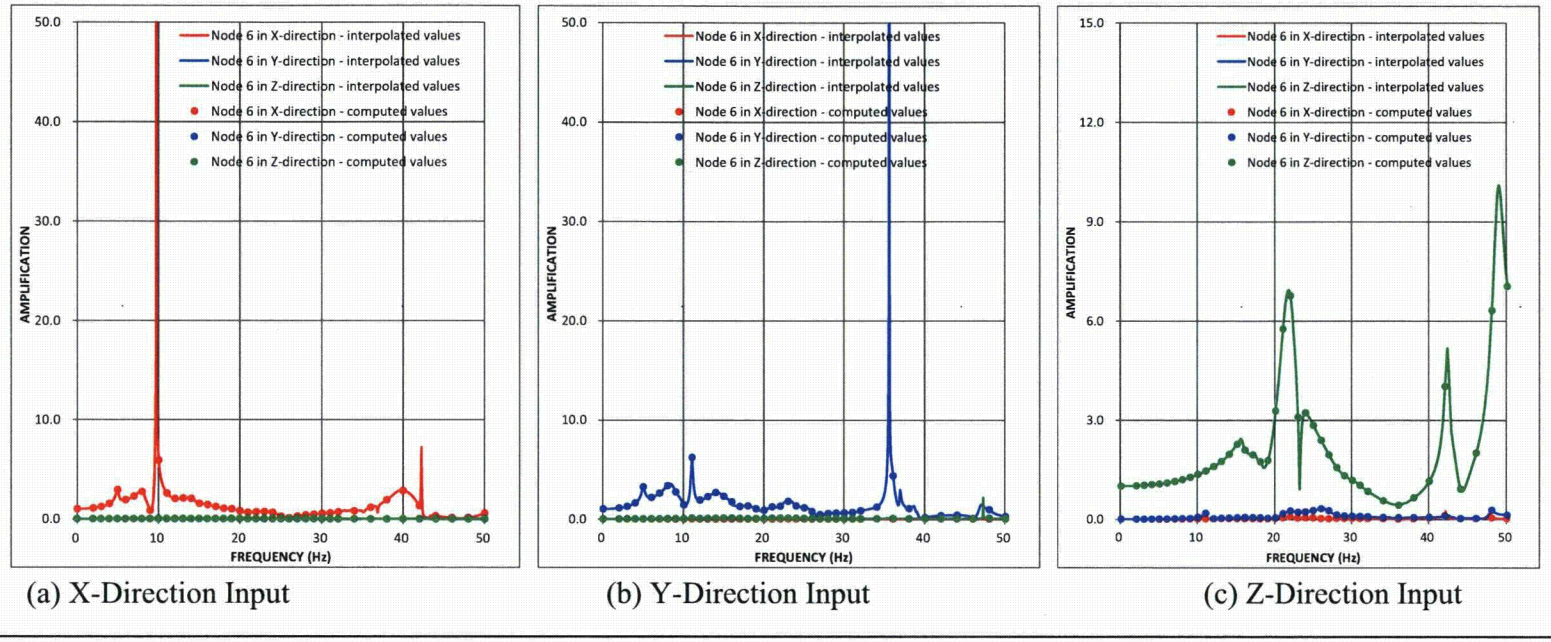

Figure 03.07.02-6(18)a Transfer functions - CB Top at Best Estimate Subsurface Profile - Case CFB1

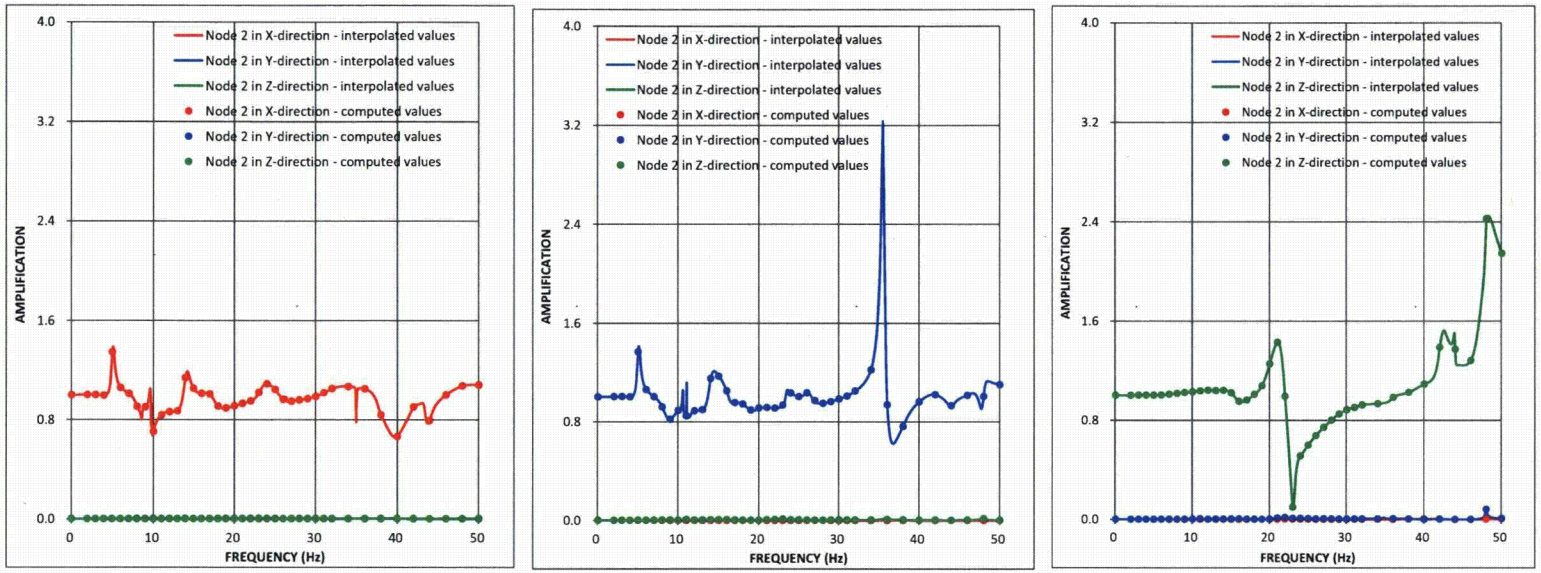

(a) X-Direction Input (b) Y-Direction Input (c) Z-Direction Input

Figure 03.07.02-6(18)b Transfer functions - CB Basemat at Best Estimate Subsurface Profile - Case CFB1

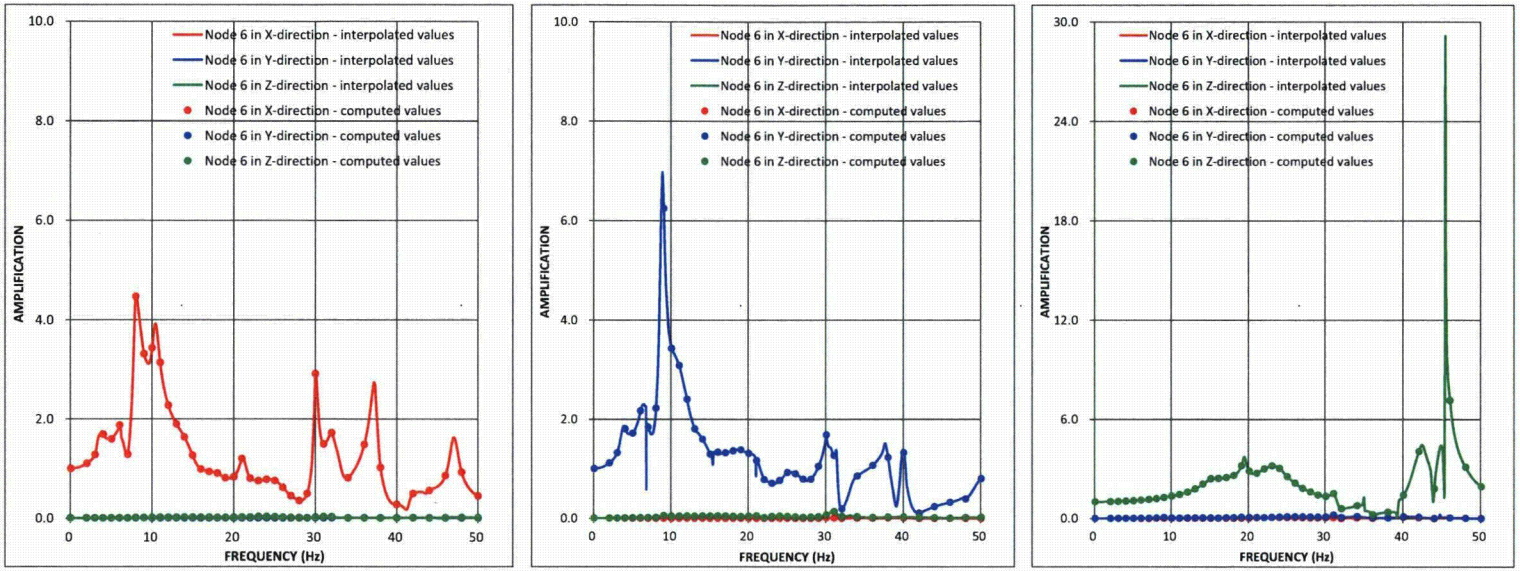

Figure 03.07.02-6(19)a Transfer functions - CB Top at Lower Bound Subsurface Profile - Case CFB1

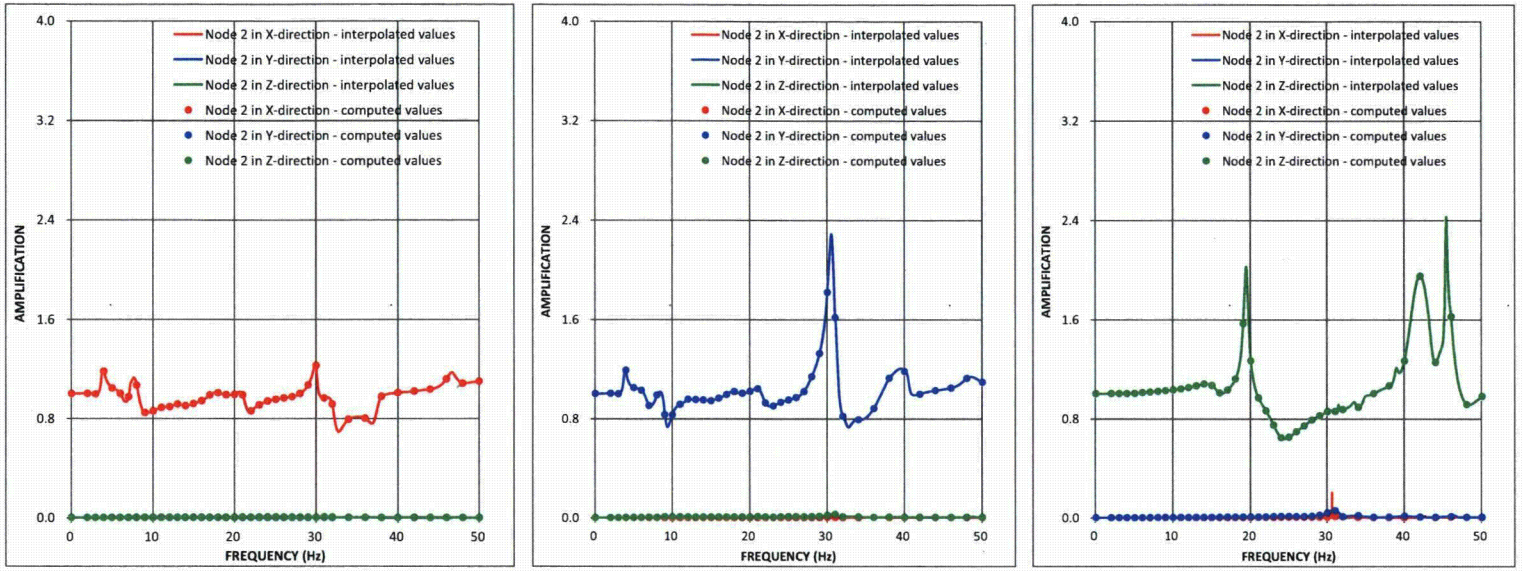

(a) X-Direction Input (b) Y-Direction Input (c) Z-Direction Input

Figure 03.07.02-6(19)b Transfer functions - CB Basemat at Lower Bound Subsurface Profile - Case CFB1

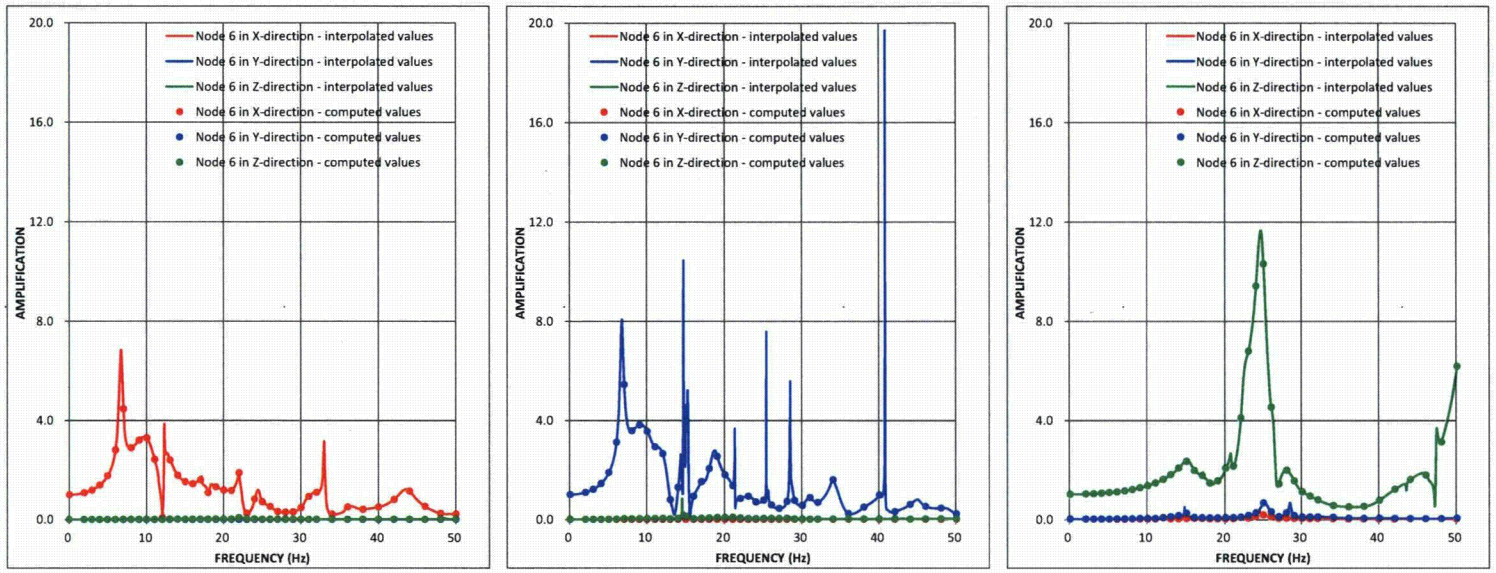

(a) X-Direction Input (b) Y-Direction Input (c) Z-Direction Input

Figure 03.07.02-6(20)a Transfer functions - CB Top at Upper Bound Subsurface Profile - Case CFB1

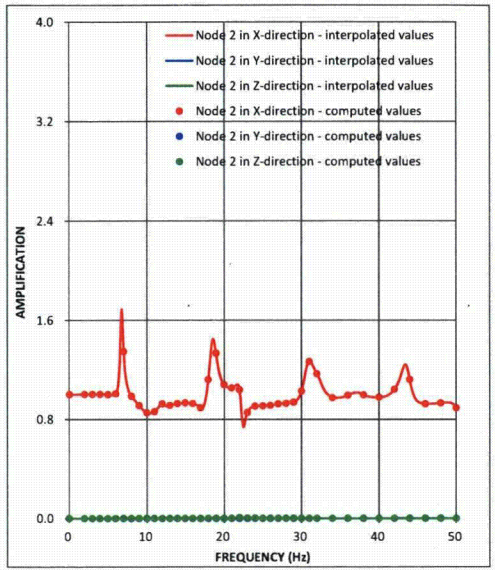

(a) X-Direction Input

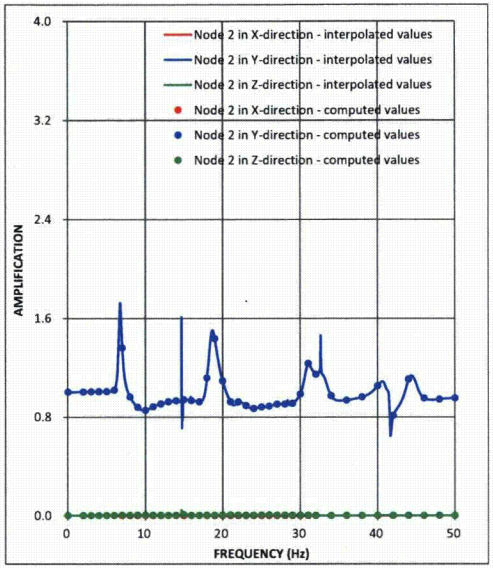

(b) Y-Direction Input

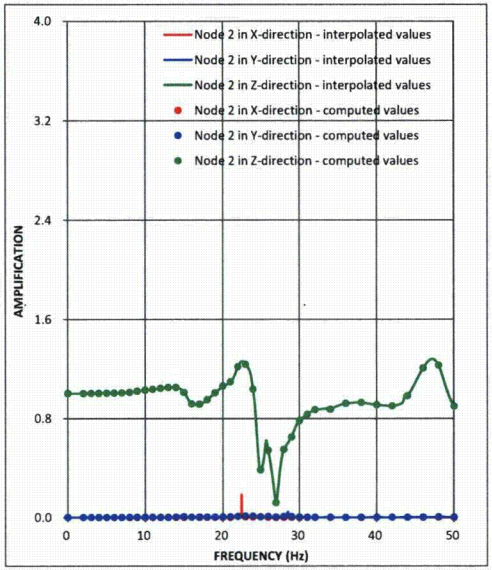

(c) Z-Direction Input

Figure 03.07.02-6(20)b Transfer functions - CB Basemat at Upper Bound Subsurface Profile - Case CFB1

Attachment 5
NRC3-12-0019
(50 pages)

Response to RAI Letter No. 70
(eRAI Tracking No. 6243)

RAI Question No. 03.07.02-8

NRC RAI 03.07.02-8

ESBWR DCD Appendix 3A.8.11 describes the SSI analyses performed to evaluate the structure-soil-structure-interaction (SSSI) effects of the RB/FB on the CB, and the effects of the CB on the FWSC. These analysis cases are termed CL-6 and FL-5 in the ESBWR DCD. Based on these limited analysis cases, it was concluded that SSSI effects were bounded by other analysis cases and would not affect the ESBWR DCD design envelope.

EF3 FSAR Figure 2.5.4-202, as modified by the markups included with the response to RAI Letter 55 Question 02.05.04-38, shows a cross section through the RB/FB, CB and FWSC with the extent of concrete fill and granular fill. Since these site conditions deviate significantly from cases CL-6 and FL-5, analyzed in the ESBWR DCD, the applicant is requested to explain how SSSI effects are evaluated between these structures. What is the basis for neglecting the granular fill in the site-specific analyses in the context of SSSI, given that these structures are deeply embedded and in close proximity to each other? What is the basis for including concrete fill between the RB/FB and CB gap? Does the addition of the stiff concrete fill between the CB and the RB/FB introduce potential interaction between the two structures?

Response

To evaluate the effects of structure-soil-structure interaction (SSSI) and embedment in the engineered granular backfill, additional SSI analyses of the Fermi 3 RB/FB, CB and FWSC considering the engineered granular backfill properties were performed, using the Design Control Document (DCD) SASSI2000 model mesh size. The subtraction method of the SASSI2000 computer program was used for these analyses. The validity of using the subtraction method is confirmed in SER-DTE-009 by using the direct method of the SASSI2000 computer program with the same model.

The subsurface profiles and input motions are the same as those shown in the response to RAI 03.07.02-6. The site-specific SSI analysis cases for the RB/FB, CB and FWSC are summarized in Table 03.07.02-8(1).

The geometry of the excavated volume for the RB/FB and CB SASSI2000 analyses are illustrated in the response to RAI 03.07.02-6 (Figures 03.07.02-6(1) through 03.07.02-6(6)). The finite element model for the FWSC SASSI2000 analyses is illustrated in Figure 03.07.02-8(1). The excavated volume for the FWSC was modeled from the top of the finished ground level grade at EL 4,500 mm to the bottom of the FWSC basemat at EL 2,150 mm. The horizontal dimensions of fill concrete are the same as the FWSC's basemat and its extends from the bottom of the FWSC basemat to the top of the bedrock at EL -6770 mm. The fill concrete is modeled with SASSI structural solid elements. The fill concrete properties are provided in Table 03.07.02-8(2).

The RB/FB SSSI effects on the CB are more significant than the CB SSSI effects on the RB/FB, because the size of the RB/FB is much larger than the CB. To evaluate the RB/FB effects on the CB, the analyses are performed by the following two steps as shown in Figure 03.07.02-8(2):

(1) Perform the RB/FB SASSI2000 analysis to obtain the in-column response at the bottom level of the CB basemat foundation (Case RFB).

(2) Perform the CB SASSI2000 analysis using the input motion obtained in Step 1 (Case CFB2).

This RB/FB and CB SSSI analysis procedure is the same procedure used in the ESBWR DCD.

Figures 03.07.02-8(3) through 03.07.02-8(11) show comparisons of floor response spectra for the Fermi 3 SSI accounting for embedment in the engineered granular backfill with the DCD Design Spectra at the top of the structure and basemat for the CB. The floor response spectra for the corresponding analysis Case CFB1 without the SSSI effect is also shown in the figures for comparison. The effect of SSSI is largest in the Y direction (East-West) floor response spectra; however, both floor response spectra without and with SSSI effect are bounded by the DCD Design Spectra in the whole frequency range. Thus the effect of SSSI between the RB/FB and CB is included in the DCD Design Spectra.

The SSSI analysis was also performed for the FWSC with CB for the same site conditions. The analysis model is composed of these two independent structures coupled through soil using the SASSI2000 computer code as shown in Figures 03.07.02- 8(1) and 03.07.02-8(2). The input motion for the coupled SSI model is the same as that used for Case CFB1 and is applied at the CB foundation level. This analysis case is named Case CFB3-FFB.

Figures 03.07.02-8(12) through 03.07.02-8(20) show comparisons of floor response spectra with the DCD Design Spectra at the top of the structure and basemat for the CB. The floor response spectra for the corresponding analysis Case CFB1 without the SSSI effect is also shown in the figures for comparison. It is confirmed from the results that the floor response spectra with the SSSI effect are bounded by DCD Design Spectra in all frequency ranges. Thus the SSSI effect of FWSC on the CB is included in the DCD Design Spectra.

Figures 03.07.02-8(21) through 03.07.02-8(23) show the comparisons of floor response spectra with the DCD Design Spectra at the top of the structure and basemat for the FWSC. It is confirmed from the results that the floor response spectra with the SSSI effect are bounded by DCD Design Spectra in all frequency ranges. Thus the SSSI effect of CB on the FWSC is included in the DCD Design Spectra.

The basis for including fill concrete between the RB/FB and CB gap is that the bedrock shear wave velocity of 6,689 ft/sec (BE) is similar to the fill concrete shear wave velocity of 7,140 ft/sec. The fill concrete top level is same as bedrock top level. Therefore, the effect of the fill concrete between the RB/FB and CB gap can be neglected.

For reference, Figures 03.07.02-8 (24) through 03.07.02-8 (29) show the transfer function values computed at each frequency for the Fermi 3 SSI analyses and the continuous transfer functions obtained by interpolation of the computed values from the Fermi 3 SSI analysis (Case CFB-FFB).

Figures 03.07.02-8 (24) through 03.07.02-8 (29) show that there are some spikes in the transfer functions; however, it can be found from the Figures that the spikes are generated from the interpolate process of SASSI2000 computer program. They are very narrow and not real transfer functions. Their effect does not appear in the FRS in Figures 03.07.02-8(12) through 03.07.02-8(23), which are calculated at intervals wider than the width of the spikes.

Proposed COLA Revision

None.

Table 03.07.02-8(1) RB/FB, CB & FWSC SSI Analysis Cases

Building	Case	ID No.	Model *1 (DCD)	Input Motion	Site Condition			Remarks
					BE	LB	UB	
RB/FB	RFB	RFB-1	Base	RB/FB FIRS	✓	--	--	
		RFB-2			--	✓	--	
		RFB-3			--	--	✓	
CB	CFB1	CFB1-1	Base	CB FIRS	✓	--	--	
		CFB1-2			--	✓	--	
		CFB1-3			--	--	✓	
CB	CFB2	CFB2-1	Base	FIRS *2	✓	--	--	RB/FB SSSI Effects are included
		CFB2-2			--	✓	--	
		CFB2-3			--	--	✓	
CB & FWSC	CFB3-FFB	CFB3-1 & FFB-1	Base	CB FIRS	✓	--	--	SSSI Effects of each Building are included
		CFB3-2 & FFB-2			--	✓	--	
		CFB3-3 & FFB-3			--	--	✓	

Note *1: As shown in DCD Table 3A.6-1, there are some models with minor modifications to evaluate the modeling effects. For this Fermi 3 SSI analysis, the most basic model, "Base" is applied.

*2: Input motion is generated from Case RFB.

Table 03.07.02-8(2) Fill Concrete Property

Unit Weight (pcf)	145
Poisson's Ratio	0.2
Shear Wave Velocity (ft/sec)	7140
Compression Wave Velocity (ft/sec)	11660
Damping Ratio (%)	4

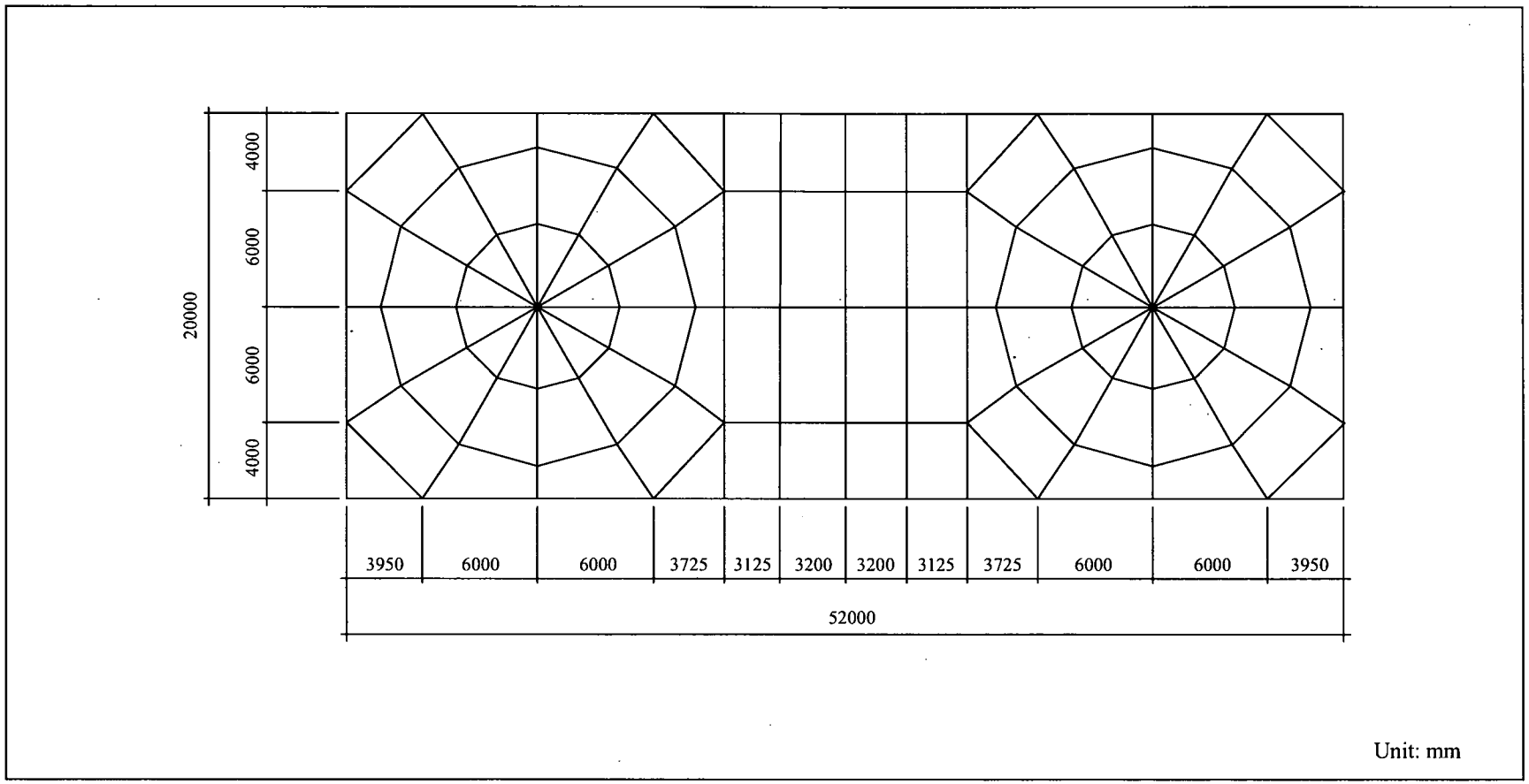

Figure 03.07.02-8(1)a SASSI2000 Plate Elements for FWSC Basemat

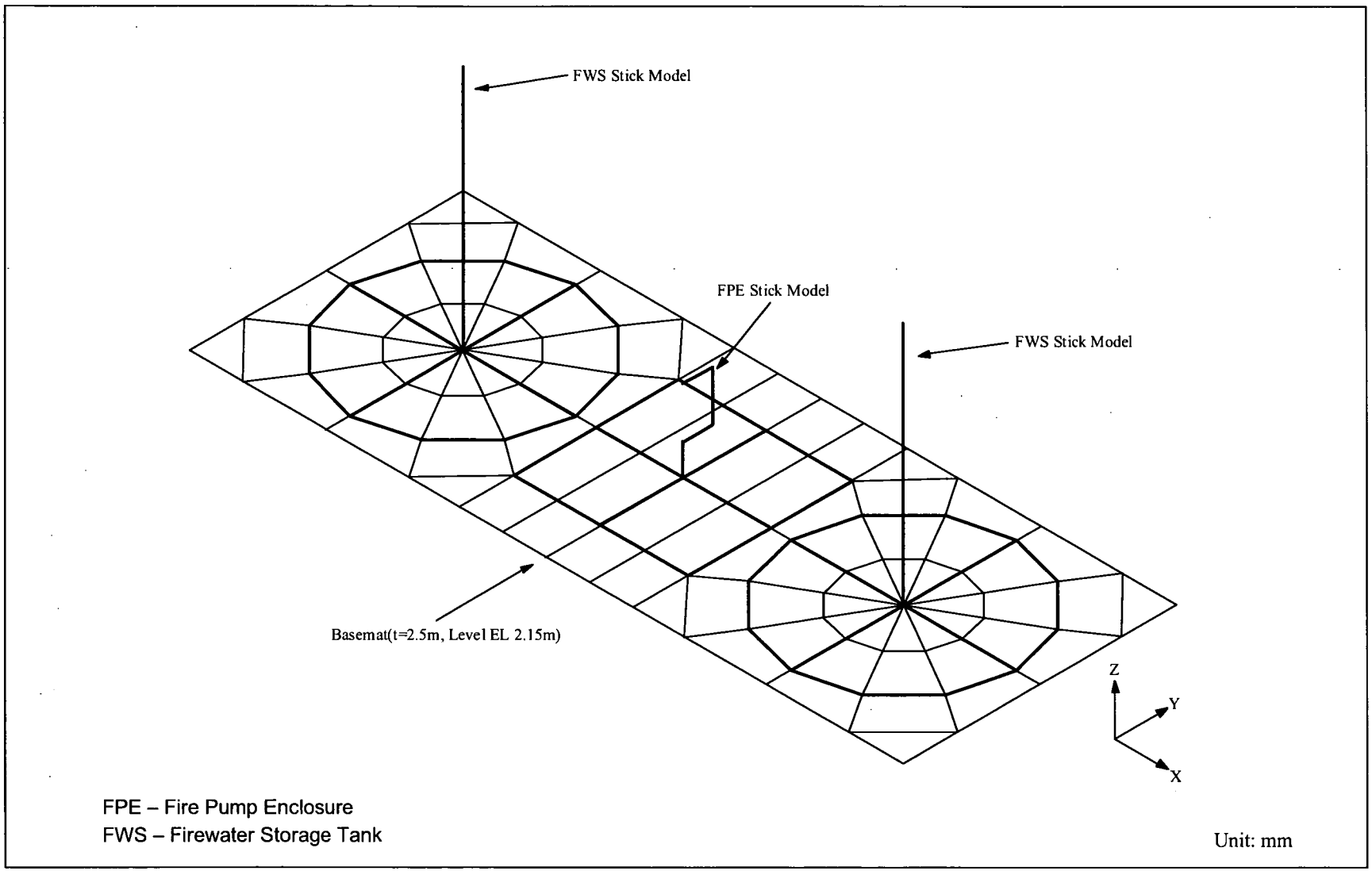

Figure 03.07.02-8(1)b Overview of SASSI2000 SSI FWSC Model

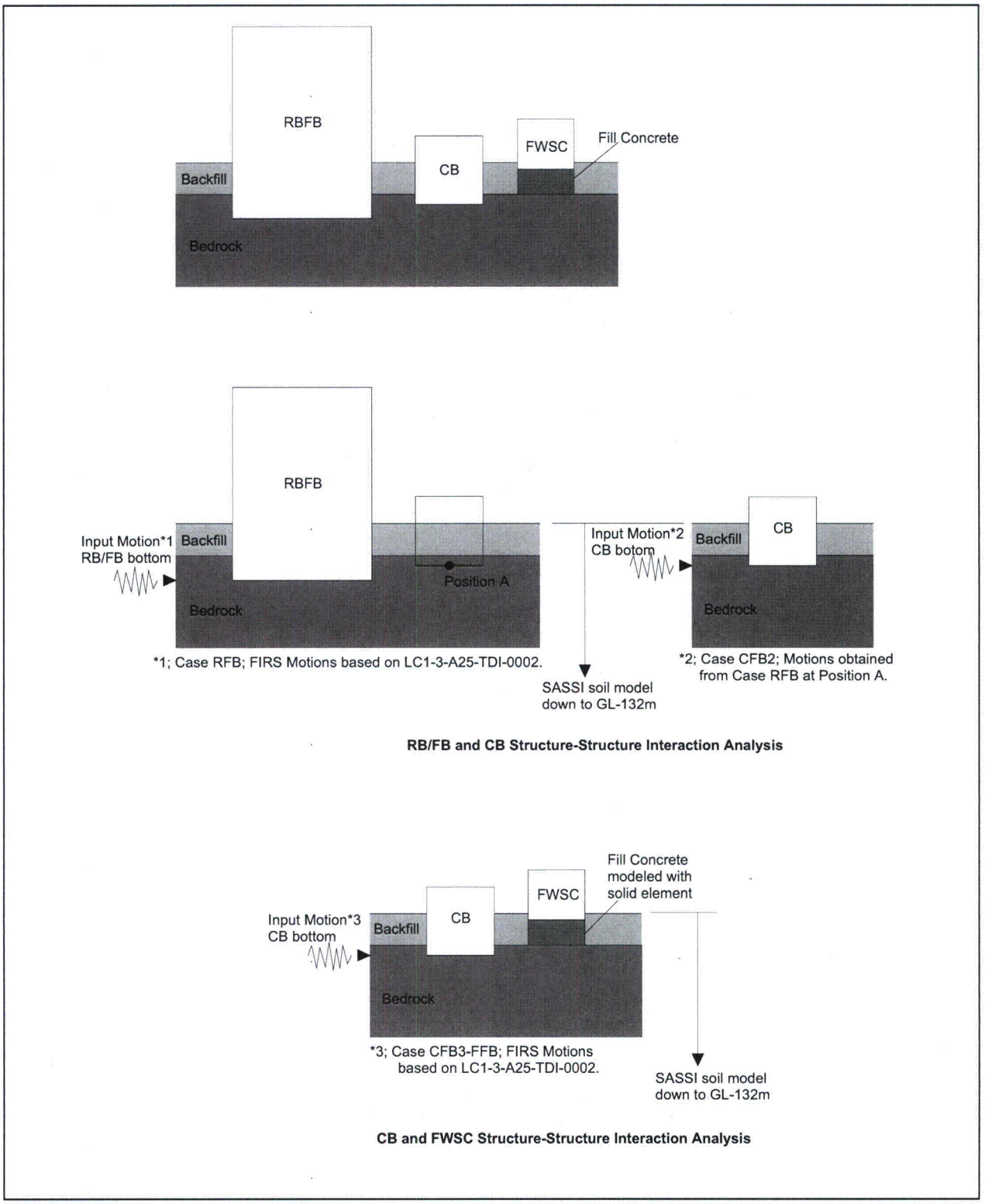

Figure 03.07.02-8(2) Structure-Soil-Structure Interaction Analysis Procedure

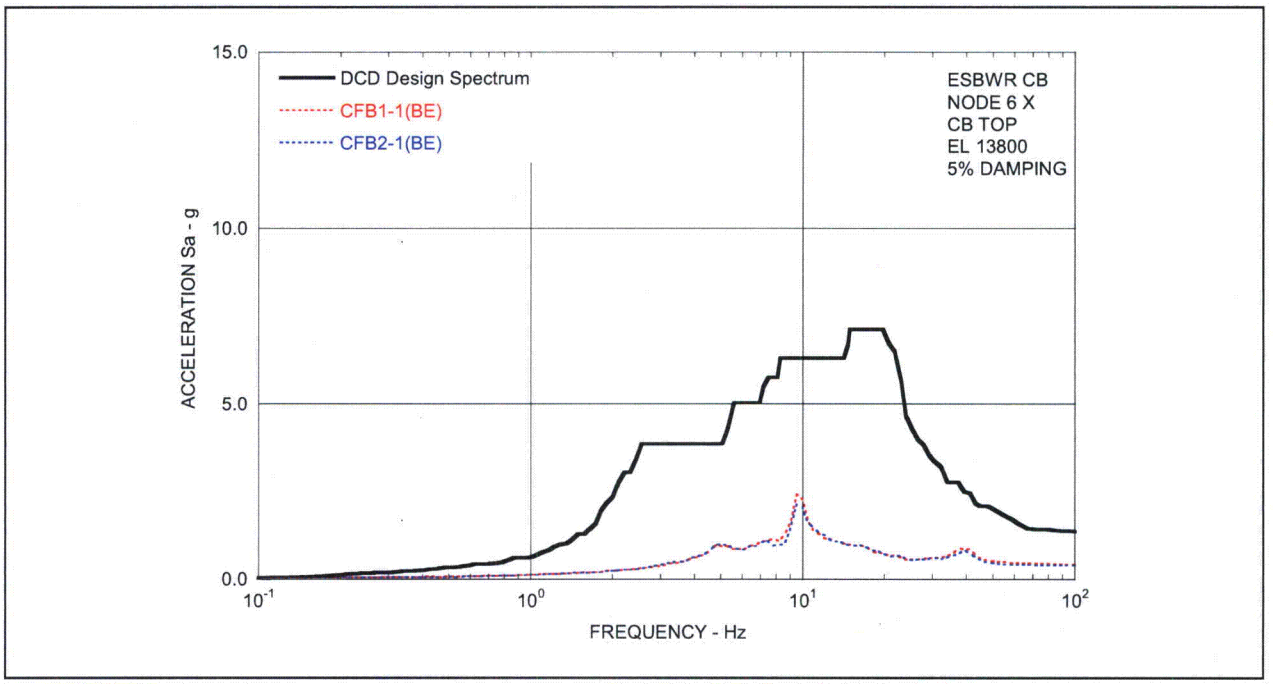

Figure 03.07.02-8(3)a Floor Response Spectra (BE) - CB Top in X-Direction - Comparison between SSI (CFB1) and SSSI including RB/FB Effects (CFB2)

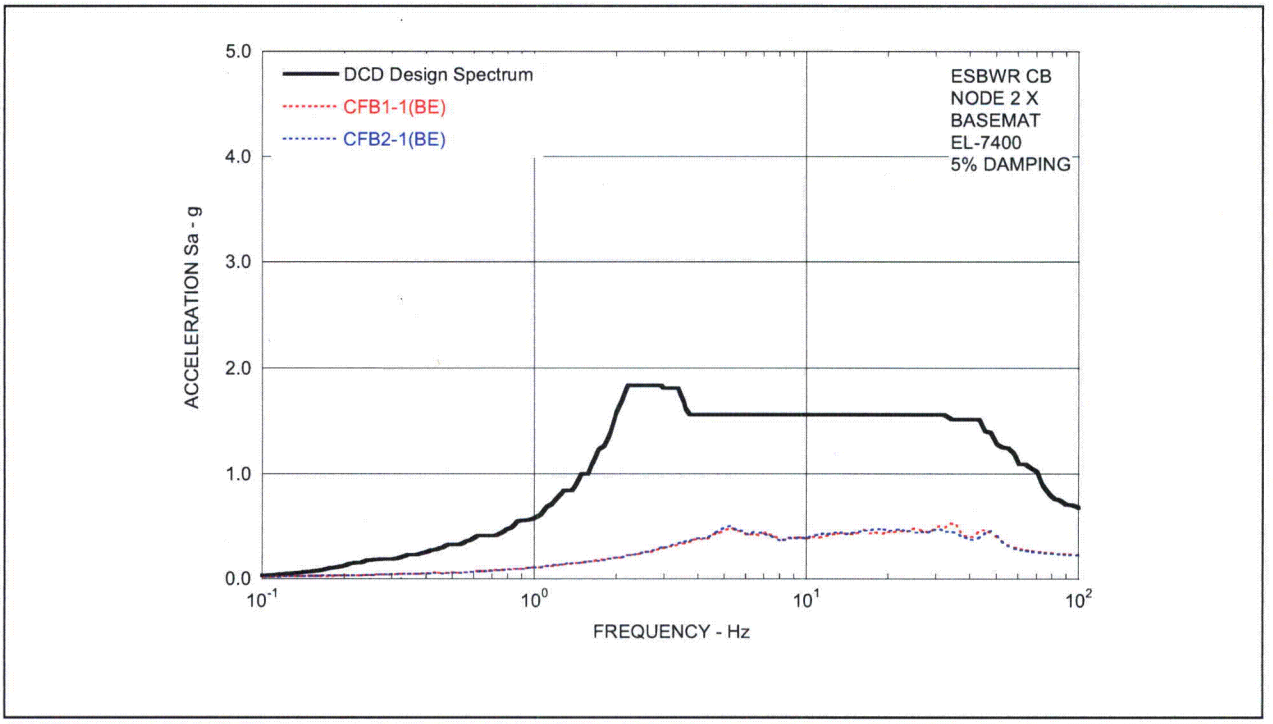

Figure 03.07.02-8(3)b Floor Response Spectra (BE) - CB Basemat in X-Direction - Comparison between SSI (CFB1) and SSSI including RB/FB Effects (CFB2)

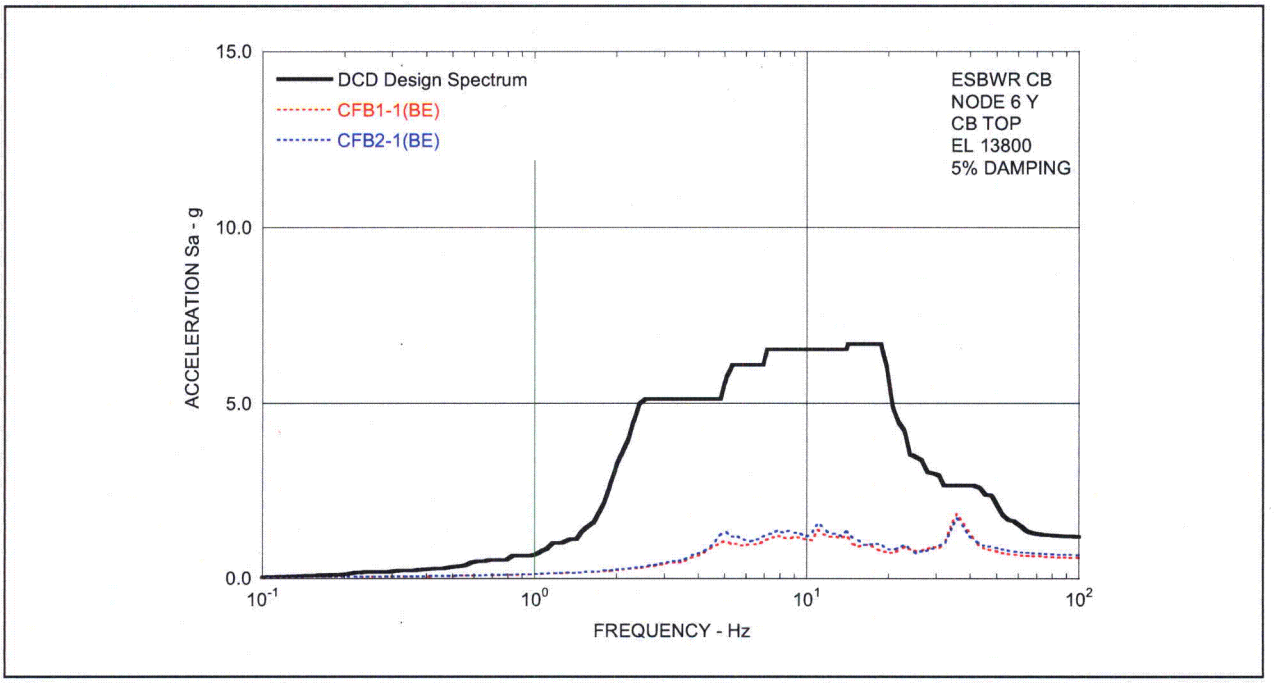

Figure 03.07.02-8(4)a Floor Response Spectra (BE) - CB Top in Y-Direction - Comparison between SSI (CFB1) and SSSI including RB/FB Effects (CFB2)

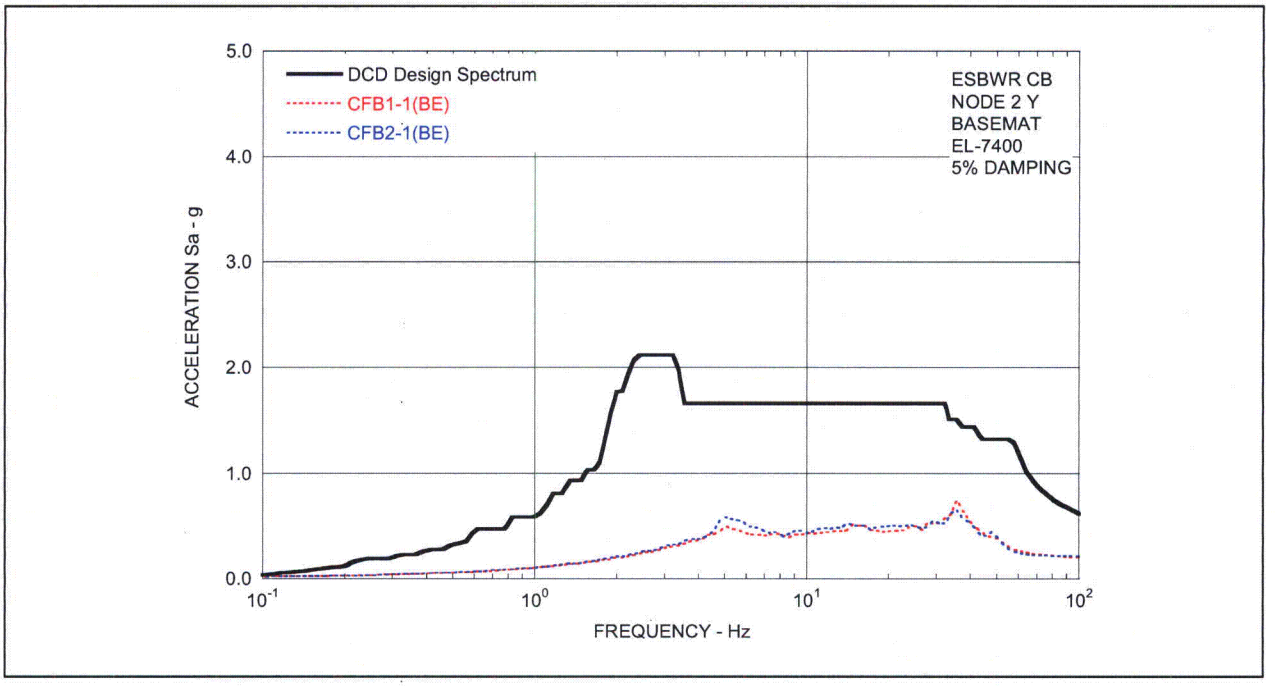

Figure 03.07.02-8(4)b Floor Response Spectra (BE) - CB Basemat in Y-Direction - Comparison between SSI (CFB1) and SSSI including RB/FB Effects (CFB2)

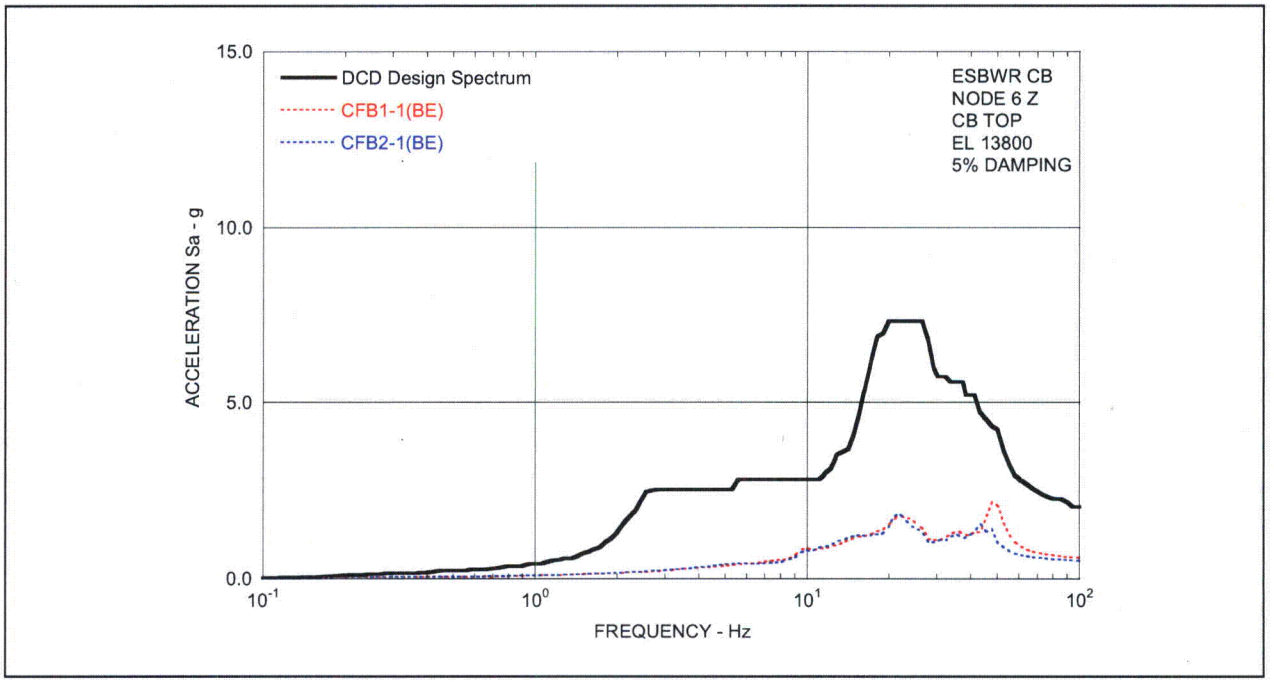

Figure 03.07.02-8(5)a Floor Response Spectra (BE) - CB Top in Z-Direction - Comparison between SSI (CFB1) and SSSI including RB/FB Effects (CFB2)

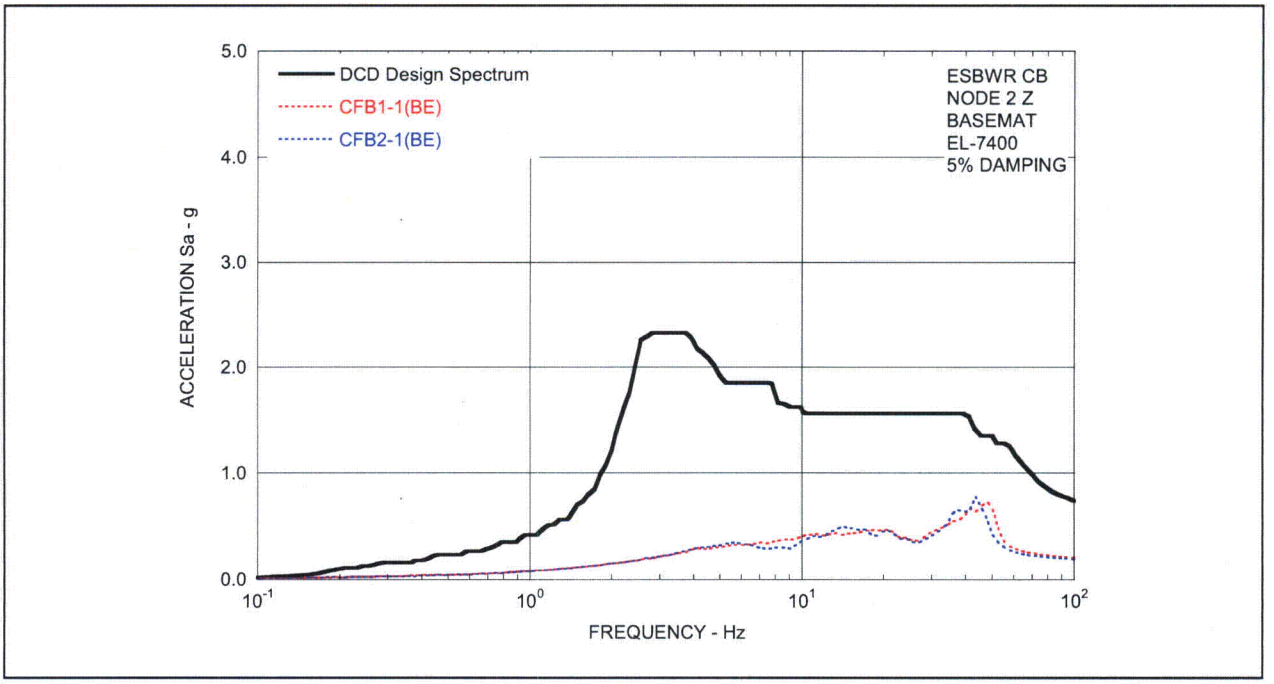

Figure 03.07.02-8(5)b Floor Response Spectra (BE) - CB Basemat in -Z-Direction - Comparison between SSI (CFB1) and SSSI including RB/FB Effects (CFB2)

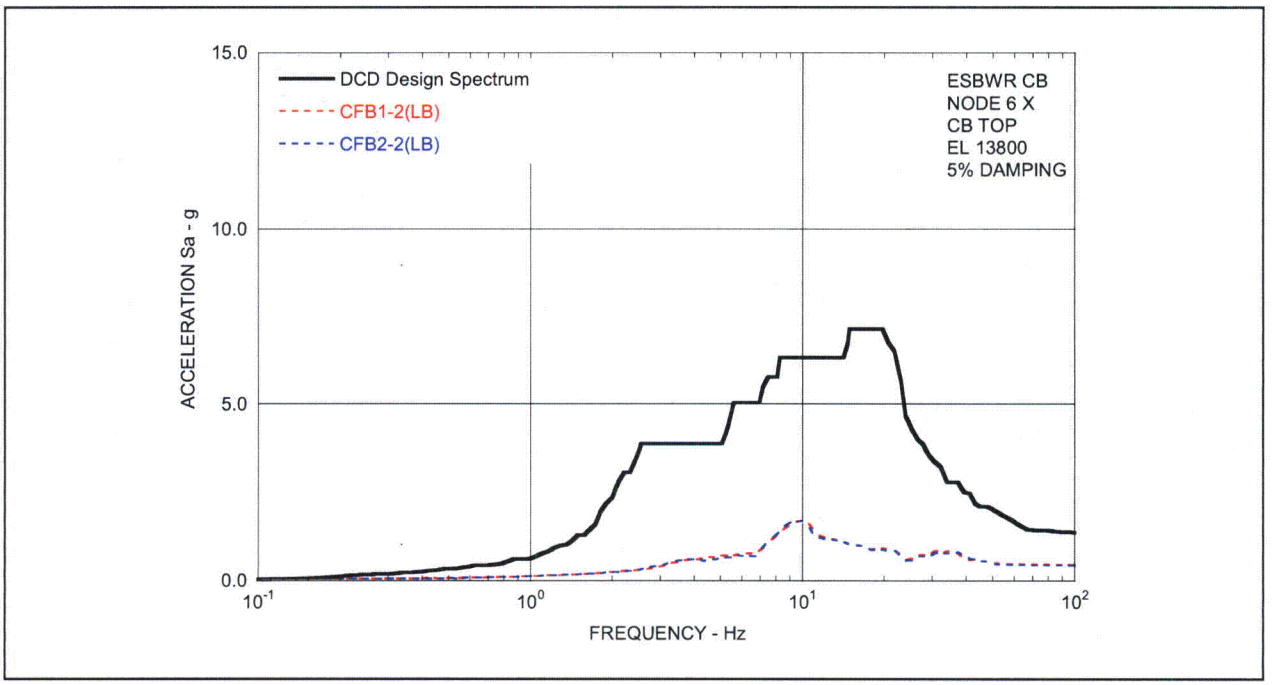

Figure 03.07.02-8(6)a Floor Response Spectra (LB) - CB Top in X-Direction - Comparison between SSI (CFB1) and SSSI including RB/FB Effects (CFB2)

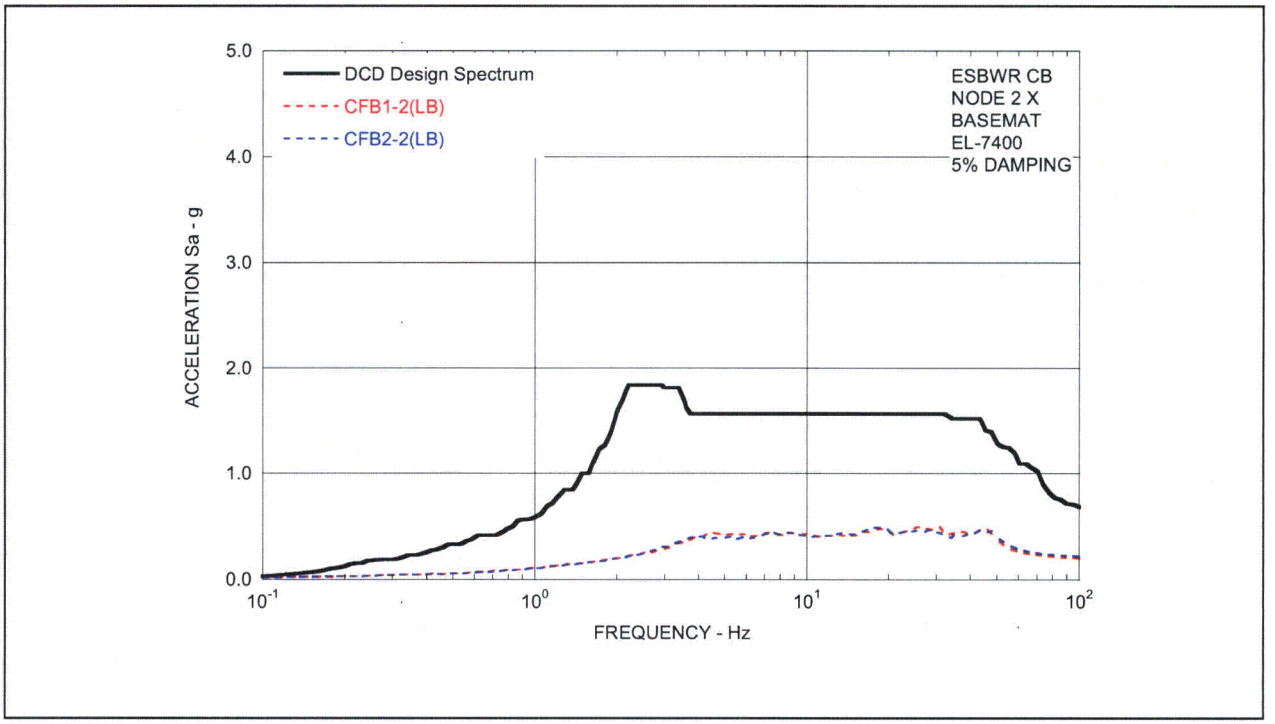

Figure 03.07.02-8(6)b Floor Response Spectra (LB) - CB Basemat in X-Direction - Comparison between SSI (CFB1) and SSSI including RB/FB Effects (CFB2)

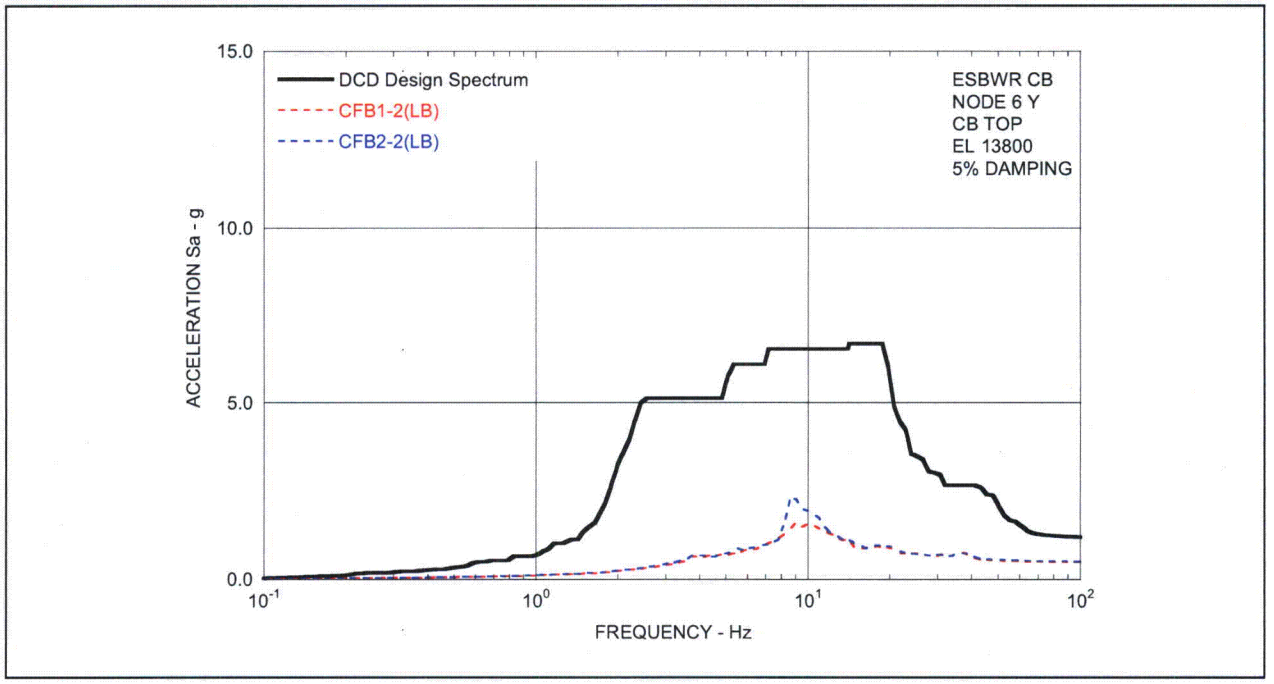

Figure 03.07.02-8(7)a Floor Response Spectra (LB) - CB Top in Y-Direction - Comparison between SSI (CFB1) and SSSI including RB/FB Effects (CFB2)

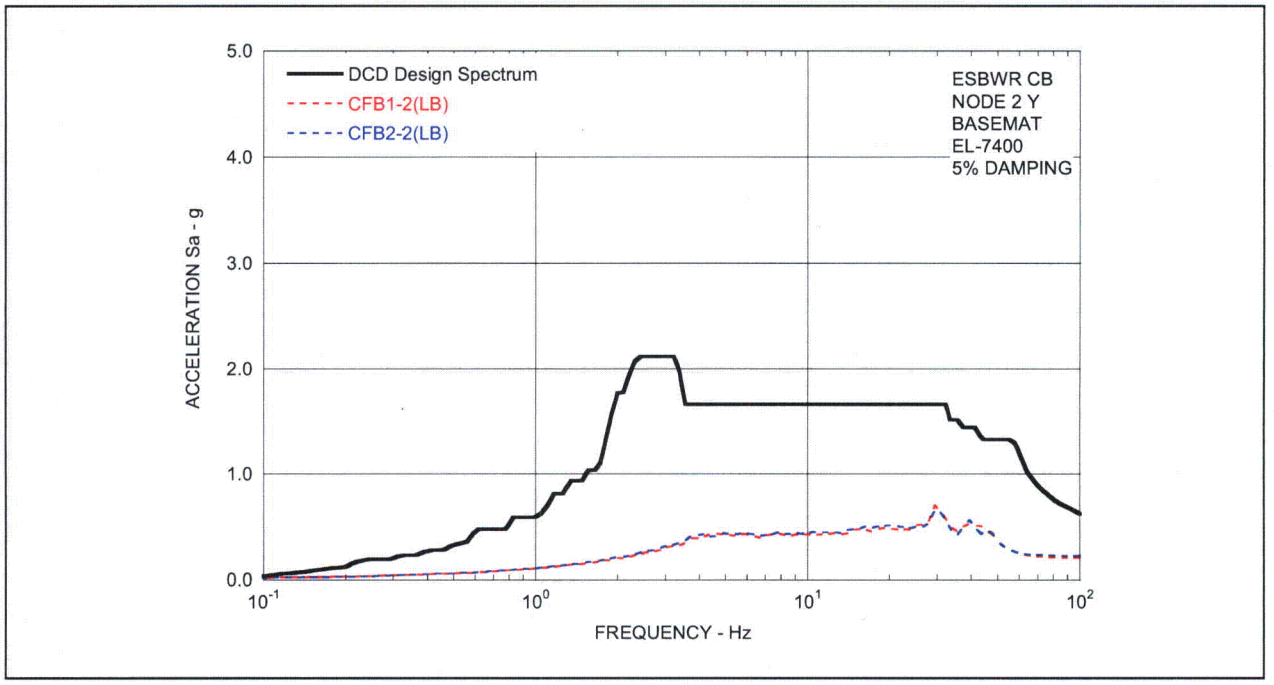

Figure 03.07.02-8(7)b Floor Response Spectra (LB) - CB Basemat in Y-Direction - Comparison between SSI (CFB1) and SSSI including RB/FB Effects (CFB2)

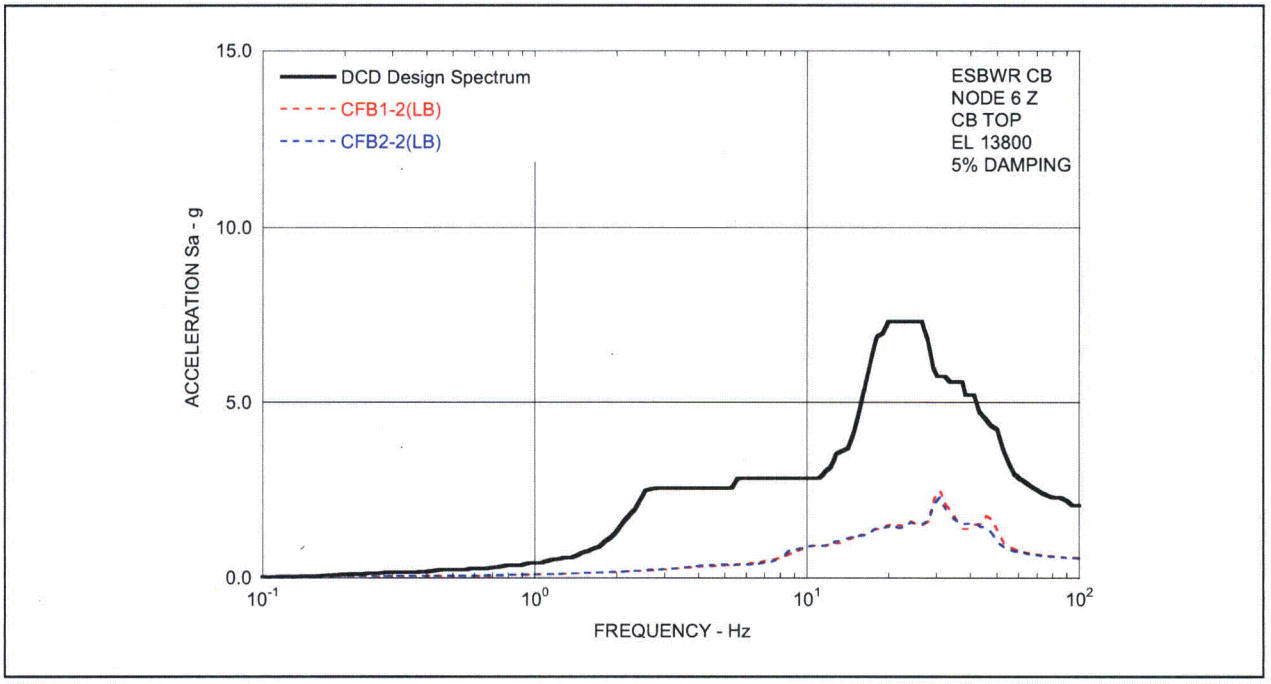

Figure 03.07.02-8(8)a Floor Response Spectra (LB) - CB Top in Z-Direction - Comparison between SSI (CFB1) and SSSI including RB/FB Effects (CFB2)

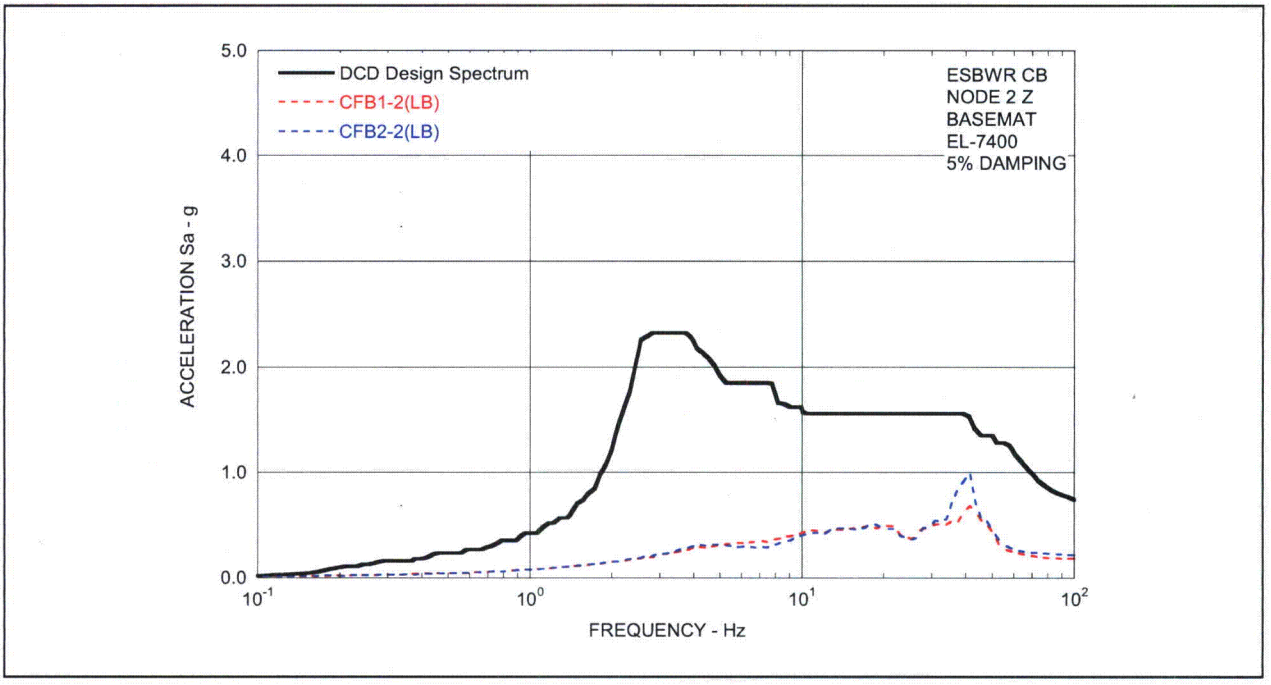

Figure 03.07.02-8(8)b Floor Response Spectra (LB) - CB Basemat in -Z-Direction - Comparison between SSI (CFB1) and SSSI including RB/FB Effects (CFB2)

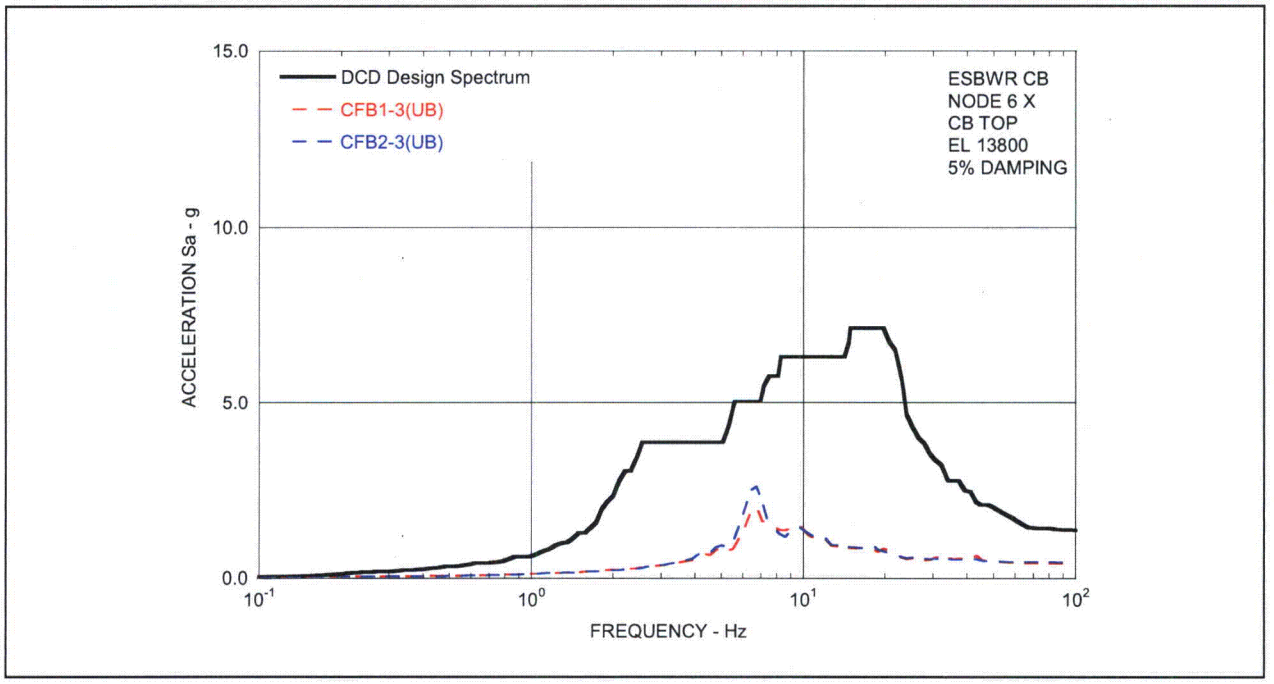

Figure 03.07.02-8(9)a Floor Response Spectra (UB) - CB Top in X-Direction - Comparison between SSI (CFB1) and SSSI including RB/FB Effects (CFB2)

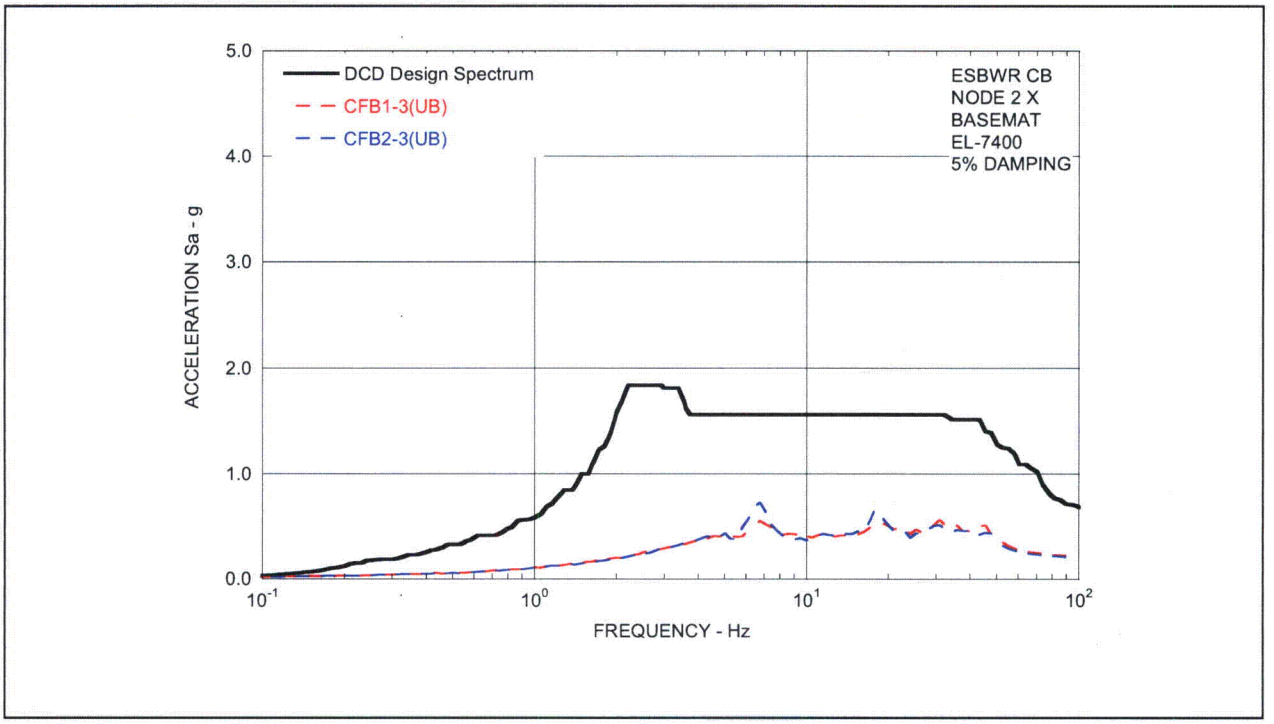

Figure 03.07.02-8(9)b Floor Response Spectra (UB) - CB Basemat in X-Direction - Comparison between SSI (CFB1) and SSSI including RB/FB Effects (CFB2)

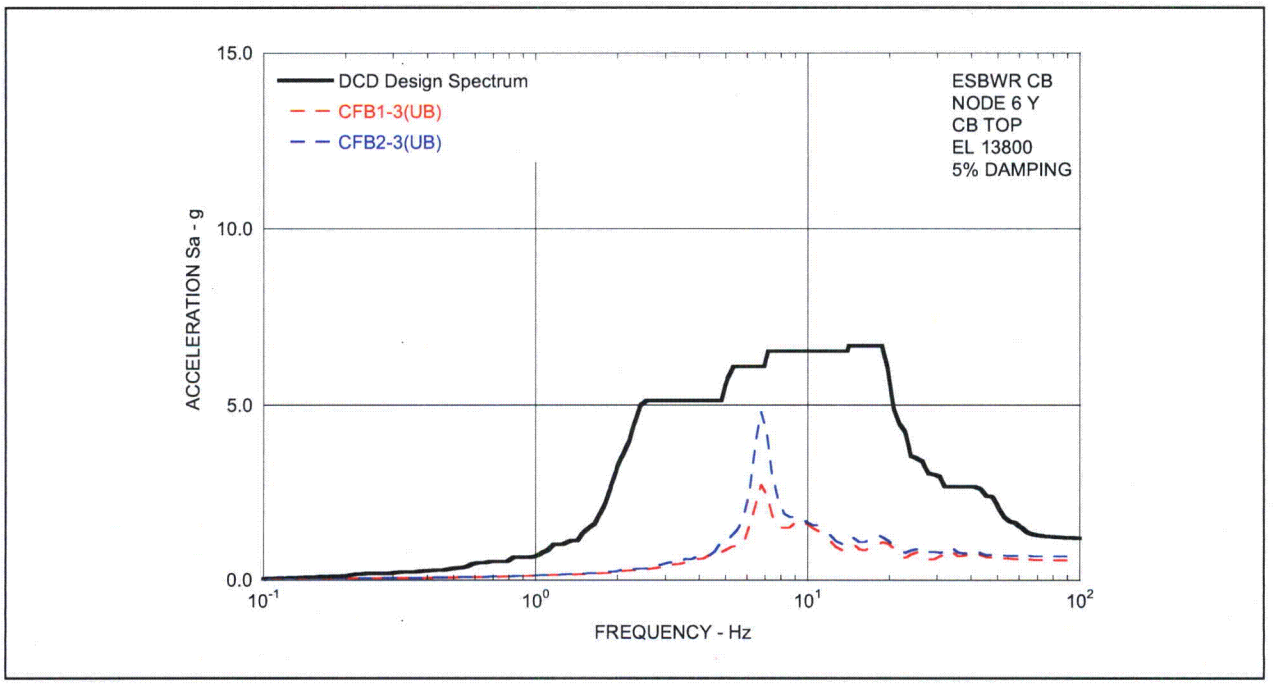

Figure 03.07.02-8(10)a Floor Response Spectra (UB) - CB Top in Y-Direction - Comparison between SSI (CFB1) and SSSI including RB/FB Effects (CFB2)

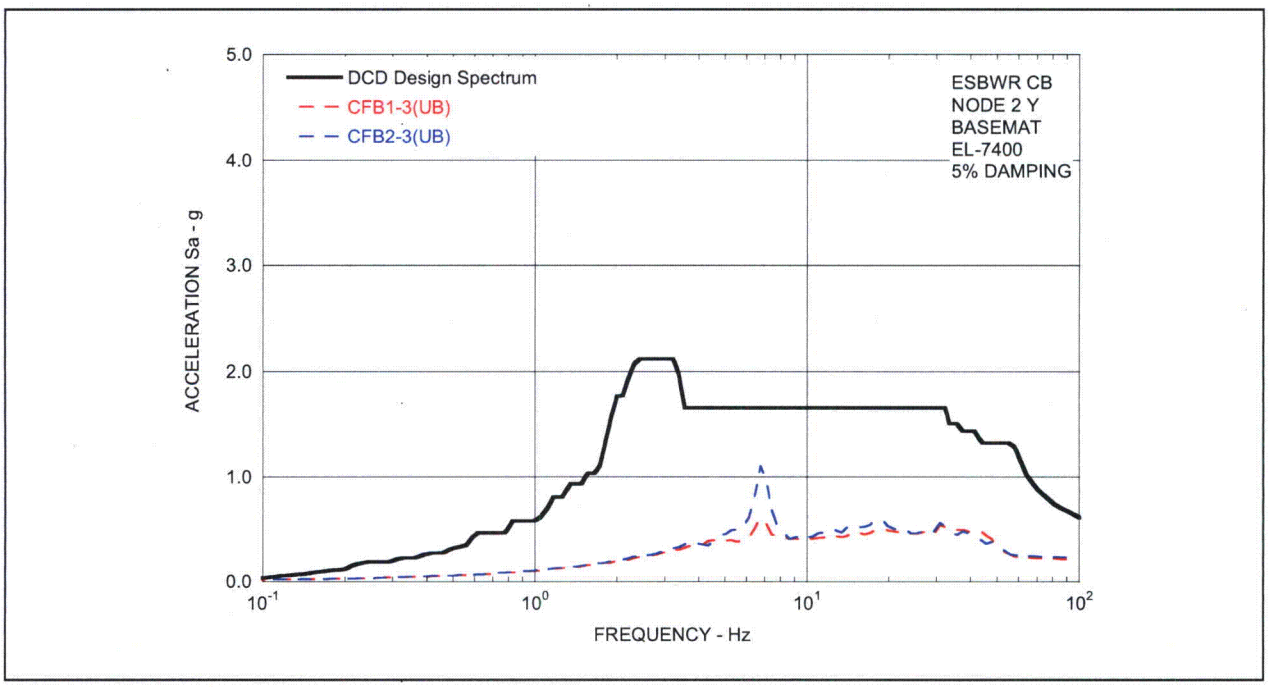

Figure 03.07.02-8(10)b Floor Response Spectra (UB) - CB Basemat in Y-Direction - Comparison between SSI (CFB1) and SSSI including RB/FB Effects (CFB2)

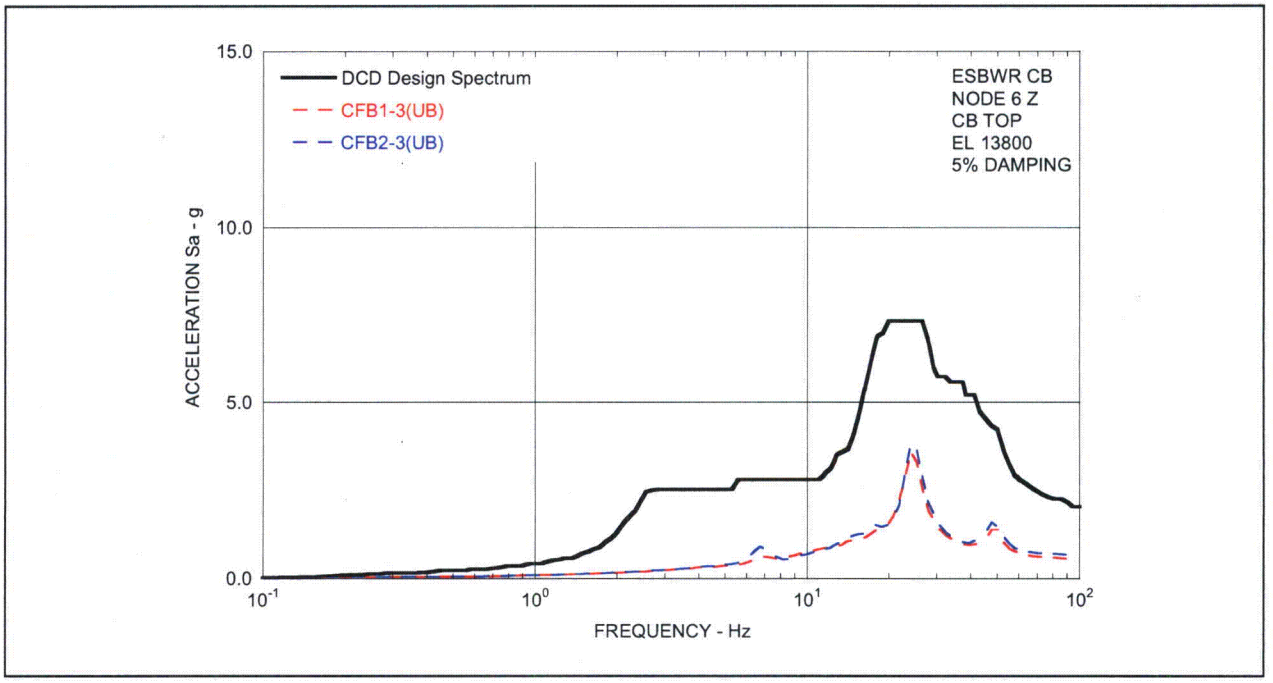

Figure 03.07.02-8(11)a Floor Response Spectra (UB) - CB Top in Z-Direction - Comparison between SSI (CFB1) and SSSI including RB/FB Effects (CFB2)

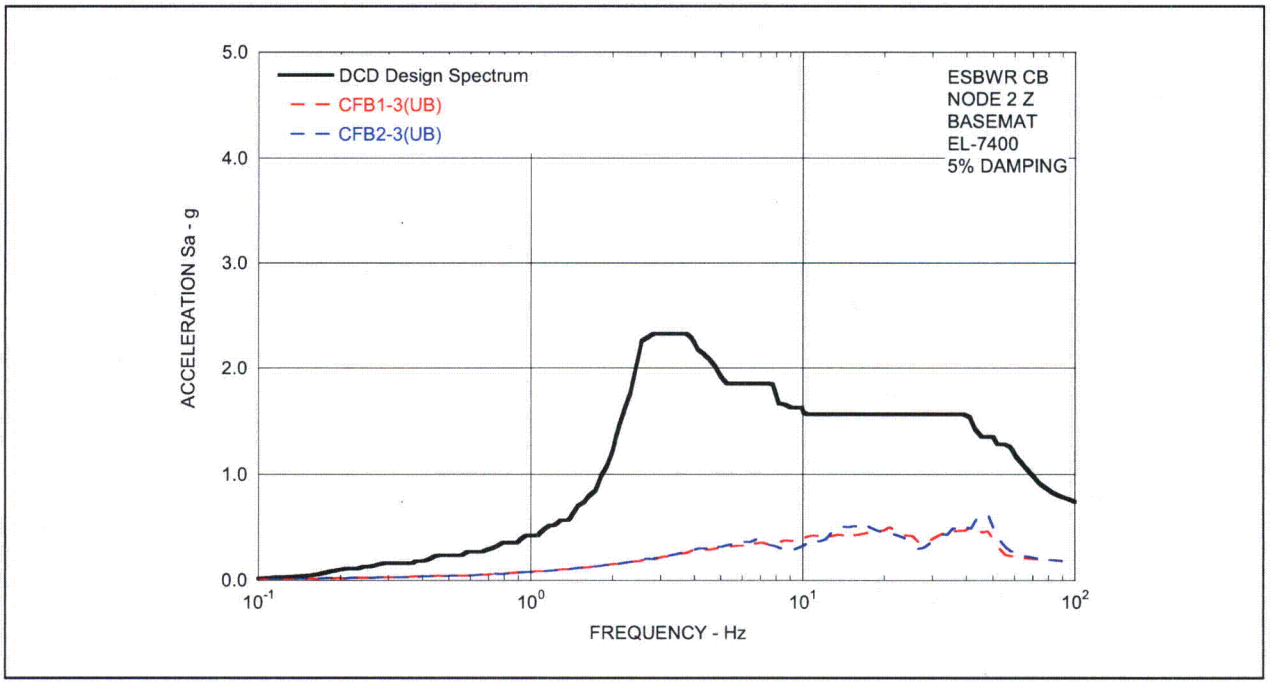

Figure 03.07.02-8(11)b Floor Response Spectra (UB) - CB Basemat in -Z-Direction - Comparison between SSI (CFB1) and SSSI including RB/FB Effects (CFB2)

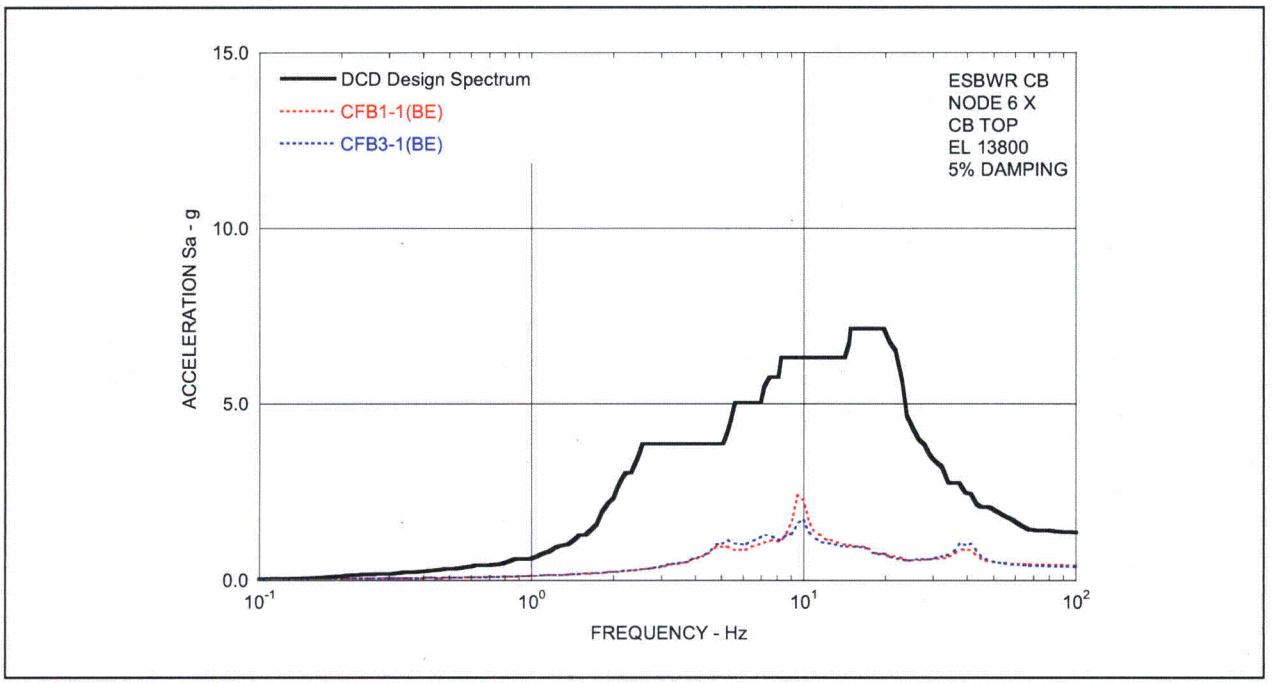

Figure 03.07.02-8(12)a Floor Response Spectra (BE) - CB Top in X-Direction - Comparison between SSI (CFB1) and SSSI including FWSC Effects (CFB3)

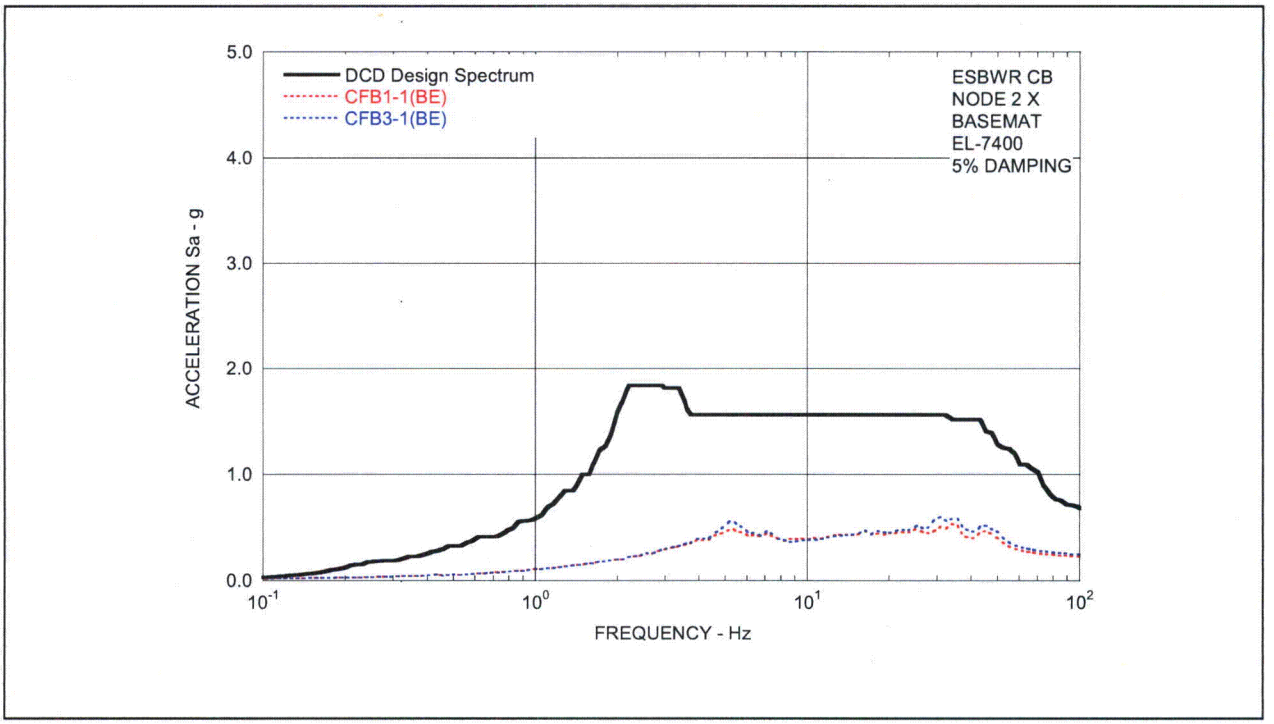

Figure 03.07.02-8(12)b Floor Response Spectra (BE) - CB Basemat in X-Direction - Comparison between SSI (CFB1) and SSSI including FWSC Effects (CFB3)

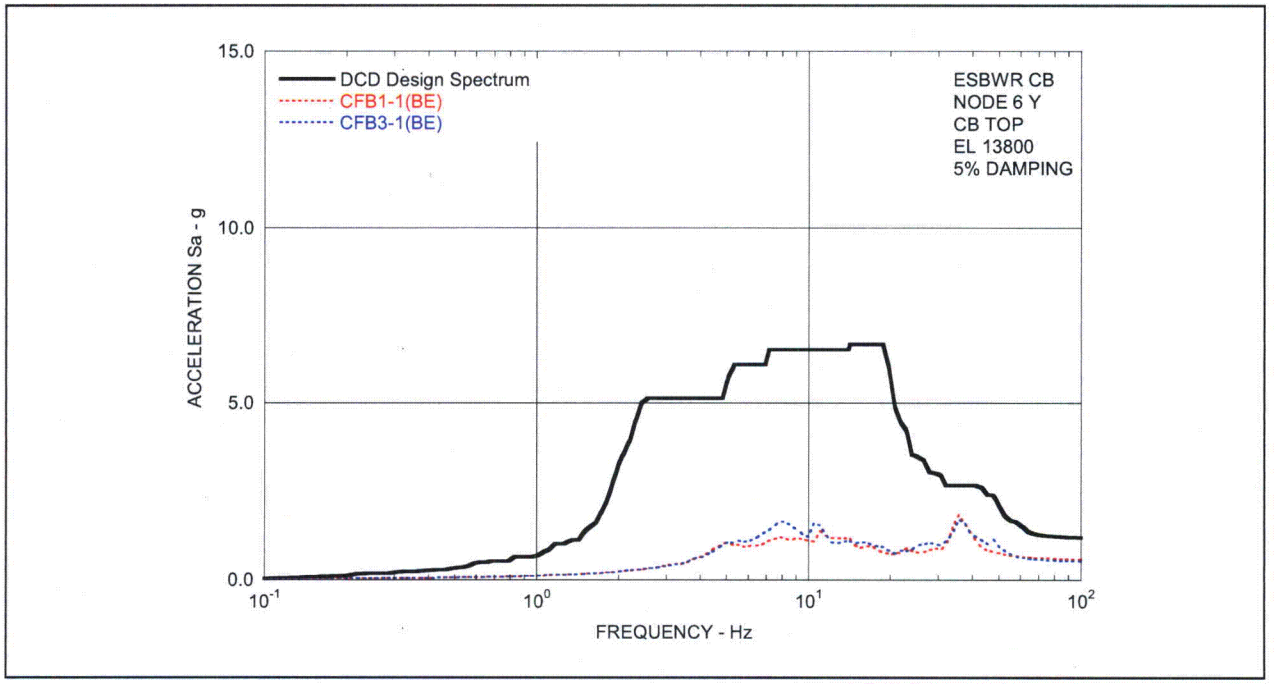

Figure 03.07.02-8(13)a Floor Response Spectra (BE) - CB Top in Y-Direction - Comparison between SSI (CFB1) and SSSI including FWSC Effects (CFB3)

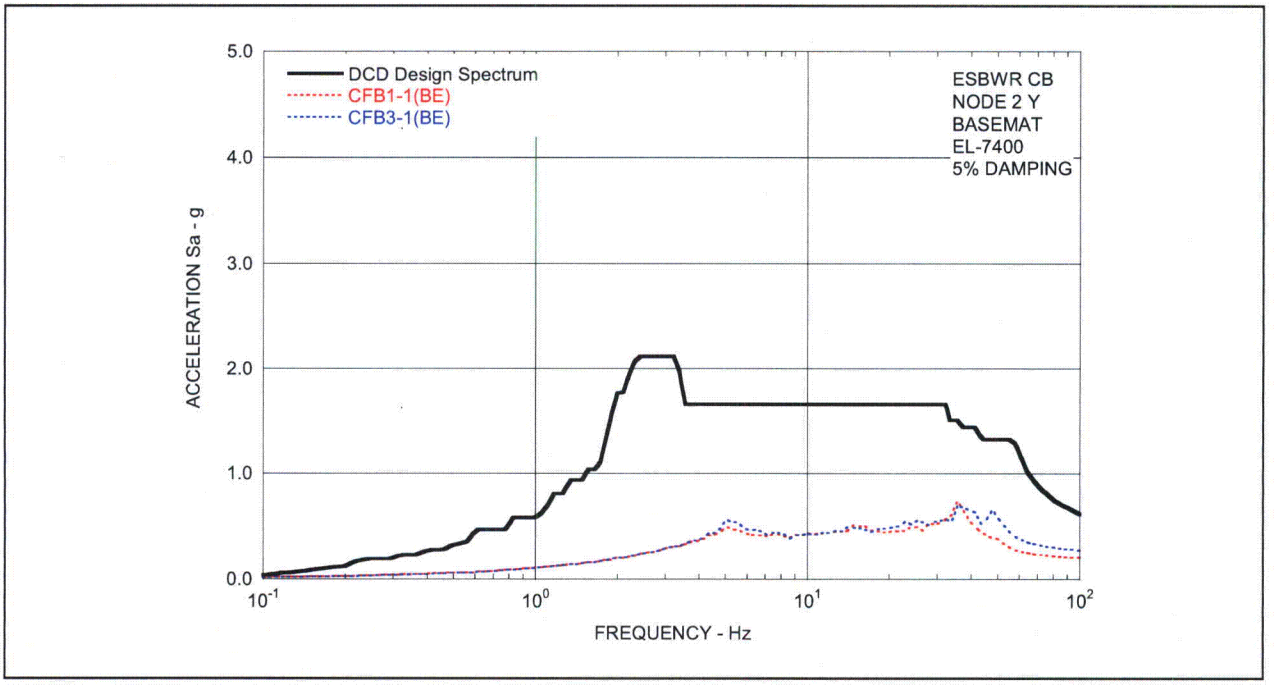

Figure 03.07.02-8(13)b Floor Response Spectra (BE) - CB Basemat in Y-Direction - Comparison between SSI (CFB1) and SSSI including FWSC Effects (CFB3)

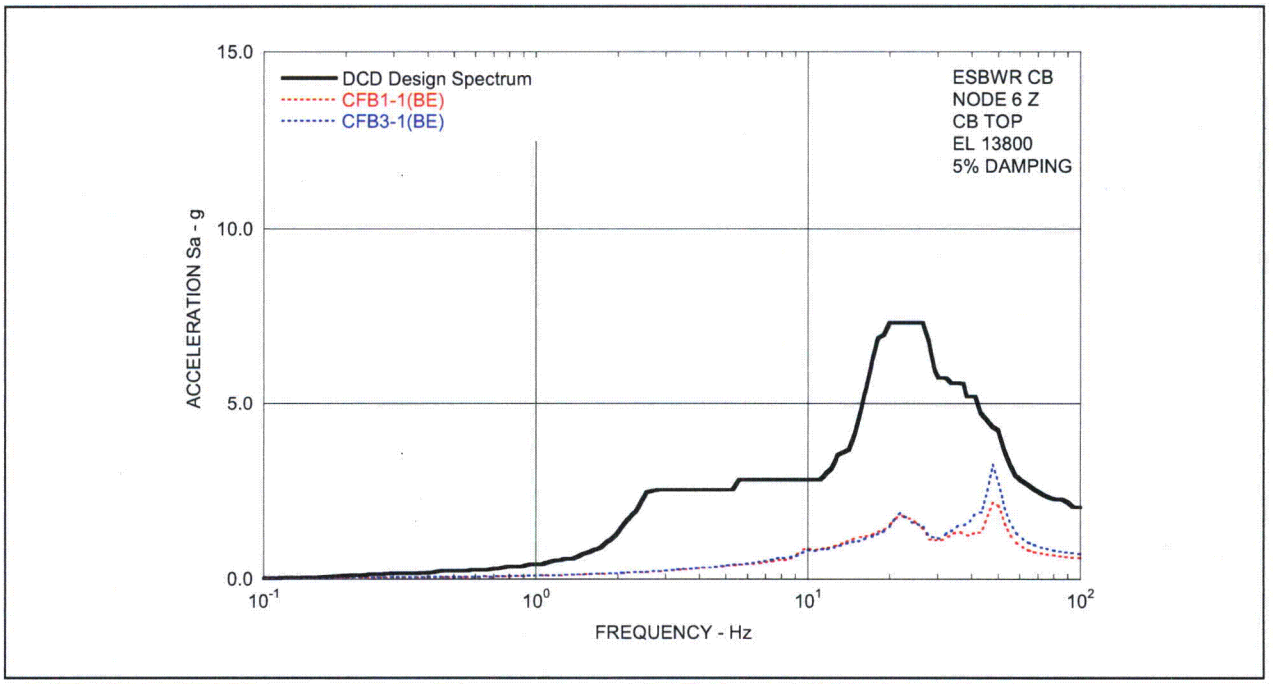

Figure 03.07.02-8(14)a Floor Response Spectra (BE) - CB Top in Z-Direction - Comparison between SSI (CFB1) and SSSI including FWSC Effects (CFB3)

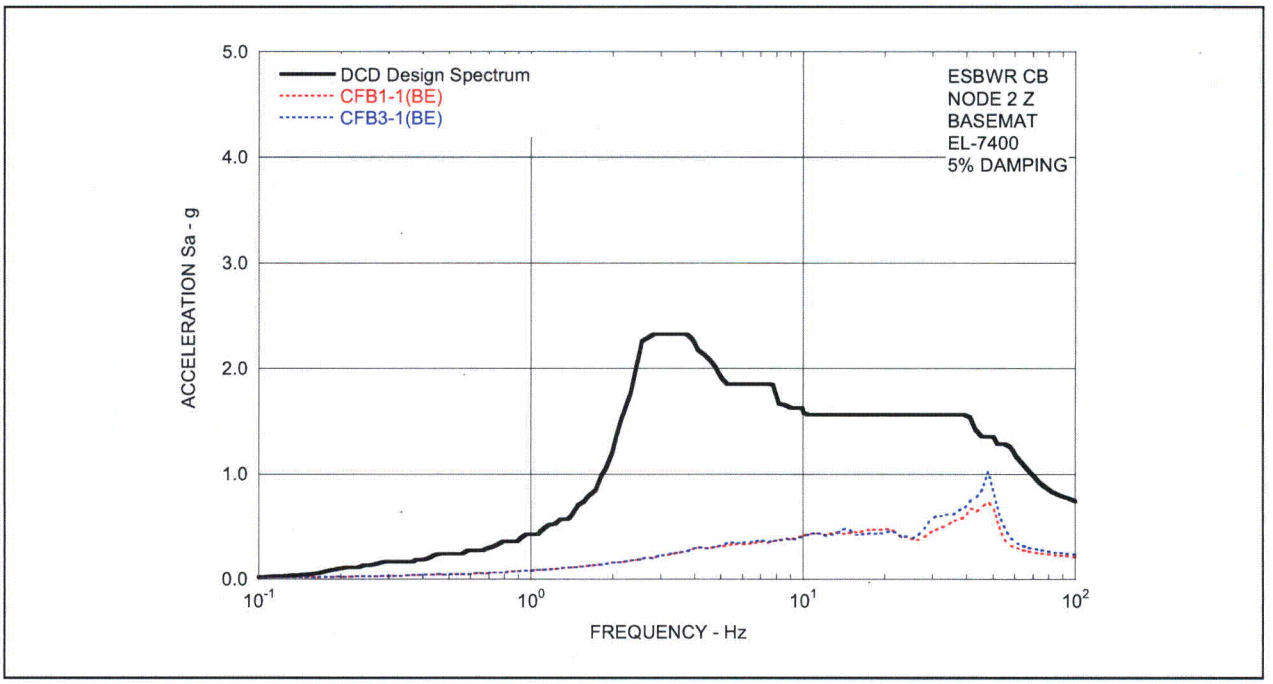

Figure 03.07.02-8(14)b Floor Response Spectra (BE) - CB Basemat in -Z-Direction - Comparison between SSI (CFB1) and SSSI including FWSC Effects (CFB3)

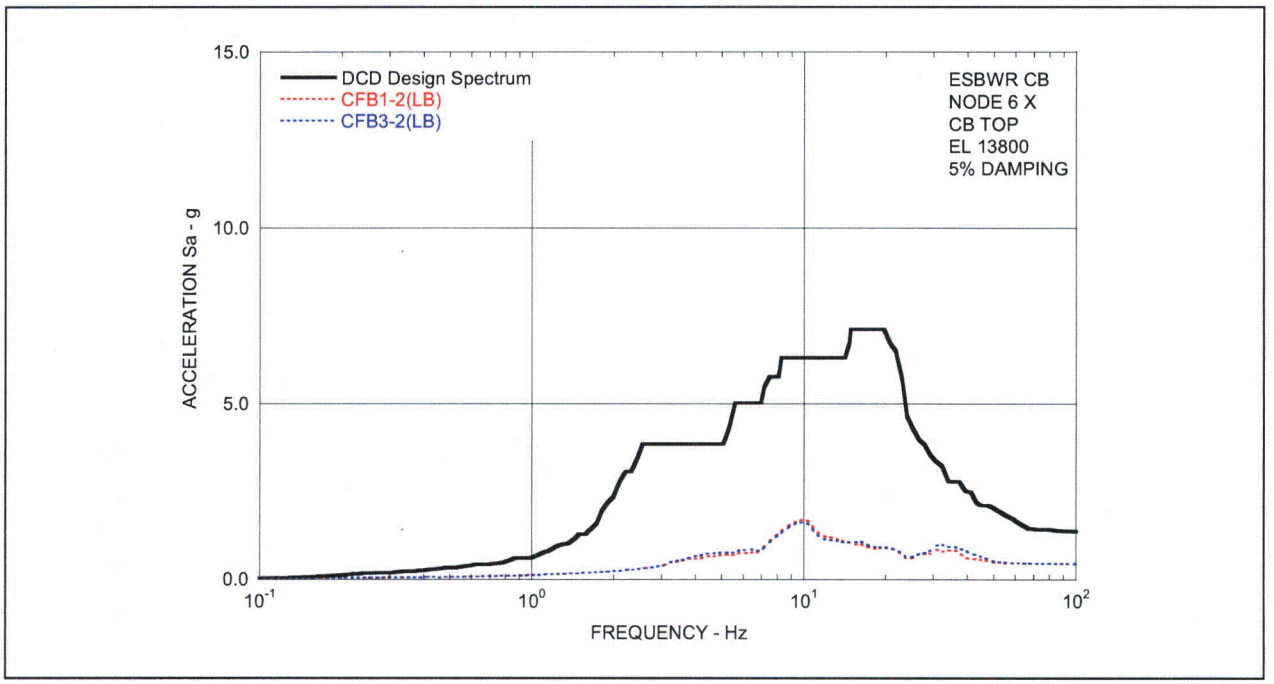

Figure 03.07.02-8(15)a Floor Response Spectra (LB) - CB Top in X-Direction - Comparison between SSI (CFB1) and SSSI including FWSC Effects (CFB3)

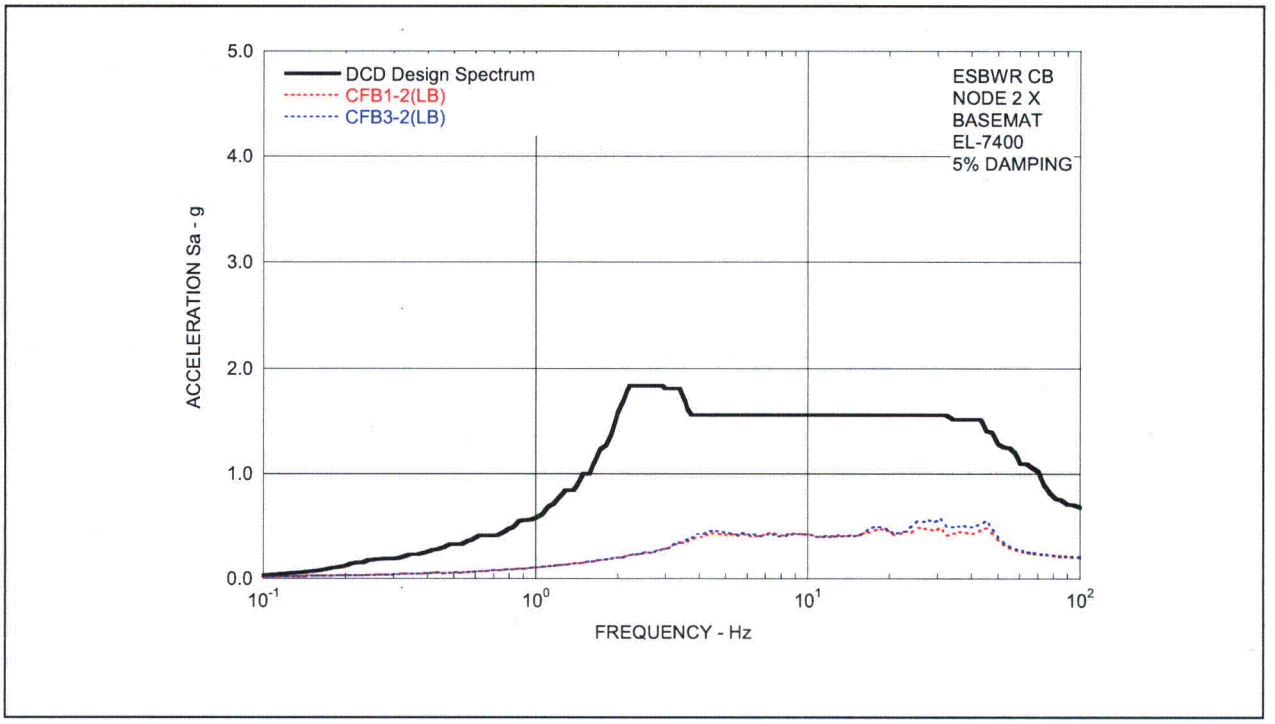

Figure 03.07.02-8(15)b Floor Response Spectra (LB) - CB Basemat in X-Direction - Comparison between SSI (CFB1) and SSSI including FWSC Effects (CFB3)

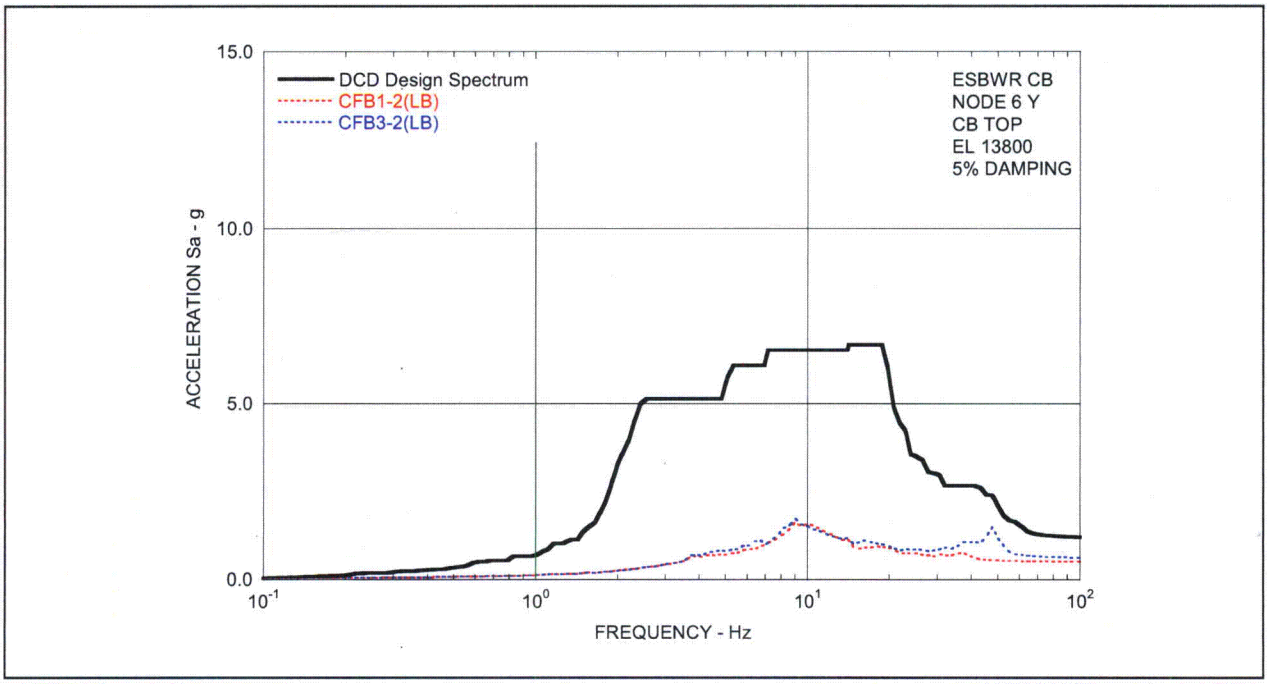

Figure 03.07.02-8(16)a Floor Response Spectra (LB) - CB Top in Y-Direction - Comparison between SSI (CFB1) and SSSI including FWSC Effects (CFB3)

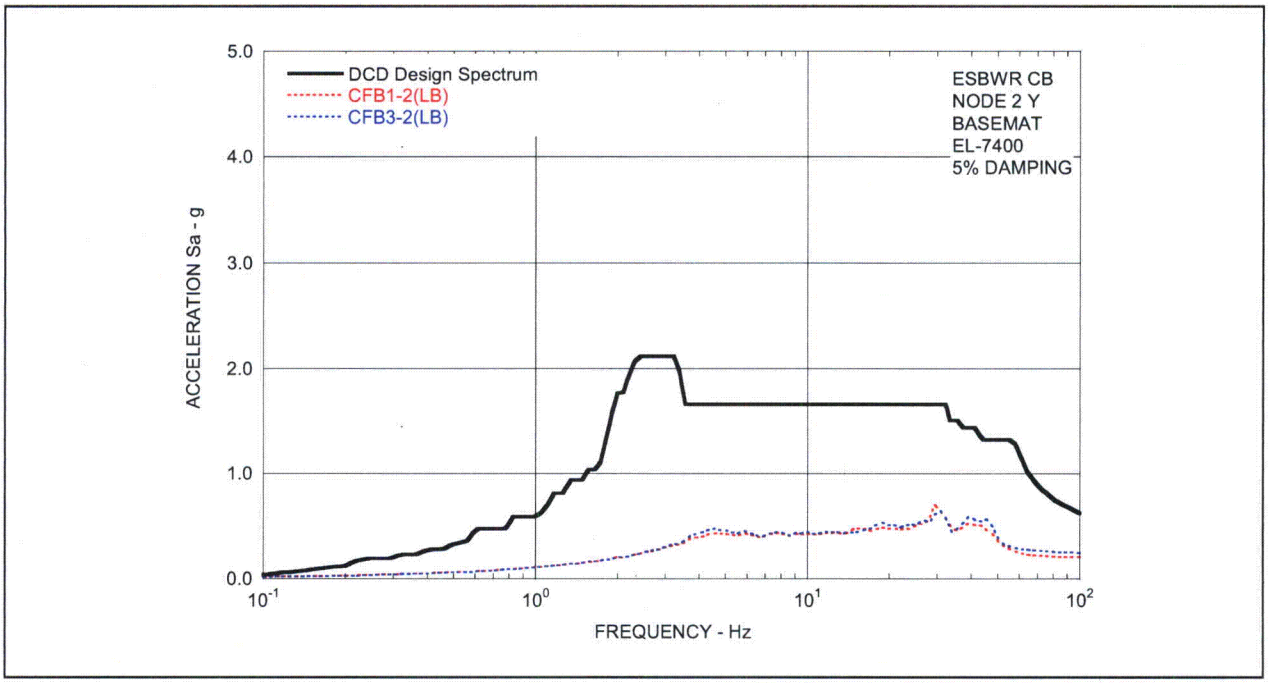

Figure 03.07.02-8(16)b Floor Response Spectra (LB) - CB Basemat in Y-Direction - Comparison between SSI (CFB1) and SSSI including FWSC Effects (CFB3)

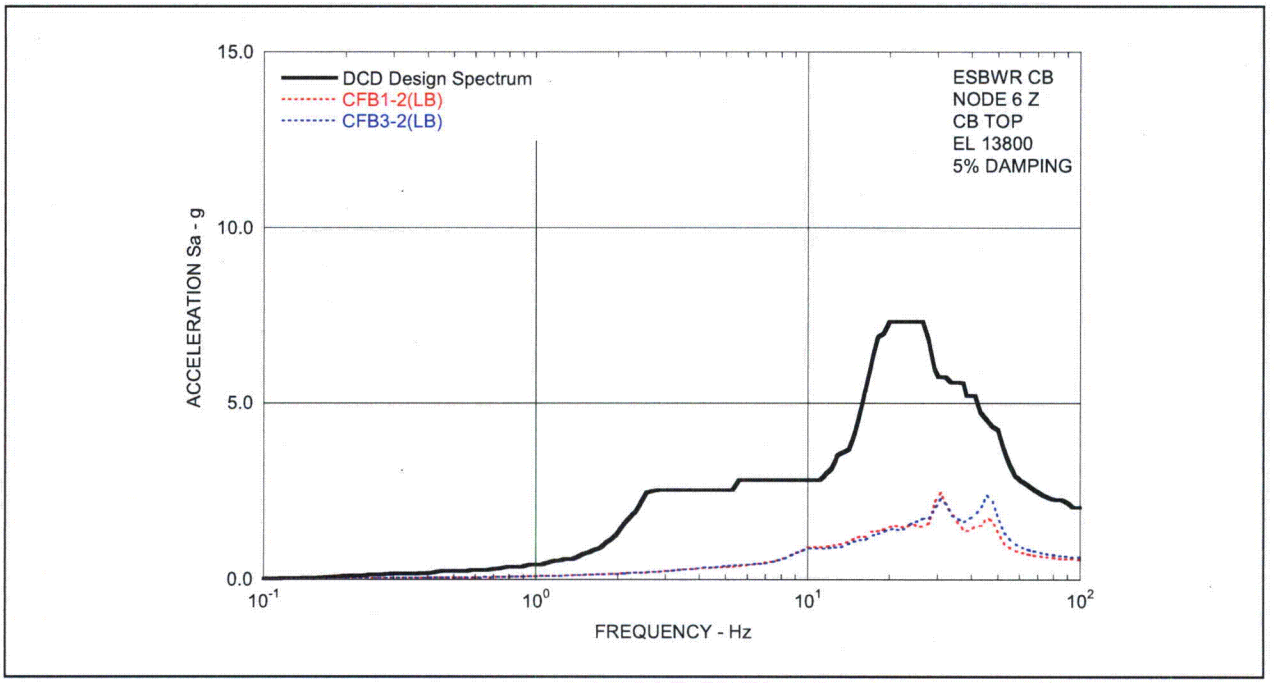

Figure 03.07.02-8(17)a Floor Response Spectra (LB) - CB Top in Z-Direction - Comparison between SSI (CFB1) and SSSI including FWSC Effects (CFB3)

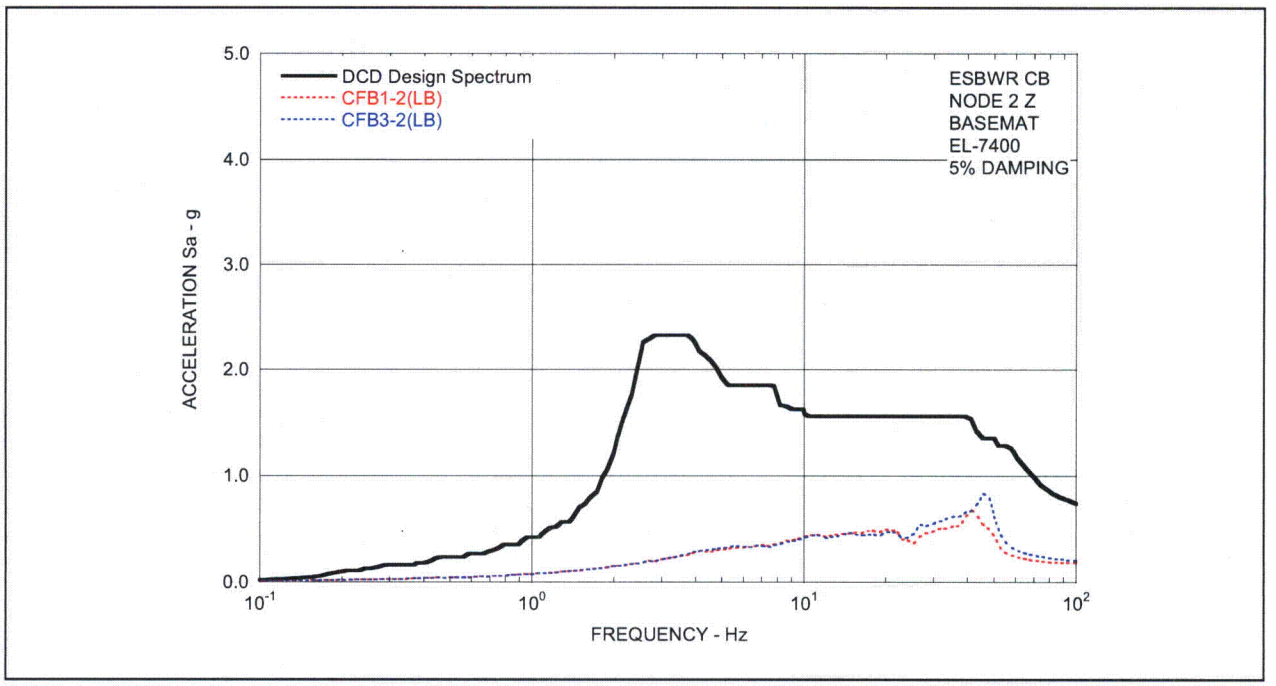

Figure 03.07.02-8(17)b Floor Response Spectra (LB) - CB Basemat in -Z-Direction - Comparison between SSI (CFB1) and SSSI including FWSC Effects (CFB3)

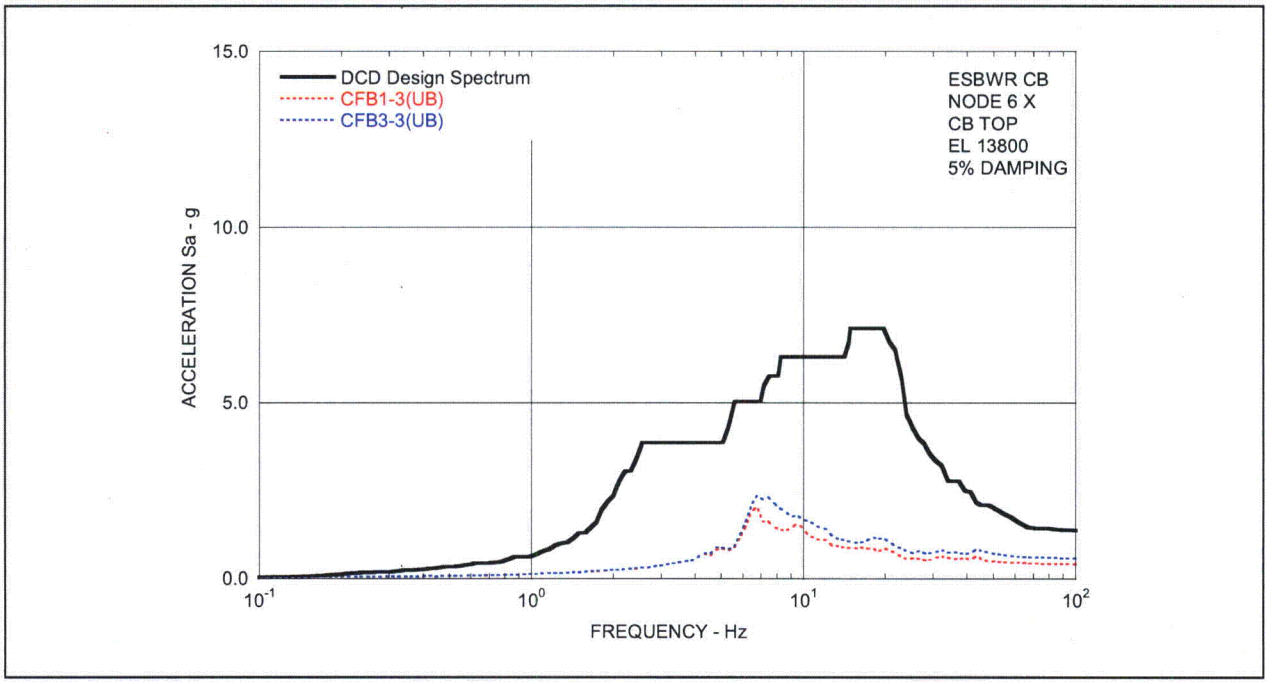

Figure 03.07.02-8(18)a Floor Response Spectra (UB) - CB Top in X-Direction - Comparison between SSI (CFB1) and SSSI including FWSC Effects (CFB3)

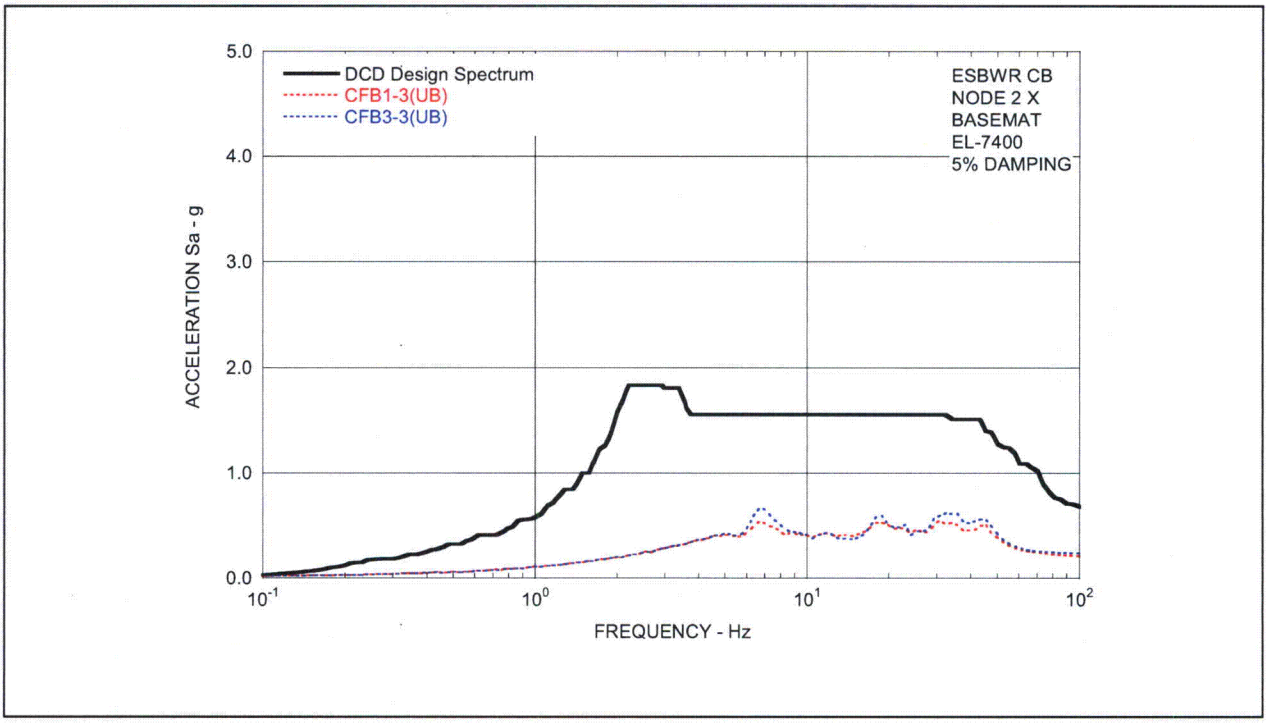

Figure 03.07.02-8(18)b Floor Response Spectra (UB) - CB Basemat in X-Direction - Comparison between SSI (CFB1) and SSSI including FWSC Effects (CFB3)

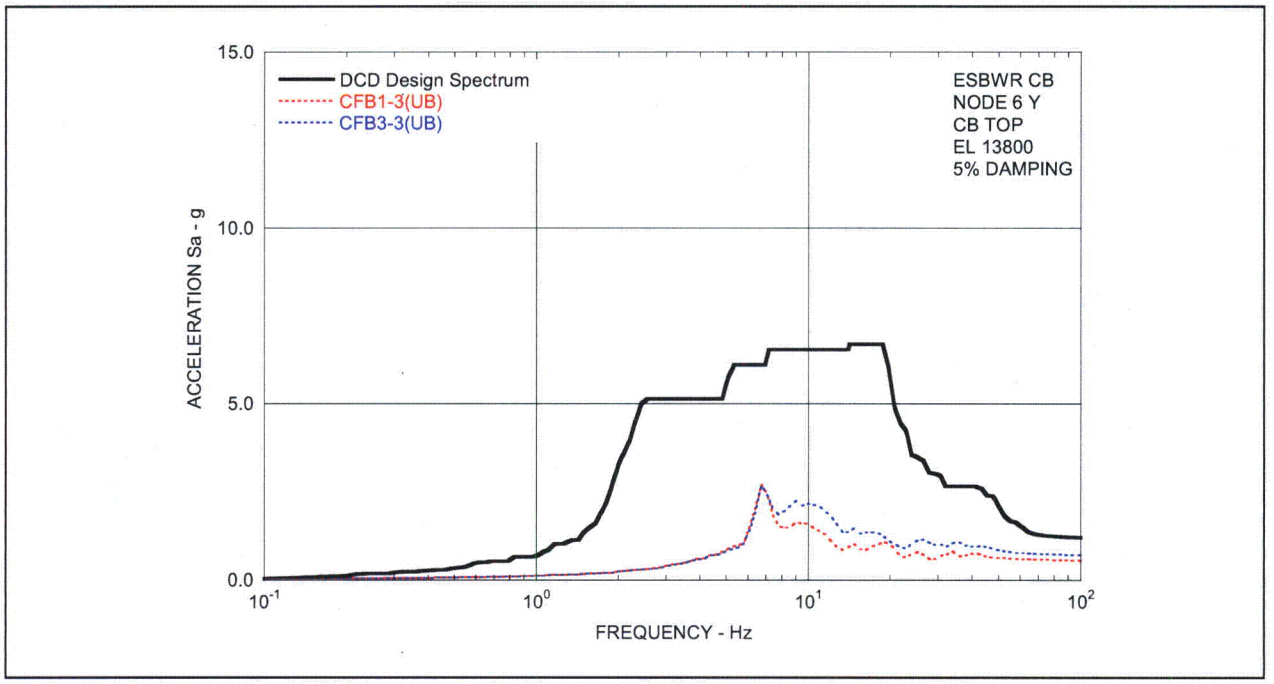

Figure 03.07.02-8(19)a Floor Response Spectra (UB) - CB Top in Y-Direction - Comparison between SSI (CFB1) and SSSI including FWSC Effects (CFB3)

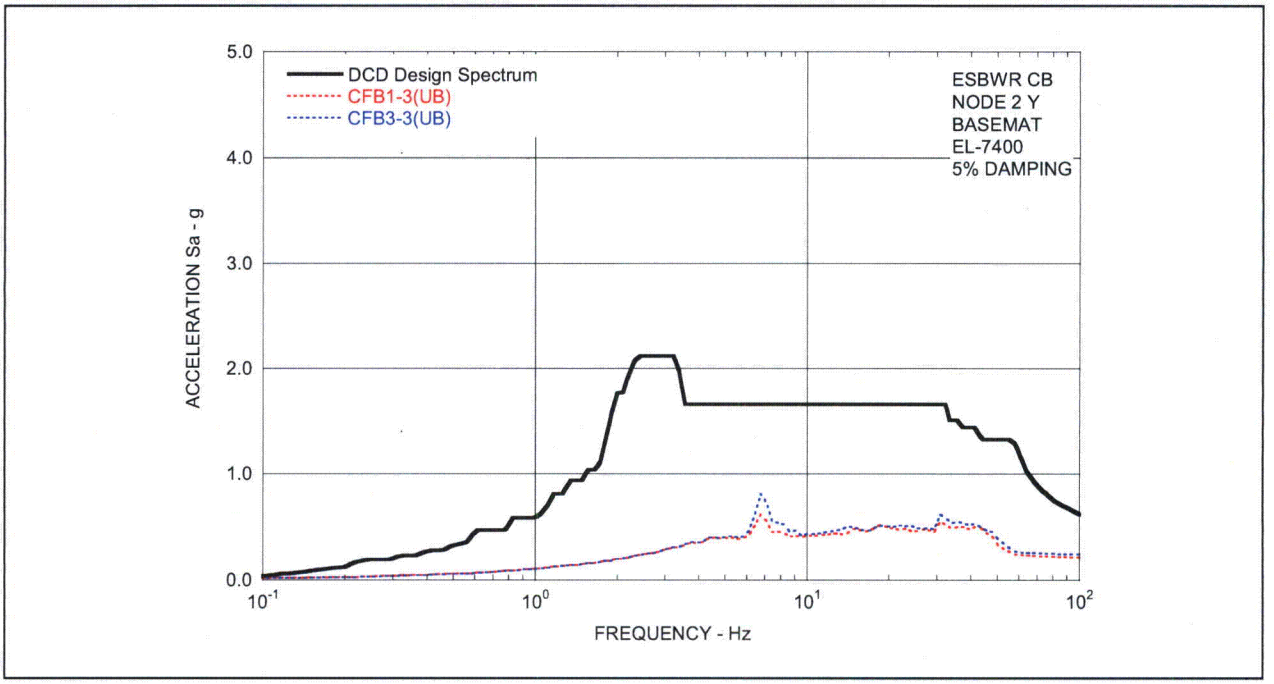

Figure 03.07.02-8(19)b Floor Response Spectra (UB) - CB Basemat in Y-Direction - Comparison between SSI (CFB1) and SSSI including FWSC Effects (CFB3)

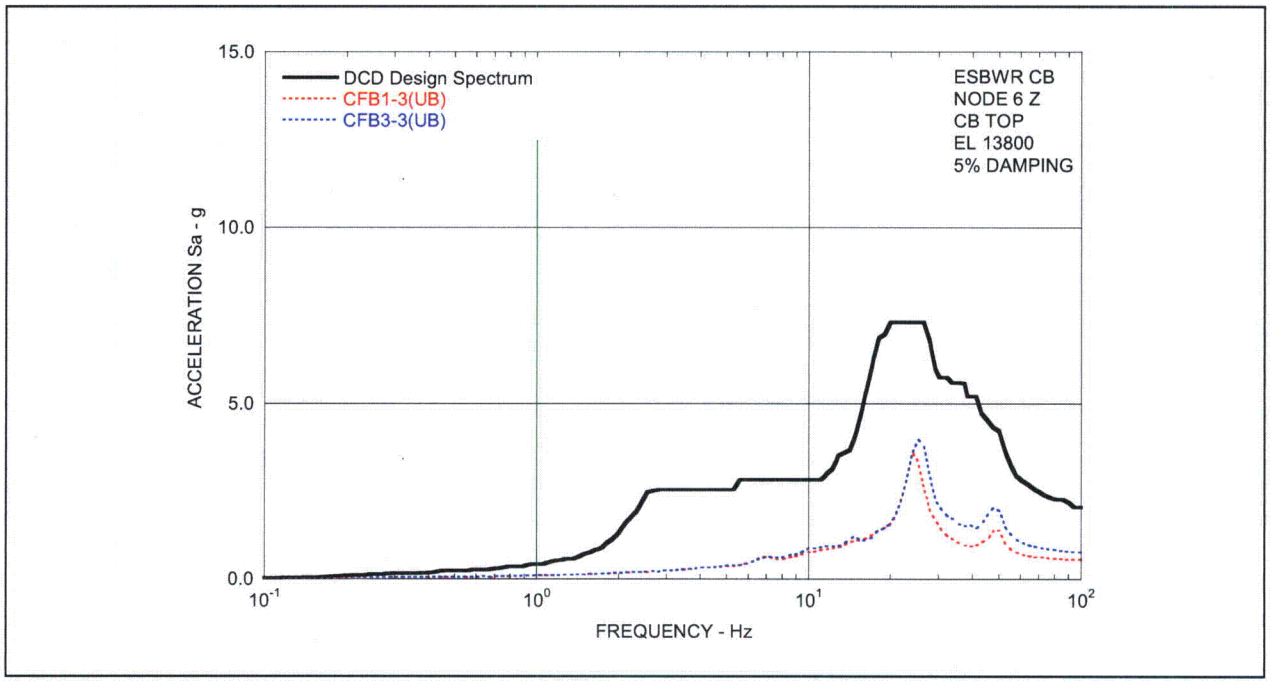

Figure 03.07.02-8(20)a Floor Response Spectra (UB) - CB Top in Z-Direction - Comparison between SSI (CFB1) and SSSI including FWSC Effects (CFB3)

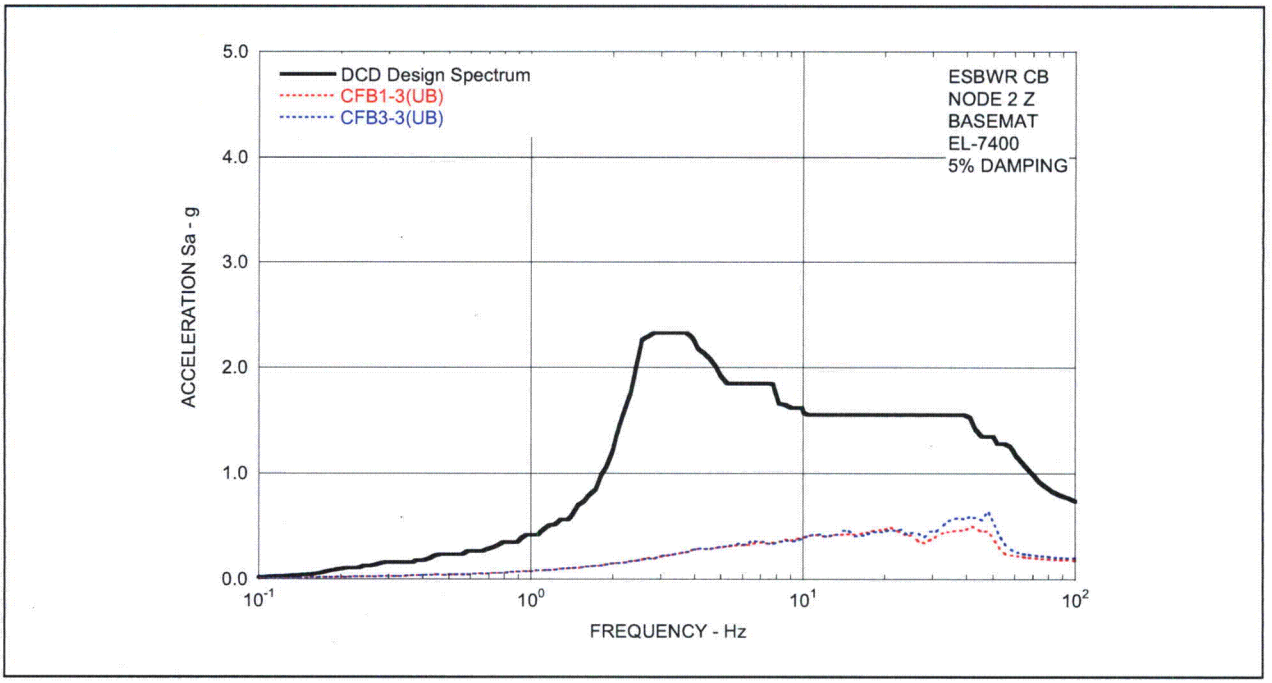

Figure 03.07.02-8(20)b Floor Response Spectra (UB) - CB Basemat in -Z-Direction - Comparison between SSI (CFB1) and SSSI including FWSC Effects (CFB3)

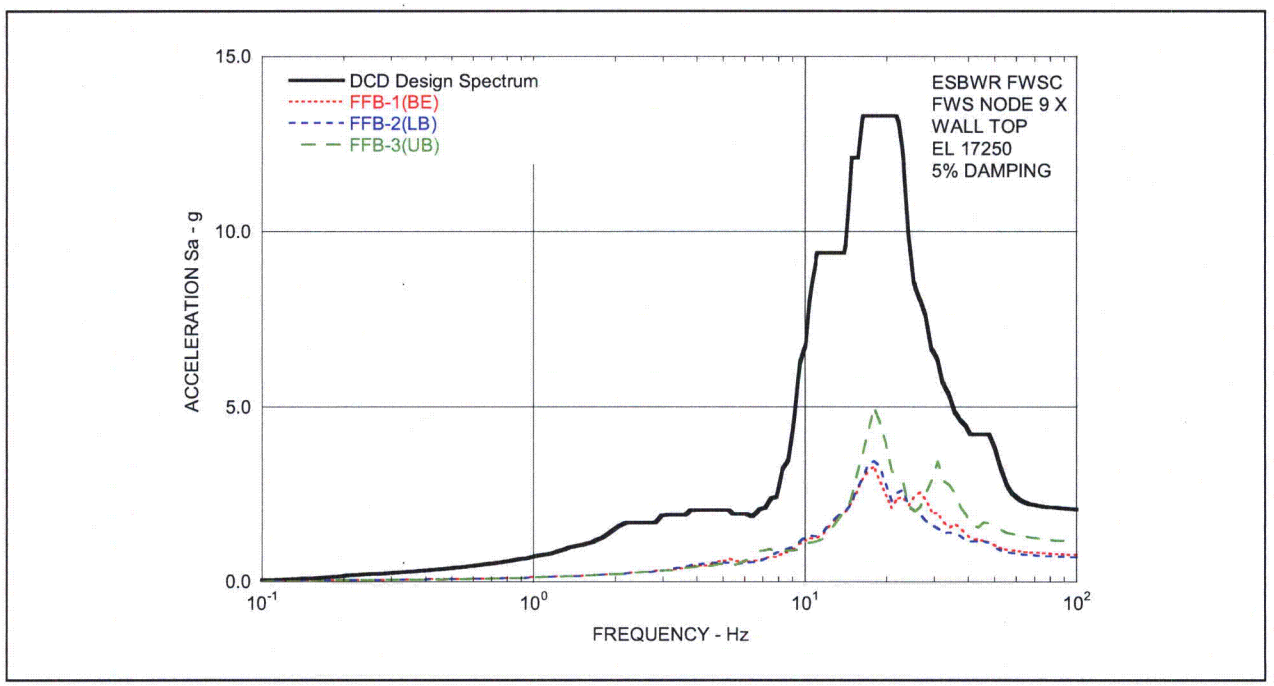

Figure 03.07.02-8(21)a Floor Response Spectra - FWS Wall Top in X-Direction - Case CFB3-FFB

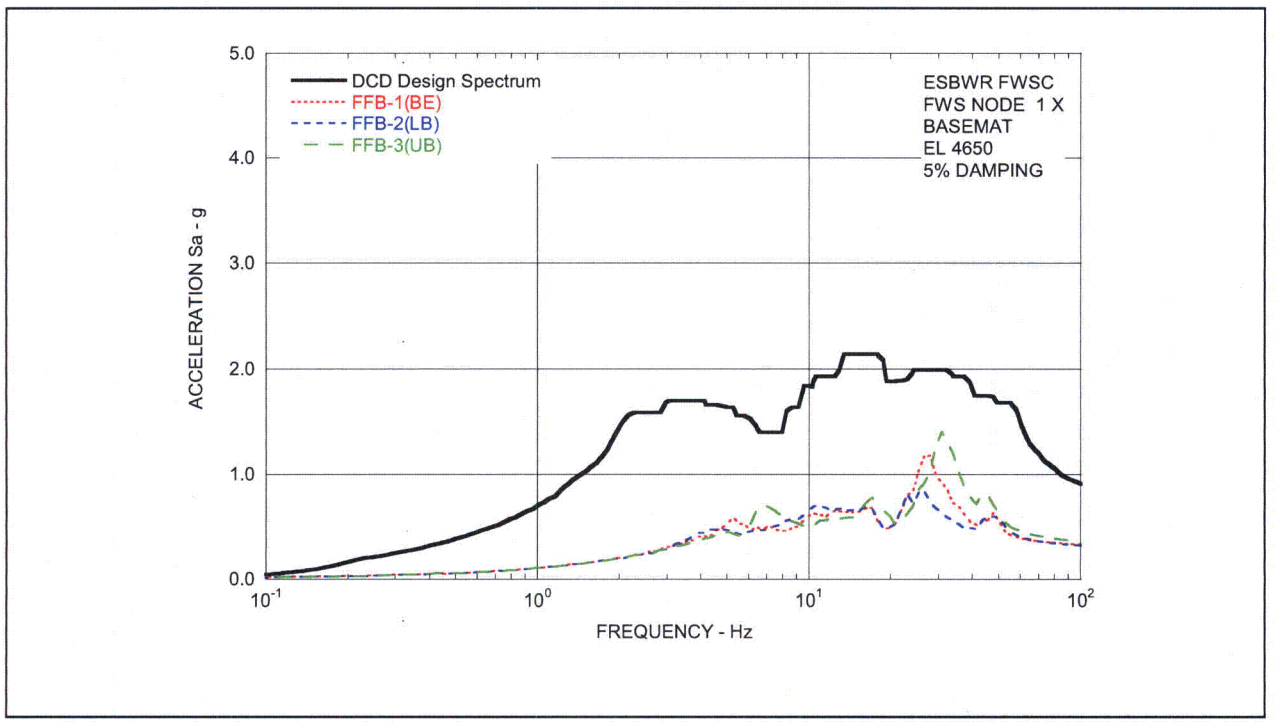

Figure 03.07.02-8(21)b Comparison of Floor Response Spectra - FWS Basemat in X-Direction - Case CFB3-FFB

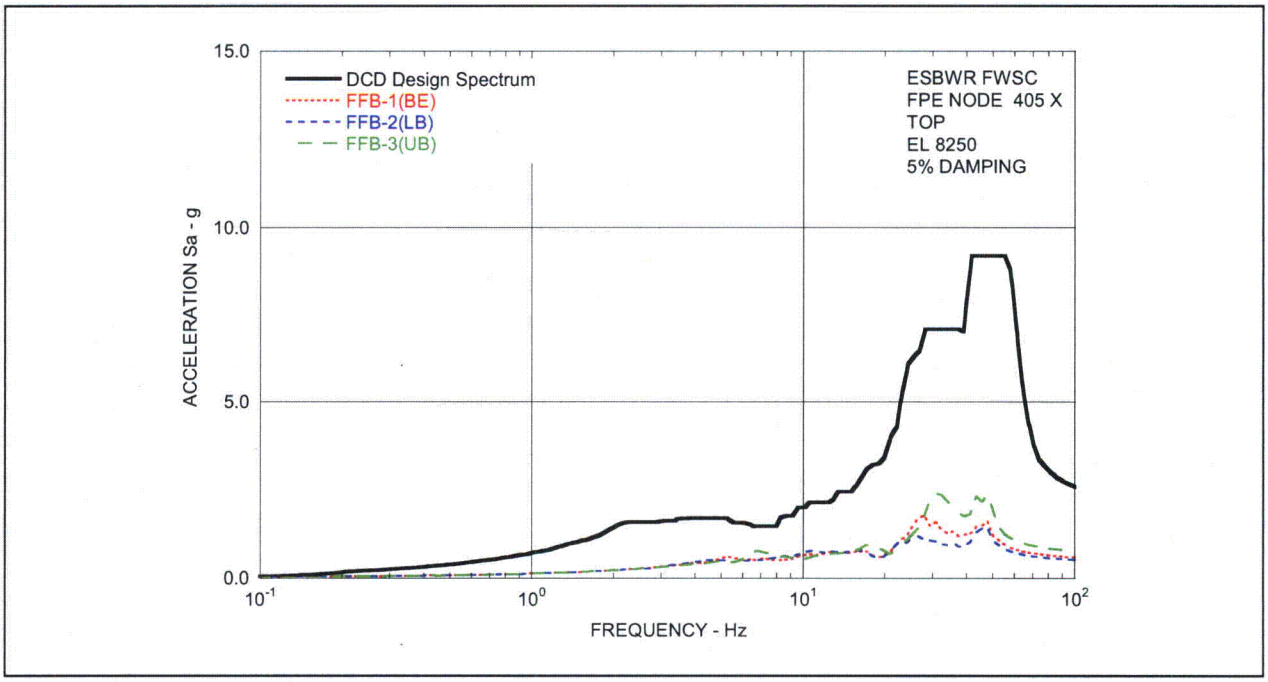

Figure 03.07.02-8(21)c Comparison of Floor Response Spectra - FPE Top in X-Direction - Case CFB3-FFB

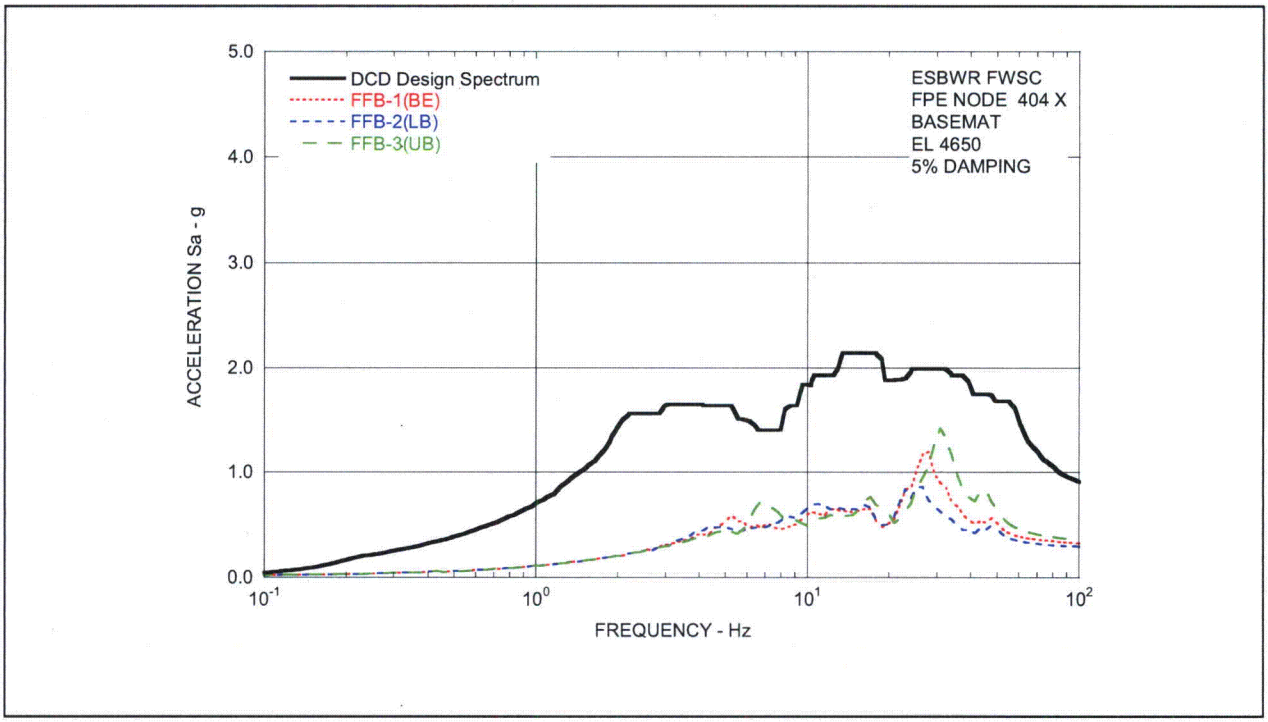

Figure 03.07.02-8(21)d Comparison of Floor Response Spectra - FPE Basemat in X-Direction - Case CFB3-FFB

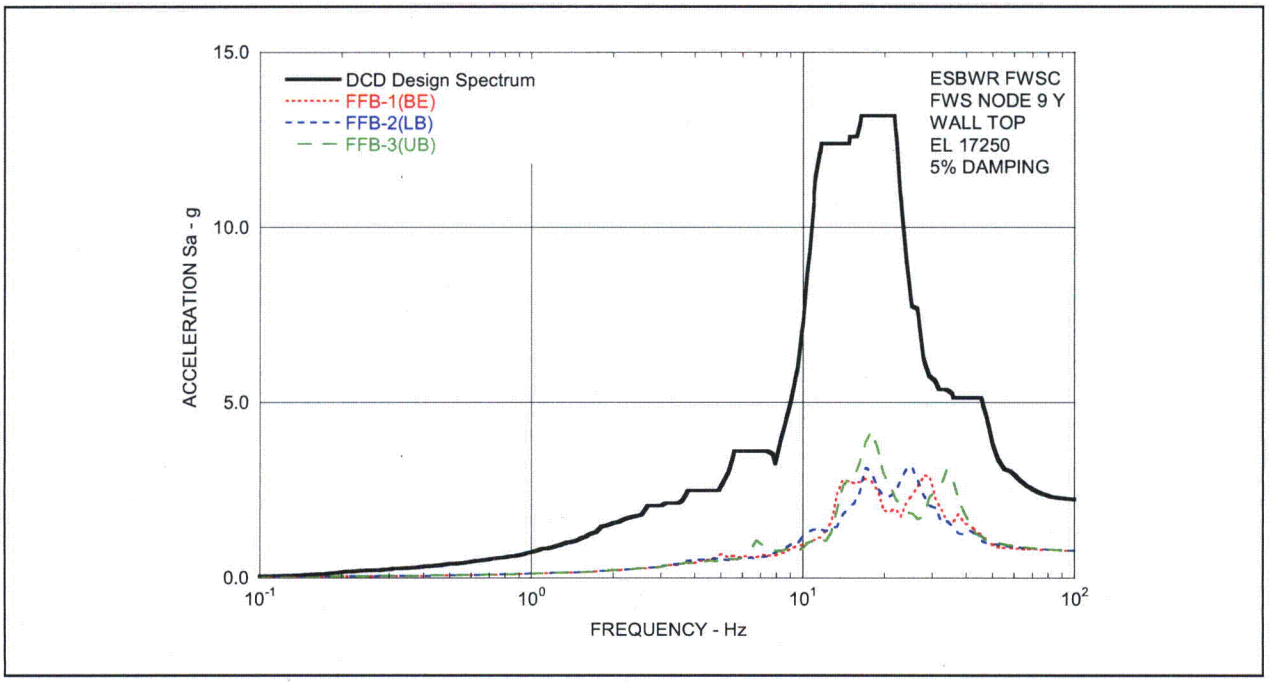

Figure 03.07.02-8(22)a Comparison of Floor Response Spectra - FWS Wall Top in Y-Direction - Case CFB3-FFB

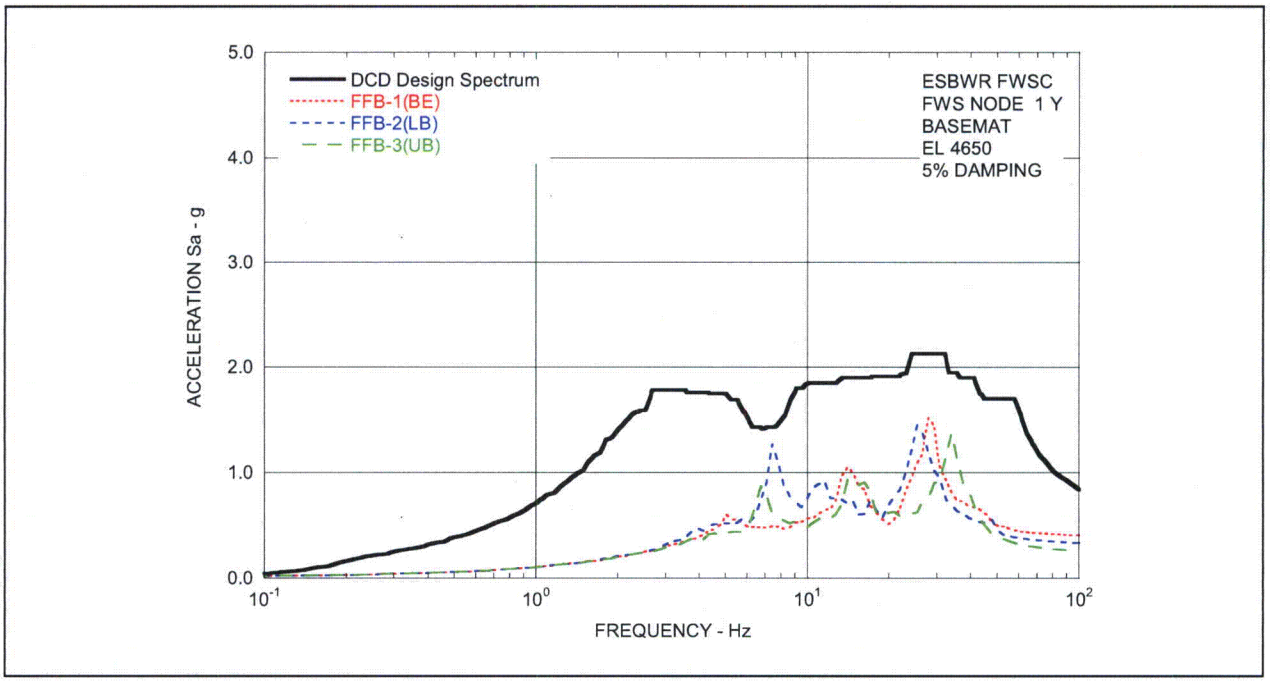

Figure 03.07.02-8(22)b Comparison of Floor Response Spectra - FWS Basemat in Y-Direction - Case CFB3-FFB

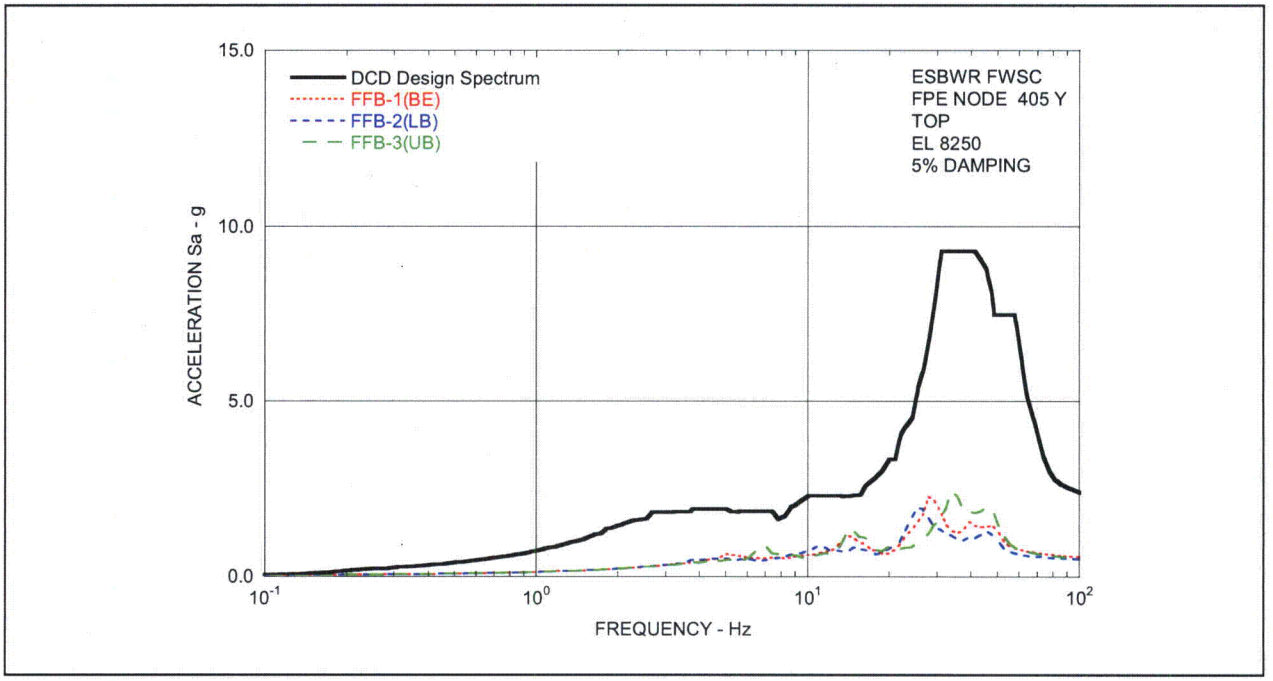

Figure 03.07.02-8(22)c Comparison of Floor Response Spectra - FPE Top in Y-Direction - Case CFB3-FFB

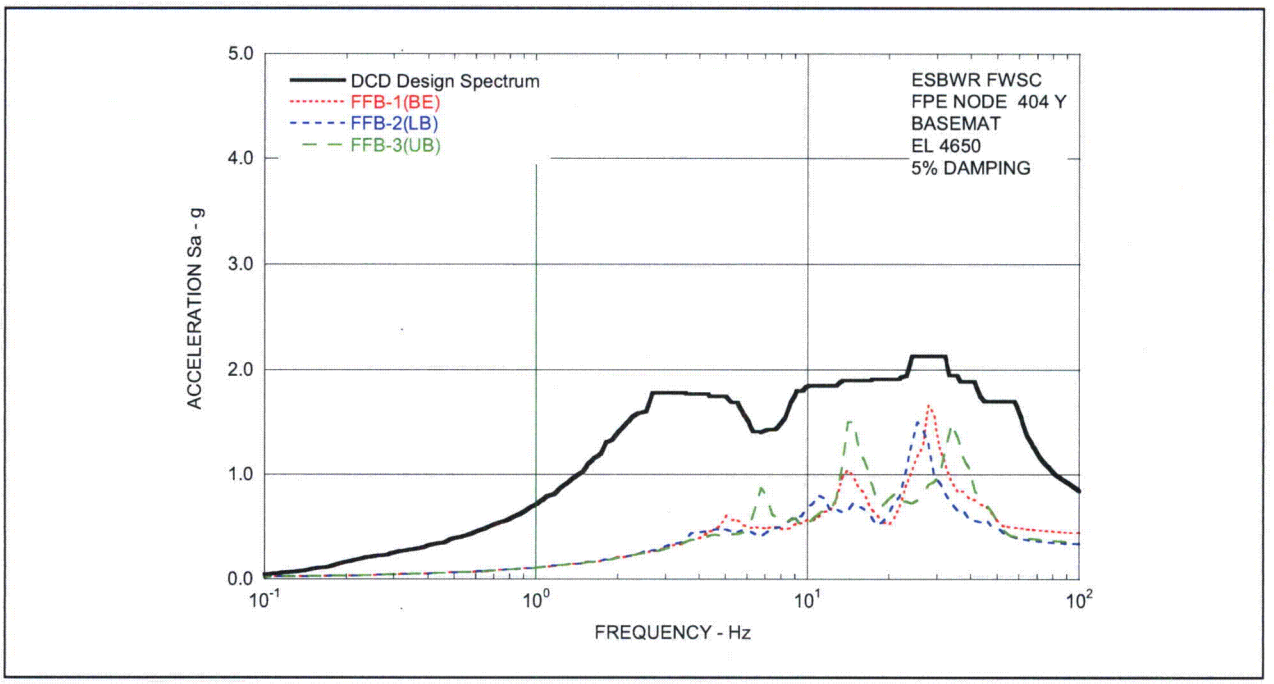

Figure 03.07.02-8(22)d Comparison of Floor Response Spectra - FPE Basemat in Y-Direction - Case CFB3-FFB

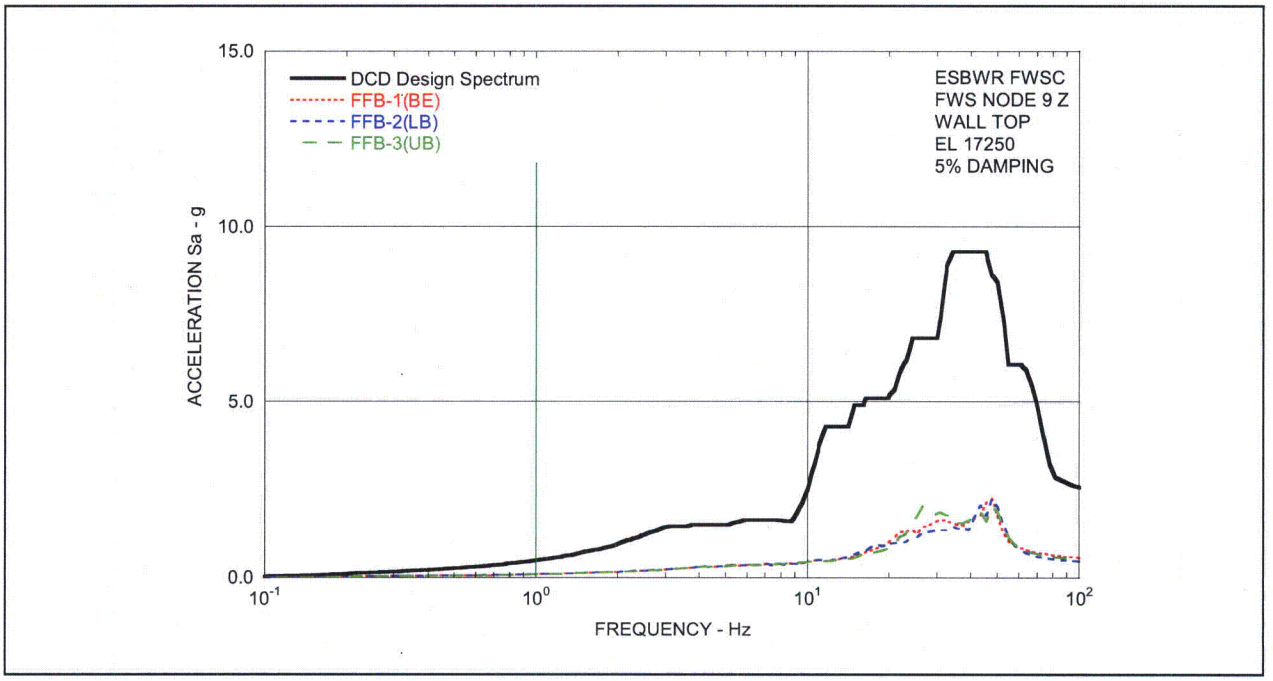

Figure 03.07.02-8(23)a Comparison of Floor Response Spectra - FWS Wall Top in Z-Direction - Case CFB3-FFB

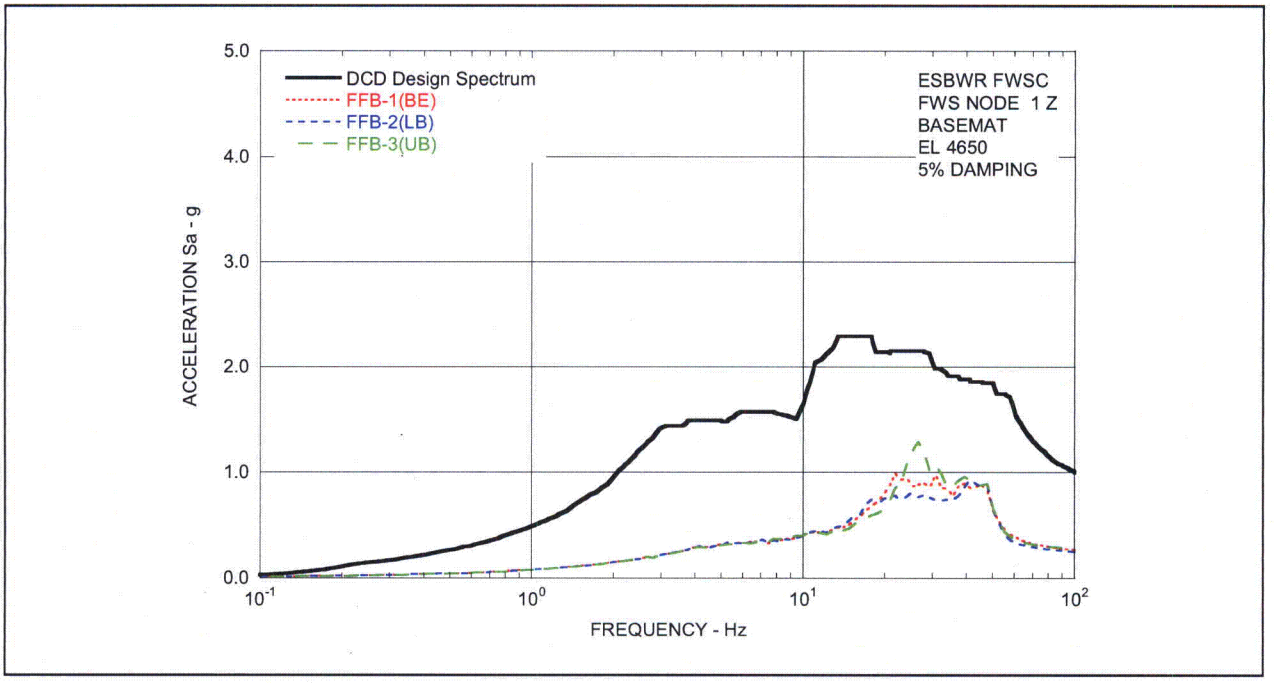

Figure 03.07.02-8(23)b Comparison of Floor Response Spectra - FWS Basemat in -Z-Direction - Case CFB3-FFB

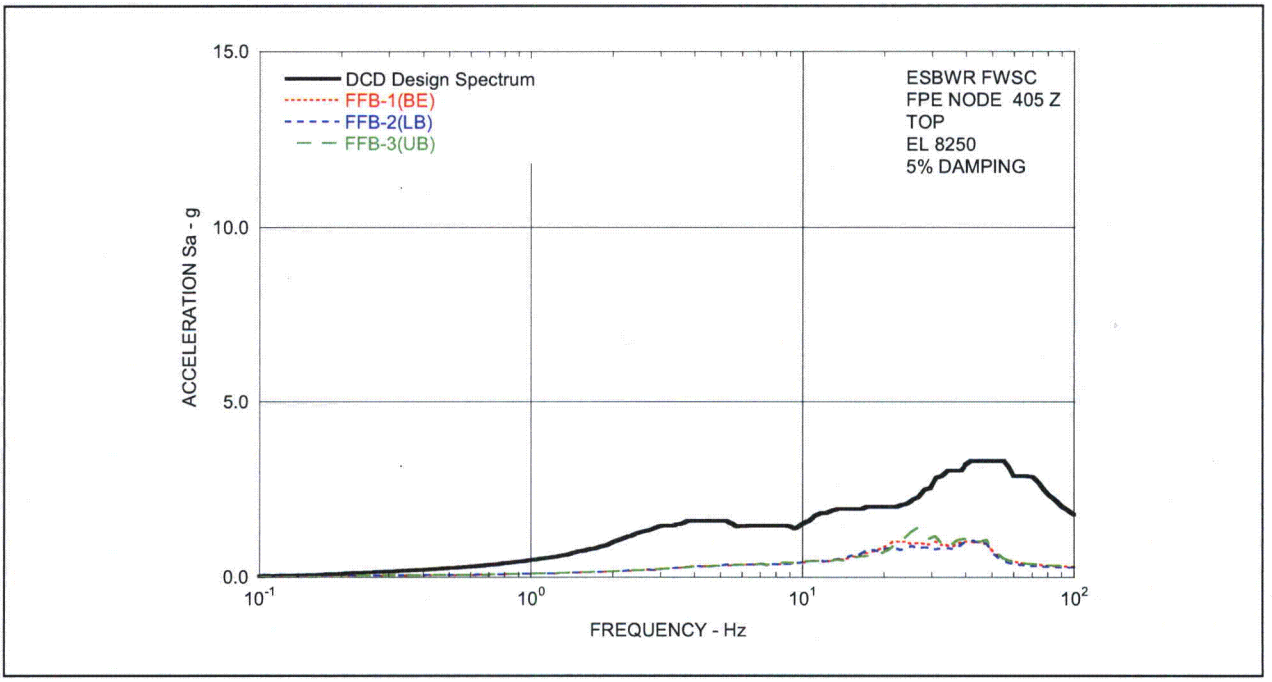

Figure 03.07.02-8(23)c Comparison of Floor Response Spectra - FPE Top in Z-Direction - Case CFB3-FFB

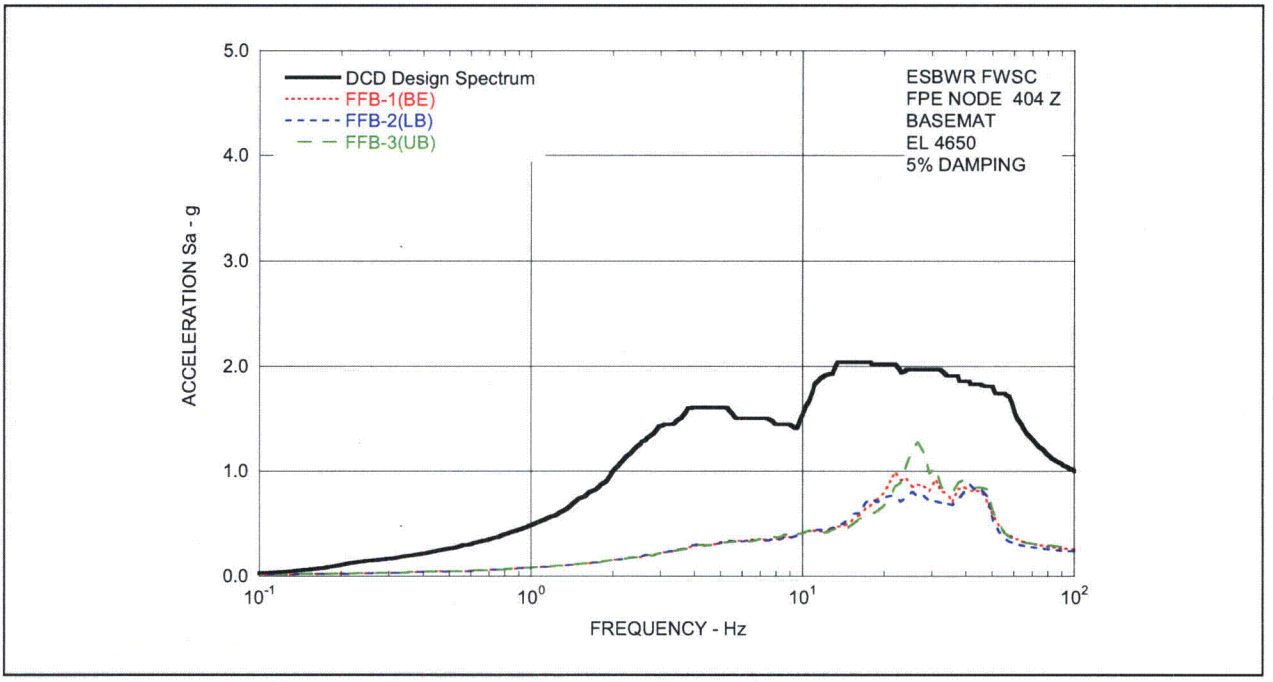

Figure 03.07.02-8(23)d Comparison of Floor Response Spectra - FPE Basemat in -Z-Direction - Case CFB3-FFB

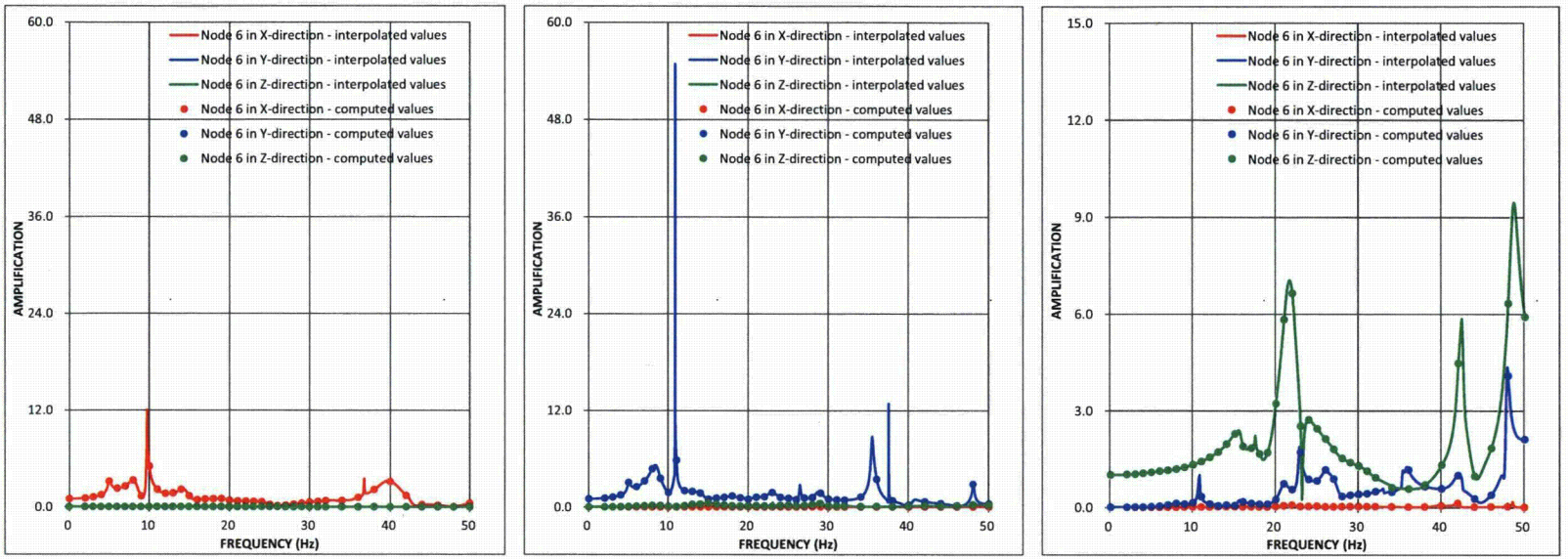

(a) X-Direction Input (b) Y-Direction Input (c) Z-Direction Input

Figure 03.07.02-8(24)a Transfer functions - CB Top at Best Estimate Subsurface Profile – Case CFB3-FFB

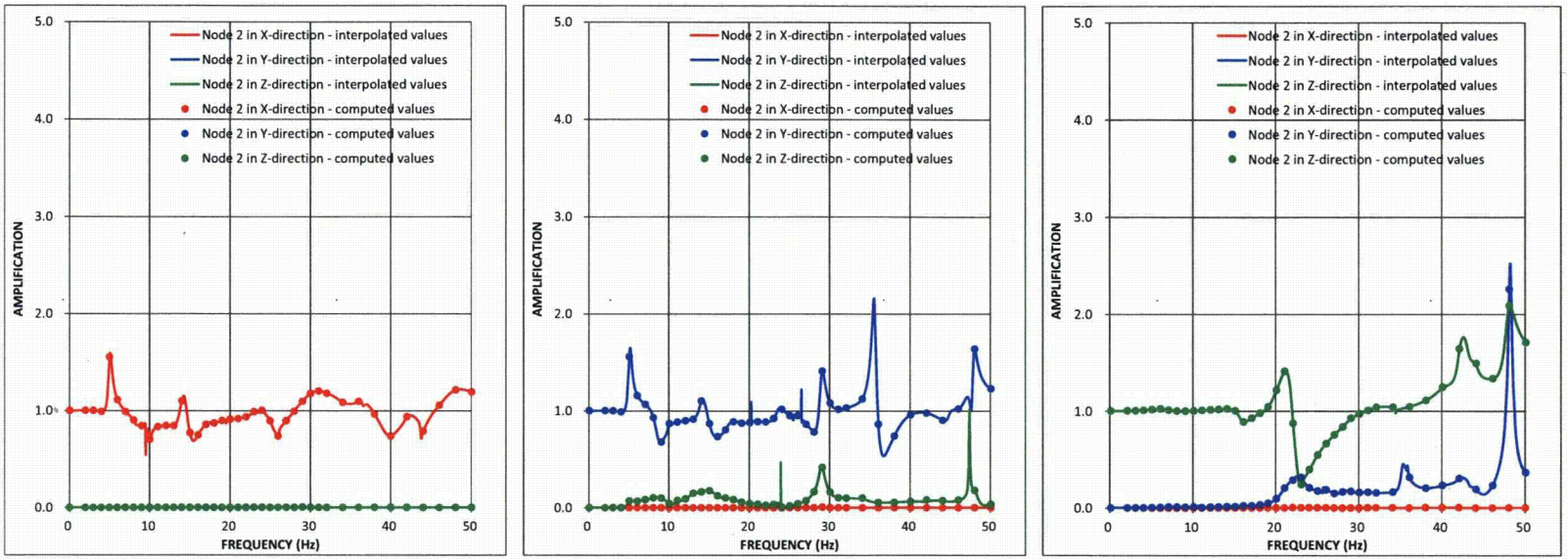

(a) X-Direction Input (b) Y-Direction Input (c) Z-Direction Input

Figure 03.07.02-8(24)b Transfer functions - CB Basemat at Best Estimate Subsurface Profile – Case CFB3-FFB

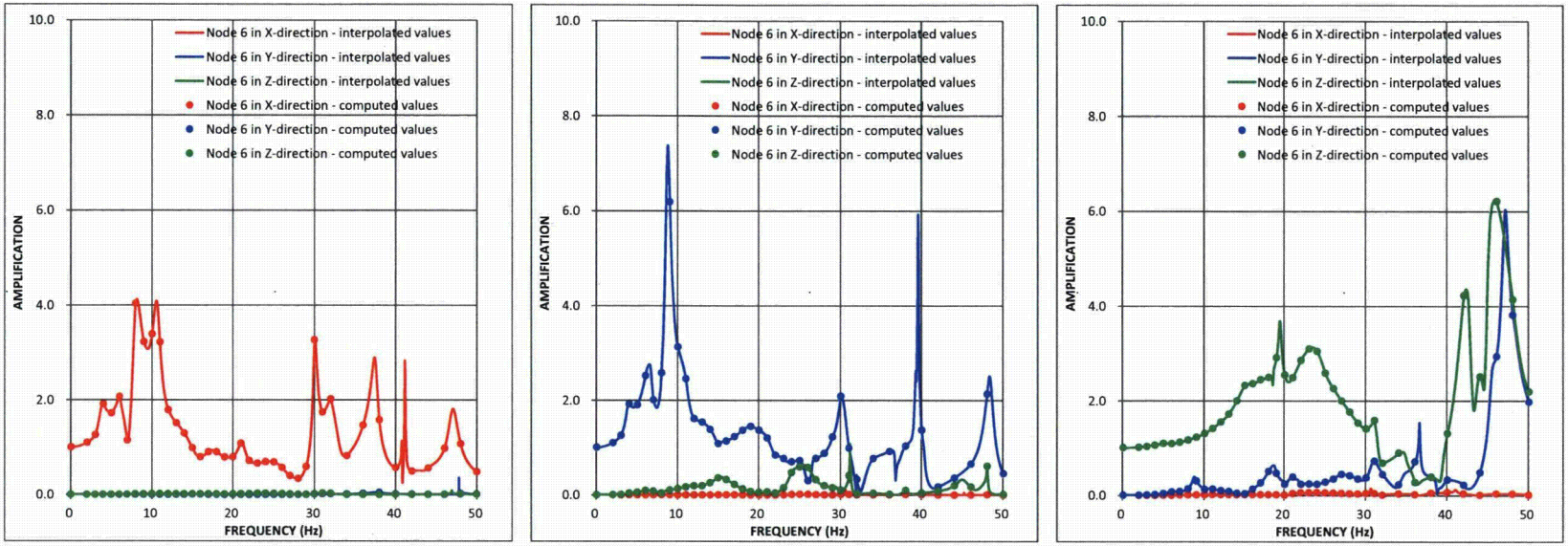

(a) X-Direction Input (b) Y-Direction Input (c) Z-Direction Input

Figure 03.07.02-8(25)a Transfer functions - CB Top at Lower Bound Subsurface Profile – Case CFB3-FFB

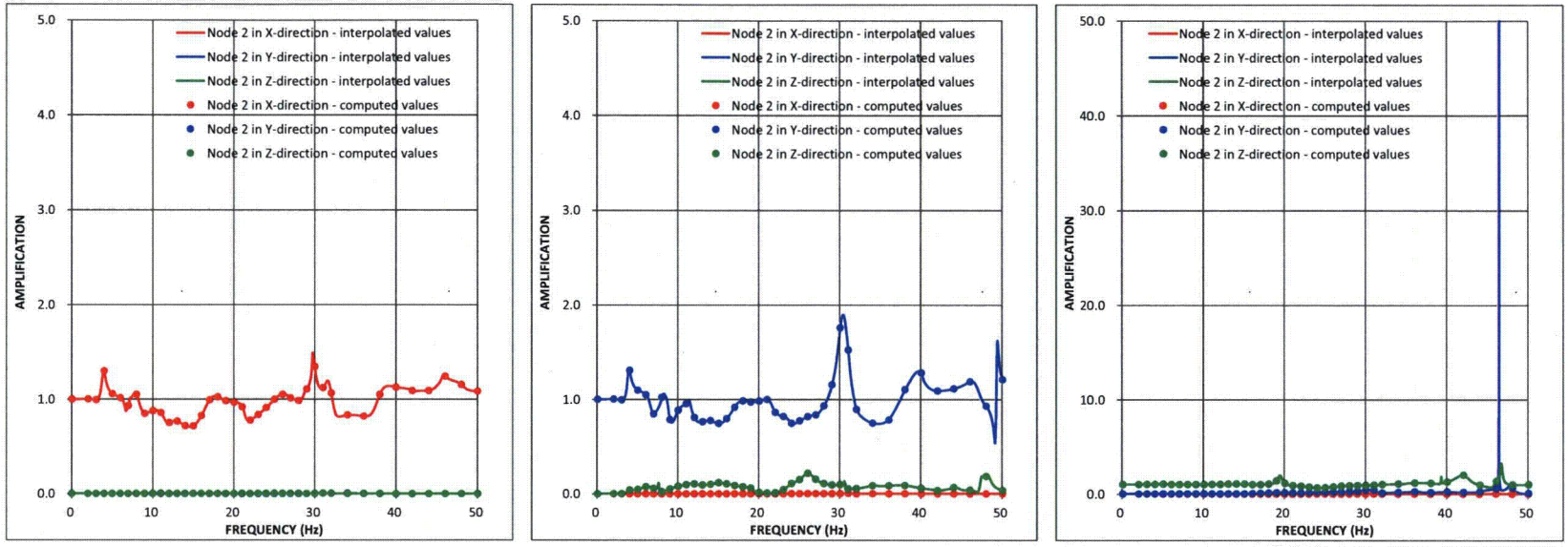

(a) X-Direction Input (b) Y-Direction Input (c) Z-Direction Input

Figure 03.07.02-8(25)b Transfer functions - CB Basemat at Lower Bound Subsurface Profile – Case CFB3-FFB

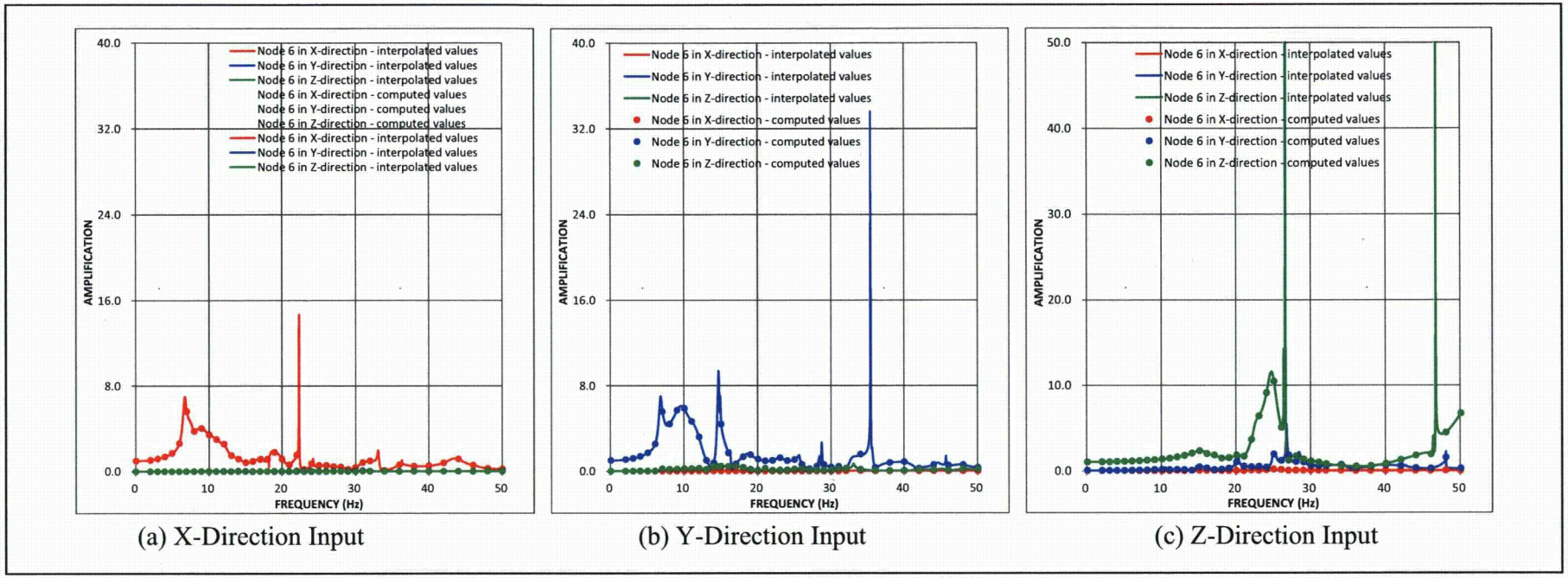

(a) X-Direction Input (b) Y-Direction Input (c) Z-Direction Input

Figure 03.07.02-8(26)a Transfer functions - CB Top at Upper Bound Subsurface Profile – Case CFB3-FFB

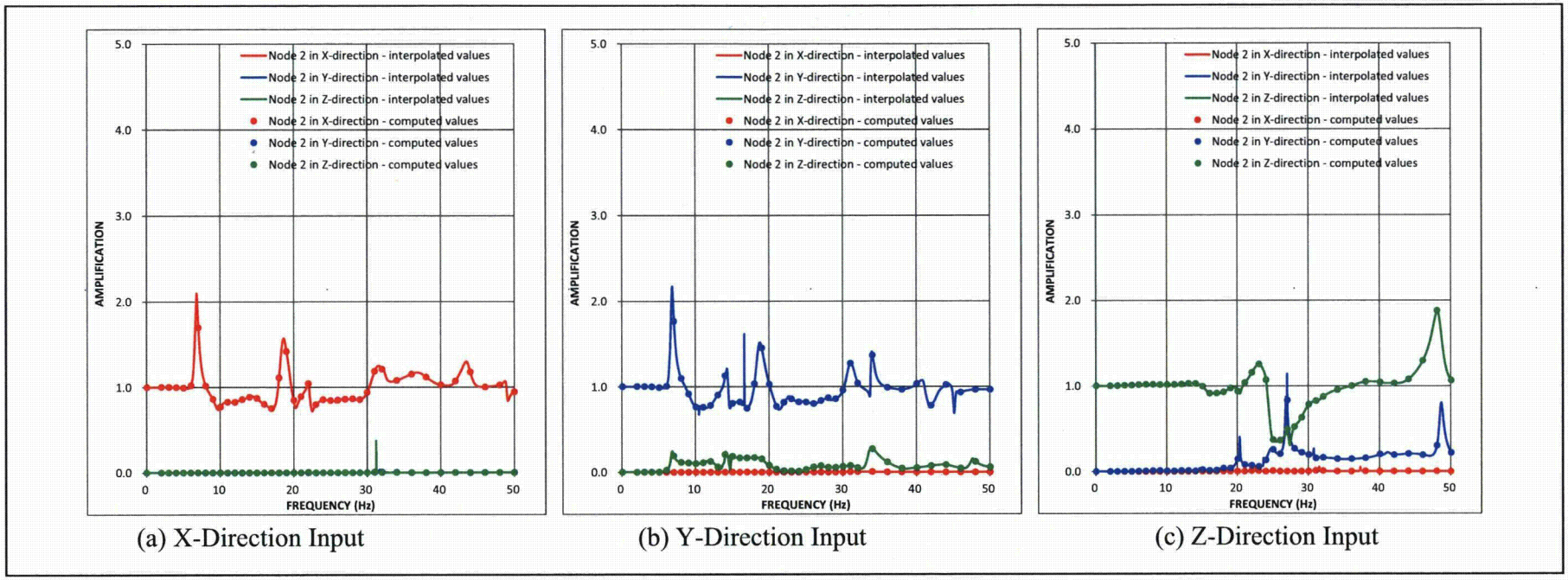

(a) X-Direction Input (b) Y-Direction Input (c) Z-Direction Input

Figure 03.07.02-8(26)b Transfer functions - CB Basemat at Upper Bound Subsurface Profile – Case CFB3-FFB

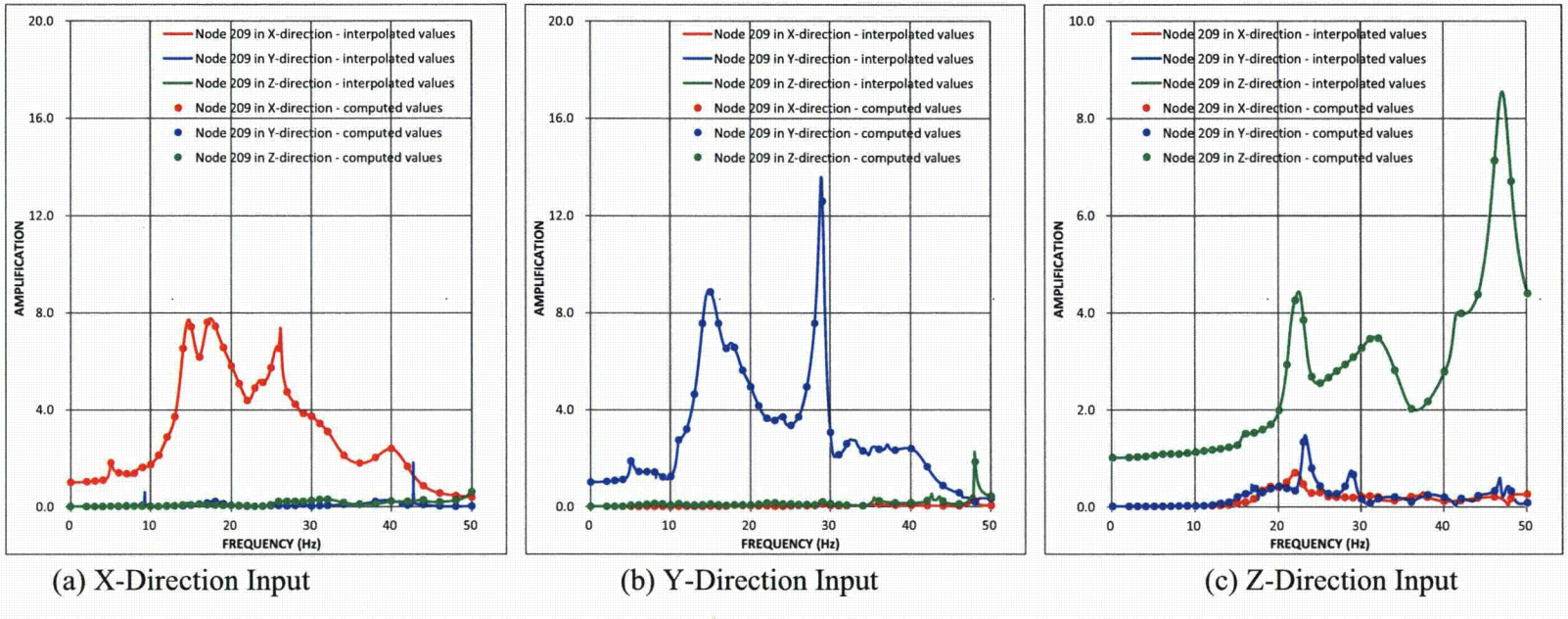

Figure 03.07.02-8(27)a Transfer functions - FWS Top at Best Estimate Subsurface Profile – Case CFB3-FFB

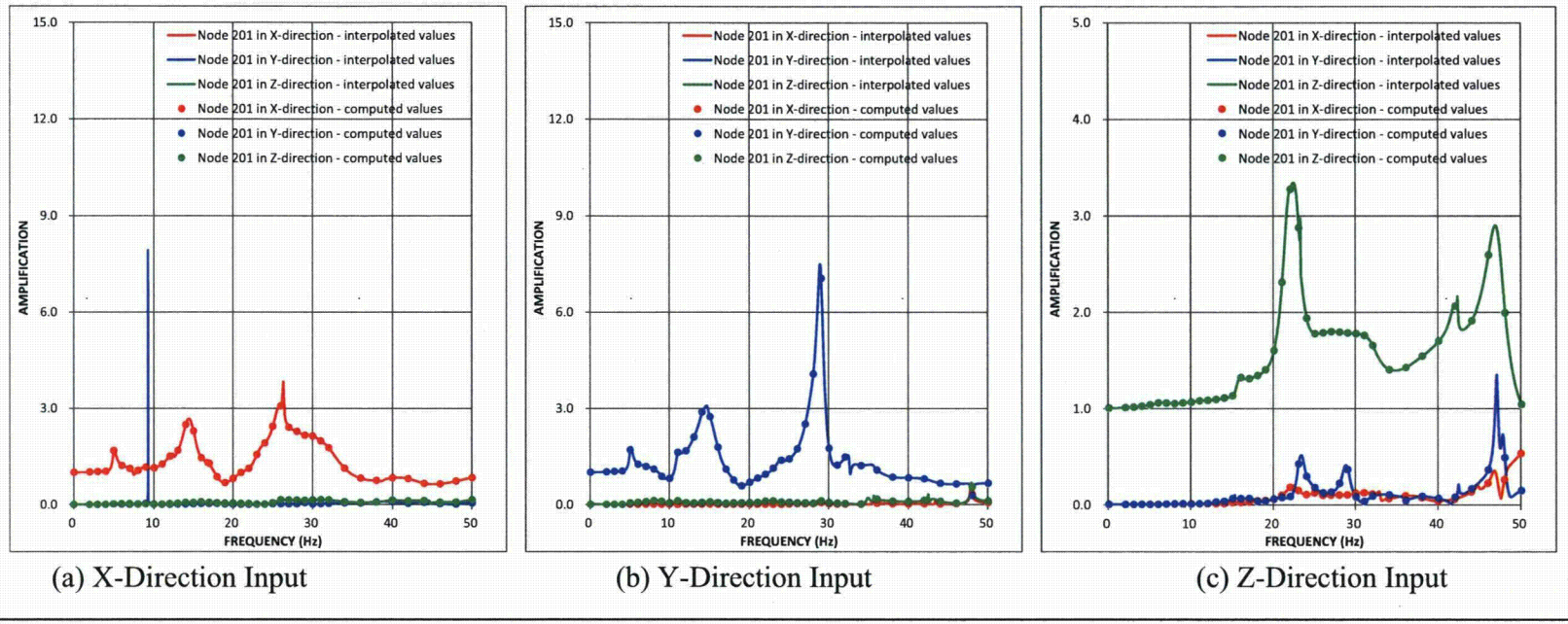

Figure 03.07.02-8(27)b Transfer functions - FWS Basemat at Best Estimate Subsurface Profile – Case CFB3-FFB

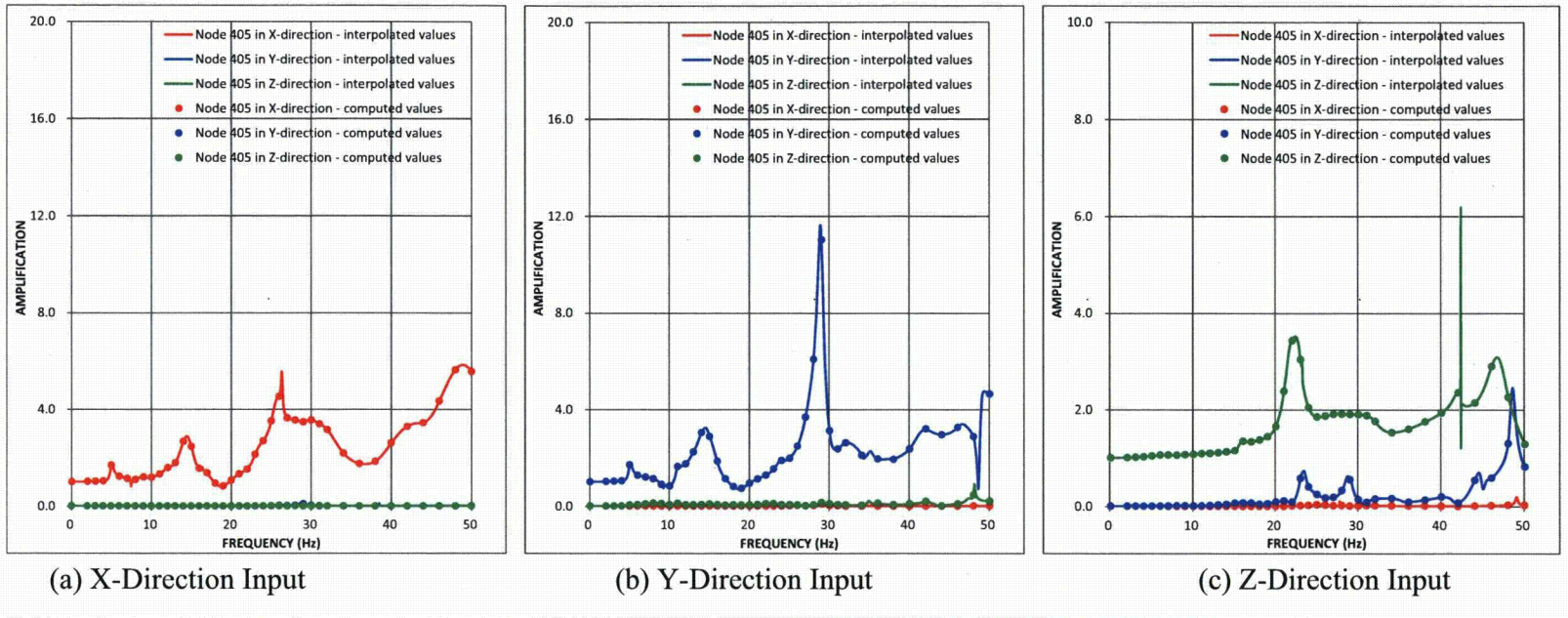

Figure 03.07.02-8(27)c Transfer functions - FPE Top at Best Estimate Subsurface Profile – Case CFB3-FFB

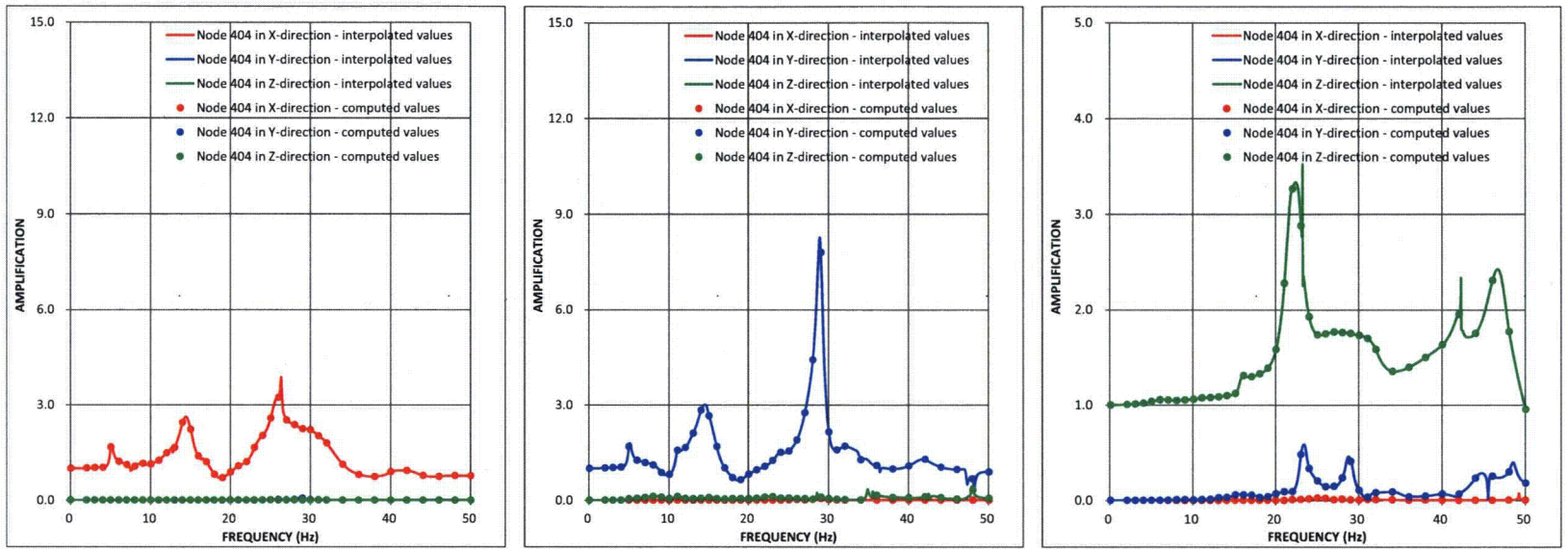

Figure 03.07.02-8(27)d Transfer functions - FPE Basemat at Best Estimate Subsurface Profile – Case CFB3-FFB

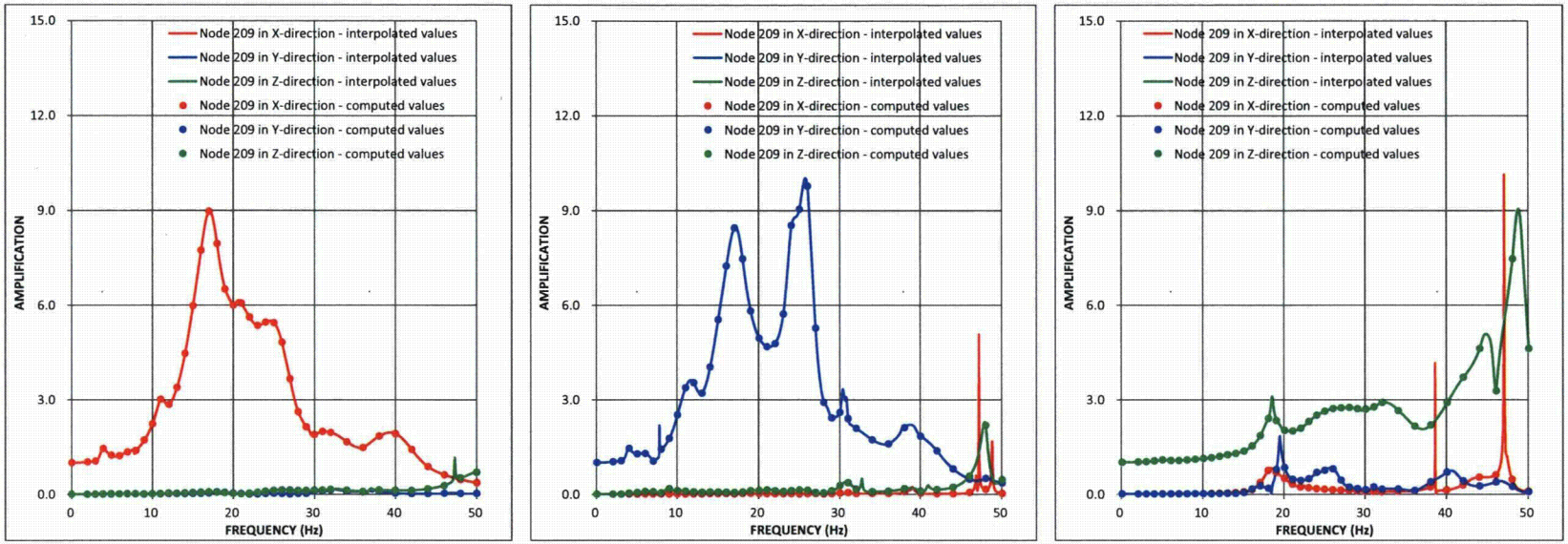

(a) X-Direction Input (b) Y-Direction Input (c) Z-Direction Input

Figure 03.07.02-8(28)a Transfer functions - FWS Top at Lower Bound Subsurface Profile – Case CFB3-FFB

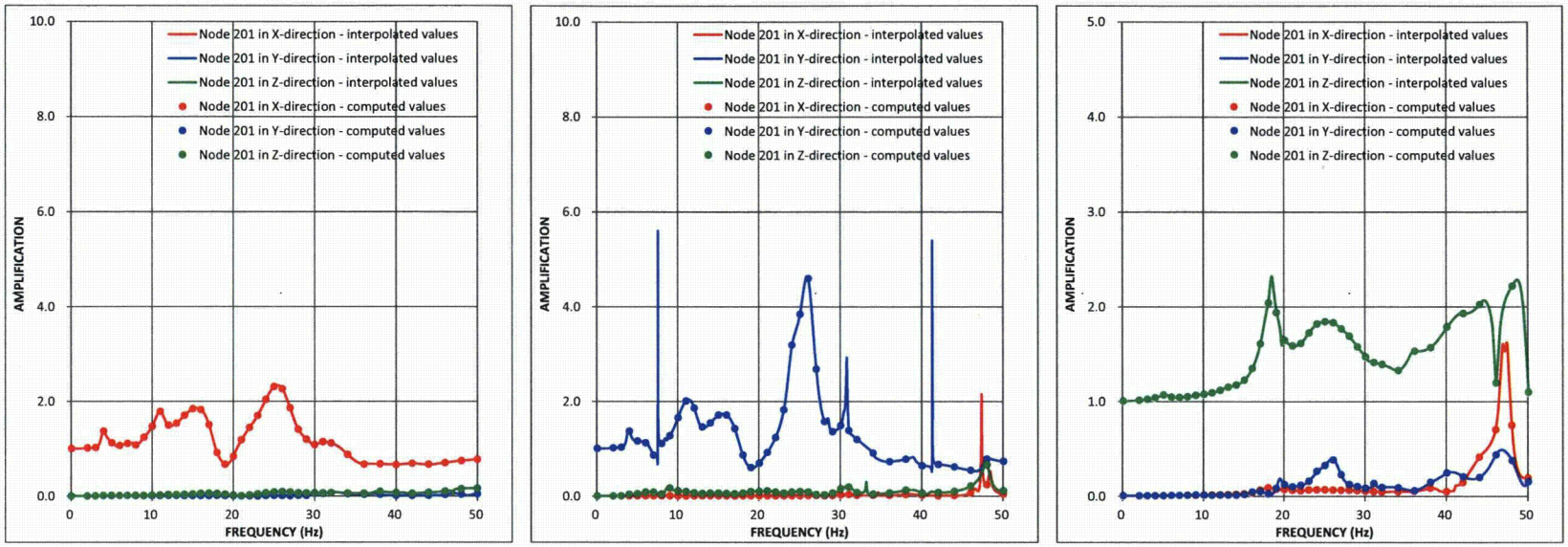

Figure 03.07.02-8(28)b Transfer functions - FWS Basemat at Lower Bound Subsurface Profile – Case CFB3-FFB

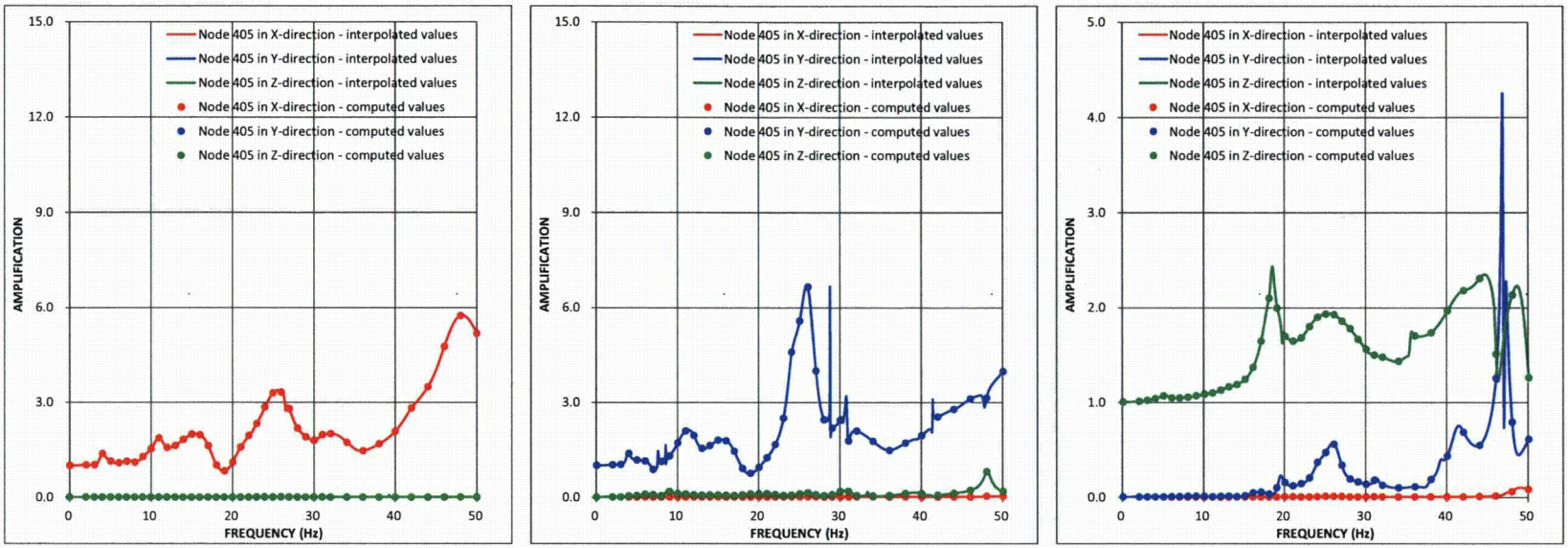

Figure 03.07.02-8(28)c Transfer functions - FPE Top at Lower Bound Subsurface Profile – Case CFB3-FFB

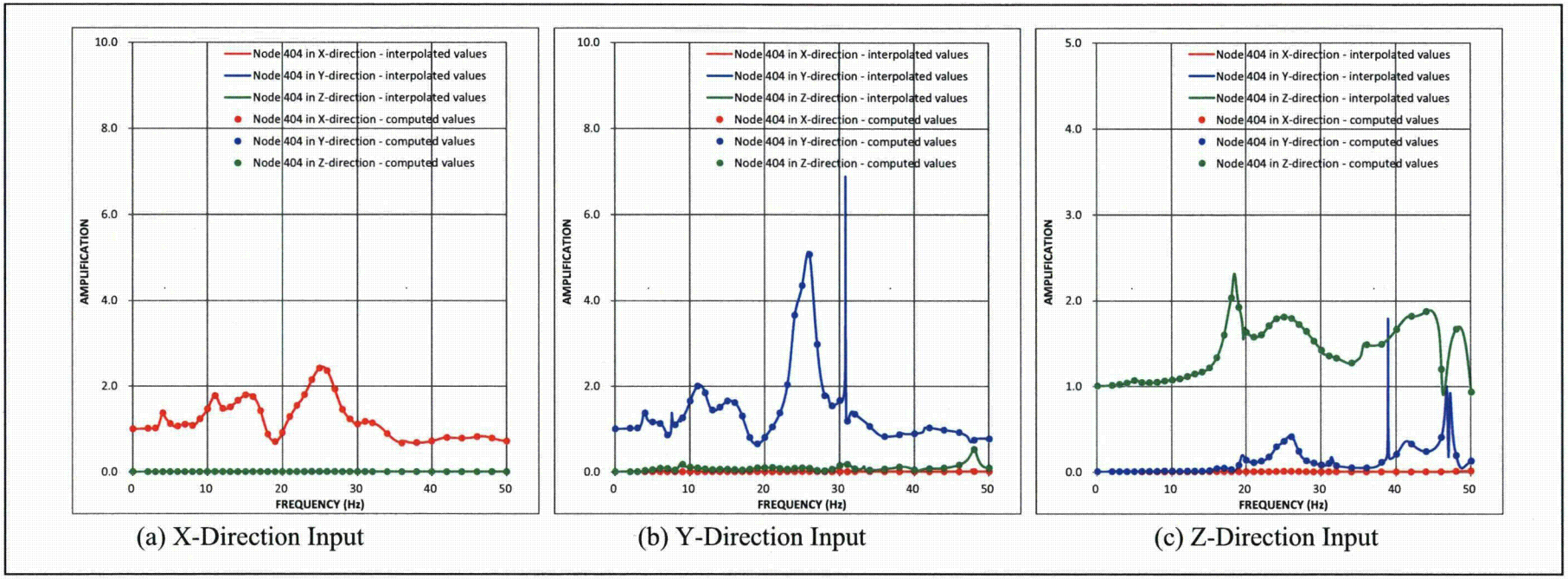

Figure 03.07.02-8(28)d Transfer functions - FPE Basemat at Lower Bound Subsurface Profile – Case CFB3-FFB

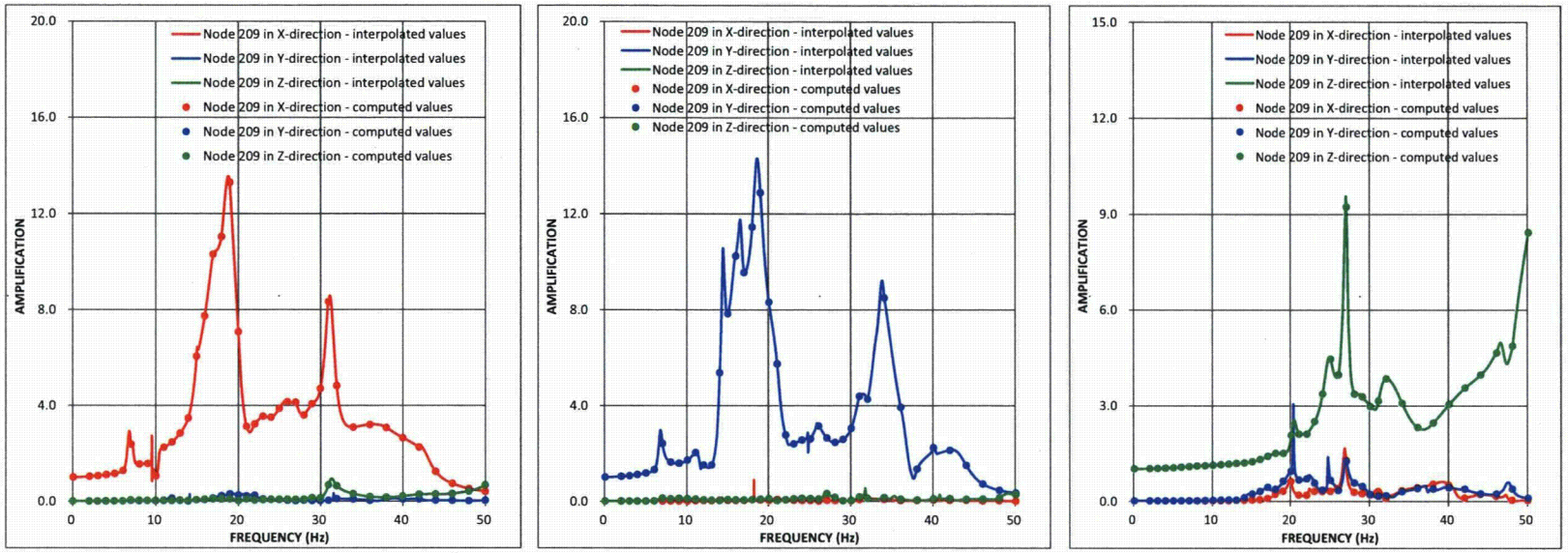

Figure 03.07.02-8(29)a Transfer functions - FWS Top at Upper Bound Subsurface Profile – Case CFB3-FFB

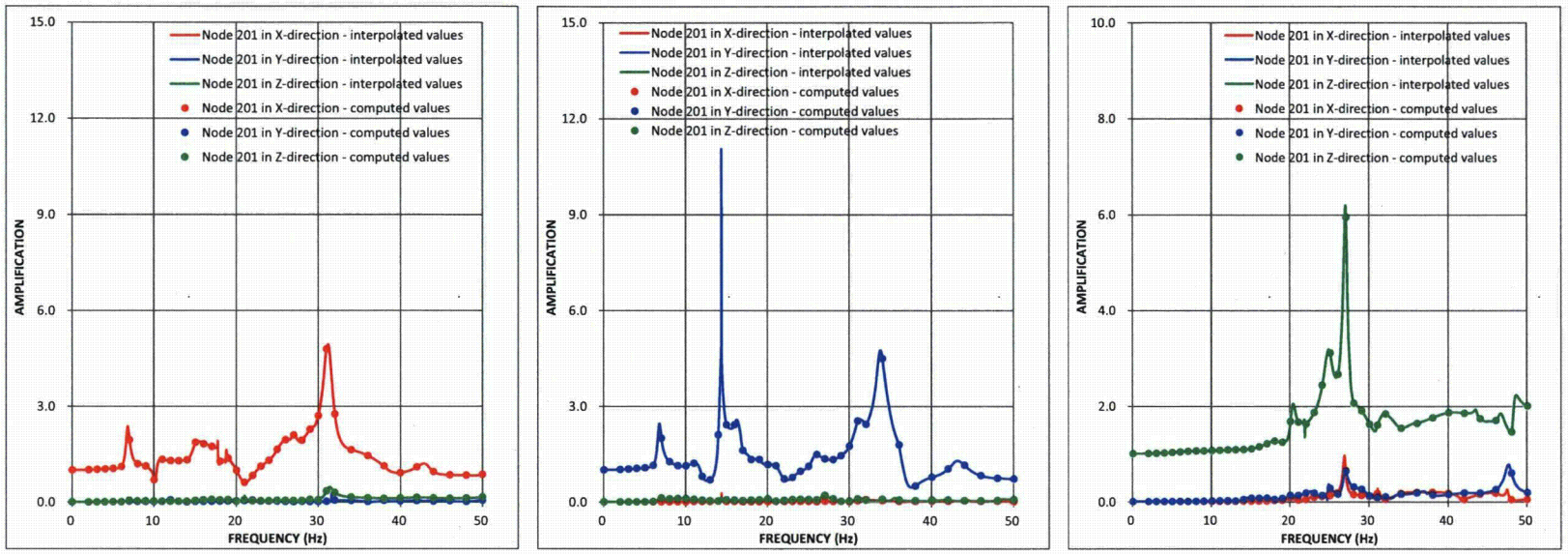

Figure 03.07.02-8(29)b Transfer functions - FWS Basemat at Upper Bound Subsurface Profile – Case CFB3-FFB

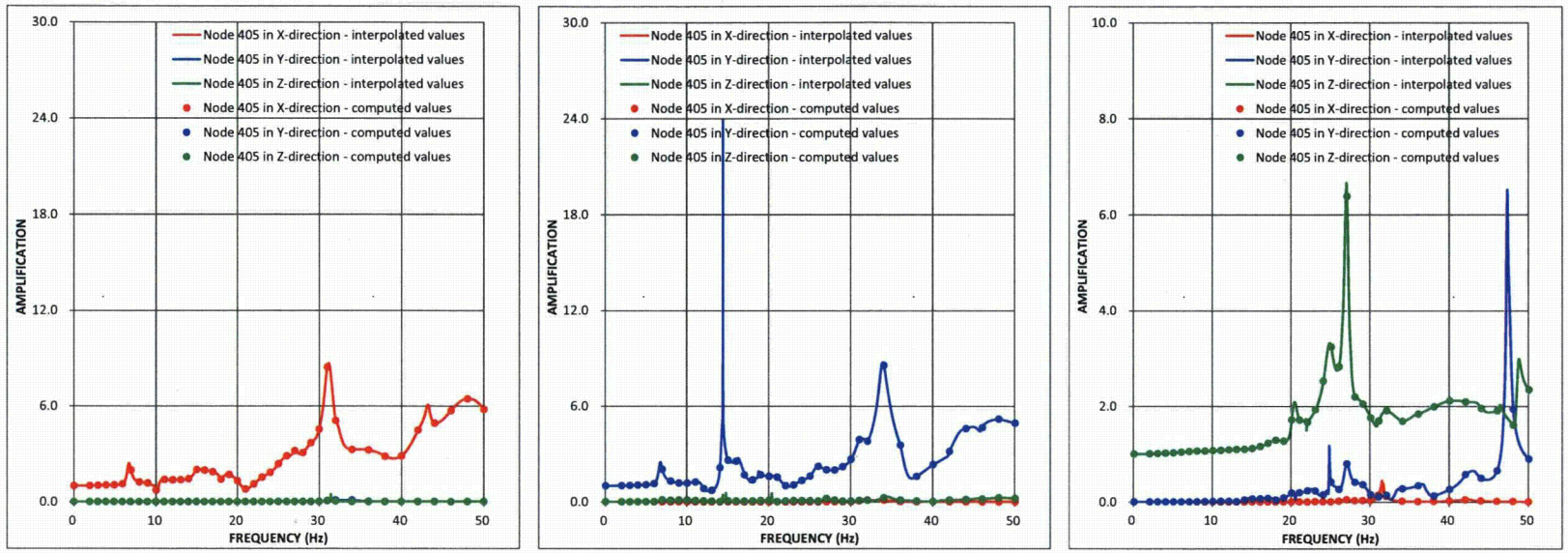

(a) X-Direction Input (b) Y-Direction Input (c) Z-Direction Input

Figure 03.07.02-8(29)c Transfer functions - FPE Top at Upper Bound Subsurface Profile – Case CFB3-FFB

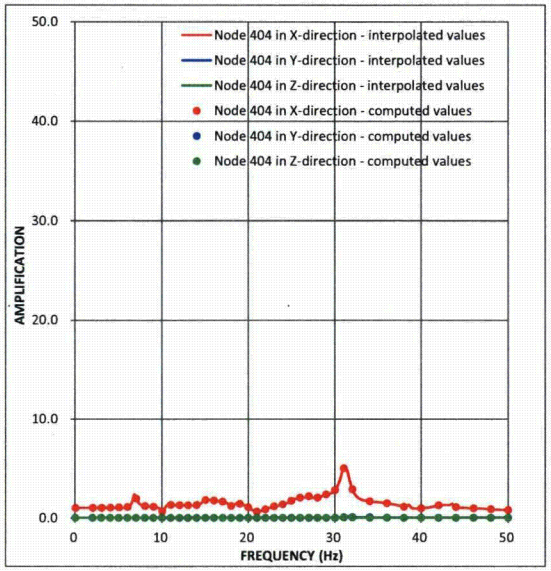

(a) X-Direction Input

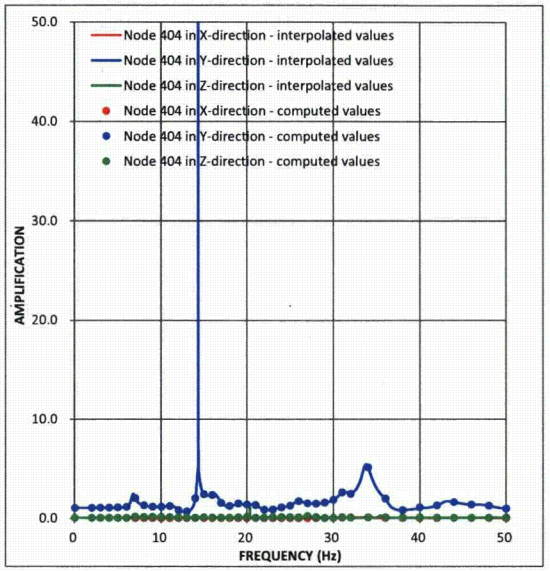

(b) Y-Direction Input

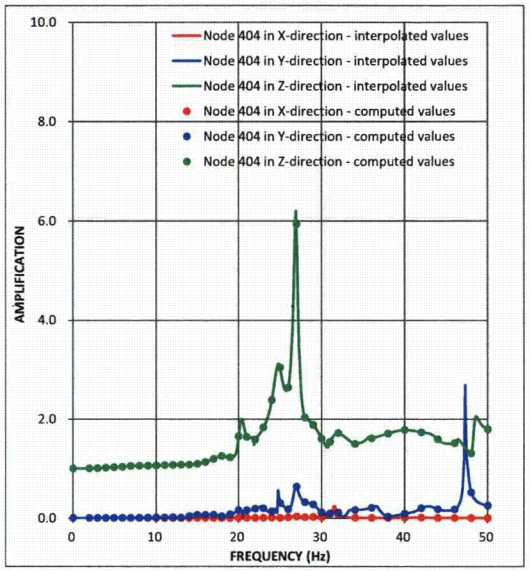

(c) Z-Direction Input

Figure 03.07.02-8(29)d Transfer functions - FPE Basemat at Upper Bound Subsurface Profile – Case CFB3-FFB

Attachment 6
NRC3-12-0019
(17 pages)

Response to RAI Letter No. 70
(eRAI Tracking No. 6245)

RAI Question No. 03.08.05-4

NRC RAI 03.08.05-4

EF3 FSAR Section 2.5.4.10.3 discusses static and dynamic lateral earth pressures for the RB/FB and CB below-grade walls at the Fermi site. At rest-conditions are assumed, consistent with the assumptions in ESBWR DCD Section 3.8.5 and Appendix 3G. These pressures are shown in EF3 FSAR Figures 2.5.4-230 and 4-231. However, no discussion is given regarding the lateral pressures on the portions of below-grade walls that are embedded in rock. Also, no discussion is given regarding additional lateral pressures due to: (i) static and dynamic surcharge loads from adjacent Seismic Category I and II structures; and (ii) effects of structure-to-structure interaction through the surrounding backfill, concrete fill, or rock.

The staff notes that the methodology used to estimate seismic lateral earth pressures is based on EF3 FSAR Reference 2.5.4-247 (Ostadan and White, 1998), which deviates from the methodology used in the ESBWR DCD Section 3.8.5, Appendix 3A, and Appendix 3G (envelope of the method described in ASCE 4-98 Section 3.5.3.2 and pressures obtained from the SSI analysis) and also from the guidance in SRP 3.8.4.II.4H.

To determine whether the lateral pressures for the RB/FB and CB below-grade walls at the Fermi site are bounded by those considered in the ESBWR DCD, provide the following information:

(a) *Comparison of seismic lateral earth pressures shown in EF3 FSAR Figures 2.5.4-230 and 4-231 with those obtained using the method described in ASCE 4-98 Section 3.5.3.2 and also with those given in ESBWR DCD Tables 3A.8.8-1 and 3A.8.8-2, and ESBWR DCD Sections 3G.1.5.2.1 and 3G.2.5.2 (Figures 3G.1-19, 3G.1-27, 3G.2-12, and 3G.2-15), which were used for the design of the walls.*

(b) *For the portions of below-grade walls that are embedded in rock, provide estimates of the seismic lateral pressures imposed by the surrounding rock, which are compatible with the results of the site-specific SSI analyses performed and with the assumptions of the sliding stability calculations discussed in EF3 FSAR Sections 3.7.2 and 3.8.5, as modified by the markups included with the response to RAI Letter 55 Question 02.05.04-38.*

(c) *Provide estimates of additional static and dynamic lateral pressures imposed from adjacent Seismic Category I and II structures. This should also include possible effects of structure-to- structure interaction through the surrounding backfill, concrete fill, or rock.*

(d) *Modify EF3 FSAR Figures 2.5.4-230 and 4-231 to incorporate the pressures discussed in items (b) and (c) above and compare with the lateral pressures given in ESBWR DCD Tables 3A.8.8-1 and 3A.8.8-2, and ESBWR DCD Sections 3G.1.5.2.1 and 3G..2.5.2, which were used for the design of the walls. If site-specific SSI analyses that consider the backfill become available, include the lateral pressures from the SSI analyses in the comparison.*

Response

(a) Comparison of seismic lateral earth pressures shown in EF3 FSAR Figures 2.5.4-230 and 4-231 with those obtained using the method described in ASCE 4-98 Section 3.5.3.2 and also with those given in ESBWR DCD Tables 3A.8.8-1 and 3A.8.8-2, and ESBWR DCD Sections 3G.1.5.2.1 and 3G.2.5.2 (Figures 3G.1-19, 3G.1-27, 3G.2-12, and 3G.2-15), which were used for the design of the walls.

The response to part (a) of this RAI was provided in Detroit Edison letter NRC3-12-0003, dated February 16, 2012 (ML12052A059).

(b) For the portions of below-grade walls that are embedded in rock, provide estimates of the seismic lateral pressures imposed by the surrounding rock, which are compatible with the results of the site-specific SSI analyses performed and with the assumptions of the sliding stability calculations discussed in EF3 FSAR Sections 3.7.2 and 3.8.5, as modified by the markups included with the response to RAI Letter 55 Question 02.05.04-38.

The lateral wall pressures imposed by the surrounding rock, which are compatible with the results of the site-specific SSI analyses performed for the licensing basis SSI analysis (i.e., no backfill), are provided in the report SER-DTF-006 for the RB/FB and CB models. The sliding stability calculations using the SSI analysis results are also provided in the SER-DTF-006 report.

In addition, the lateral wall pressures imposed by the surrounding rock and engineered granular backfill, which are compatible with the results of the site-specific SSI analyses that include backfill are provided in the response to RAI 03.07.02-6 in the report SER-DTF-008 for the RB/FB and CB models.

In the both reports, it was confirmed that the lateral soil pressures are less than the DCD wall capacity passive pressures for the RB/FB and less than the DCD design soil pressures for the CB.

In the report SER-DTF-006, it was confirmed that the actual factors of safety for overturning, sliding, and floatation are greater than the required factor of safety, and that the site-specific dynamic bearing pressure demands are less than the allowable dynamic bearing capacity in Section 2.5.4.10 in the Fermi 3 FSAR.

(c) Provide estimates of additional static and dynamic lateral pressures imposed from adjacent Seismic Category I and II structures. This should also include possible effects of structure-to- structure interaction through the surrounding backfill, concrete fill, or rock.

The additional static and dynamic lateral pressures imposed from adjacent Category I and II structures are estimated using the results of SSSI analyses of the RB/FB, CB and FWSC, which are provided in the response to RAI 03.07.02-8.

The site-specific SSI analysis cases for the RB/FB, CB and FWSC are summarized in Table 03.08.05-4(1).

Figures 03.08.05-4(1) and 03.08.05-4(2) show the lateral soil pressures on the CB imposed from the RB/FB (Case CFB2) and FWSC (Case CFB3-FFB), respectively. These pressures are compared with the lateral soil pressures computed from the equivalent static pressure analysis in ASCE 4-98.

The lateral soil pressure loads for the exterior walls are calculated by averaging lateral soil pressures in Figures 03.08.05-4(1) and 03.08.05-4(2) along each wall height which is a floor height excluding the thickness of slabs. The calculated soil pressures are provided in Tables 03.08.05-4(2) and 03.08.05-4(3), respectively for impact of the RB/FB on the CB (Case CFB2) and the impact of the FWSC on the CB (Case CFB3-FFB), along with the Fermi 3 SASSI2000 SSSI enveloping lateral soil pressures and the DCD design soil pressures. The calculated Fermi 3 SSSI lateral soil pressures are less than the DCD design soil pressures.

Figures 03.08.05-4(1) and 03.08.05-4(2) demonstrate that the Fermi 3 SSSI SASSI2000 lateral soil pressures are generally bounded by the ASCE 4-98 lateral soil pressures; however, at the elevation close to the engineered granular backfill/bedrock transition (EL -6,770 mm), the Fermi 3 SSSI SASSI2000 lateral soil pressures exceed the ASCE 4-98 soil pressures. However, when evaluated using the averaged soil pressures in Tables 03.08.05-4(2) and 03.08.05-4(3), the Fermi 3 SSSI SASSI2000 lateral soil pressures are confirmed to be less than or equal to the DCD design soil pressures.

This portion of the response provides supplemental information regarding the following supplemental request made by the staff at the audit conducted during the week of April 23, 2012.

> *For the RB acting on the CB, staff indicated the kinematic approach proposed by GEH may not capture inertial effects on wall pressures.*

For this supplemental response, the potential impact of the RB/FB wall deflections on the lateral soil pressures on the CB wall and the CB wall deflections on the lateral soil pressures on the RB/FB wall were evaluated. The RB/FB and CB wall deflections were estimated using the soil-structure interaction (SSI) analyses deflections for the individual RB/FB and CB modeled with SASSI2000 computer software for the fully embedded condition that includes the engineered granular backfill. Estimated wall deflections from SSI analyses of the individual RB/FB and CB are presented in Table 1. The deflections presented in Table 1 are the difference between the displacements at each floor level relative to where the embedded walls connect to the top of the RB/FB or CB basemats. The top of the embedded walls are at Elevation 4.65 m (DCD standard plant elevation), which is 150 mm above the finished ground level grade.

To consider a bounding condition, the maximum wall deflections were selected from Table 1 irrespective of whether they correspond to the same case, irrespective of the direction of the deflection, and without considering when the deflections occur. The maximum deflection of the RB/FB is 1.24 mm and the maximum deflection of the CB is 2.09 mm. If these deflections are assumed to be out of phase and occur at the same time, the maximum relative deflection of the RB/FB and CB toward each other is 3.33 mm (0.13 in).

For the RB/FB or CB to apply additional lateral soil pressures to each other due to lateral wall deflections, the following are needed:

1. The RB/FB wall must deflect into (toward) the engineered granular backfill between the RB/FB and CB sufficiently to cause lateral soil pressures on the CB wall.

2. The CB wall must deflect into (toward) the engineered granular backfill between the RB/FB and CB sufficiently to cause lateral soil pressures on the RB/FB wall.

For the ESBWR, the RB/FB and CB are separated by approximately 32 to 33 ft (10 m) [DCD Figure 1.2-11].

When a wall deflects into soil, passive lateral soil pressures will develop if there is enough movement to mobilize the shear strength of the soil. To fully mobilize the passive lateral soil pressure, an estimated rotation of the top of an embedded wall into the engineered granular backfill of 0.002 times the wall height is required (Reference 1). The equivalent RB/FB and CB embedded wall height is approximately 37 ft, which is from the top of bedrock (Fermi 3 elevation 552 ft NAVD 88) to the finished ground level grade (Fermi 3 elevation 589.3 ft NAVD 88). Below the top of bedrock the foundations are restrained from deflecting by fill concrete used to backfill the excavations within the bedrock; therefore, there will essentially be no lateral translation of the RB/FB and CB walls pushing against the engineered granular backfill. Assuming the engineered granular backfill is not moving, the wall deflection to fully develop the passive lateral soil pressure is about 0.002 * 37 ft * 12 in/ft, which equals 0.89 in (23 mm).

The 1 to 2 mm RB/FB and CB wall deflections into engineered granular backfill are much smaller than the 23 mm needed to fully mobilize the passive lateral soil pressure. These 1 to 2 mm deflections will result in non-linear deformations within the engineered granular backfill that are localized near the RB/FB and CB walls, rather than being evenly distributed across the 32 to 33 ft (10 m) width of the engineered granular backfill. Therefore, it is anticipated that the small, 1 to 2 mm, deflections of the RB/FB or CB walls will not cause additional loads to transfer through the 32 to 33 ft (10 m) of engineered granular backfill between the RB/FB and CB to impact the lateral soil pressures on the RB/FB or CB walls.

In conclusion, the SSI wall deflections of the RB/FB and CB are small and, therefore, there will be no additional lateral soil pressures on the walls of the RB/FB or CB through the 32 to 33 ft (10 m) of engineered granular backfill.

References:

1. Department of the Navy, Naval Facilities Engineering Command, *Design Manual 7.2, Foundations and Earth Structures*, NAVFAC DM-7.2, May 1982.

(d) Modify EF3 FSAR Figures 2.5.4-230 and 4-231 to incorporate the pressures discussed in items (b) and (c) above and compare with the lateral pressures given in ESBWR DCD Tables 3A.8.8-1 and 3A.8.8-2, and ESBWR DCD Sections 3G.1.5.2.1 and 3G..2.5.2, which were used for the design of the walls. If site-specific SSI analyses that consider the backfill become available, include the lateral pressures from the SSI analyses in the comparison.

For cases without engineered granular backfill, see Attachment 7 (SER-DTF-006, Figures 5.4-1 and 5.4-2). For cases with engineered granular backfill, see Attachment 4 (response to RAI 03.07.02-6). For cases considering adjacent structures, see response (c) above. No FSAR change is required.

Proposed COLA Revision

None.

Table 03.08.05-4(1) RB/FB, CB & FWSC SSI Analysis Cases

Building	Case	ID No.	Model *1 (DCD)	Input Motion	Site Condition			Remarks
					BE	LB	UB	
RB/FB	RFB	RFB-1	Base	RB/FB FIRS	✓	--	--	
		RFB-2			--	✓	--	
		RFB-3			--	--	✓	
CB	CFB2	CFB2-1	Base	FIRS *2	✓	--	--	RB/FB SSSI Effects are included
		CFB2-2			--	✓	--	
		CFB2-3			--	--	✓	
CB & FWSC	CFB3-FFB	CFB3-1 & FFB-1	Base	CB FIRS	✓	--	--	SSSI Effects of each Building are included
		CFB3-2 & FFB-2			--	✓	--	
		CFB3-3 & FFB-3			--	--	✓	

Note *1: As shown in DCD Table 3A.6-1, there are some models with minor modifications to evaluate the modeling effects. For this Fermi 3 SSI analysis, the most basic model, "Base" is applied.

*2: Input motion is generated from Case RFB.

Table 03.08.05-4(2) Comparison of Lateral Soil Pressure - CB - Case CFB2

Floor Level (m)	C1 and C5 Averaged Soil Pressure (MPa)			CA and CD Averaged Soil Pressure (MPa)			Envelope (MPa)		DCD Design Soil Pressure (MPa)	
	CFB2-1 (BE)	CFB2-2 (LB)	CFB2-3 (UB)	CFB2-1 (BE)	CFB2-2 (LB)	CFB2-3 (UB)	C1 and C5 Wall	CA and CD Wall	C1 and C5 Wall	CA and CD Wall
4.65										
Slab										
3.95 -2.00	0.11	0.09	0.12	0.13	0.11	0.14	0.12	0.14	0.22	0.22
Slab										
-2.50 -7.40	0.15	0.13	0.14	0.18	0.15	0.16	0.15	0.18	0.18	0.18

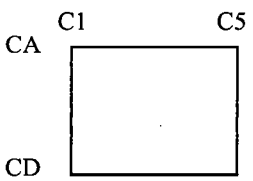

Table 03.08.05-4(3) Comparison of Lateral Soil Pressure - CB - Case CFB3-FFB

Floor Level (m)	C1 and C5 Averaged Soil Pressure (MPa)			CA and CD Averaged Soil Pressure (MPa)			Envelope (MPa)		DCD Design Soil Pressure (MPa)	
	CFB3-1 (BE)	CFB3-2 (LB)	CFB3-3 (UB)	CFB3-1 (BE)	CFB3-2 (LB)	CFB3-3 (UB)	C1 and C5 Wall	CA and CD Wall	C1 and C5 Wall	CA and CD Wall
4.65										
Slab										
3.95 -2.00	0.11	0.09	0.11	0.12	0.10	0.12	0.11	0.12	0.22	0.22
Slab										
-2.50 -7.40	0.15	0.13	0.14	0.17	0.14	0.16	0.15	0.17	0.18	0.18

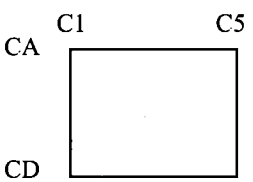

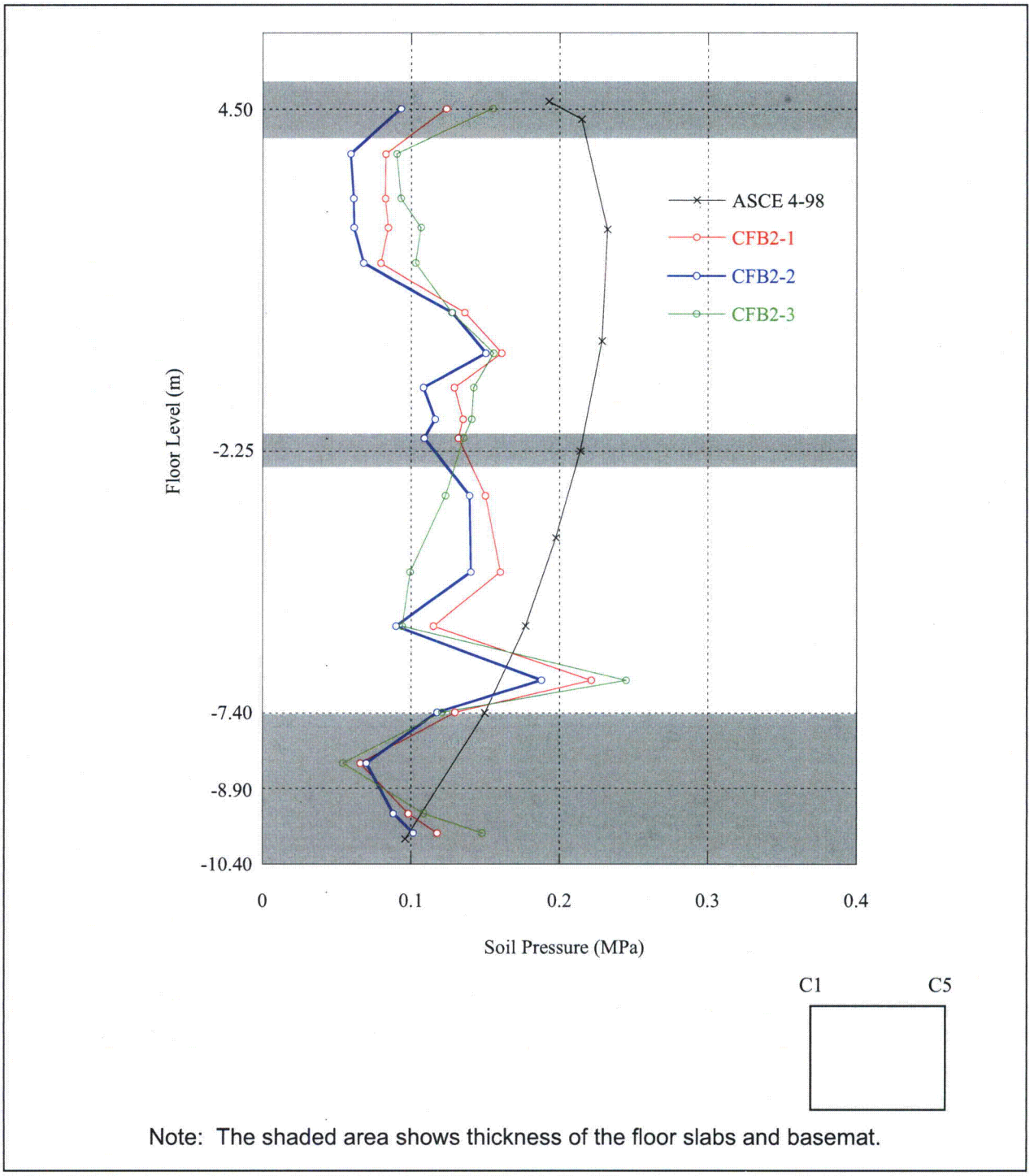

Figure 03.08.05-4(1)a Lateral Soil Pressure including RB/FB SSSI Effects - CB C1 Wall - Case CFB2

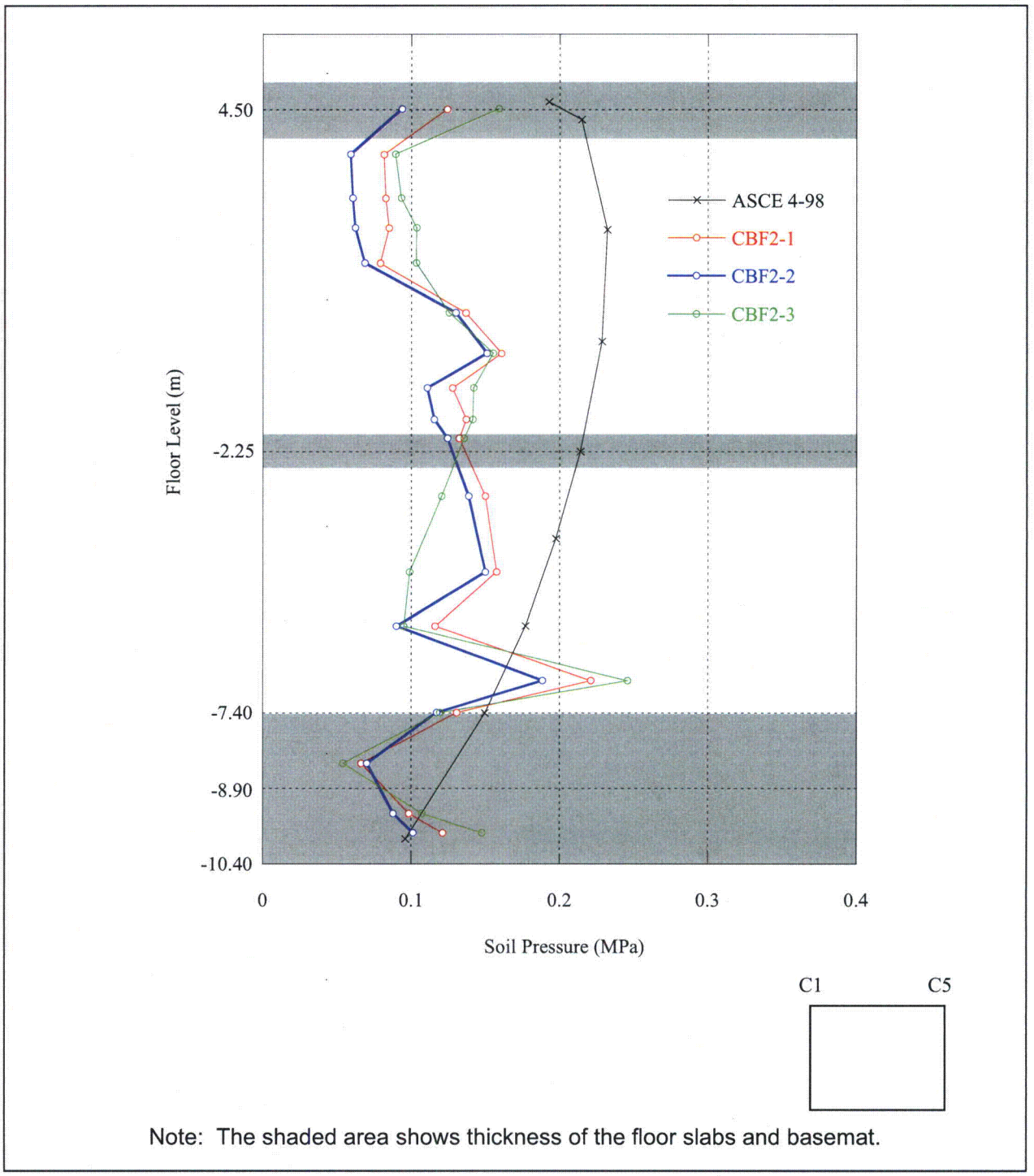

Note: The shaded area shows thickness of the floor slabs and basemat.

Figure 03.08.05-4(1)b Lateral Soil Pressure including RB/FB SSSI Effects - CB C5 Wall - Case CFB2

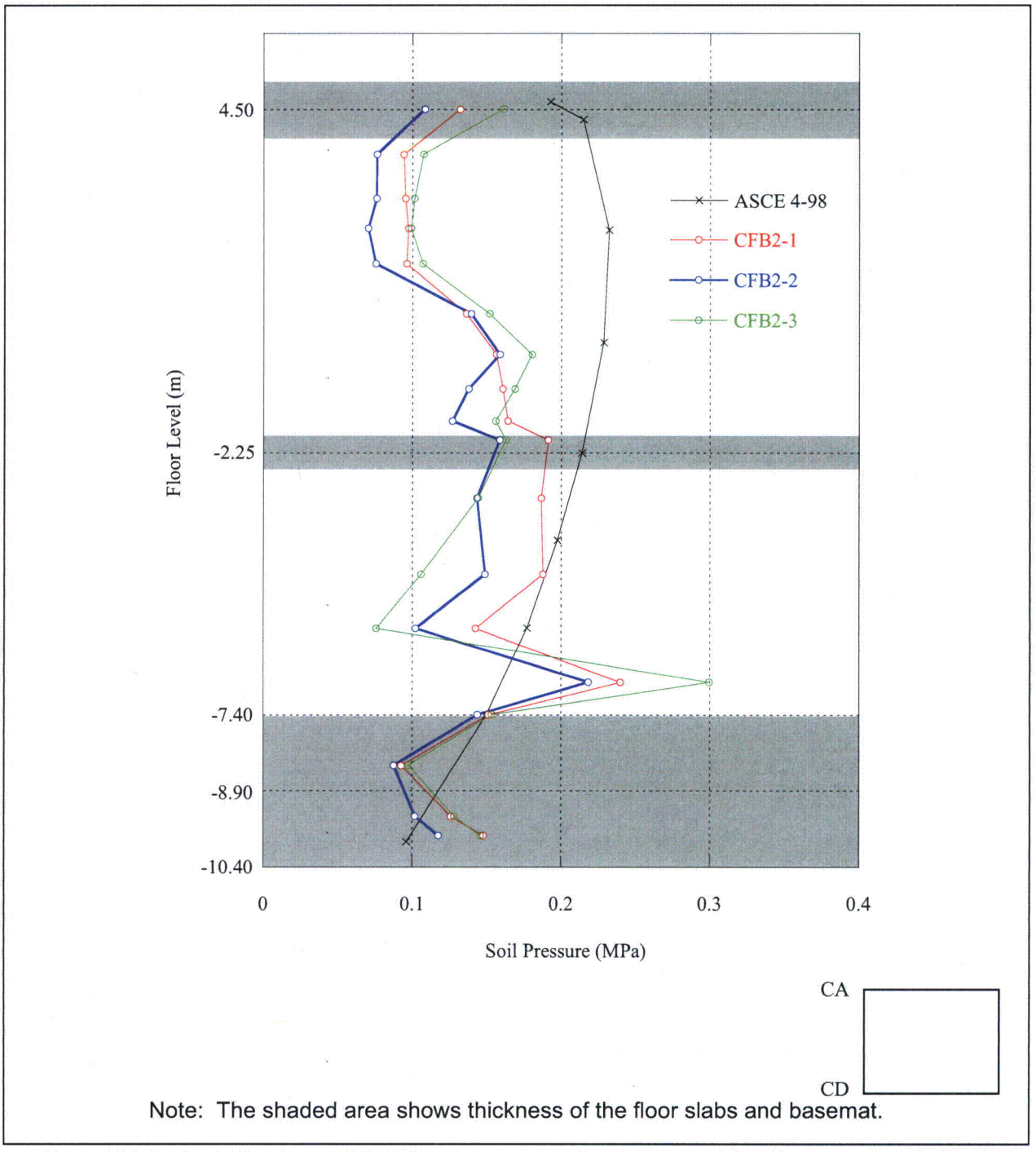

Note: The shaded area shows thickness of the floor slabs and basemat.

Figure 03.08.05-4(1)c Lateral Soil Pressure including RB/FB SSSI Effects - CB CA Wall - Case CFB2

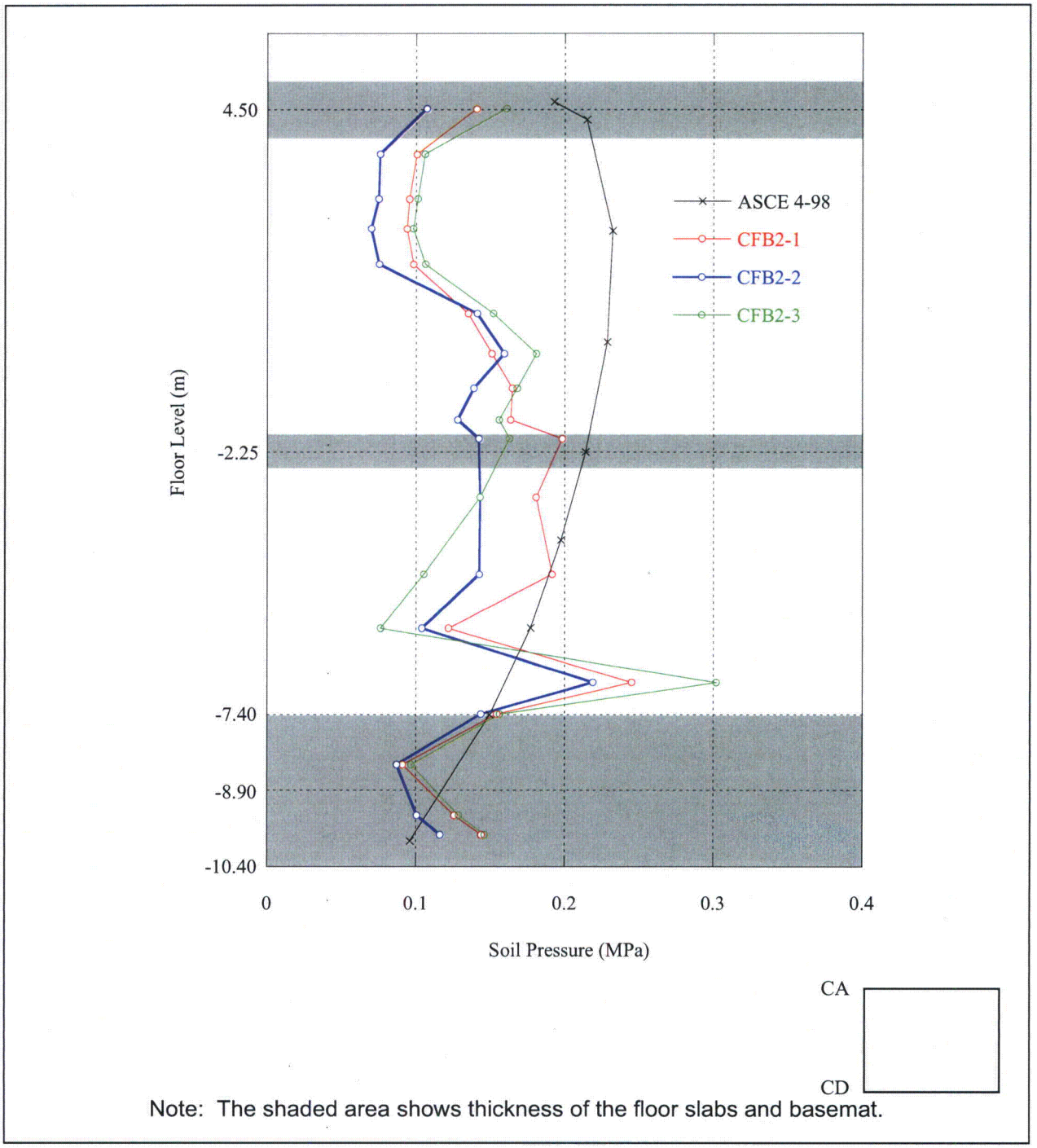

Note: The shaded area shows thickness of the floor slabs and basemat.

Figure 03.08.05-4(1)d Lateral Soil Pressure including RB/FB SSSI Effects - CB CD Wall - Case CFB2

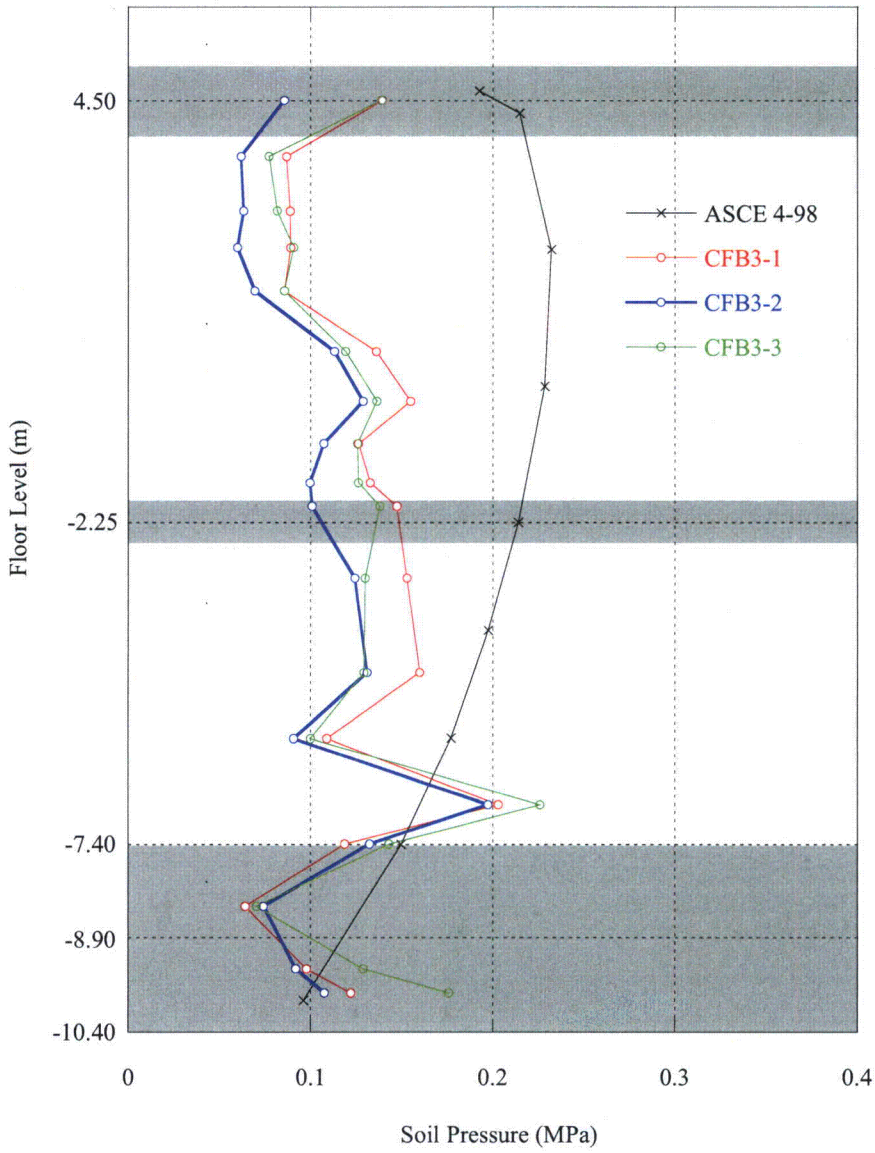

Note: The shaded area shows thickness of the floor slabs and basemat.

Figure 03.08.05-4(2)a Lateral Soil Pressure including FWSC SSSI Effects - CB C1 Wall - Case CFB3-FFB

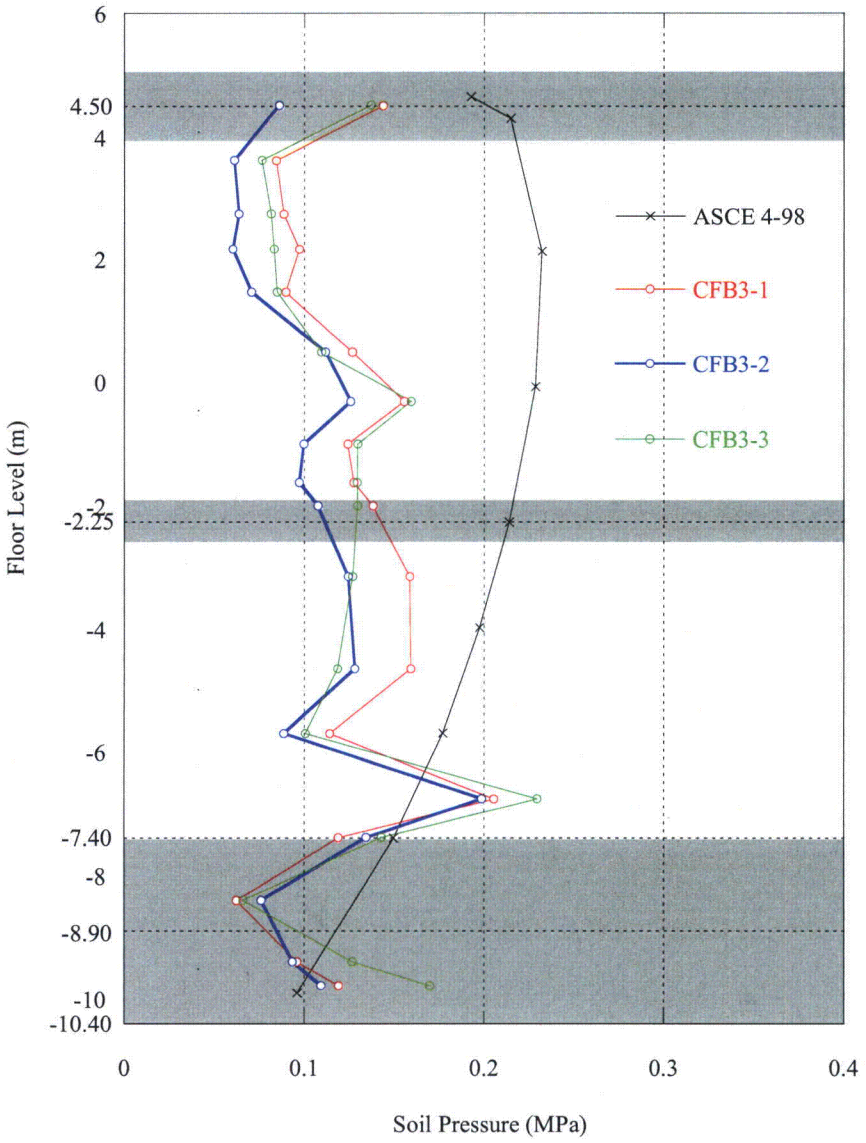

Note: The shaded area shows thickness of the floor slabs and basemat.

Figure 03.08.05-4(2)b Lateral Soil Pressure including FWSC SSSI Effects - CB C5 Wall - Case CFB3-FFB

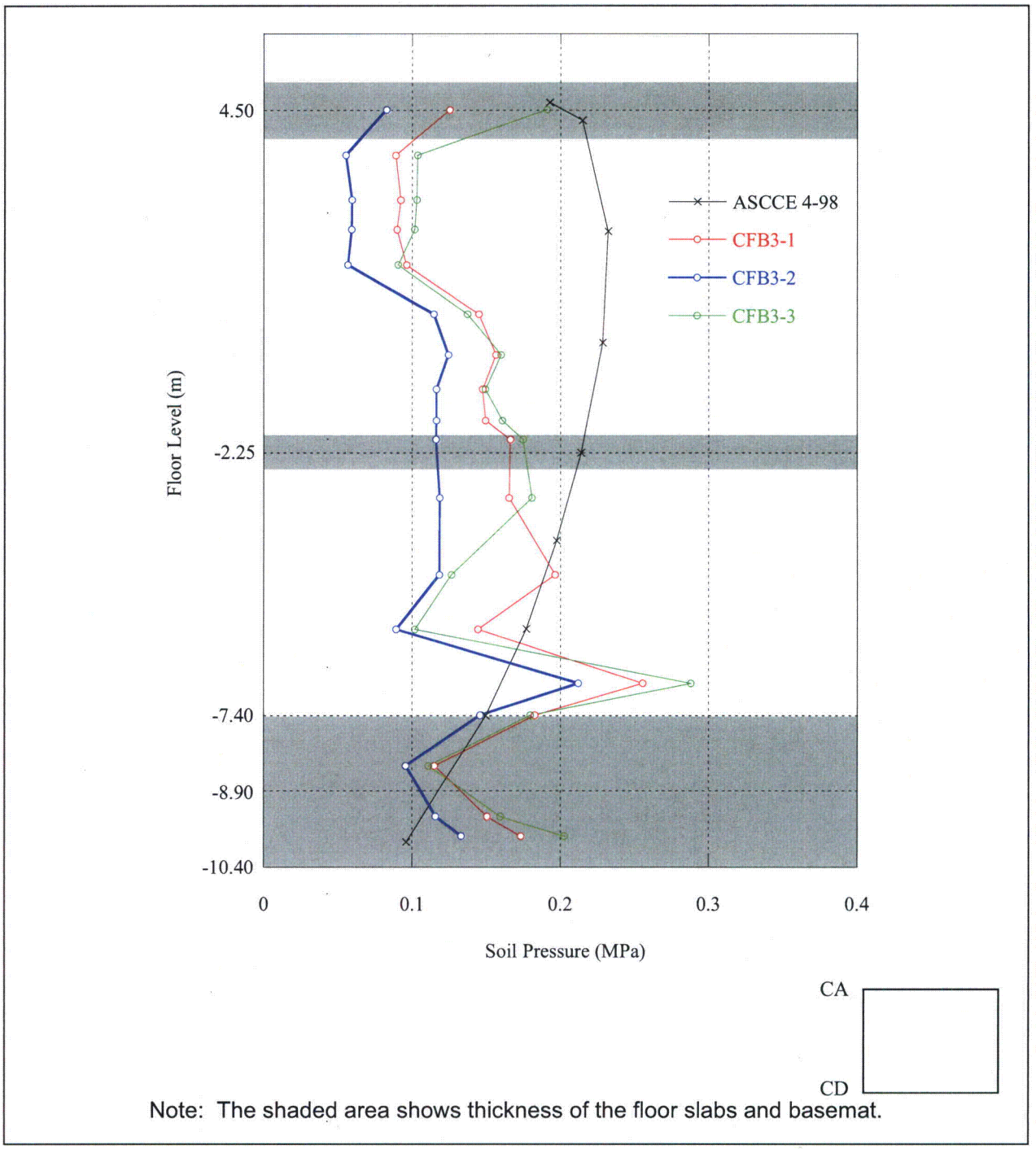

Note: The shaded area shows thickness of the floor slabs and basemat.

Figure 03.08.05-4(2)c Lateral Soil Pressure including FWSC SSSI Effects - CB CA Wall - Case CFB3-FFB

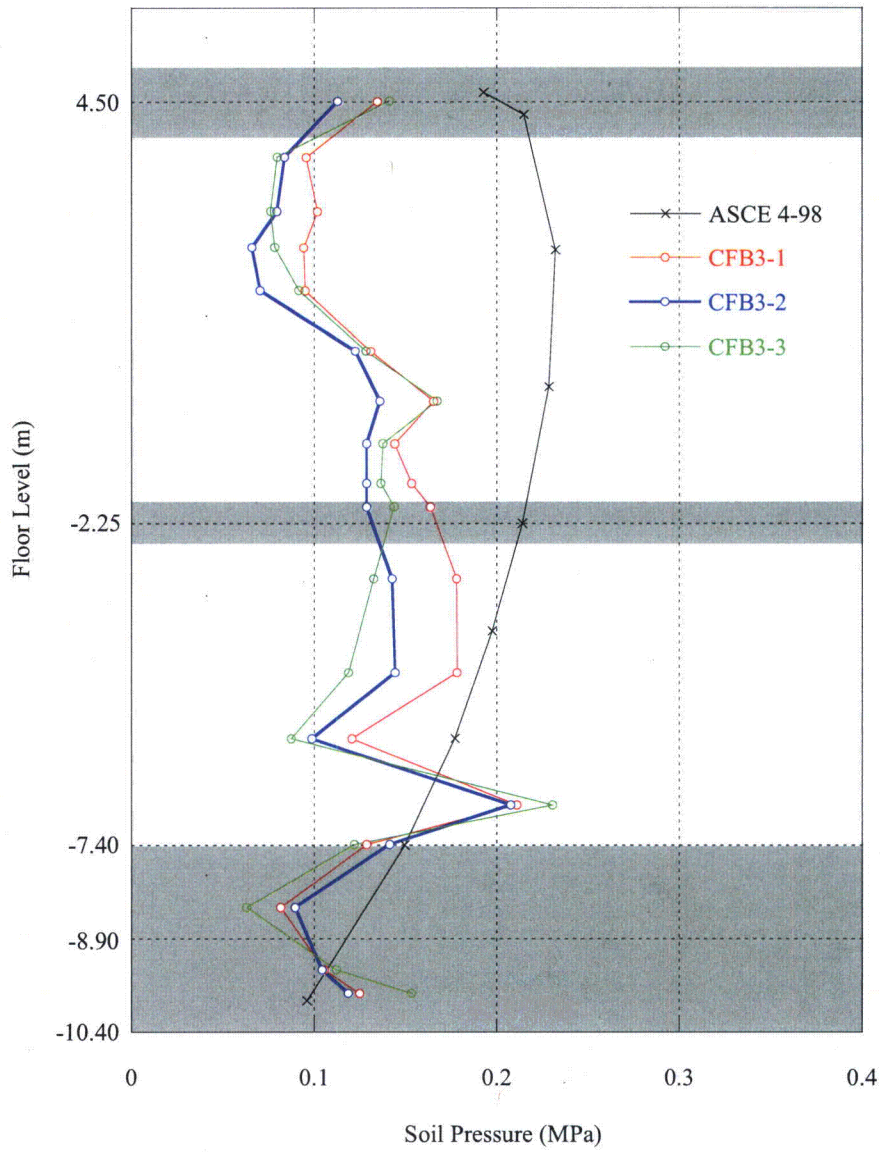

Note: The shaded area shows thickness of the floor slabs and basemat.

Figure 03.08.05-4(2)d Lateral Soil Pressure including FWSC SSSI Effects - CB CD Wall - Case CFB3-FFB

Table 1
Relative Wall Deflections for Fully Embedded Conditions

Reactor Building/Fuel Building

Elevation (m)	Relative Displacement (mm)					
	BE		LB		UB	
	W-dir.	E-dir.	W-dir.	E-dir.	W-dir.	E-dir.
4.65	1.22	1.06	1.24	1.19	0.94	0.94
-1.00	0.64	0.67	0.70	0.67	0.57	0.57
-6.40	0.29	0.27	0.21	0.22	0.19	0.20
-11.50	Reference Point (top of building basemat)					

Control Building

Elevation (m)	Relative Displacement (mm)					
	BE		LB		UB	
	W-dir.	E-dir.	W-dir.	E-dir.	W-dir.	E-dir.
4.65	1.06	1.15	0.90	0.89	2.02	2.09
-2.00	0.53	0.52	0.37	0.45	0.96	0.98
-7.40	Reference Point (top of building basemat)					